EXPLORING LIVER AND ADIPOSE TISSUE ALTERATIONS IN THE NATURAL COURSE OF NON-ALCOHOLIC FATTY LIVER DISEASE: A LIPIDOMIC APPROACH

Gerard Baiges Gaya

GERARD BAIGES GAYA

EXPLORING LIVER AND ADIPOSE TISSUE ALTERATIONS IN THE NATURAL COURSE OF NON-ALCOHOLIC FATTY LIVER DISEASE: A LIPIDOMIC APPROACH

INTERNATIONAL DOCTORAL THESIS

Supervised by:

Professor Jorge Joven Maried

Professor Jorge Camps Andreu

Department of Medicine and Surgery

UNIVERSITAT
ROVIRA i VIRGILI

Reus, Tarragona, Spain

2022

UNIVERSITAT ROVIRA I VIRGILI
EXPLORING LIVER AND ADIPOSE TISSUE ALTERATIONS IN THE NATURAL COURSE OF NON-ALCOHOLIC FATTY LIVER DISEASE: A LIPIDOMIC
Gerard Baiges Gaya

UNIVERSITAT ROVIRA I VIRGILI
EXPLORING LIVER AND ADIPOSE TISSUE ALTERATIONS IN THE NATURAL COURSE OF NON-ALCOHOLIC FATTY LIVER DISEASE: A LIPIDOMIC
Gerard Baiges Gaya

UNIVERSITAT ROVIRA i VIRGILI

FAIG CONSTAR que aquest treball, titulat “Exploring liver and adipose tissue alterations in the natural course of non-alcoholic fatty liver disease: a lipidomic approach”, que presenta Gerard Baiges Gaya per a l’obtenció del títol de Doctor amb menció internacional, ha estat realitzat sota la meva direcció al Departament de Medicina i Cirurgia d’aquesta universitat.

HAGO CONSTAR que el presente trabajo, titulado “Exploring liver and adipose tissue alterations in the natural course of non-alcoholic fatty liver disease: a lipidomic approach”, que presenta Gerard Baiges Gaya para la obtención del título de Doctor con mención internacional, ha sido realizado bajo mi dirección en el Departamento de Medicina y Cirugía de esta universidad.

I STATE that the present study, entitled “Exploring liver and adipose tissue alterations in the natural course of non-alcoholic fatty liver disease: a lipidomic approach”, presented by Gerard Baiges Gaya for the award of the degree of Doctor with an international distinction, has been carried out under my supervision at the Department of Medicine and Surgery of this university.

Reus, 26 de agost de 2022/ Reus, 26 de agosto de 2022/ Reus, 2022 August 26

Els directors de la tesis doctoral
Los directores de la tesis doctoral
Doctoral thesis supervisors

Professor Jorge Joven Maried

Dr. Jorge Camps Andreu

UNIVERSITAT ROVIRA I VIRGILI
EXPLORING LIVER AND ADIPOSE TISSUE ALTERATIONS IN THE NATURAL COURSE OF NON-ALCOHOLIC FATTY LIVER DISEASE: A LIPIDOMIC
Gerard Baiges Gaya

ACKNOWLEDGMENTS

M’agradaria agrair a totes aquelles persones que en major o menor mesura han contribuït a dur a terme aquesta tesi.

En primer lloc, al Dr. Jorge Joven per obrir-me les portes del CRB ara fa 8 anys. Gràcies per totes les lliçons i consells que m’has transmès durant aquesta etapa de creixement professional i personal.

Al Dr. Jordi Camps, per la paciència i ajuda rebuda en els moments crítics i pels consells que m’han ajudat tan dins i fora del laboratori.

A les meves primeres tutores del CRB Fedra i Noemí. Gràcies per cuidar-me, ensenyar-me i aconsellar-me en tot moment. Heu sigut un referent en el meu camí.

A l’Anna i al Salva, gràcies per ajudar-me quan us he necessitat. Us desitjo el millor.

Als meus nens de pràctiques, gràcies per deixar-me créixer al vostre costat. En especial, gràcies, Maria Mercado, per impulsar-me a aprendre cada dia més resolent totes les nostres preguntes. Desitjo que tinguis un futur brillant dins del món de la ciència.

A l’Helena i l’Andrea, gràcies per treballar amb mi colze a colze i fer posible que les coses surtin. Estic segur que us espera un futur prometedor.

A totes les persones de la Facultat de Medicina i Ciències de la Salut que he tingut el plaer de conèixer, en especial al Dr. Jordi Blanco, Dra. Josepa Girona i al Dr. Lluís Masana. Gràcies per ajudar-me i facilitar-me el camí en tot moment.

Al Dr.Toni Vidal-Puig, gracias por acogerme y abrirme las puertas de su grupo de investigación durante mi estancia en Cambridge. Ha sido un enorme placer poder ver y aprender de cerca todo lo que hacéis. Al Dr. Guillaume Bidault, thank you so much for taught me in the lab and for all the good moments in the Cambridge University. Al Dr. Sergio Rodríguez gràcies infinites per tot el que has fet per mi dins i fora del laboratori. M’has ajudat a créixer i millorar dins del món científic i a veure les coses d’una altra manera. Espero que puguem seguir en contacte amb tots vosaltres. Moltes gràcies per tot.

Al Dr. Selvakumar Anbalagan, thank you very much for your help, time, and patience. It was a pleasure to meet you. I am sure that we will keep in touch.

Al Dr. Raúl Durán y al Dr. Josep Jiménez, gracias por permitir-me aprender con vosotros el mundo de los cultivos celulares. Fue una gran experiencia y os estoy muy agradecido.

Al meva princesa Elisabet, gràcies per ser el meu punt de suport en tot moment i per aguantar-me en les bones i no tan bones. Gràcies per compartir amb mi totes les anècdotes dins i fora del laboratori, però sobretot per ser la meva companya de vida. T’estimo.

A la meva mare Dolors, gràcies per confiar i recolzar-me en tot moment. Ets un pilar imprescindible per a mi. Al Robert, gràcies per preocupar-te per mi i cuidar-me sempre. Al meu pare Javier, gràcies per ajudar-me sempre i vetllar pel meu futur. A l'Àlex, per transmetre'm energia positiva en tot moment i ser una font de coneixement per a qualsevol que estigui al teu costat.

A la iaia i la padrina, gràcies per escoltar-me i donar-me suport en cada pas del meu camí. A les tietes Mònica i Yolanda, gràcies per celebrar amb mi totes les victòries i recolzar-me en els moments difícils. A l'Evaristo, per contagiar-me sempre d'alegria i riures i donar-me consells en els moments crítics. Us estimo a tots.

Finalment, als meus amics de la infància, en especial, Mata, Pipa, Esteban i Colom gràcies per recordar-me els bons moments i estar-hi sempre. Sou família.

UNIVERSITAT ROVIRA I VIRGILI
EXPLORING LIVER AND ADIPOSE TISSUE ALTERATIONS IN THE NATURAL COURSE OF NON-ALCOHOLIC FATTY LIVER DISEASE: A LIPIDOMIC
Gerard Baiges Gaya

UNIVERSITAT ROVIRA I VIRGILI
EXPLORING LIVER AND ADIPOSE TISSUE ALTERATIONS IN THE NATURAL COURSE OF NON-ALCOHOLIC FATTY LIVER DISEASE: A LIPIDOMIC
Gerard Baiges Gaya

"Ningún precio es demasiado alto por el privilegio de ser uno mismo"

Friedrich Nietzsche

UNIVERSITAT ROVIRA I VIRGILI
EXPLORING LIVER AND ADIPOSE TISSUE ALTERATIONS IN THE NATURAL COURSE OF NON-ALCOHOLIC FATTY LIVER DISEASE: A LIPIDOMIC
Gerard Baiges Gaya

Abbreviations

UNIVERSITAT ROVIRA I VIRGILI
EXPLORING LIVER AND ADIPOSE TISSUE ALTERATIONS IN THE NATURAL COURSE OF NON-ALCOHOLIC FATTY LIVER DISEASE: A LIPIDOMIC
Gerard Baiges Gaya

4-HNE: 4-hydroxy-2-nonenal

ACAT: acyl-CoA: cholesterol O-acyltransferases

ACC: acetyl-CoA carboxylase

AGPAT: 1-acylglycero-3-phosphate O-acyltransferase

AMPK: AMP-activated protein kinase

Apo: apolipoprotein

ARA: arachidonic acid

ASAT: abdominal subcutaneous adipose tissue

ATF6: activating transcription factor 6

CCL2: chemokine (C-C motif) ligand 2

CD36: fatty acid translocase

CE: cholesterol esters

CETP: cholesteryl ester transfer protein

CHOP: CCAAT-enhancer-binding protein homologous protein

CHT: high-affinity transporter

CIDEA: cell death-inducing DFA-like effector

CK: choline kinase

CL: cardiolipin

CPT1: carnitine palmitoyl transferase 1

CT: CTP: posphocholines cytidylyltransferase

CTL: intermediate-affinity transporters

CTP: phosphocholines and cytidyl triphosphate

DGAT: diacylglycerol acyltransferases

DPPC: dipalmitoyl-phosphatidylcholine

EK: ethanolamine kinase

ER: endoplasmic reticulum

ERAD: ER-associated protein degradation

ET: CTP-phosphoethanolamine cytidylyltransferase

FABP: fatty-acid binding protein

GRP78: chaperone protein glucose-regulated protein 78

GSAT: gluteo-femoral subcutaneous adipose tissue

HDL-p: high-density lipoprotein particles

IDL-p: intermediate-density lipoprotein particles

IL: interleukin

IRE1: inositol-requiring enzyme-1α

JNK: Jun-N-terminal kinase

LCL: lysocardiolipin

LCLAT: lyso-cardiolipin acyltransferase

LDL: low-density lipoprotein particles

LPAAT: lyso-phosphatidic acid acyltransferase

LPAF: lyso-platelet-activating factor

LPC: lysophosphatidylcholines

LPCAT: lysophosphatidylcholine acyltransferase

LPE: lysophosphatidylethanolamine

LPEAT: lysophosphatidylethanolamine acyltransferase

LPG: lysophosphatidylglycerol

LPGAT: lysophosphatidylglycerol acyltransferase

LPI: lysophosphatidylinositol

LPIAT: lysophosphatidylinositol acyltransferase

LPLAT: lysophosphospholipid acyltransferase

LPS: lysophosphatidylserine

MBOAT: membrane bound O-acyltransferase

MDA: malondialdehyde

MUHO: metabolic unhealthy obese

NAFL: non-alcoholic fatty liver

NAFLD: non-alcoholic fatty liver disease

NASH: non-alcoholic steatohepatitis

NEFAs: non-esterified fatty acids

OCT: low-affinity organic cation transporters

OVAT: omental visceral adipose tissue

PA: phosphatidic acid

PAF: platelet-activating factor

PAI1: plasminogen activator inhibitor- 1

PC: phosphatidylcholine

PE: phosphatiylethanolamine

PEMT: phosphatidylethanolamine N-methyltransferase

PERK: PRKR-like endoplasmic reticulum kinase

PG: phosphatidylglycerol

PGP: phosphatidylglycerol-phosphate

PGP-Pase: phosphatidylglycerolphosphate phosphatase

PGPS: phosphatidylglycerolphosphate synthase

PI: phosphatidylinositol

PIS: phosphatidylinositol synthase

PS: phosphatidylserine

PSD: phosphatidylserine decarboxylase

PSS: phosphatidylserine synthase

RBP4: retinol-binding protein 4

ROS: reactive oxygen species

SCD: stearoyl-CoA desaturase

SM: sphingomyelins

TCA: tricarboxylic acid cycle

TNF-α: tumour necrosis factor alpha

VAT: visceral adipose tissue

VLDL-p: very-low-density lipoprotein particles

UNIVERSITAT ROVIRA I VIRGILI
EXPLORING LIVER AND ADIPOSE TISSUE ALTERATIONS IN THE NATURAL COURSE OF NON-ALCOHOLIC FATTY LIVER DISEASE: A LIPIDOMIC
Gerard Baiges Gaya

UNIVERSITAT ROVIRA I VIRGILI
EXPLORING LIVER AND ADIPOSE TISSUE ALTERATIONS IN THE NATURAL COURSE OF NON-ALCOHOLIC FATTY LIVER DISEASE: A LIPIDOMIC
Gerard Baiges Gaya

INDEX

UNIVERSITAT ROVIRA I VIRGILI
EXPLORING LIVER AND ADIPOSE TISSUE ALTERATIONS IN THE NATURAL COURSE OF NON-ALCOHOLIC FATTY LIVER DISEASE: A LIPIDOMIC
Gerard Baiges Gaya

ABSTRACT

BACKGROUND AND AIMS: Obesity is a worldwide health concern in which 60-90% of patients will develop non-alcoholic fatty liver disease (NAFLD), the primary hepatic manifestation of metabolic syndrome. The adipose tissue dysfunction results in a limited capacity for expansion, and the free fatty acids flux is redirected into the liver which leads to ectopic fat accumulation. The excessive accumulation of hepatic saturated fatty acids and cholesterol can promote endoplasmic reticulum stress and mitochondrial dysfunction, which in turn generate an inflammatory and oxidative stress environment leading to non-alcoholic steatohepatitis (NASH). At present, no drugs have been approved for long-term treatment of NAFLD. Therefore, lifestyle interventions are the first-line treatment for this metabolic disorder. Herein, we study the lipid metabolism alterations produced in NASH development to identify potential pharmacological targets. Additionally, we test metformin as a drug for NASH prevention or remission combined with dietary interventions.

METHODS: In Study I, 5-week-old C57BL/6J male mice were fed on a standard chow diet (CD), high-fat diet (HFD), or high-fat high-sucrose diet (HFHSD) for 20 weeks to develop a phenotype associated with the diagnosis of NASH. In Study II, 5-week-old C57BL/6J male mice were fed on a CD or HFHSD for 20 or 40 weeks to study the ageing effects as well as to evaluate the metformin effectiveness in the prevention of NASH. Additionally, halfway study, some C57BL/6J male mice fed on an HFHSD were switched to CD to mimic the caloric restriction.

RESULTS: After 20 weeks of dietary treatment, HFHSD-fed mice develop a phenotype associated with the diagnosis of NASH. Thus, mice fed on an HFHSD showed more hepatic macrovascular steatosis than HFD-fed mice, as well as higher levels of markers related to oxidative stress and inflammation such as 4-hydroxy-nonenal, CD11b, CCL2, and the activation of the JNK pathway. Additionally, this metabolic context was related to alterations in the autophagy-associated proteins and the activation of hepatic *de novo* lipogenesis. Given that hepatic *de novo* lipogenesis is one of the strongest pathways activated in our model, we considered testing the efficacy of metformin as a lipogenesis inhibitor for the prevention of NASH. After 20 and 40 weeks of treatment, we observed that HFHSD-fed and the HFHSD-fed + metformin mice showed higher scores of hepatic steatosis, lobular inflammation, and ballooning than the CD-fed mice. Thus, the phenotype developed was associated with the diagnosis of NASH. Moreover,

HFHSD-fed mice showed higher concentrations of glucose, cholesterol, and total lipoproteins as well as higher alanine aminotransferase activities than the CD-fed mice and independently of metformin administration. Our lipidomic data showed an accumulation of hepatic cholesterol esters and a decrease in phosphatidylcholines in mice fed HFHSD and HFHSD + metformin. Moreover, we observed changes in the fatty acid composition of hepatic triglycerides and diglycerides characterized by the decrease in the polyunsaturated fatty acid content. Age-associated effects were observed mainly in the visceral and subcutaneous adipocytes. In addition, we observed that 45-week-old mice exhibited higher levels of triglycerides and diglycerides, whereas the levels of phospholipids decreased compared to 25-week-old mice independently of dietary treatment. Finally, we observed that mice receiving caloric restriction showed a reduction in body weight as well as a decrease in glucose, cholesterol, and total lipoprotein concentration, resulting in lower hepatic steatosis scores than those mice that did not receive caloric restriction. Of note, the combination of caloric restriction with metformin resulted in higher body weight reduction and better outcomes in hepatic steatosis resolution than caloric restriction alone.

CONCLUSION: Our studies show that HFHSD-fed mice develop NASH after 20 weeks of dietary treatment, and they can be a good mouse model to recapitulate the metabolic disorders observed in patients with NASH. We also found that metformin should not be used as a preventive strategy for NASH. However, this pharmaceutical compound could be useful to potentiate the metabolic effects of caloric restriction.

Financial support: The present work was supported by grants PI18/00921 and PI21/00510 and doctoral fellowship (FI1900097) from the Instituto de Salud Carlos III and co-financed by the European Social Fund (ESF) “investing in your future”.

Unió Europea
Fons Social Europeu
L’FSE inverteix en el teu futur

UNIVERSITAT ROVIRA I VIRGILI
EXPLORING LIVER AND ADIPOSE TISSUE ALTERATIONS IN THE NATURAL COURSE OF NON-ALCOHOLIC FATTY LIVER DISEASE: A LIPIDOMIC
Gerard Baiges Gaya

JUSTIFICATION

UNIVERSITAT ROVIRA I VIRGILI
EXPLORING LIVER AND ADIPOSE TISSUE ALTERATIONS IN THE NATURAL COURSE OF NON-ALCOHOLIC FATTY LIVER DISEASE: A LIPIDOMIC
Gerard Baiges Gaya

Obesity is a metabolic disease that increases the risk of developing cardiovascular disease, type 2 diabetes, fatty liver, musculoskeletal disorders, and several cancers. In the last decades, the prevalence of obesity worldwide has increased from 4.7% to 13.1% (1975 – 2016). In parallel, the prevalence of non-alcoholic fatty liver disease (NAFLD) has substantially grown, affecting now up to 24% of the worldwide population. NAFLD is a complex disease that worsens over time and spans from simple steatosis (NAFL) to steatohepatitis (NASH) and fibrosis, and in the long term, a significant number of patients develop cirrhosis or hepatocellular carcinoma, requiring liver transplantation.

The degree of hepatic steatosis is largely determined by the flux of lipids entering the hepatocyte. The lipid flux is dependent on the synthesis (*de novo* lipogenesis) or uptake of lipids (lipoproteins and fatty acids) contributing to lipid input into the hepatocyte, whereas lipoprotein export and lipid oxidation determine lipid output. As a result of alterations in any of these processes, intracellular fat accumulates within the liver, causing steatosis.

In this context, white adipose tissue (AT) has been demonstrated to have a crucial role in managing lipid flux into the liver. When there is an abundant nutrient supply, the AT adapts physiologically and enlarges by hyperplasia and hypertrophy, safely storing the surplus of energy in the form of triglycerides. However, when the nutrients exceed the capacity of AT to expand, the lipid fluxes are redirected to the liver (1). Briefly, when reaching the liver, the free fatty acids are esterified into cholesterol esters and triglycerides by acyl-CoA cholesterol acyltransferases (ACATs) and diacylglycerol-O-acyltransferases (DGATs) respectively and incorporated into the hepatic lipid droplets (LDs). The synthesis of glycerophospholipids (GPs) by the endoplasmic reticulum (ER) supports the biogenesis of lipid droplets, the membranes of which are mainly composed of phosphatidylcholines (PC) (50%) and phosphatidylethanolamines (PE) (~25%). Qualitative changes in the composition of LDs surface can compromise the LDs stability, favouring/impairing the fusion of LDs. For example, the decrease in the PC:PE ratio or PC deficiency results in large LDs. Moreover, the alteration of the glycerophospholipid composition affects the synthesis of very-low-density lipoprotein particles (VLDL-p), and as a result, these VLDL are less stable and susceptible to being degraded within the liver leading to the accumulation of hepatic fat (2).

GPs biosynthesis is tightly regulated by the Kennedy pathway (*de novo* biosynthesis) when the GPs requirements are high. GPs composition and diversity are maintained through a remodelling process of de-acylation and re-acylation by the Land's cycle that compromised the coordinated action of several enzymes such as Phospholipase A_2 that catalyse the phospholipid de-acylation of fatty acid linked to the sn-2 position, lysophospholipid acyltransferases (LPLAT) that re-acylates the lysophospholipid at the sn-2 position and acyl-CoA synthetase (ACLs) that activate polyunsaturated fatty acids by the covalent union to CoA to be used by LPLATs. Interestingly, several clinical studies have provided evidence that the serum and hepatic lipidome of NASH patients is altered, suggesting that disturbances in either the biosynthetic and/or remodelling pathways of GPs could be important contributors to the natural course of NAFLD (3,4). Nevertheless, little is known about what those changes are when changes take place during the natural course of the disease and how those changes contribute (if so) to the pathophysiology of this metabolic disorder.

Thus, to characterise an accurate and robust profiling of the lipidome during the different stages of NAFLD progression may contribute to the understanding of how the different stages relate at the molecular level providing not only prognostic but also therapeutical value. On the other side, the use of mice under different nutritional and environmental challenges to recapitulate the "human disease" has enabled the dissection and discovery at the molecular level of key metabolic aspects of NAFLD and facilitates the integrative approach when considering the crosstalk and relevance of different organs to the liver disease that otherwise would not have been obtained from human samples for ethical reasons.

Considering the importance of lipid metabolism and adipose tissue function for the development of metabolic disorders, in the present thesis, we aimed to elucidating the contribution of lipids to NASH development, characterizing the hepatic and adipose tissue lipidome in the context of obesity and diabetes as well as identifying the drivers involved in the NASH resolution under caloric restriction combined with metformin. Thus, we developed a NASH mouse model using C57BL/6J male mice under a high-fat high sucrose diet (HFHSD) that recapitulates a typical American/European diet. For the

NASH resolution, we used NASH-established mice that were then switched to a standard chow diet (CD). Using this swap from HFHSD to CD in mice treated or not with metformin, we identified the synergic effects between caloric restriction and metformin and which lipid changes were involved during the resolution. In this thesis, hepatic and adipose tissue lipids have been analysed by state-of-the-art lipidomic methods (EURECAT facility), which allow the quantification of thousands of lipid species. In addition, the investigation of oxidative stress and inflammatory markers, as well as tissue histology, biochemical and lipoprotein analyses, were also done.

INTRODUCTION

UNIVERSITAT ROVIRA I VIRGILI
EXPLORING LIVER AND ADIPOSE TISSUE ALTERATIONS IN THE NATURAL COURSE OF NON-ALCOHOLIC FATTY LIVER DISEASE: A LIPIDOMIC
Gerard Baiges Gaya

Chapter 1. Obesity

The pathophysiology of obesity is multidimensional and involves environmental, genetic, and psychosocial factors (5). However, ultimately body weight gain arises from disruptions in energy balance. In this context, hypertrophy and hyperplasia mechanisms lead to enlarge adipose tissue and becoming obese when body fat exceeds >25% in men and >35% in women (6).

1.1. Prevalence

The prevalence of obesity has nearly tripled since 1975. Thus, in 2016 over 650 million people globally were obese (15 % of women and 11% of men). The overall obesity prevalence increased in all world regions, although with variations among world economies. The World Bank assigns the countries' economies to four income groups - low, lower-middle, upper-middle, and high-income countries (7). Thus, as a country's per capita income increases also increases the burden of obesity, showing that obesity remains a serious health concern in high-income countries (Fig.1.).

Women's prevalence of obesity exceeds that of men's as a country's capita income decreases (9.9% of women and 3.6% of men in low-income countries), whereas sex differences disappear (24.7% of women and 24.1% of men) in high-income countries. This suggests that intrinsic-country drivers (food, social and cultural environments) of women's and men's may not be the same (Fig.1.).

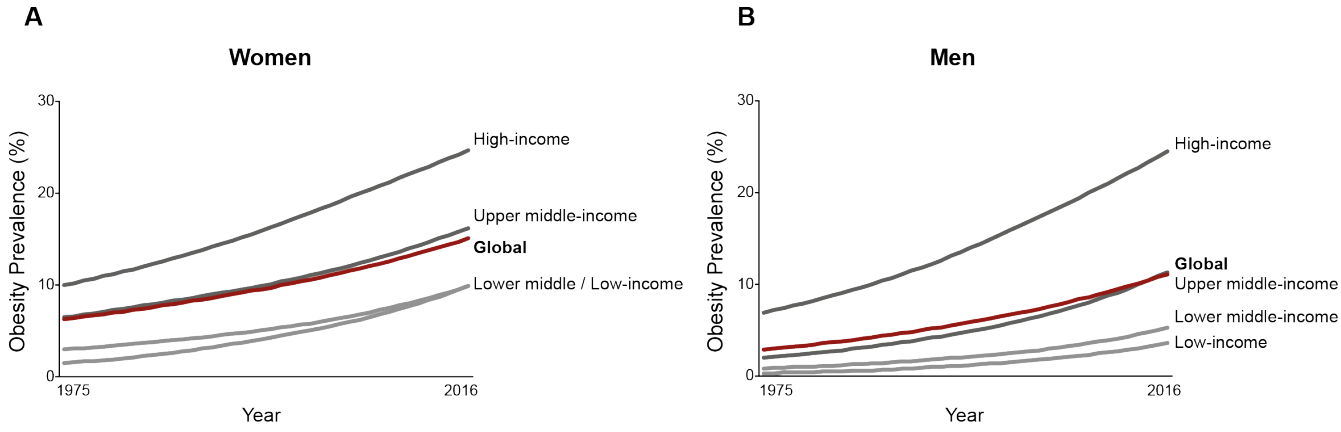

Fig.1. (**A**) Women and (**B**) men prevalence in obesity according to four income groups- low, lower-middle, upper-middle, and high-income countries. Red, dark-grey, and sky-grey lines show global, upper/high

income, and lower-low-income countries obesity prevalence, respectively, in women and men. Data collection from World Health Organization (8).

1.2 Body fat distribution

The main function of adipocytes from white adipose tissue is to store energy in the form of triglycerides and release free fatty acids according to energy-balance needs. Adipocytes are large spherical cells that store triglycerides in the form of a unilocular droplet that occupies 90% of the cell volume. White adipose tissue is in two anatomical regions of the body: visceral (omental and mesenteric) and subcutaneous (abdominal and gluteo-femoral). The functional differences in adipose tissue are observed not only between regional depots but also according to their localisation (9,10). Transcriptional profiling reveals that omental visceral (OVAT) and abdominal subcutaneous adipose tissue (ASAT) display a similar gene expression signature and are different from gluteo-femoral subcutaneous adipose tissue (GSAT), suggesting different roles in upper and lower body depots (11,12). Indeed, human studies have demonstrated that the release of nonesterified fatty acids in the overnight fasted state, as well as the triglycerides turnover, is higher in the upper body than in lower body depots. Moreover, a study published in 2010 demonstrated that lower-body depots have a preference for hydrolysis of fatty acids from very low-density lipoproteins versus chylomicrons compared to upper-body depots (13). This suggests that upper body fat is the primary site for the immediate storage of diet-derived fat (VAT and ASAT), whereas GSAT (lower body depot) is a site for long-term storage. Indeed, the enlargement mechanisms of adipose tissue also differ among depot sites. In this sense, upper body fat has a preference for hypertrophy growth (adipocyte size), while lower body fat shows evidence of hyperplasia (adipocyte number).

During the development of obesity, not all fat accumulation contributes to metabolic complications. Thus, obese people with an upper-body fat distribution pattern tend to have an increase in the likelihood of insulin resistance (IR) by 80%, whereas a preference for fat accumulation in GSAT decreases the likelihood of IR by 48%. Therefore, the preferential enlargement of upper body fat correlates with cardiometabolic risk (14) and NAFLD progression (15).

1.2. Adipose tissue as a secretory organ

In addition to the importance of white adipose tissue to store the excess energy supply in the form of triglycerides, it also acts as an endocrine organ that secretes a wide range of bioactive proteins. These molecules collectively termed adipokines, include the following: cytokines and related proteins [leptin, tumour necrosis factor-alpha, TNF--α, interleukin-6, IL-6, and chemokine (C-C motif) ligand 2, CCL2]; proteins of the fibrinolytic cascade (plasminogen activator inhibitor- 1, PAI1); complement-related proteins such as adiponectin, and other biologically active peptides such as omentin, retinol-binding protein 4 (RBP4) and vaspin (10,16). The secreted adipokine profile is not only affected by the degree of adiposity but also by body fat distribution. Therefore, people with gynoid fat distribution (lower body fat accumulation) display an adipokine profile characterised by insulin-sensitiser and anti-inflammatory properties, which in turn are associated with metabolically healthy obesity. On the other side, preferences in android distribution (upper-body fat accumulation) display adipokines profiles related to insulin resistance and pro-inflammatory response, contributing to metabolically unhealthy obesity

For example, in GSAT the secreted levels of leptin and adiponectin are higher than in upper-body fat, which is associated with insulin sensitivity. However, adipokines such as RBP4 and PAI1 are primarily secreted by the upper body fat and increase insulin resistance and the risk of thrombotic disorders, respectively (Table 1).

Table 1. Sources and functions of key adipokines.

Adipokine	Primary source(s)	Depot region	Changes in MUHO	Function
Adiponectin	Adipocytes	Lower body	Low	Insulin sensitizer, anti-inflammatory
CCL2	Preadipocytes, macrophages	Upper body	High	Monocyte recruitment
IL-6	Preadipocytes, macrophages, adipocytes	Upper body	High	Insulin resistance
Leptin	Adipocytes	Lower body	High	Appetite control
Omentin	Stromal vascular cells	Upper body	Low	Insulin sensitizer, anti-inflammatory

PAI1	Preadipocytes	Upper body	High	Insulin resistance, pro-thrombotic
RBP4	Preadipocytes, adipocytes	Upper body	High	Implicated in systemic insulin resistance
TNF-α	Preadipocytes, macrophages, and adipocytes	Upper body	High	Inflammation, antagonism of insulins signalling
Vaspin	Adipocytes	Upper body	High	Insulin sensitizer

CCL2: chemokine (C-C motif) ligand 2; IL: interleukin; PAI-1: plasminogen activator inhibitor- 1; MUHO: metabolically unhealthy obesity; RBP4: retinol-binding protein 4; TNF: tumour necrosis factor.

1.3. Obesity associated complications

As discussed above, the white adipose tissue is the primary organ for lipid storage and can enlarge as a response to an abundant nutrient supply. The expansion of adipose tissue is a process that involves the mechanisms of hyperplasia and hypertrophy. Thus, during adipogenesis (hyperplasia), new adipocytes are recruited by differentiation from preadipocytes, providing the adipose tissue with more capacity to uptake the excess lipids, while hypertrophy increases the lipid storage into existing adipocytes. However, the adipogenesis process in upper body fat is limited and therefore depends on hypertrophy, which has a finite storage capacity. During adipose tissue expansion, the extracellular matrix is remodelled to guarantee safe expansion; however, in the long term the adipose tissue becomes dysfunctional, generating an environment with insulin resistance and higher rates of lipolysis (17). Thus, dysfunctional adipocytes produce a wide range of NFκB-dependent cytokines that enhance the inflammatory response (18–20). The increase of pro-inflammatory cytokines such as TNF-α results in the increase of lipolysis, which drives the free fatty acids fluxes to the bloodstream and the liver (21). Additionally, the uptake of diet-derived lipids (chylomicrons) by the adipose tissue is impaired, forming a vicious positive feedback loop of lipid fluxes to peripheral tissues (22,23). Moreover, the increase of upper-body fat mass results in changes in adipokines profile secretion, such as the reduction of adiponectin. Indeed, it has been reported that adiponectin is able to inhibit the hepatic *de novo* lipogenesis, stimulates the oxidation of free fatty acids as well as ameliorates insulin sensitivity (23). Therefore, dysfunctional adipose tissue potentiates adverse metabolic outcomes, which can lead to the risk of suffering dyslipidaemia, type 2 diabetes, and NAFLD.

Chapter 2. Non-alcoholic fatty liver disease

Fatty liver disease was first described in 1836 by the English physician and scientist Thomas Addison, although he reported cases of fatty liver related to excessive alcohol intake. In 1860, Friedrich von Frerichs, a German physician, and pathologist, described the link between dietary habits and fatty liver, and Ludwig J. *et.a.l* described the term non-alcoholic steatohepatitis as a progressive form of fatty liver disease in 1980 (24,25).

2.1 Non-alcoholic fatty liver disease spectrum

NAFLD encompasses a spectrum of diseases that starts with non-alcoholic fatty liver (NAFL), which is defined as the presence of >5% lipid accumulation within hepatocytes and affects over 25% worldwide population. If the lipid accumulation is chronic in time results in the accumulation of toxic lipid species. This type of lipid species might produce endoplasmic stress, oxidative stress, and mitochondrial dysfunction, resulting in inflammation and hepatocyte degeneration (ballooning), which are characteristic of non-alcoholic steatohepatitis (NASH) (26). The prevalence of NASH is estimated at 60% among biopsied NAFLD patients, and over time 41% of patients with NASH develop fibrosis, 22% of patients with advanced fibrosis progress to cirrhosis, and over 2% of patients with cirrhosis develop hepatocellular carcinoma within three years (26,27) (Fig.2.).

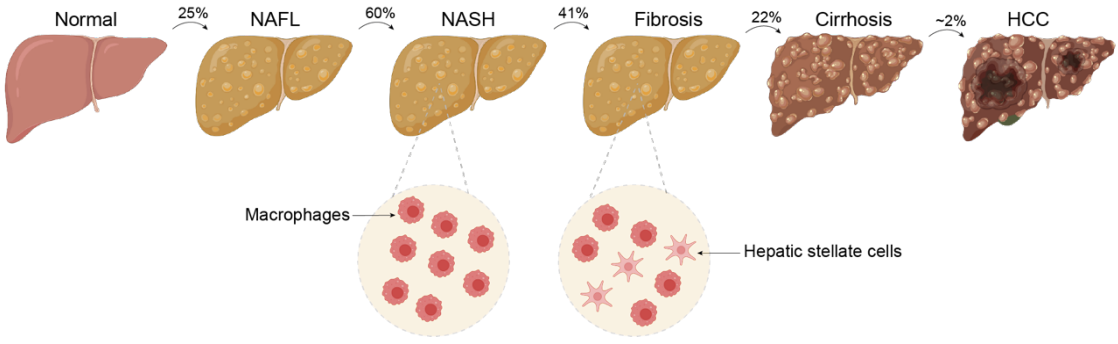

Fig.2. NAFLD disease spectrum.

HCC, hepatocellular carcinoma; NAFL: non-alcoholic fatty liver; NASH: non-alcoholic steatohepatitis. Illustration adapted from Ferguson D *et.al* (26).

2.1 The pathophysiology of non-alcoholic fatty liver disease

Lipidomic studies show that the initial hepatic lipid accumulation occurs when the liver's capacity to use, store, and export lipids are overwhelmed by the increase of free fatty acids fluxes from adipose tissue and, therefore, lipids are stored in the form of triglycerides that are considered inert by hepatic cells. However, as liver disease advances from simple steatosis (NAFL) to NASH, it results in the accumulation of toxic lipid species. This includes diglycerides (28), saturated fatty acids (29), ceramides (30), and free cholesterol (31). Moreover, these disorders have been associated with the deficiency of essential lipid species for cell viability, such as phospholipids and unsaturated fatty acids. Indeed, excessive levels of toxic lipids might promote endoplasmic reticulum stress, oxidative stress, and mitochondrial dysfunction. Therefore, the profile of lipid accumulation in the liver might be determinant in the progression of the disease, which in turn will also depend on the systemic metabolic environment, genetic background, dietary pattern, and exercise.

In this sense, subjects with obesity overfeeding with saturated fatty acids and carbohydrates tend to have increased hepatic lipid deposition compared to subjects feeding with unsaturated fat. Additionally, the saturated fatty acid overfeeding increases the toxic lipid species such as ceramides, which were associated with increased insulin resistance (29). Therefore, saturated dietary-enriched patterns might interact with hepatic lipidome increasing the risk of suffering NAFLD and type 2 diabetes, whereas preferences in monounsaturated and polyunsaturated fatty acids can help in the prevention of these metabolic disorders (32).

Indeed, subjects with NASH have alterations in elongase and desaturase enzymes involved in the synthesis of long-chain and very-long-chain fatty acids, resulting in the increase of saturated and significant decrease in polyunsaturated fatty acids (33). This suggests that hepatic lipotoxicity is not only related to the amount of lipids but also to the qualitative aspect of lipids.

Chapter 3. Lipotoxicity

The excessive accumulation of toxic lipids may alter the normal function of intracellular organelles, such as the endoplasmic reticulum (ER) and mitochondria (34).

3.1. Endoplasmic reticulum stress

Hepatic ER stress occurs under exposure to high levels of saturated fatty acids (predominantly palmitic acid and stearic acid). In this context, the chaperone protein glucose-regulated protein 78 (GRP78) is released by ER, resulting in the activation of inositol-requiring enzyme-1α (IRE1α), PRKR-like endoplasmic reticulum kinase (PERK), and activating transcription factor-6 (ATF6) (35). Thus, IRE1 mediates the activation of TRAF2, a protein of the TNF receptor superfamily, and Jun-N-terminal kinase1/2 (JNK1/2), a critical mediator of insulin resistance and hepatic cell death. Additionally, PERK and ATF result in the activation of CCAAT-enhancer-binding protein homologous protein (CHOP), which is involved in the apoptotic pathway (Fig.3.) (35).

Of note, mice with the deletion of gene encoding stearoyl-CoA desaturase-1 (SCD1), which is involved in the conversion of saturated to monounsaturated fatty acids, showed an increase in hepatic CHOP levels as a result of the ER stress (36).

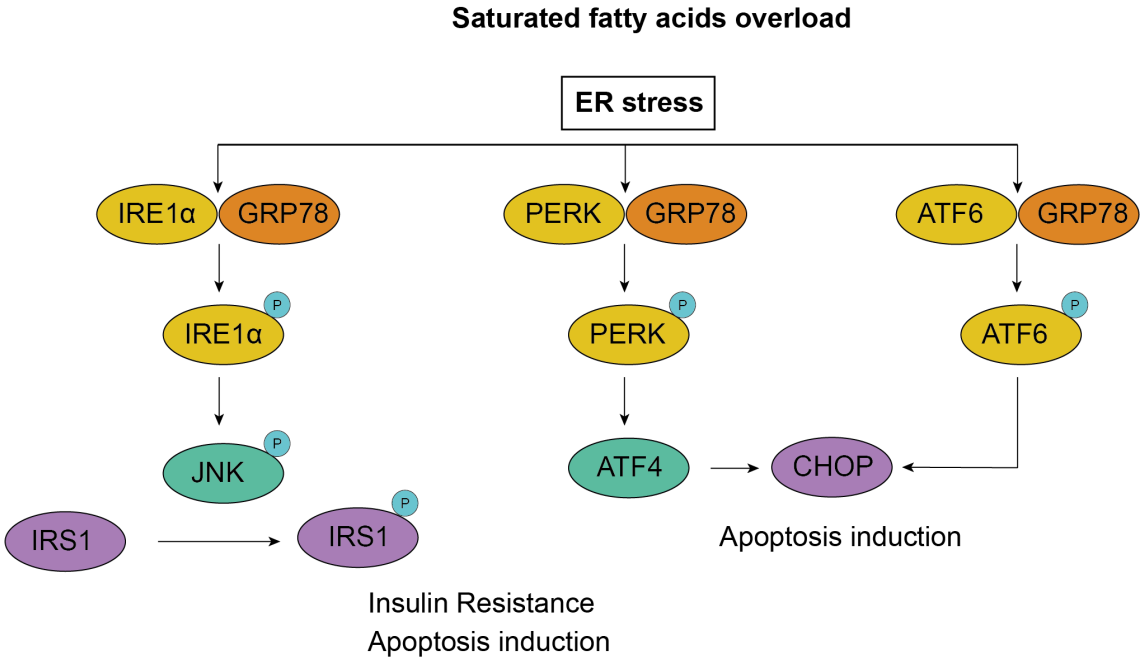

Fig.3. Endoplasmic reticulum stress signalling.

ATF: activating transcription factor; CHOP: CCAT-enhancer binding protein homologous protein; ER: endoplasmic reticulum; GRP78: chaperone protein glucose-regulated protein 78; IRE1α: inositol-requiring-enzyme 1α; JNK: Jun-N-terminal kinase; PERK: PRKR-like endoplasmic reticulum kinase.

3.2. Mitochondrial dysfunction

In normal conditions, free fatty acids are transferred to the mitochondria via carnitine palmitoyl transferase 1 (CPT1). Fatty acids are oxidised in the mitochondrial matrix, breaking down acyl-CoA to form acetyl-CoA and then being metabolised in the tricarboxylic acid cycle (TCA). This catabolic process that involves the electron transport chain generates H_2O. However, the impairment of the electron transport chain leads to a leakage of electrons and a subsequent increase of superoxide ($O_2^{\cdot}$) and hydrogen peroxide (H_2O_2). Alternatively, the long-chain fatty acids may be oxidised in the peroxisomes, but the peroxisomal B-oxidation produces H_2O_2, which is transformed into hydroxyl radical ($HO^{\cdot}$). Thus, the excessive levels of reactive oxygen species (ROS) result in the peroxidation of polyunsaturated fatty acids, which are transformed into 4-hydroxy-2-nonenal (4-HNE) and malondialdehyde (MDA). Indeed, these highly reactive aldehyde compounds increase in patients with NASH compared to patients with simple steatosis (37,38). Of note, another feature of NASH is the reduction in the activity of antioxidant enzymes such as catalase (39), glutathione peroxidase, and superoxide dismutase (40).

In this context, the oxidative stress environment in the liver leads to the increase of dysfunctional mitochondria. The autophagy process is involved in the quality control of organelles, eliminating those that are damaged or dysfunctional. However, chronic exposure to saturated fatty acids decreases the autophagy process, resulting in autophagosomes accumulation and damaged mitochondria (41,42).

Indeed, the deletion in mice of Atg7 or Atg14 genes involved in the autophagy machinery increased the hepatic steatosis and cholesterol content. This suggests that the impairment in the autophagy process can promote NAFLD (43). Of note, patients with NASH showed an increase in hepatic p62 protein compared to NAFL patients, evidencing the importance of autophagy in human disease (44).

Chapter 4. Lipoprotein metabolism

Cholesterol, cholesterol esters, and triglycerides are the main lipids in plasma, and they are transported through lipoproteins. These lipoproteins play an important role in the transport of dietary lipids, in the transport of lipids from the liver to peripheral tissues, and the transport of lipids from peripheral tissues to the liver (45).

The apolipoprotein B (ApoB100 and 48) is the main component of all atherogenic lipoproteins (chylomicrons, very-low-density lipoproteins, VLDL, intermediate density lipoproteins, IDL, and low-density lipoproteins, LDL) (Fig.4.), whereas apo A-I and apo-AII are components of high-density lipoproteins (HDL).

Table 2. Lipoprotein classes properties

Lipoprotein	Density (g/mL)	Size (nm)	Major lipids	Major apoproteins
Chylomicrons	<0.930	75-1200	TG	Apo-B48, Apo C, Apo E, Apo A-1, A-II, A-IV
Chylomicron remnants	0.930 – 1.006	30-80	TG, Chol	Apo B-48, Apo E
VLDL	0.930 – 1.006	30-80	TG	Apo B-100, Apo E, Apo C
IDL	1.006 – 1.019	25-35	TG,Chol	Apo B-100, Apo E, Apo C
LDL	1.019 – 1.063	18-25	Chol	Apo B-100
HDL	1.063 – 1.210	5-12	Chol	Apo A-I, Apo A-II, Apo C, Apo E

Apo: apolipoproteins; Chol: cholesterol; HDL: high density lipoprotein; IDL: intermediate density lipoproteins; LDL: low density lipoprotein; TG: triglyceride; VLDL: very low-density lipoprotein.

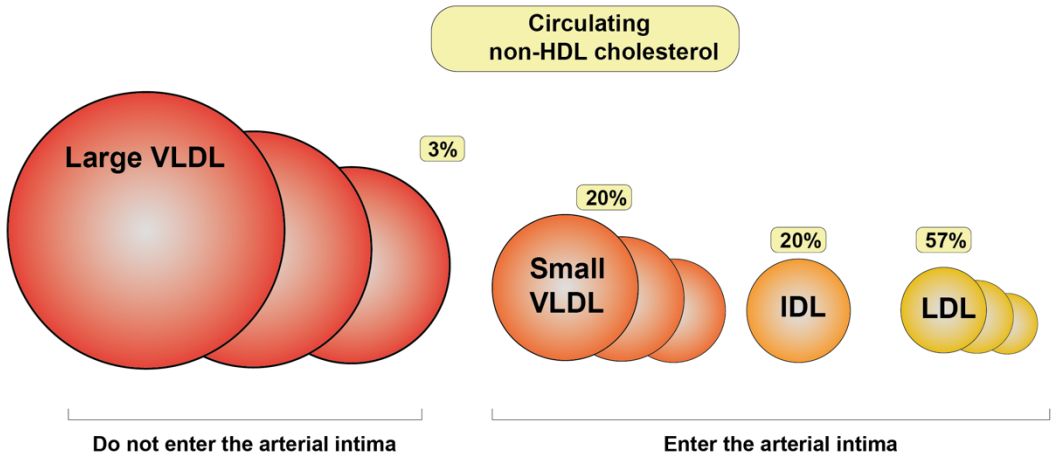

Fig.4. Apo-B containing lipoproteins

IDL: intermediate density lipoproteins; LDL: low density lipoproteins; VLDL: very low-density lipoproteins. Adapted from Holmes. MV *et.al* (46).

4.1 Chylomicrons

Dietary fatty acids are transported by chylomicrons via the intestinal lymphatic system and enter the bloodstream in the left subclavian vein. During circulation, triglycerides are removed in peripheral tissues. After that, chylomicrons are cleared from circulation by the liver via apo E receptors (47).

4.2. Very-low density lipoprotein and low-density lipoprotein metabolism

VLDL particles are syntesized in the liver (ER), where hepatic cholesterol and triglycerides are packaged into apoB-containing VLDL particles and then are secreted in the bloodstream to supply triglycerides to peripheral tissues such as adipose tissue and skeletal muscle (48). The triglyceride hydrolysis from VLDL results in the formation of IDL, wich are enriched in cholesterol esters and acquire Apo E from HDL. In this context, the liver removes 50% of IDL particles from circulation. The rest of IDL undergoes triglyceride hydrolysis by hepatic lipase leading to a decrease in the content of triglycerides, which leads to the formation of LDL. After that, LDL particles are cleared via the LDL receptor in the liver (49,50).

4.3 High-density lipoprotein metabolism and reverse cholesterol transport

Peripheral tissues accumulate cholesterol through the uptake of circulating lipoproteins and *de novo* cholesterol synthesis. However, they do not have mechanisms for cholesterol metabolization. Thus, the HDL particles play a crucial role in the uptake of cholesterol from peripheral tissues. The core of cholesterol esters in HDL particles can be transferred to the liver via SR-BI receptors. Alternatively, the cholesteryl ester transfer protein (CETP) can transfer cholesterol from HDL particles to Apo-B containing lipoproteins, and then they are degraded by the liver via the LDL receptor (51,52). This cholesterol can be converted to bile acids, steroid hormones, or esterified in cholesterol esters and incorporated into the lipid droplet.

Chapter 5. Lipid metabolism

5.1. Fatty acid synthesis

Many lipids are synthesised from fatty acids, which can vary in chain length and in degrees of unsaturation. Moreover, fatty acids are major components of triglycerides, phospholipids, cholesterol esters, and other complex lipids. Hepatic fatty acids derive either from exogenous sources or from *de novo* lipogenesis. The liver is supplied with non-esterified fatty acids (NEFAs) from two sources: The major contribution comes from adipose tissue (lipolysis), while the diet-derived triglycerides (chylomicrons) represent a smaller contribution. Then, NEFAs are transported across the plasma membrane, mainly via fatty-acid binding protein (FABP), caveolins, and fatty acid translocase (CD36) to enter the hepatocyte. On the other side, hepatic *de novo* lipogenesis uses Acetyl-CoA (from glycolysis) to generate malonyl-CoA and then palmitoyl-CoA by acetyl-CoA carboxylase and fatty acid synthase, respectively. The palmitoyl-CoA is then elongated and desaturated to produce molecules of various lengths and degrees of saturation (Fig.5.) (53).

SCD1 enzyme catalyses the introduction of the first double bond in the *cis*-delta-*9* position of several saturated fatty acids, mainly palmitoyl-CoA and stearoyl-CoA, to generate palmitoleoyl-CoA and oleoyl-CoA, respectively (54). Humans cannot synthesise polyunsaturated fatty acids. Thus, linoleic (18:2) and alpha-linolenic (18:3) acids must be obtained from the diet. Once absorbed, the essential fatty acids are activated by acyl-CoA synthetase through the covalent union to CoA to be converted (by desaturase and elongase activities) into long-chain polyunsaturated fatty acids such as arachidonic acid (20:4) (55). After that, arachidonic acid can be used to increase the degree of unsaturation of phospholipids or metabolised in inflammatory mediators (56).

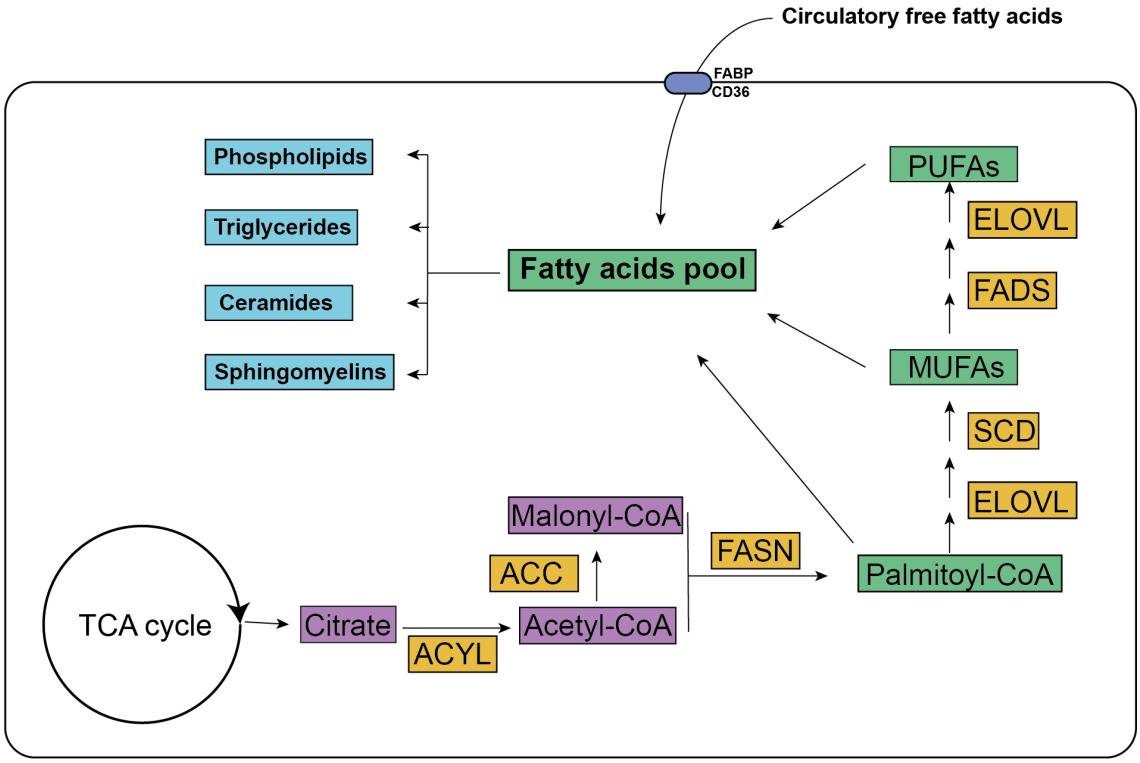

Fig.5. Fatty acid synthesis and uptake

ACC: Acetyl-CoA carboxylase; ACYL: ATP-citrate synthase; CD36: fatty acid translocase; ELOVL: elongation of very long chain fatty acids; FABP: fatty acid binding protein; FAD: fatty acid desaturase; FASN: fatty acid synthase; MUFAs: monounsaturated fatty acids PUFAs: polyunsaturated fatty acids; SCD: stearoyl-CoA desaturase; TCA: tricarboxylic acid.

5.2. Neutral lipids synthesis

Triglycerides and cholesterol esters are the major lipids that are stored in the hepatic lipid droplets or secreted in lipoprotein particles. Thus, hepatic long-chain fatty acids are esterified to glycerol-3-P and to free cholesterol to generate triglycerides and cholesterol ester, respectively. Different enzymes are involved in each case, all restricted to the ER. Triglycerides are the product of diacylglycerol acyltransferases (DGAT1 and DGAT2), which catalyse the acylation of a diglyceride, while cholesterol esters are made by acyl-CoA: cholesterol O-acyltransferases (ACAT1 and ACAT2) (57). Of note, the most abundant fatty acids esterified to triglycerides are oleate (C18:1n9), palmitate (C16:0), and linoleate (C18:2n6), resulting around 85% of all triglycerides. The next most abundant are palmitoleate (C16:1n7), stearate (C18:0), and vacceneate (C18:1n7), which in turn account for a further 8% of free fatty acids (58).

The lipid droplet is the main storage for neutral lipids, but the number, size, and composition can vary according to the metabolic state of the cell (59). Despite varying morphologically, all lipid droplets have a similar structural organization. Thus, lipid droplets are surrounded by a phospholipid monolayer that encloses triglycerides and cholesterol esters mainly. The lipid droplet biogenesis emerges from the ER. Thus, the triglycerides and cholesterol esters are deposited between the leaflets of the ER bilayer. Then, seipin protein, a membrane protein, and other lipid droplet biogenesis factors are recruited to the lens structure and facilitate the growth of the nascent lipid droplet.

After that, the expansion of the neutral lipid lens results in the lipid droplet budding from the ER membrane. Indeed, in this step, the composition of the phospholipid monolayer is critical for lipid droplet budding, which can lead to membrane instability (59). After budding, the lipid droplet expands, which occurs with the fusion of lipid droplets through the transfer of neutral lipids from ER membrane to the lipid droplet, or through the synthesis of triglycerides on the lipid droplet surface. In this context, new phospholipids are recruited to expand the lipid droplets. In parallel, proteins with functions such as membrane trafficking and protein degradation are recruited. The lipid-droplet-associated proteins can be divided into two classes: 1) Proteins that are recruited from the ER (Class I proteins), and 2) proteins recruited from the cytosol (Class II proteins). For example, ER-associated protein degradation (ERAD) belongs to class I proteins, and is involved in recognising, extracting, and ubiquitinate proteins for their clearance (60). On the other side, the class II proteins are recruited to the surface of lipid droplets, which are involved in recognising and restoring packing defects in the phospholipid monolayer. In contrast to bilayers, phospholipids monolayers are prone to exhibit packing defects, particularly under high surface tensions (61,62).

The lipid droplets can interact with different organelles such as ER, other lipid droplets, mitochondria, lysosomes, and peroxisomes (63):

<u>Lipid droplet-ER contacts:</u>

Around 85% of lipid droplets in mammalian cells remain in contact with ER but not tethered.

Lipid droplet-lipid droplet contact:

As mentioned above, the lipid droplets in mammalian cells can expand through the fusion of two lipid droplets mediated by cell death-inducing DFA-like effector (CIDEA).

Lipid droplet-mitochondria contact:

Under nutrient deprivation, the mitochondria obtain the fatty acids from lipid droplets for the energy production via β-oxidation and the citric acid cycle.

Lipid droplet-lysosome contact:

It has been observed both prolonged and short interaction between lipid droplets and lysosomes, resulting in the hydrolysis of triglycerides and cholesterol esters.

Lipid droplet-peroxisome contact:

In humans the β-oxidation occurs in mitochondria; however, the β-oxidation of very-long chain fatty acids and branched fatty acids occurs in the peroxisomes.

5.3. Glycerophospholipid biosynthesis.

The glycerophospholipid phosphatidylcholine (PC) is the most abundant phospholipid in mammalian cells, comprising 40-50% of total phospholipids, followed by phosphatidylethanolamine (PE), phosphatidylserine (PS), sphingomyelin (SM), cardiolipin (CL), and phosphatidylinositol (PI) (Table 2). The phospholipid biosynthesis is required for the normal secretion of very-low-density particles (VLDL-p), lipid droplet formation, and mitochondrial function. Therefore, alterations in the biosynthesis of phospholipids are associated with metabolic disorders, including NAFLD.

Table 2. Phospholipid composition in mammalian organelles (% of total phospholipids).

Lipid	ER	IMM	OMM	Lysosomes	Nuclei	Golgi	Plasma membrane
PC	57	41	49	42	52	45	43
PE	21	38	34	21	25	17	21
SM	4	2	2	16	6	12	23
PI	9	2	9	6	4	9	7
PS	4	1	1	1	6	4	4
CL	0	16	5	0	0	0	0
Other	5	<1	<1	14	7	13	2

CL: cardiolipin; ER: endoplasmic reticulum; IMM: inner mitochondrial membrane; OMM: outer mitochondrial membrane; PC: phosphatidylcholine; PE: phosphatidylethanolamine; PI: phosphatidylinositol; PS: phosphatidylserine; SM: sphingomyelin.

5.3.1. Phospholipid precursor biosynthesis

The phospholipid biosynthesis requires a diglyceride unit in the form of CDP-diglyceride or diglyceride. These two precursors are generated from phosphatidic acid. Briefly, glycerol-3-phosphate is transformed into lysophosphatidic acid by glycerol-3-phosphate acyltransferase. Then, lysophosphatidic acid is converted into phosphatidic acid (PA) by acyltransferase activities that are restricted to the ER and outer mitochondrial membrane. After that, the enzyme phosphatidic acid phosphatase removes the inorganic phosphate from PA to yield diglyceride. Alternatively, the CDP-diglyceride is obtained from the reaction between CTP and phosphatidic acid by CDP-diglyceride synthase (64).

5.3.2 Phosphatidylcholine de novo biosynthesis from diglycerides

The de novo biosynthesis of PC and PE, also called the Kennedy pathway, was described by Kennedy and Weiss in 1956 (65). The synthesis of PC requires that choline enters the cell through choline transporters. These include high-affinity transporter (CHT1), intermediate-affinity transporters (CTL family), and low-affinity organic cation transporters (OCT family). Then, choline is phosphorylated by ATP to form phosphocholine by choline kinase (CK). After that, phosphocholines and cytidyl triphosphate (CTP) are converted to CDP-choline via the CTP: posphocholine cytidylyltransferase (CT). Finally, the CDP-choline is transferred in the ER to a diglyceride, thereby generating PC (66,67).

On the other side, the liver can also use an additional pathway for the synthesis of PC. In this sense, the phosphatidylethanolamine N-methyltransferase (PEMT) catalyses three methylation reactions to convert PE to PC, using the S-adenosylmethionine as the methyl-group donor. Thus, this pathway is considered to provide ~30% of PC in the liver (68,69).

5.3.3. Phosphatidylethanolamine de novo biosynthesis from diglycerides

The main pathways used by mammalian cells for the biosynthesis of PE are the *Kennedy pathway* and the phosphatidylserine decarboxylase (PSD) pathway. Briefly, in the Kennedy pathway, ethanolamine is phosphorylated to phosphoethanolamine by ethanolamine kinase (EK), a cytosolic protein. CTP-phosphoethanolamine cytidylyltransferase (ET) converts phosphoethanolamine and CTP to CDP-ethanolamine, which is then transferred with a diglyceride to generate PE in the ER (70).

The other important pathway for the synthesis of PE is the decarboxylation of phosphatidylserine (PS). The PS synthesis is made by a base-exchange reaction from either PC (via PS synthase-1) or PE (via PS synthase-2) in the ER membranes. Then, the PS is transported into mitochondria and decarboxylated to PE by phosphatidylserine decarboxylase (PSD) in the inner mitochondrial membrane. Of note, mice with the deletion of the PSD gene have embryonic lethality, whereas a PSD reduction activity by 20% increase the PC/PE molar ratio in the mitochondria and impairs cell survival. This suggests that PSD activity is essential to provide PE to the mitochondrial membrane(70).

5.3.4. Phospholipid *de novo* biosynthesis from CDP-diglycerides

The phosphatidylinositol (PI), phosphatidylglycerol (PG), and cardiolipin (CL) biosynthesis are made from CDP-diglycerides. Briefly, the PI synthase (PIS) catalyses the reaction between CDP-diglycerides and myo-inositol in the ER to generate PI. Alternatively, the phosphatidylglycerol-phosphate (PGP) synthase (PGPS) can generate PGP from the reaction between glycerol-3-P and CDP-diglyceride. Then, the dephosphorylation of PGP by PGP-phosphatase results in the synthesis of PG. Finally, the synthesis of CL is required that a PG unit be combined with a CDP-diglyceride molecule, catalysed by cardiolipin synthase(CLS)(64).

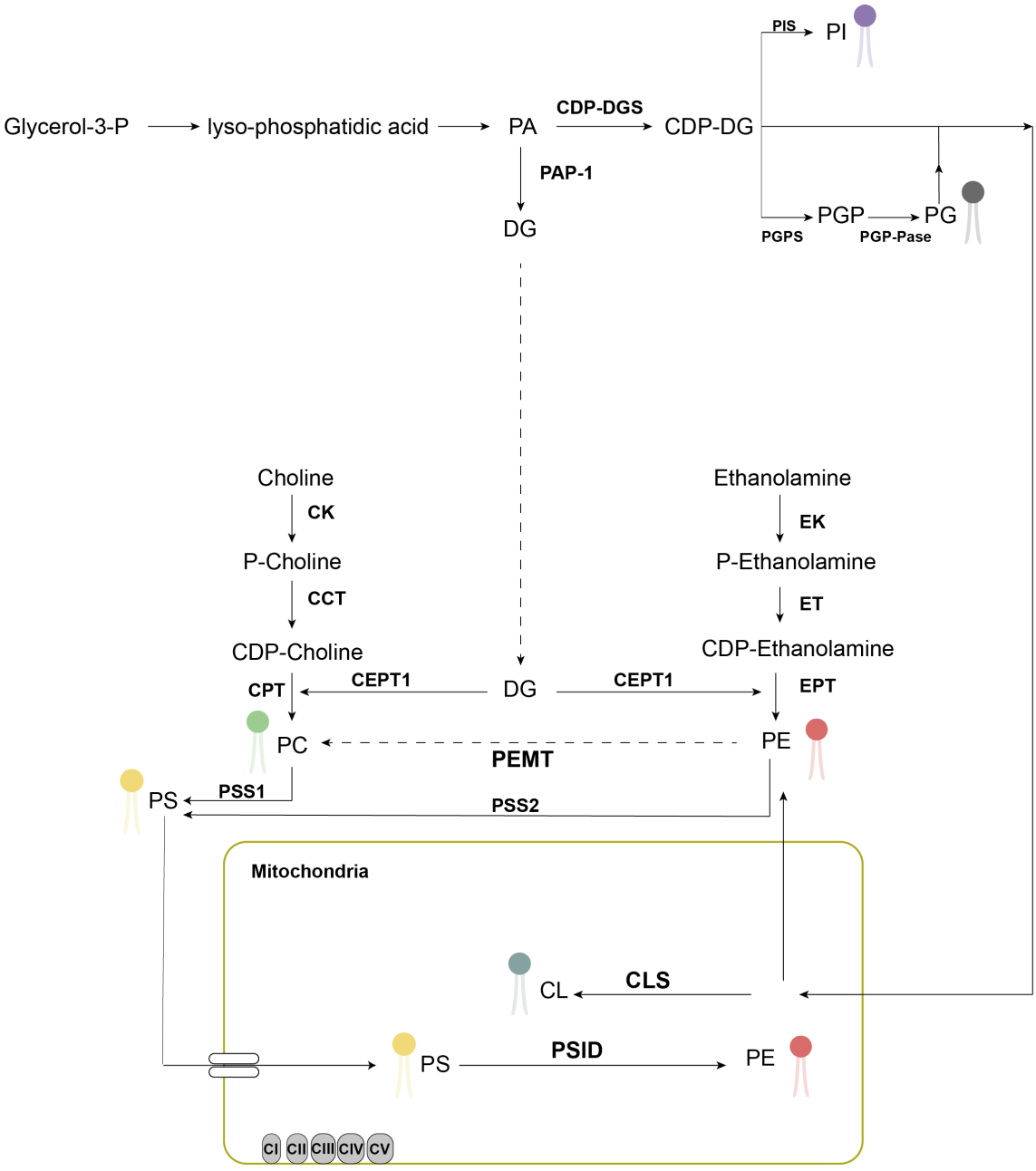

Fig.6. Phospholipid biosynthesis.

CCT: cytidyltransferase; CK: choline kinase; CL: cardiolipin; CLS: cardiolipin synthase; CPT: cholinephosphotransferase; DG: diglyceride; CDP-DGS: cdp-diglyceride synthase; EPT: CDP-ethanolamine:1,2-diglyceride ethanolaminephosphotransferase; ET: ctp-phosphoethanolamine cytidylyltransferase; EK: ethanolamine kinase; PA: phosphatidic acid; PAP-1: phosphatidic acid phosphatase-1; PC: phosphatodylcholine; PE: phosphatidylethanolamine; PEMT: phosphatidylethanolamine methyltransferase; PG: phosphatidylglycerol; PGP-Pase: phosphatidylglycerolphosphate phosphatase; PGPS: phosphatidylglycerolphosphate synthase; PI: phosphatidylinositol; PIS: phosphatidylinositol synthase PSID: phosphatidylserine decarboxylase; PS: phosphatidylserine; PSS: phosphatidylserine synthase.

Chapter 6. Phospholipid remodelling (Lands Cycle)

The phospholipids synthesised by the Kennedy pathway contain saturated and monounsaturated fatty acids. To incorporate polyunsaturated fatty in the sn-2 position of phospholipids, a phospholipase A_2 first cleaves the fatty acyl group (saturated or monounsaturated) from the sn-2 position of phospholipids to then incorporate a polyunsaturated fatty acid by lysophosphospholipid acyltransferase (LPLAT). Therefore, the Lands cycle contributes to maintaining a different content and composition of different classes of glycerophospholipids such as PA, PC, PE, PS, PI, PG, and CL (Fig.4.).

So far, there have been identified two different families of LPLATs, such as 1-acylglycerol-3-phosphate O-acyltransferase (AGPAT) and the membrane-bound O-acyltransferase (MBOAT), in which each enzyme displays distinct activities and substrate preferences (Table 3) (71).

Table 3. Lysophospholipids acyltransferase properties.

Family	Enzyme	Enzymatic activity	Substrate preference	Product
AGPAT	LPAAT	LPA	22:6-CoA	PA
	LCLAT	LCL, LPI, LPG	18:2-CoA 18:0-CoA (sn-1 position of LPI)	CL, PI, PG
	LPGAT	LPG	16:0-CoA, 18:0-CoA, 18:1-CoA	PG
	LPCAT1	LPC, LPAF, LPG	16:0-CoA, 18:2-CoA, 18:3-CoA	PAF, PG, DPPC
	LPCAT2	LPC, LPG	20:4-CoA	PAF, PC

	LPEAT	LPE, LPG, LPS, LPC	18:1-CoA, 20:4-CoA	PE, PG, PS, PC
MBOAT	LPIAT1	LPE	20:4-CoA, 20:5-CoA	PE
	LPCAT3	LPC, LPE, LPS	20:4-CoA, 18:2-CoA	PC, PE, PS
	LPCAT4	LPC, LPE	18:1-CoA	PC, PE
	LPEAT1	LPE	18:1-CoA	PE

AGPAT: 1-acylglycero-3-phosphate O-acyltransferase; CL: cardiolipin; DPPC: dipalmitoyl-phosphatidylcholine; LCL: lysocardiolipin; LCLAT: lyso-cardiolipin acyltransferase; LPAAT: lyso-phosphatidic acid acyltransferase; LPAF: lyso-platelet-activating factor; LPC: lysophosphatidylcholine; LPCAT: lysophosphatidylcholine acyltransferase; LPE: lysophosphatidylethanolamine; LPEAT: lysophosphatidylethanolamine acyltransferase; LPG: lysophosphatidylglycerol; LPGAT: lysophosphatidylglycerol acyltransferase; LPI: lysophosphatidylinositol; LPIAT: lysophosphatidylinositol acyltransferase; LPS: lyso phosphatidylserine; MBOAT: membrane bound O-acyltransferase; PA: phosphatidic acid; PAF: platelet-activating factor; PC: phosphatidylcholine; PE: phosphatidylethanolamine; PG: phosphatidylglycerol; PI: phosphatidylinositol; PS: phosphatidylserine.

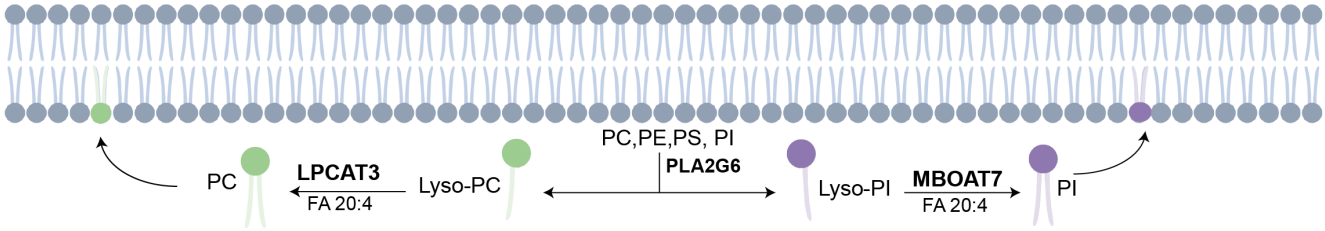

Fig.7. Phospholipid remodelling.
LPCAT3: lysophosphatidylcholine acyltransferase 3; MBOAT7: membrane bound O-acyltransferase 7; PC: phosphatidylcholine; PE: phosphatidylethanolamine; PI: phosphatidylinositol; PS: phosphatidylserine; PLA2G6; phospholipase A_2 group VI.

Chapter 7. Phospholipids regulates lipoprotein metabolism

Changes in both PC content and fatty acyl composition of phospholipids regulate the very-low-density lipoprotein particles (VLDL-p) secretion and the lipid metabolism in the liver.

Phospholipids (PC represents 70% of total phospholipids) and free cholesterol are the main lipids on the surface of lipoproteins, surrounding mainly the cholesterol esters and triglycerides. In normal conditions, the hepatic VLDL-p requires apolipoprotein B100 and PC for assembly and secretion of VLDL-p from ER lumen. Thus, when insufficient lipids are available for the formation of stable apo-B100, the excess of apo-B100 is degraded.

In this sense, the deletion of the PEMT gene in chow diet-fed mice results in a decrease in the secretion of triglycerides, apoB-100, and PC by 70%. Moreover, previous studies observed that rats fed on a choline-deficient diet had lower hepatic PC concentrations and elevated hepatic triglycerides content, while plasma triglycerides were reduced because of reduced VLDL secretion (72). Moreover, the deletion of choline kinase in mice results in lower plasma triglycerides and apoB100 because of reduced VLDL secretion (72,73).

On the other side, the fatty acyl-chain composition of PC also acts as a regulator of VLDL secretion. In normal situations, the incorporation of polyunsaturated fatty acids in the sn2-position of phospholipids contributes to maintaining membrane fluidity. Thus, the incorporation of polyunsaturated fatty acids into the membranes of ER participates in the transfer of lipids from ER to apoB100. However, deletion of hepatic LPCAT3 in mice, which incorporates the arachidonic acid in the sn-2 position of phospholipids, results in impairment of VLDL lipidation and secretion and consequently increases the hepatic triglycerides content (74). Of note, polyunsaturated fatty acids-rich membranes result in more flexible membranes that enable efficient triglycerides transfer to high-density lipoprotein.

Chapter 8. Phospholipids regulates lipid droplets

As mentioned before, lipid droplets store triglycerides and cholesterol esters to prevent the lipotoxicity of fatty acids. In normal situations, the core of lipid droplets is surrounded by phospholipids, predominantly PC and PE. Indeed, when the synthesis of PC is inhibited, the triglycerides storage increase, resulting in larger lipid droplets (75,76). This phenomenon also occurs when the content in PE increases, promoting the lipid droplet fusion of smaller droplets into larger ones (77). Therefore, the amount of PC regulates the size of lipid droplets.

On the other side, the degree of saturation of phospholipids also alters the lipid droplet dynamics. Thus, the deletion of LPCAT 1 and LPCAT2 gens in mice results in the increase of lipid droplets without altering the amount of neutral lipids (78).

HYPOTHESIS AND OBJECTIVES

UNIVERSITAT ROVIRA I VIRGILI
EXPLORING LIVER AND ADIPOSE TISSUE ALTERATIONS IN THE NATURAL COURSE OF NON-ALCOHOLIC FATTY LIVER DISEASE: A LIPIDOMIC
Gerard Baiges Gaya

Hypothesis

Disruption in the energy balance leads to alterations in AT function and expansion, which is a major factor for the liver becoming a primary organ to buffer the surplus of fat. Thus, the hypothesis under study is that during the development of NASH, the lipidome profiling of liver and adipose tissue is modified and can be reversed after caloric restriction combined with metformin. Therefore, these approaches will allow identifying the lipid alterations involved in the development and resolution of NASH as well as provide evidence about the effectiveness of metformin as a coadjuvant treatment and identify novel potential therapeutical targets for this metabolic disorder.

General Aim:

The major aim of this study is to identify the lipid signature of liver and adipose tissue, specifically in obese male mice with NASH, and the lipid changes associated with NAFLD resolution. To address these:

Aim 1:

To establish a mouse model that recapitulates the hepatic steatosis, inflammation, and oxidative stress fingerprint as observed in patients with NASH

Aim 2:

To identify the main metabolic and lipidomic drivers and mechanisms involved during NASH development.

Aim 3:

To establish the impact of ageing on the lipid signature of liver and adipocytes of mice with NASH.

Aim 4:

To determine and correlate lipid and biochemical changes associated with weight loss and NAFLD remission.

Aim 5:

To assess and evaluate the effects of metformin on NASH prevention as well as the synergic effects between caloric restriction and metformin occurring during NAFLD remission in mice.

METHODS

UNIVERSITAT ROVIRA I VIRGILI
EXPLORING LIVER AND ADIPOSE TISSUE ALTERATIONS IN THE NATURAL COURSE OF NON-ALCOHOLIC FATTY LIVER DISEASE: A LIPIDOMIC
Gerard Baiges Gaya

4.1 Ethical considerations

All animal experiments were conducted in accordance with Directive 86/609/CEE of the Council of the European Union and the Animal Ethics Committee of Rovira i Virgili University and with approval from the Directorate General of Environmental Policies and the Natural Environment of the Government of Catalonia. C57BL/6J male mice were housed 4 per cage in each experiment and were kept in a temperature-controlled environment (22 ± 2ºC) with a 12-h/12-h light-dark cycle, with "lights on" corresponding to 8 am and fed with a standard chow diet (CD), high-fat diet (HFD), high-fat high sucrose diet (HFHSD) and water *ad libitum*.

4.2 Study design

Study I

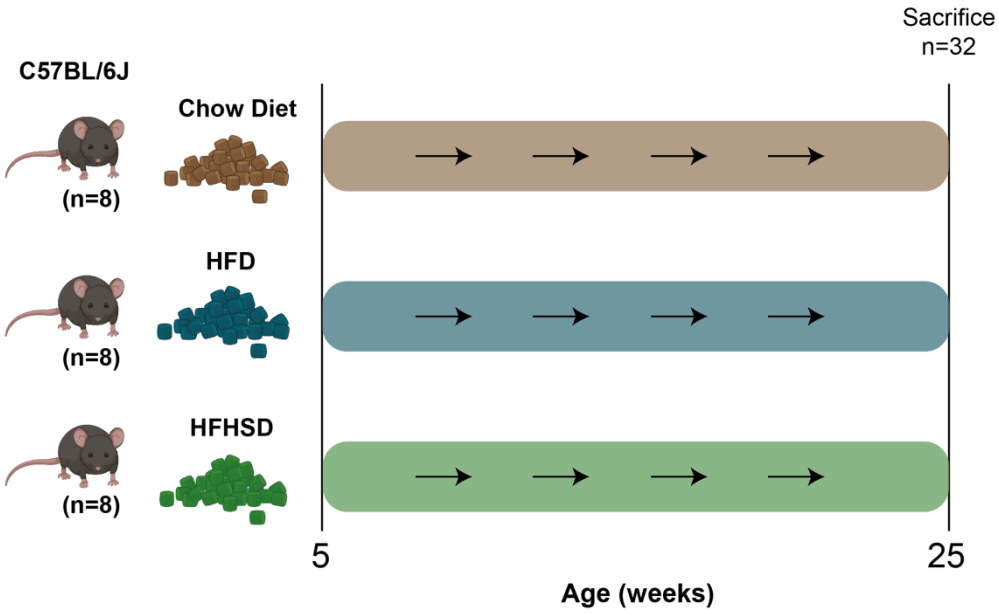

Fig.8. Study design of **Study I**

Study I was based on the hypothesis that giving mice a high-fat high-sucrose diet for 20 weeks may lead to NASH development. Blood, liver, and adipose tissue samples were collected. The efficacy of dietary treatment was analysed by examining liver histology. The inflammatory and oxidative environment in the liver was analysed by immunohistochemistry, western blot, and colorimetric assays to determine antioxidant enzyme activities. Additionally, metabolomics approaches were conducted in the liver and adipose tissue to explore the dietary metabolic response.

Study II

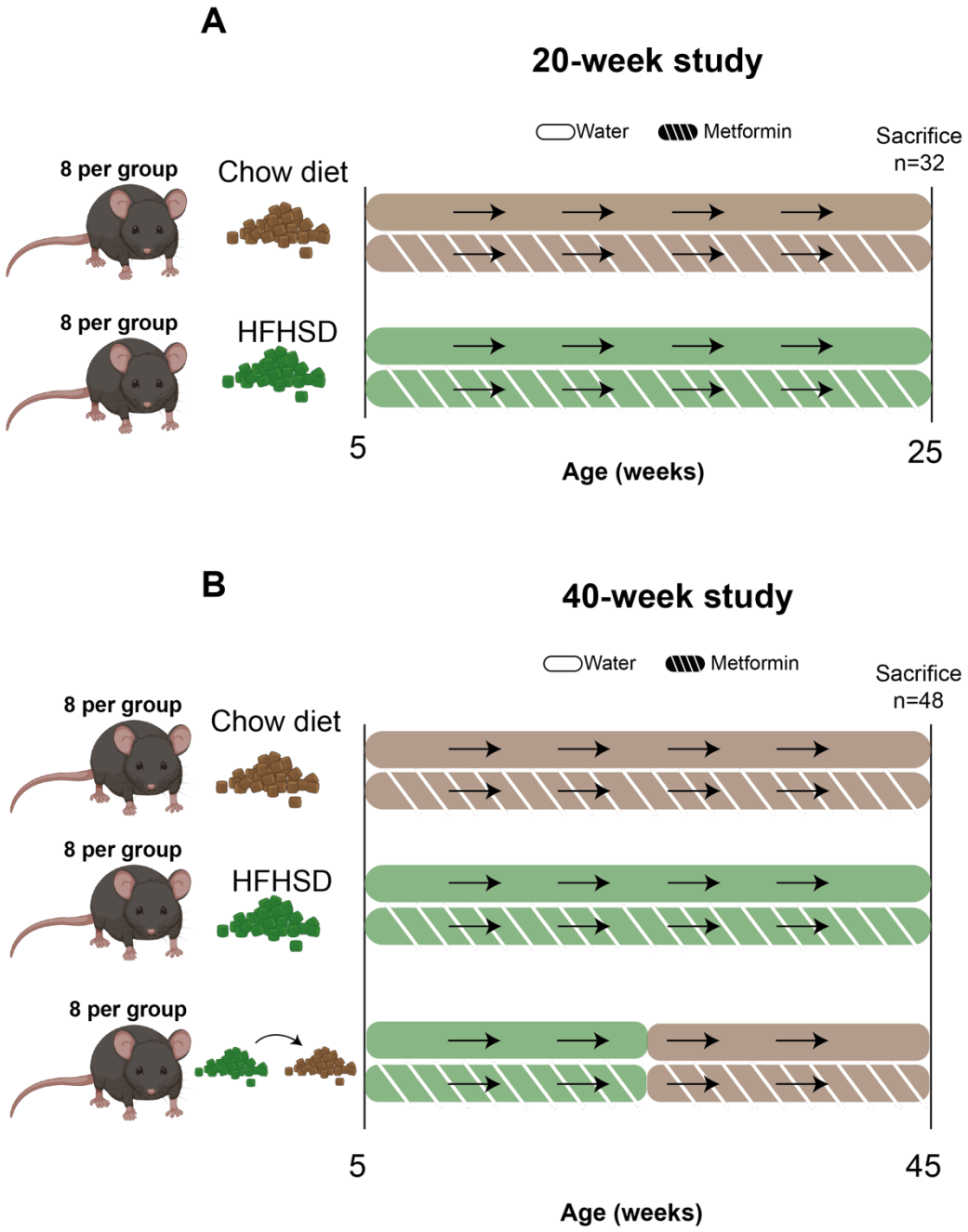

Fig.9. Study design scheme of (A) 20 and (B) 40 weeks study**.**

In **Study II**, we studied the metformin effects on NASH prevention in a 20-week experimental design (Fig 9A), while the metformin effectiveness in combination with caloric restriction was analysed in a 40-week experimental design (Fig 9B). Blood samples were collected to determine biochemical and lipoprotein profiles. Furthermore, liver and adipocytes from visceral and subcutaneous adipose tissue were collected to dissect lipid changes in the development and remission of NASH.

4.3 Statistical analysis

Study I

All data are shown as means, with error bars showing the standard error of the mean. Non-parametric Wilcoxon-rank sum test was used for comparison between the two groups. Test results with *p* values below 0.05 were considered significant. Multivariate statistics were analysed by MetaboAnalyst version 4.0. Analysis was performed, and graphs were generated using SPSS and GraphPad Prism software. Graphs and figures were edited for presentation using Adobe Illustrator CC 2020 software.

Study II

All bar plots are shown as means, with error bars showing standard deviation, whereas box plots are represented as means, with error bars showing minimum and maximum. Lollipop plots of the mean for each lipid class of experimental groups are drawn, whereas volcano plots show the statistical significance (p-value) versus the magnitude of change (fold change). Non-parametric Wilcoxon-rank sum test was used for comparison between the two groups, and *p* values below 0.05 were considered significant. Linear discriminant analysis (LDA) was used to show the lipid signature differences between groups. All bar and box plots were generated using GraphPad Prism 9 software, while lollipop, volcano, and LDA plots were generated using Jupyter Notebook written in Python code. Graphs and figures were edited for presentation using Adobe Illustrator CC 2020 software.

RESULTS

UNIVERSITAT ROVIRA I VIRGILI
EXPLORING LIVER AND ADIPOSE TISSUE ALTERATIONS IN THE NATURAL COURSE OF NON-ALCOHOLIC FATTY LIVER DISEASE: A LIPIDOMIC
Gerard Baiges Gaya

STUDY I: HEPATIC METABOLIC ADAPTATION AND ADIPOSE TISSUE EXPANSION ARE ALTERED IN MICE WITH STEATOHEPATITIS INDUCED BY HIGH-FAT HIGH-SUCROSE DIET

UNIVERSITAT ROVIRA I VIRGILI
EXPLORING LIVER AND ADIPOSE TISSUE ALTERATIONS IN THE NATURAL COURSE OF NON-ALCOHOLIC FATTY LIVER DISEASE: A LIPIDOMIC
Gerard Baiges Gaya

Journal Pre-proof

Hepatic metabolic adaptation and adipose tissue expansion are altered in mice with steatohepatitis induced by high-fat high sucrose diet

Gerard Baiges-Gaya , Salvador Fernández-Arroyo , Fedra Luciano-Mateo , Noemí Cabré , Elisabet Rodríguez-Tomàs , Anna Hernández-Aguilera , Helena Castañé , Marta Romeu , Maria-Rosa Nogués , Jordi Camps , Jorge Joven

PII: S0955-2863(20)30591-X
DOI: https://doi.org/10.1016/j.jnutbio.2020.108559
Reference: JNB 108559

To appear in: *The Journal of Nutritional Biochemistry*

Received date: 22 March 2020
Revised date: 5 October 2020
Accepted date: 21 November 2020

Please cite this article as: Gerard Baiges-Gaya , Salvador Fernández-Arroyo , Fedra Luciano-Mateo , Noemí Cabré , Elisabet Rodríguez-Tomàs , Anna Hernández-Aguilera , Helena Castañé , Marta Romeu , Maria-Rosa Nogués , Jordi Camps , Jorge Joven , Hepatic metabolic adaptation and adipose tissue expansion are altered in mice with steatohepatitis induced by high-fat high sucrose diet, *The Journal of Nutritional Biochemistry* (2020), doi: https://doi.org/10.1016/j.jnutbio.2020.108559

Highlights

- High-fat high-sucrose diets (HF-HSD) promote NAFLD and NASH in mice
- HF-HSD is associated with oxidative stress and inhibition of hepatic autophagy
- HF-HSD produces metabolic inflexibility associated with mitochondrial damage
- NASH is related to changes in adipose tissue dynamics and fatty acid accumulation

Research Paper

Hepatic metabolic adaptation and adipose tissue expansion are altered in mice with steatohepatitis induced by high-fat high sucrose diet

Gerard Baiges-Gaya[a,b], Salvador Fernández-Arroyo[a,b] Fedra Luciano-Mateo[a,b], Noemí Cabré[a,b], Elisabet Rodríguez-Tomàs[a,b], Anna Hernández-Aguilera[a,b], Helena Castañé[a,b], Marta Romeu[c], Maria-Rosa Nogués[c], Jordi Camps[a,b,*], Jorge Joven[a,b,d,*]

[a] *Universitat Rovira i Virgili, Departament de Medicina i Cirurgia, Facultat de Medicina, Reus, Spain*

[b] *Unitat de Recerca Biomèdica, Hospital Universitari de Sant Joan, Institut d'investigació Sanitària Pere Virgili, Reus, Spain*

[c] *Universitat Rovira i Virgili, Departament de Ciències Mèdiques Bàsiques, Facultat de Medicina, Unitat de Farmacologia, Reus, Spain*

[d] *Campus of International Excellence Southern Catalonia, Tarragona, Spain*

*Corresponding authors at: Unitat de Recerca Biomèdica, Hospital Universitari de Sant Joan, C. Sant Joan s/n, 43201 Reus, Spain

E-mail addresses: jcamps@grupsagessa.com (J. Camps) or jjoven@grupsagessa.com (J. Joven).

Email addresses:

GBG: gerard.baiges@iispv.cat; SFA: salvador.fernandezarroyo@gmail.com; FLM: fedra.luciano@gmail.com ; NC: ncabre@scripps.edu; ERT: elisabet.rodriguez@urv.cat; AHA: anna.hernandeza@gmail.com; HC: helena.castanev@gmail.com; MR: marta.romeu@urv.cat; MRN: mariarosa.nogues@urv.cat; JC: jcamps@grupsagessa.com; JJ: jjoven@grupsagessa.com.

Running Title: NASH and diet-induced metabolic alterations in mice

ABSTRACT

Background: Obesity is a chronic progressive disease with several metabolic alterations. Non-alcoholic fatty liver disease (NAFLD) is an important co-morbidity of obesity that can progress to non-alcoholic steatohepatitis (NASH), cirrhosis or hepatocarcinoma. This study aimed at clarifying the molecular mechanisms underlying the metabolic alterations in hepatic and adipose tissue during high-fat high-sucrose diet-induced NAFLD development in mice.

Methods: Twenty-four male mice (C57BL/6J) were randomly allocated into 3 groups (n=8 mice per group) to receive a chow diet, a high-fat diet (HFD), or a high-fat high-sucrose diet (HF-HSD) for 20 weeks. At sacrifice, liver and adipose tissue were obtained for histopathological, metabolomic, and protein expression analyses.

Results: HF-HSD (but not HFD) was associated with NASH and increased oxidative stress. These animals presented an inhibition of hepatic autophagy and alterations in AMP-activated protein kinase/mammalian target of rapamycin activity. We also observed that the ability of metabolic adaptation was adversely affected by the increase of damaged mitochondria. NASH development was associated with changes in adipose tissue dynamics and increased amounts of saturated fatty acids, monounsaturated fatty acids and polyunsaturated fatty acids in visceral adipose tissue.

Conclusion: HF-HSD led to a metabolic blockage and impaired hepatic mitochondria turnover. In addition, the continuous accumulation of fatty acids produced adipose tissue dysfunction and hepatic fat accumulation that favored the progression to NASH.

[Abstract word count: 216]

Keywords: Adipose tissue; autophagy; NAFLD; NASH; obesity; sucrose

Abbreviations:

4-HNE, 4-hydroxy-2-nonenal; ACC1, acetyl-CoA carboxylase 1; ACC2, acetyl-CoA carboxylase 2; ACLY, ATP citrate-lyase; AMPK, AMP-activated protein kinase; ATG7, autophagy-related protein 7; CA, cholic acid; CAC, citric acid cycle; CAT, catalase; CCL2, chemokine (C-C motif) ligand 2; CD, chow diet; CD11b, cluster of differentiation 11b; CD163, cluster of differentiation 163; CLEC4F, c-type lectin domain family 4; c-Jun, Jun proto-oncogene; DNL, de novo lipogenesis; F4/80, EGF-like module-containing mucin-like hormone receptor-like 1; FAH, fumarylacetoacetate hydrolase; FAO, fatty acid oxidation; FASN, fatty acid synthase; FRAP, ferric ion reducing antioxidant power; GPx, glutathione peroxidase; GR, glutathione reductase; HFD, high fat diet; HSL, hormone sensitive lipase; HF-HSD, high-fat high-sucrose diet; IDH, Isocitrate dehydrogenase; iWAT; inguinal white adipose tissue; LC3B, microtubule-associated proteins 1A/1B light chain 3B; MAPK, mitogen activated protein kinase; MFN2, mitofusin 2; mTOR, mammalian target of rapamycin; NAFLD, non-alcoholic fatty liver disease; NASH, non-alcoholic steatohepatitis; OGDH; oxoglutarate dehydrogenase; P62, sequestosome 1; PARKIN, E3 ubiquitin- protein ligase parkin; pgWAT, perigonadal white adipose tissue; PINK1, PTEN-induced putative kinase 1; PLSDA, partial least squares discriminant analysis; PON1, paraoxonase 1; PPP, pentose phosphate pathway; PUFA, polyunsaturated fatty acids; SAT, subcutaneous adipose tissue; SDHA, succinate dehydrogenase, SOD, superoxide dismutase; SFA, saturated fatty acids; TNFα, tumor necrosis factor-α; TOM20, translocase outer membrane 20; UCP-1, uncoupling protein 1; VAT, visceral adipose tissue; VIP, variable importance in projection; WAT, white adipose tissue.

1. Introduction

The prevalence of obesity has increased in recent decades and this phenomenon constitutes a serious health problem worldwide [1]. Non-alcoholic fatty liver disease (NAFLD) is an important co-morbidity of obesity. The most severe form of NAFLD is non-alcoholic steatohepatitis (NASH) which, currently, represents the main reason for liver transplantation [2]. Abnormal nutrient intake is a fundamental contributor to obesity and the related metabolic liver disease. Several studies linked the consumption of fat and sugars with the development of obesity [3,4]. However, the molecular mechanisms that can explain these effects of diets are poorly understood. The complex interactions between the liver and adipose tissue makes necessary the study NAFLD from a global metabolic perspective [5,6] since these organs are involved in the regulation of whole-body energy homeostasis, and have a great capacity of adaptation to metabolic needs. An excessive nutrient intake promotes triglyceride storage and, thereby, an increase in adipocyte size of white adipose tissue (WAT) while maintaining homeostasis. However, there is a large variation in adipocyte metabolism within and between individuals [7–9]. Subcutaneous adipose tissue (SAT) represents around 80% of WAT and constitutes the main reservoir of lipid storage. The magnitude of adiposity is influenced by the growth potential of adipose cells and their ability to induce turnover of triglycerides [10,11]. Indeed, when the ability of SAT to release fatty acids is reduced, accumulation of fat in visceral adipose tissue (VAT) and ectopic fat deposition on metabolic organs such as liver or muscle may occur [10]. Moreover, it has been reported in both humans and animal models that the dysfunction of adipose tissue lead to metabolic inflexibility [12-14]. As a result, large visceral fat cells are produced, and the liver captures excess circulating fatty acids leading to an increase in hepatic fat accumulation which can produce an inflammatory response [15]. The accumulation of defective mitochondria and malfunctioning cytoplasmatic protein progressively increases which results in autophagy suppression and progression to steatohepatitis [16,17].

In this study, we investigated the differences physiological and metabolic implicated on NAFLD development and alterations of adipose tissue caused by two

different types of western diets, supporting the concept that the dietetic pattern established it is decisive point in the impaired metabolic flexibility.

2. Methods

2.1. Animal care and diets

All experiments were performed in compliance with the guidelines established by the Committee on Animal Care of the *Universitat Rovira i Virgili* and conform to the Animal Research: Reporting of *In Vivo* Experiments (ARRIVE) guidelines. Four-week-old male mice (C57BL/6J) were obtained from Charles River Laboratories (Wilmington, MA, USA) and acclimatized to the animal house for 1 week. All mice were housed in groups of four and maintained in environmentally controlled conditions (temperature 22-24ºC, 12h dark-light cycles and 51-53% relative humidity).

Animals received food and water *ad libitum* and were monitored daily for health status. Body weight and food intake were recorded weekly. After acclimatization, mice were randomly allocated into 3 groups (n=8 mice per group) to receive either a standard chow diet (CD, A04, Scientific Animal Food & Engineering, Augy, France), a high-fat diet (HFD, D12492, Ssniff Speziäten GmbH, Ferdinand-Gabriel-Weg, Germany), or a high fat high-sucrose diet (HF-HSD, TD08811, Harlan Laboratories Inc., Madison, WI, USA) for 20 weeks. Diet compositions are shown in Supplementary Table 1. At the end of the experiment, mice were sacrificed following a12h fast. The liver, adipose tissue and sera were collected and stored at -80ºC for biochemical and molecular analyses, or preserved in formalin for histopathological analysis.

2.2. Standard biochemical analyses

Serum concentrations of glucose, cholesterol and triglycerides were determined by standard tests in a Cobas Mira automated analyzer (Roche Diagnostics, Rotkreuz, Switzerland).

2.3. Histological analysis

Liver and adipose tissue samples were fixed in formalin and embedded in paraffin for hematoxylin and eosin staining. The degree of hepatic impairment was estimated using the NAFLD activity score (NAS score). This scoring system is based on

histological features classified into three categories: steatosis (graded from 0 to 3), lobular inflammation (graded from 0 to 2) and hepatocellular ballooning (graded from 0 to 2) were assessed by an experienced pathologist [18]. Samples were considered to have NASH when the NAS score was ≥5. The average adipocyte size from visceral and subcutaneous adipose tissue was estimated using the ImageJ 1.51 software (National Institutes of Health, Bethesda, MD, USA) with the macro MRI's adipocyte tool.

2.4. Immunohistochemistry

To assess differences in oxidation and inflammation between the groups of mice, we analyzed the hepatic immunohistochemical expressions of 4-hydroxy-2-nonenal (marker of lipid peroxidation), paraoxonase-1 (an antioxidant enzyme), chemokine (C-C motif) ligand-2 (CCL2), tumor necrosis factor-α (TNF-α), F4/80 antigen (marker of total number of macrophages, both pro- and anti-inflammatory), cluster differentiation 11b (CD11b, marker of pro-inflammatory macrophages), cluster differentiation 163 (CD163, marker of anti-inflammatory macrophages), and C-type lectin domain (CLEC4F, marker of Kupffer cells and infiltrating monocytes) [19,20]. The employed primary antibodies are described in Supplementary Table 2. Unstained paraffin-embedded tissues were deparaffinized and rehydrated before antigen retrieval detection with 10 mM of sodium citrate or Tris-EDTA (10mM Tris Base, 1mM EDTA) at pH 9.0 for 40 min at 95ºC. Endogenous peroxidase activity was blocked using EnVison™ FLEX Peroxidase-Blocking Reagent (Agilent Technologies, Santa Clara, CA, USA) for 25 minutes, and BSA 2% (Sigma Aldrich, St. Louis, MO, USA) was used to block non-specific binding sites. Sections were incubated overnight with the corresponding primary antibody, washed (twice for 4 min) with phosphate-buffered saline with glycine, and incubated with EnVison™ FLEX/HRP (Agilent Technologies) for 1h at room temperature. In the final step, slides were washed with phosphate-buffered saline with glycine (twice for 4 min) and incubated with EnVison™ FLEX DAB + Chromogen (Agilent Technologies). Photographs were taken with an optical microscope (Eclipse E600, Nikon, Tokyo, Japan) and NIS-Elements F 4.00.00 software. Positively-stained areas were calculated using the ImageJ 1.51 software (National Institutes of Health, Bethesda, MD, USA) with the plug-in versatile wand tool.

2.5. Plasma antioxidant capacity assay

Plasma antioxidant capacity was measured by the ferric ion reducing antioxidant power (FRAP) assay, as described previously [21] and performed using a Biotek Power Wave XS microplate reader equipped with Gen5 software (Biotek Instruments, Winooski, VT, USA). Trolox was used as a standard. Results were expressed as mmol of Trolox Equivalents per liter (TE/L)

2.6. Hepatic antioxidant enzyme assays

Liver tissues (150 mg) were homogenized with a Politron (Thomas Scientific, Swedesboro, NJ, USA) in 0.2M cold sodium phosphate buffer at pH 6.25. The crude soluble fraction was obtained by ultra-centrifugation at 105,000 x g for 60 min at 4°C (Kontron 50TI rotor and Centrikon T-1045 centrifuge, Kontron Instruments, Augsburg, Germany). The supernatants were dispensed into aliquots to determine the different enzymes. Protein content was measured with the Bradford method [22] using bovine serum albumin as standard. Total superoxide dismutase (SOD) and catalase (CAT) activities were measured as previously described [23,24]; results are presented as U/g tissue and mmol/g tissue, respectively. Glutathione reductase (GR) and glutathione peroxidase (GPX) activities were measured in a Cobas Mira automated analyzer (Roche) [25]; the results are presented as U/g tissue.

2.7. Targeted metabolomics

We analyzed the hepatic concentrations of metabolites from glycolysis, pentose-phosphate pathway, citric acid cycle (CAC), and amino acids as described in detail previously [26]. Briefly, samples were injected into a 7890A gas chromatograph coupled with an electron impact source to a 7200-quadrupole time-of-flight mass spectrometer equipped with a 7693 auto-sampler module and a J&W Scientific HP-5MS column (30 m × 0.25 mm, 0.25 µm; Agilent Technologies).

2.8. Targeted lipidomics

Adipose tissues (10 mg) were homogenized in a Precellys 24 homogenizer (Bertin Technologies, Montigny, France) and polar lipids were extracted by adding 250 µL of methanol containing the selected internal standards described in Supplementary

Table 3. Samples were centrifuged at 15,000 rpm for 10 min at 4 ºC. The supernatants were dispensed into glass vials for liquid chromatography and mass spectrometry (LC-MS) analysis. Stock standards for calibration curves were dissolved in methanol at the concentrations described in Supplementary Table 4. A series of 10 concentrations of the internal standards mixture was prepared and dispensed into glass vials for LC-MS analysis. Samples (5 μl) were injected into a 1290 Infinity ultra-high-pressure liquid chromatograph (UHPLC) coupled to a 6550 quadrupole-time-of-flight mass spectrometer (QTOF) using a dual jet stream electrospray ionization (ESI) source (Agilent Technologies). The samples were injected in duplicate into the LC-MS system working in positive and negative mode. Supplementary Table 5 describes the retention times, *m/z* and polarity (positive or negative) in detecting each lipid species, as well as the standards employed. The UHPLC system was equipped with a binary pump (G4220A), an autosampler (G4226A) thermostat-controlled at 4ºC, and an Acquity BEH C_{18} column 1.7 μm, 2.1 mm × 100 mm (Waters Corp., Milford, MA, USA) thermostat-controlled at 40 ºC. The mobile phase consisted of A: water + 0.05% formic acid; B: acetonitrile + 0.05 formic acid. The flow rate was 0.3 mL/min. The gradient used was as follows: 0 min, 2% B; 2 min, 50% B; 10 min, 98% B; from 10 to 13 min, gradient was maintained at 98% B for column cleaning; 14 min, 2% B followed by a post-run of 4 min under the same conditions for column re-conditioning. For the ESI source, the optimized parameters were as follows: gas temperature 225 ºC, drying gas flow 11 L/min, nebulizer 35 psi, sheath gas temperature 300 ºC and sheath gas flow 12 L/min For the QTOF-MS, the capillary, nozzle and fragmentor voltages were set at 3500 V, 500 V and 380 V, respectively.

2.9. GC-MS and LC-MS metabolites quantification

Metabolites and lipid species were quantified using Mass Hunter Quantitative Analysis B.07.00 (Agilent Technologies). Lipid characterization was done by matching their accurate mass and isotopic distributions to the Metlin-PCDL database (Agilent Technologies) allowing a mass error of 10 ppm and a score higher than 80 for isotopic distribution. To ensure the tentative characterization, chromatographic behavior of pure standards and corroboration with Lipid Maps database (www.lipidmaps.org) was performed.

2.10. Immunoblotting analysis

Frozen hepatic tissues (30 mg) were homogenized with 300 µL of 0.25M sucrose. Adipose tissues (100 mg) were homogenized with 200 µl RIPA (Sigma Aldrich) in a 2mL safe-lock Eppendorf tube. Both buffers contained phosphatase (Roche Diagnostics) and protease inhibitors (Roche Diagnostics). After centrifugation (14,000 rpm, 4ºC, 20 min) the protein concentration was analyzed in the aqueous phase using a NanoDrop2000 spectrophotometer (Thermo Fisher Scientific Inc. Waltham, MA, USA). We analyzed the hepatic expressions of AMP-activated protein kinase (AMPK) and acetyl-CoA carboxylase (ACC) and their inactive phosphorylated forms pAMPK and pACC, hormone sensitive lipase (HSL) and pHSL, mammalian target of rapamycin complex 1 (mTORC1) and pmTORC1, autophagy-related protein 7 (ATG7), microtubule-associated proteins 1A/1B light chain 3B (LC3B), mitofusin 2 (MFN2), total oxidative phosphorylation (OXPHOS), CCL2, CD11b, CD163, c-Jun and p-c-Jun, sequestosome-1 (P62) and pP62, PTEN-induced putative kinase 1 (PINK1), E3 ubiquitin-protein ligase parkin (PARKIN), translocase outer membrane 20 (TOM20), fatty acid synthase (FASN) and uncoupling protein 1 (UCP-1). Denatured proteins (50 µg) from frozen tissue were subjected to 8%–14% sodium dodecyl sulfate polyacrylamide gel or nitrocellulose membrane electrophoresis with a Trans-Blot Turbo Transfer System (Bio-Rad Laboratories, Hercules, CA, USA). Membranes were incubated for 1h in a blocking solution (5% non-fat dry milk in Tris-buffered saline with 0.1% Tween-20). Samples were, then, incubated with the corresponding primary antibody as described in Supplementary Table 2. The following day, membranes were washed (thrice for 10 min) in Tris-buffered saline and incubated for 1h at room temperature in the presence of polyclonal goat anti-rabbit (HRP) antibody (Agilent Technologies). Membranes were washed again (thrice for 10 min) in Tris-buffered saline and enhanced with SuperSignal West Femto chemiluminescent substrate (ThermoFisher) and image were digitally captured using de ChemiDoc MP System (Bio-Rad). Bands were quantified using Image Lab software (Bio-Rad) and the protein expressions were normalized with a housekeeping protein (FAH).

2.11. Extraction and quantification of RNA

Total RNA was extracted from liver using RNeasy kit (Qiagen, Barcelona, Spain) according to the manufacturer's instructions, and was purified by chloroform extraction and isopropanol precipitation. RNA concentration and purity were determined using Nanodrop ND-2000 spectrophotometer (Thermofisher Scientific). Quantitative gene expression was evaluated by qPCR on a 7900HT Fast Real-Time PCR System using TaqMan Gene Expression Assay (Applied Biosystems) with the primer sequences ATP-citrate lyase (Mm01302282_m1), isocitrate dehydrogenase 1 (Mm00516030_m1), isocitrate dehydrogenase 2 (Mm00612429_m1), oxoglutarate dehydrogenase (Mm00803119_m1) and succinate dehydrogenase (Mm01352366_m1). Beta-2-microglobulin (B2M) was employed as housekeeping gene.

2.12. Statistical analysis

Data are presented as mean ± standard error of the mean (SEM) unless otherwise indicated. Differences between groups were analyzed by the Mann-Whitney *U*-test with the SPSS package, version 22.0. MetaboAnalyst 4.0 (available at http://www.metaboanalyst.ca/) was used to generate scores/loading plots and Heatmaps. Multivariate statistics were used to improve the analysis of complex raw data and pattern recognition. The supervised partial least squares discriminant analysis (PLSDA) method was employed to distinguish the compared groups according to metabolomic data. The relative magnitude of observed changes was evaluated using the variable importance in projection (VIP) score. Statistical significance was defined when p value was <0.05.

3. Results

3.1. HFD and HF-HSD promoted NAFLD, but only HF-HSD promoted NASH

Mice fed HFD and HF-HSD showed a faster gain in body weight than the CD-fed group (Fig. 1A). The relative food intake was higher in the CD-fed group due to the lower energy density of this diet, but there were no differences in calorie intake between groups (Fig. 1B and C). At sacrifice, animals fed HFD and HF-HSD showed significantly higher serum cholesterol concentrations than CD-fed animals, but only

mice fed HF-HSD showed significantly increased circulating glucose and triglycerides (Fig. 1D). Hepatic histology was normal in CD-fed mice. In contrast, animals fed HFD showed a general loss of hepatocyte structure, and with an increase in cytosolic fat accumulation characteristic of NAFLD. In mice fed HFD, fat accumulation was observed predominantly as micro-vesicular steatosis with some ballooning. Histopathological alterations were more severe in mice fed HF-HSD. This group, apart from presenting micro-vesicular steatosis in the peri-central area, had macro-vesicular steatosis in the peri-portal area, severe ballooning, and lobular inflammation (Fig. 1F). In mice fed HFD and HF-HSD, changes in liver histology were accompanied with a significant increase of liver weight compared to CD-fed animals. Only mice fed HF-HSD showed NAS scores >5: indicating the presence of NASH.

3.2. HF-HSD was associated with oxidative stress and inflammation

In mice fed HF-HSD, we found a significantly increased hepatic immunohistochemical expression of 4-hydroxy-2-nonenal, which is the most abundant product derived from peroxidation of polyunsaturated fatty acids. The expression of the antioxidant enzyme PON1 remained unmodified (Fig. 2A). This increase in lipid peroxidation was accompanied by lower hepatic SOD, CAT and GPX activities, while there were no significant changes in GR. In addition, these mice showed a significant decrease in plasma FRAP (Fig. 2B). Moreover, the oxidative stress environment was corroborated with the activation of c-Jun (Ser 73), which is a major redox-sensitive component (Fig. 2C).This general increase in oxidative stress may stimulate inflammatory response. To investigate this issue, we focused on markers present in macrophages that are key players in initiating an immune response. Our results showed that mice fed HFD and HF-HSD had a lower expression of CLEC4F and F4/80 than CD-fed animals (Supplementary Fig.1A). In addition, CD163 expression was also lower; indicating a poor anti-inflammatory response in mice fed HF-HSD and HFD. The lower anti-inflammatory capacity was accompanied by the increase of pro-inflammatory marker CD11b in both groups, although the increase was stronger in the HF-HSD group. Moreover, expression of the inflammatory chemokine (C-C motif) ligand-2 (CCL2) was significantly increased in mice fed HF-HSD (Supplementary Fig. 1B).

3.3. HF-HSD was associated with metabolic inflexibility in adapting to excess nutrient intake

PLDSA analysis showed significant global liver differences in energy balance-related metabolites between the different diets administered. VIP analysis showed that the variations in the metabolite profile were attributed mainly to oxaloacetate, fructose-6-P, fructose-1,6-BisP, glucose-6-P, α-ketoglutarate, 6-P-gluconate, citrate, and ribose-5-P, all of which had VIP values >1 (Supplementary Fig. 2). HFD and HF-HSD produced different alterations in metabolites of the CAC cycle, glycolysis, amino acids and pentose-phosphate pathway (PPP) (Table 1, Supplementary Fig. 3). HFD-fed mice had significant increases of some metabolites involved in pathways of glycolysis and PPP, whereas animals fed HF-HSD had lower levels of these metabolites than CD-fed mice. Immunoblotting analyses (Fig. 3A) suggested that mice fed HF-HSD had a poorer metabolic adaptation (metabolic inflexibility) due to a relative incapacity to oxidize the accumulated lipids and to an increase the lipogenic pathways via the upregulation of ACC1 and FASN. In contrast to mice fed HF-HSD, animals fed HFD showed an adequate metabolic adaptation by increasing the mitochondrial fatty acid oxidation via the inhibition of ACC2, and downregulation of key proteins in pathways of lipogenesis. We also investigated whether this switch in liver metabolism was related to alterations in mitochondrial proteins. We found low levels of mitochondrial complexes II, III and V, suggesting a decrease in the capacity to oxidize succinate to fumarate and to produce ATP. Finally, we analyzed the gene expression of ATP-citrate lyase (ACLY), isocitrate dehydrogenase 1 and 2 (IDH1 and 2), oxoglutarate dehydrogenase (OGHD) and succinate dehydrogenase (SDHA) (Fig. 3B). The mice fed HF-HSD showed a great increase expression of ACLY and IDH1 and a moderate increase of SDHA and OGDHA, suggesting a rewriting metabolic flux towards lipogenesis. As such, these results suggest that the increase in hepatic *de novo* lipogenesis (DNL) in mice fed HF-HSD might be a compensatory response to the lowered capacity for oxidative metabolism in the mitochondria.

3.4. HF-HSD promoted defective mitochondrial clearance via autophagy

We evaluated whether autophagy was inhibited within the context of metabolic inflexibility. As shown in Fig. 4, the activation of AMP-activated protein kinase (AMPK) suggested the activation of autophagy , with the formation of auto-phagosomes and the increase in LC3II in the HF-HSD group. However, the increase in P62 levels suggests a blockage in the final step of the pathway resulting in the accumulation of non-degraded auto-phagosomes. We further assessed whether the inhibition of autophagy was associated with the inhibition of ubiquitin-dependent mitophagy. For this purpose, we determined the levels of pP62, PINK and PARKIN that are necessary for normal mitophagy function. As shown in Fig. 4, we observed high levels of all three proteins, indicating a high number of malfunctioning mitochondria and accumulation of proteins awaiting degradation. Finally, we investigated the capacity of the mitochondria to incorporate new mitochondrial pre-proteins through the TOM20 pathway. We observed that the levels of this protein were lower; indicating, again, a metabolic blockage of the mitochondria. All these results indicate a poorer metabolic adaptation in animals fed HF-HSD.

3.5. Diet induces metabolic re-programming of adipose tissue

The results obtained so far indicate that liver metabolism was strongly altered in the mice fed HF-HSD. But we were curious to know whether different diets change the adipose tissue dynamics. As shown in Fig. 5A-C, the adipocyte size increased (hypertrophy) in the peri-gonadal WAT (pgWAT) and the inguinal WAT (iWAT) of the groups fed HFD and HF-HSD. Following this observation, we studied the role of several proteins involved in processes related to lipogenesis and to lipolysis. We observed a downregulation of ACC1 and HSL, resulting in a lower capacity to store (lipogenesis) and to remove (lipolysis) excess triglycerides, and lower thermogenic capacity by UCP-1 (Fig 5D).

3.6. HF-HSD is associated with the accumulation of visceral lipid species

We proceeded to measure the concentrations of a wide range of lipid species in the liver, pgWAT and iWAT. Results of the individual lipids measured are summarized in Supplementary Tables 6, 7 and 8. Globally, lipid content differed according to the

diet administered, and to the anatomical location of the tissue in which the measurements were made. There was a significant accumulation of saturated fatty acids (SFA) and polyunsaturated fatty acids (PUFA) in pgWAT as well as iWAT of the mice fed HF-HSD; while the HFD-group showed a decrease in SFA in iWAT, and no changes in pgWAT in the animals fed CD (Supplementary Fig. 4). In contrast, the content of PUFA was decreased in iWAT of mice fed HFD and HF-HSD, while PUFA content in pgWAT was only decreased in the HFD-group. In addition, there were variations in the concentrations of bile acid metabolites; a decrease in cholic acid (CA) metabolites only in iWAT of the HF-HSD-group; suggesting an impairment in energy expenditure [27]. These results suggest that the impairment of iWAT function in mice fed HF-HSD completely abolished the capacity of the animal to store excess circulating free fatty acids, while promoting lipid accumulation in pgWAT (Fig. 6).

4. Discussion

Results of the present study show that, in mice receiving a high-fat diet, the addition of sucrose promotes the development of NASH. In this context, sucrose acts as a lesion enhancer by inducing the inhibition of autophagy and fatty acid oxidation and, concomitantly, activating *de novo* lipogenesis. Also, the sucrose induces adipose tissue dynamic changes. Both HFD and HF-HSD diets were obesogenic but the effects produced at the metabolic and mechanistic level were different. Previous studies evidenced the lack of consensus on the most effective diets (and duration of exposure to them) to induce metabolic alterations and related pathologies such as diabetes, metabolic syndrome, NAFLD or NASH [28]. In rats, the feeding of HFD or HF-HSD caused steatosis, but not NASH [29,30], while diets with a very high sucrose content (without excess fat), were able to promote steatosis and NASH [31,32]. In contrast, a diet high in sucrose and fat does induce steatosis [33] as well as NASH [34,35] in mice. Earlier reports [36,37] indicated that different diets act as modulators of different alterations in metabolism, depending on the nutritional composition of the diets. A more recent report [38] showed that fructose supplementation in HFD alters the mitochondrial protein acetylation involved in hepatic fatty acid oxidation (FAO).

We have corroborated these observations in a long-term study showing that the administration of a HF-HSD to mice, not only induces metabolic changes in liver

but also in different regions of adipose tissue. These findings correlated with the aggravation of NAFLD and the appearance of NASH. We also observed that sucrose supplementation in HFD promoted oxidative stress and activation of the immune response i.e. the immune cells developed an imbalance of pro-inflammatory/anti-inflammatory markers in favor of an increase in pro-inflammatory CD11b expression. This observation is supported by other reports showing that the administration of high-fat, high-cholesterol, high-sugar diet [39] or high-fat high-cholesterol diet [40] in mice promoted an increase of CD11b levels and the number of M1 macrophages. In addition, the upregulation of inflammatory response was associated with an increase in oxidative stress through the inhibition of hepatic SOD, CAT and GPx activity and the activation of c-Jun. One report indicated that obese patients with NASH had a lower antioxidant defense capacity [41], which was in line with another report in a murine NASH model [42]. Further, this obesogenic phenotype was linked to changes in metabolic regulation. Strikingly, the activation of AMPK and mTORC1 was different depending on the diet. In the present study, the administration of HF-HSD stimulated AMPK without effecting autophagy activation, since the process was blocked at the last step of lysosome fusion. With regard to this observation, it is of note that the activation of AMPK is known to induce autophagy in general while, in contrast, mTORC1 promotes the inhibition of autophagosome formation [43]. For example, mice deficient in carboxylesterase 1d (Ces1d) are protected from NAFLD induction by HF-HSD *via* activation of AMPK [44]. However, other factors such as the exposure to certain lipid species, the activation of Rubicon (a negative regulator of autophagy), or the preference of autophagosomes to fuse with endosomes (low hydrolysis efficiency) may regulate the autophagosome-lysosome fusion step [45–47]. This could explain the increase of LC3-II and P62 observed in HF-HSD. A recent study in mice with NAFLD [48] reported that a decrease in oxidative phosphorylation proteins was associated with an increase in some mitophagy markers. However, the same study found that proteasomal degradation activity was reduced, suggesting that ATP deficiency because of reduced stability of oxidative phosphorylation complex subunits contributed to inhibition of ubiquitin-proteasome and activation of mitophagy. Moreover, another study in mice fed with a high-fat diet showed an increase in the activities of complex I and complex II and an increase in ATP production [49]. On the other hand, there are

some reports indicating that complexes I and III are required to normal autophagy flux and their suppression led to autophagy inhibition [50,51]. Moreover, the inhibition of Complex V with oligomycin has been reported to promote mitochondrial dysfunction and death in cell cultures [52] and in Alzheimer disease, the low expression of CI, CII, CIII, CIV and CV was associated with a mitophagy failure [53]. Our results support the hypothesis of a reduction in autophagy/mitophagy in mice fed an HF-HSD diet, despite having a downregulation of CII, CIII and CV. Results obtained to-date can be open to more than one interpretation, and different diets or different weeks of treatment make difficult to reach a consensus.

We noted that HFD administration produced a decrease of LC3-II and P62 levels, reflecting a normal autophagic flux; albeit this was associated with the surprising activation of mTORC1. One explanation of this autophagy flux could be the activation of p38-mitogen-activated protein kinase (p38 MAPK) that, under certain stress stimuli, may induce autophagy activation, thus acting as a compensatory measure to restore homoeostasis [54,55]. In this context, we found that HFD is associated with the activation of p38 MAPK, implying that this factor might be a countermeasure to defend liver tissue from injury. Of note is that HF-HSD promoted the activation of PINK1/PARKIN pathway and the increase in MFN2 and p-P62 levels; suggesting an activation of the mitophagy machinery as consequence of abnormal mitochondrial accumulation. It is of further note that, despite the role assigned to PINK1/PARKIN pathway in the clearance of abnormal mitochondria (mitophagy), the results demonstrated a low capacity of the lysosome to degrade autophagosomes, thus precluding the elimination of damaged mitochondria. In concordance with our findings, a previous report highlighted that the increase of MFN2 and PINK1/PARKIN pathway was linked to clearance of abnormal mitochondria in cardiomyocytes. The authors suggested that PINK1 phosphorylates MFN2 to attract, and bind, PARKIN to promote the ubiquitination of mitochondrial proteins [56]. In this context, other reports observed that the genetic ablation of MFN2 in liver, or in specific neurons, causes mitochondrial dysfunction and alterations in morphology [57,58]. Further, a recent report showed that PINK/PARKIN pathway controls the specific degradation of MFN 1 and 2 rather than the global mitochondrial ubiquitination; thus indicating

pathways other than ubiquitin may label damaged mitochondria [59]. However, the implication of diet in the mitochondrial state seems to be more complex than expected due to a contradictory results from a few studies. These discrepancies can be due to a qualitative and quantitative variations of dietary composition that influence the transition of NAFL to NASH [60].

We also observed that the activation of AMPK/mTORC1 promoted the activation of ACC1 in mice fed HF-HSD, and the inhibition of ACC2 in mice fed HFD: processes related to hepatic DNL and FAO respectively. Indeed, an explanation for this switch in ACC1/ACC2 activation might be the presence, or absence, of fructose in the diet; reports have suggested that fructose consumption enhances fatty acid synthesis [61,62]. However, a recent study indicates that this response might depend on the mouse strain: thus emphasizing the importance of the genetic background in experimental-animal studies [63]. Of note is that supplementation of HFD with sucrose promoted a different metabolic response to that of HFD alone. The exposure to HF-HSD caused a decrease in the concentrations of metabolites of glycolysis, while HFD caused an increase. The high numbers of damaged mitochondria and insulin resistance may block glucose oxidation via CAC in favor of induction of reductive carboxylation which supports the biosynthesis of lipids [64,65]. Finally, we observed that adipose tissue may be crucial in aggravating NAFLD, and its progression to NASH. Indeed, administering HFD or HF-HSD was sufficient to induce pgWAT and iWAT hypertrophy. We also observed that both diets induced a metabolic re-programing of adipose tissue, independently of the anatomical localization. As such, these diets produced an increase in phosphorylated AMPK levels that led to the inhibition of lipolysis, accompanied by a downregulation of ACC1; a process related to DNL. Some evidence indicated that the downregulation of DNL appears to be a mechanism responsible for insulin resistance in adipose tissue [66-68]. However, adipose tissue is the largest organ and its metabolic function not only differs between anatomical regions but also within regions, implying a complex regulation network. Of considerable note is that there was an increase in the levels of SFA, MUFA and PUFA in iWAT and, more importantly, in pgWAT of mice fed HF-HSD. Our results are in agreement with a report showing that VAT contained more MUFA than SAT as a result

of a higher activity of long-chain fatty acid elongase 6 and steaoryl-CoA desaturase-1; two enzymes involved in the elongation and desaturation of fatty acids[69]. This observation can be explained by a decreased ability of subcutaneous adipose tissue to expand contributing to deposition into visceral adipose tissue and the liver. Several reports suggest that the reduction of visceral adipose tissue concomitantly reduces insulin resistance and glucose levels in humans, and increases lifespan in animal models [70–72]. In contrast, the reduction of subcutaneous adipose tissue has been reported not to improve insulin sensitivity, and the subcutaneous increase in adipose tissue is considered complicit in the metabolic complications related to obesity [73,74]. Our current findings highlight the interconnection between these organs and their involvement in metabolic disease progression.

The mechanisms by which HF-HSD induces NAFLD and NASH are complex. Indeed, and regardless of the results obtained in our study, reports have shown that HF-HSD impairs phosphorylation of protein kinase B (PKB/Akt), hyperphosphorylation of insulin receptor substrate-1, activation of poly (ADP-ribose) polymerase 1 (PARP-1), altered mitochondrial function, and autophagy in experimental models. Conversely, the administration of several nutraceuticals corrected these alterations while activating anti-oxidative signaling pathways, reducing inflammation and modifying gut microbiota [75-81]. The combined results of studies published to-date highlight the close relationship between oxidative stress, mitochondrial dysfunction, alterations in autophagy and excessive accumulation of lipids in the development of NASH induced by HF-HSD.

This study has potential translational implications to human pathology. Our results point towards adipose tissue dysfunction as an important contributor to the progression of NAFLD to NASH and, as such, highlight the potential of adipose tissue as a therapeutic target for the management of metabolic complications of obesity. The results also highlight the importance of understanding the impact of two dietary patterns which, in our present case, were sufficient to induce two different phenotypes. We conclude that the administration of a HF-HSD under metabolic blockage conditions led to an oxidative and inflammatory environment, and negated the restoration of damaged hepatic mitochondria. In addition, the continuous

accumulation of fatty acids resulted in dysfunctional adipose tissue, and hepatic fat accumulation that favored the progression to NASH. Finally, the results here exposed unveil the importance of dietary background and their complex role in the regulation of metabolism. A limitation of the present study is that modifications in the autophagy process have been studied indirectly, by analyzing the expression of some regulatory factors. Dynamic studies, measuring autophagy flux activity would be necessary to fully demonstrate this hypothesis.

Funding

This study was supported by grants PI15/00285 and PI18/00921 from the *Instituto de Salud Carlos III* (Madrid, Spain); co-funded by European Social Fund (ESF); "Investing in your future" and the *Agència de Gestió d'Ajuts Universitaris i de Recerca* (SGR00436).

Author contributions

Gerard Baiges-Gaya, Jordi Camps, Jorge Joven: Conceptualization; Gerard Baiges-Gaya, Jordi Camps: Data curation; Gerard Baiges-Gaya, Jordi Camps, Jorge Joven: Formal analysis; Marta Romeu, Maria-Rosa Nogués, Jorge Joven: Funding acquisition; Gerard Baiges-Gaya, Salvador Fernández-Arroyo, Fedra Luciano-Mateo, Noemí Cabré, Elisabet Rodríguez-Tomàs, Anna Hernández-Aguilera, Helena Castañé: Investigation; Gerard Baiges-Gaya, Salvador Fernández-Arroyo, Fedra Luciano-Mateo, Noemí Cabré, Elisabet Rodríguez-Tomàs, Anna Hernández-Aguilera, Helena Castañé: Methodology; Jordi Camps, Jorge Joven: Project administration; Salvador Fernández-Arroyo, Marta Romeu, Maria-Rosa Nogués, Jorge Joven: Resources; Gerard Baiges-Gaya, Salvador Fernández-Arroyo: Software; Jordi Camps, Jorge Joven: Supervision; Gerard Baiges-Gaya, Jordi Camps, Jorge Joven: Validation; Jordi Camps: Visualization; Gerard Baiges-Gaya: Writing – original draft; Jordi Camps: Writing – review & editing.

Declaration of competing interest

None.

REFERENCES

[1] González-Muniesa P, Mártinez-González M-A, Hu FB, Després J-P, Matsuzawa Y, F Loos RJ, et al. Obesity, considered by many as a 21st century epidemic. Nat Publ Gr 2017;3:1–18. https://doi.org/10.1038/nrdp.2017.34.

[2] Friedman SL, Neuschwander-Tetri BA, Rinella M, Sanyal AJ. Mechanisms of NAFLD development and therapeutic strategies. Nat Med 2018;24:908–22. https://doi.org/10.1038/s41591-018-0104-9.

[3] Van Dam RM, Seidell JC. Carbohydrate intake and obesity. Eur J Clin Nutr 2007. 61 suppl 1;s75–99. https://doi.org/10.1038/sj.ejcn.1602939.

[4] Stanhope KL. Sugar consumption, metabolic disease and obesity: The state of the controversy. Crit Rev Clin Lab Sci 2016;53:52–67 https://doi.org/10.3109/10408363.2015.1084990.

[5] Schuster S, Cabrera D, Arrese M, Feldstein AE. Triggering and resolution of inflammation in NASH. Nat Rev Gastroenterol Hepatol 2018;15:349–64. https://doi.org/10.1038/s41575-018-0009-6.

[6] Kim D, Kim W, Joo SK, Han J, Kim JH, Harrison SA, et al. Association between body size-metabolic phenotype and nonalcoholic steatohepatitis and significant fibrosis. J Gastroenterol 2019. https://doi.org/10.1007/s00535-019-01628-z.

[7] Hoffstedt J, Arner E, Wahrenberg H, Andersson DP, Qvisth V, Löfgren P, et al. Regional impact of adipose tissue morphology on the metabolic profile in morbid obesity. Diabetologia 2010;53:2496–503. https://doi.org/10.1007/s00125-010-1889-3.

[8] Tchkonia T, Thomou T, Zhu Y, Karagiannides I, Pothoulakis C, Jensen MD, et al. Mechanisms and metabolic implications of regional differences among fat depots. Cell Metab 2013;17:644–56. https://doi.org/10.1016/j.cmet.2013.03.008.

[9] White UA, Tchoukalova YD. Sex dimorphism and depot differences in adipose tissue function. Biochim Biophys Acta-Mol Basis Dis 2014;1842:377–92. https://doi.org/10.1016/j.bbadis.2013.05.006.

[10] Arner P, Bernard S, Salehpour M, Possnert G, Liebl J, Steier P, et al. Dynamics of human adipose lipid turnover in health and metabolic disease. Nature 2011;478:110–3. https://doi.org/10.1038/nature10426.

[11] Tchoukalova YD, Votruba SB, Tchkonia T, Giorgadze N, Kirkland JL, Jensen MD. Regional differences in cellular mechanisms of adipose tissue gain with overfeeding. Proc Natl Acad Sci U S A 2010;107:18226–31. https://doi.org/10.1073/pnas.1005259107.

[12] Frayn, K. Adipose tissue as a buffer for daily lipid flux. *Diabetologia* **45,** 1201–1210 (2002). https://doi.org/10.1007/s00125-002-0873-y

[13] Virtue S, Petkevicius K, Moreno-Navarrete JM, Jenkins B, Hart D, Dale M, et al. Peroxisome Proliferator- Activated Receptor γ2 Controls the Rate of Adipose Tissue Lipid Storage and Determines Metabolic Flexibility. Cell Rep. 2018;24(8):2005-2012.e7. doi:10.1016/j.celrep.2018.07.063[14] Asterholm IW, Mundy DI, Weng J, Anderson

[14] RG, Scherer PE. Altered mitochondrial function and metabolic inflexibility associated with loss of caveolin-1. Cell Metab. 2012;15(2):171-185. doi:10.1016/j.cmet.2012.01.004

[15] Mendez-Sanchez N, Cruz-Ramon VC, Ramirez-Perez OL, Hwang JP, Barranco-Fragoso B, Cordova-Gallardo J. New aspects of lipotoxicity in nonalcoholic steatohepatitis. Int J Mol Sci 2018;19: pii: E2034. https://doi.org/10.3390/ijms19072034.

[16] Lim JS, Mietus-Snyder M, Valente A, Schwarz JM, Lustig RH. The role of fructose in the pathogenesis of NAFLD and the metabolic syndrome. Nat Rev Gastroenterol Hepatol 2010;7:251–64. https://doi.org/10.1038/nrgastro.2010.41.

[17] Yamada T, Murata D, Adachi Y, Itoh K, Kameoka S, Igarashi A, et al. Mitochondrial stasis reveals p62-mediated ubiquitination in parkin-independent mitophagy and mitigates nonalcoholic fatty liver disease. Cell Metab 2018;28:588–604. https://doi.org/10.1016/j.cmet.2018.06.014.

[18] Kleiner DE, Brunt EM, Van Natta M, Behling C, Contos MJ, Cummings OW, et al. Design and validation of a histological scoring system for nonalcoholic fatty liver disease. Hepatology 2005;15:1313–21. https://doi.org/10.1002/hep.20701.

[19] Luciano-Mateo F, Cabré N, Fernández-Arroyo S, Baiges-Gaya G, Hernández-Aguilera A, Rodríguez-Tomàs E, et al. Chemokine (C-C motif) ligand 2 gene ablation protects low-density lipoprotein and paraoxonase-1 double deficient mice from liver injury, oxidative stress and inflammation. Biochim Biophys Acta - Mol Basis Dis 2019;1865:1555–1566. https://doi.org/10.1016/j.bbadis.2019.03.006.

[20] Cabré N, Luciano-Mateo F, Fernández-Arroyo S, Baiges-Gayà G, Hernández-Aguilera A, Fibla M, et al. Laparoscopic sleeve gastrectomy reverses non-alcoholic fatty liver disease modulating oxidative stress and inflammation. Metabolism 2019;99:81–89. https://doi.org/10.1016/j.metabol.2019.07.002.

[21] Benzie IFF, Strain JJ. The ferric reducing ability of plasma (FRAP) as a measure of "antioxidant power": The FRAP assay. Anal Biochem 1996;239:70–6. https://doi.org/10.1006/abio.1996.0292.

[22] Bradford MM. A rapid and sensitive method for the quantitation of microgram quantities of protein utilizing the principle of protein-dye binding. Anal Biochem 1976;72:248–54. https://doi.org/10.1016/0003-2697(76)90527-3.

[23] Misra HP, Fridovich I. The role of superoxide anion in the autoxidation of epinephrine and a simple assay for superoxide dismutase. J Biol Chem 1972;247:3170–5.

[24] Cohen G, Dembiec D, Marcus J. Measurement of catalase activity in tissue extracts. Anal Biochem 1970;34:30–8. https://doi.org/10.1016/0003-2697(70)90083-7.

[25] Wheeler CR, Salzman JA, Elsayed NM, Omaye ST, Korte DW. Automated assays for superoxide dismutase, catalase, glutathione peroxidase, and glutathione reductase activity. Anal Biochem 1990;184:193–9. https://doi.org/10.1016/0003-2697(90)90668-Y.

[26] Riera-Borrull M, Rodríguez-Gallego E, Hernández-Aguilera A, Luciano F, Ras R, Cuyàs E, et al. Exploring the Process of Energy Generation in Pathophysiology by Targeted Metabolomics: Performance of a Simple and Quantitative Method. J Am Soc Mass Spectrom. 2016;27(1):168-177. https:// doi:10.1007/s13361-015-1262-3

[27] Watanabe M, Houten SM, Mataki C, Christoffolete MA, Kim BW, Sato H, et al. Bile acids induce energy expenditure by promoting intracellular thyroid hormone activation. Nature 2006;439:484–9. https://doi.org/10.1038/nature04330.

[28] Melo BF, Sacramento JF, Ribeiro MJ, Prego CS, Correia MC, Coelho JC, et al. Evaluating the impact of different hypercaloric diets on weight gain, insulin resistance, glucose intolerance, and its comorbidities in rats. Nutrients 2019;11: pii: E1197. https://doi.org/10.3390/nu11061197.

[29] Roberts MD, Mobley CB, Toedebush RG, Heese AJ, Zhu C, Krieger AE, et al. Western diet-induced hepatic steatosis and alterations in the liver transcriptome in adult Brown-

Norway rats. BMC Gastroenterol 2015;15:151. https://doi.org/10.1186/s12876-015-0382-3.

[30] Fakhoury-Sayegh N, Trak-Smayra V, Khazzaka A, Esseily F, Obeid O, Lahoud-Zouein M, et al. Characteristics of nonalcoholic fatty liver disease induced in wistar rats following four different diets. Nutr Res Pract 2015;9:350–7. https://doi.org/10.4162/nrp.2015.9.4.350.

[31] Ragab SMM, Abd Elghaffar SK, El-Metwally TH, Badr G, Mahmoud MH, Omar HM. Effect of a high fat, high sucrose diet on the promotion of non-alcoholic fatty liver disease in male rats: The ameliorative role of three natural compounds. Lipids Health Dis 2015;14:83. https://doi.org/10.1186/s12944-015-0087-1.

[32] Acosta-Cota S de J, Aguilar-Medina EM, Ramos-Payán R, Ruiz-Quiñónez AK, Romero-Quintana JG, Montes-Avila J, et al. Histopathological and biochemical changes in the development of nonalcoholic fatty liver disease induced by high-sucrose diet at different times. Can J Physiol Pharmacol 2019;97:23–36. https://doi.org/10.1139/cjpp-2018-0353.

[33] Wang S, Yang FJ, Shang LC, Zhang YH, Zhou Y, Shi XL. Puerarin protects against high-fat high-sucrose diet-induced non-alcoholic fatty liver disease by modulating PARP-1/PI3K/AKT signaling pathway and facilitating mitochondrial homeostasis. Phyther Res 2019;33:2347–2359. https://doi.org/10.1002/ptr.6417.

[34] Verbeek J, Lannoo M, Pirinen E, Ryu D, Spincemaille P, Elst I Vander, et al. Roux-en-y gastric bypass attenuates hepatic mitochondrial dysfunction in mice with non-alcoholic steatohepatitis. Gut 2015;64:673–83. https://doi.org/10.1136/gutjnl-2014-306748.

[35] Verbeek J, Spincemaille P, Vanhorebeek I, Van Den Berghe G, Vander Elst I, Windmolders P, et al. Dietary intervention, but not losartan, completely reverses non-alcoholic steatohepatitis in obese and insulin resistant mice. Lipids Health Dis 2017;16:46. https://doi.org/10.1186/s12944-017-0432-7.

[36] Drescher HK, Weiskirchen R, Fülöp A, Hopf C, De San Román EG, Huesgen PF, et al. The influence of different fat sources on steatohepatitis and fibrosis development in the western diet mouse model of non-alcoholic steatohepatitis (NASH). Front Physiol 2019;10:770. https://doi.org/10.3389/fphys.2019.00770.

[37] Softic S, Gupta MK, Wang GX, Fujisaka S, O'Neill BT, Rao TN, et al. Divergent effects of

glucose and fructose on hepatic lipogenesis and insulin signaling. J Clin Invest 2017;11:4059–4074. https://doi.org/10.1172/JCI94585.

[38] Softic S, Meyer JG, Wang GX, Gupta MK, Batista TM, Lauritzen HPMM, et al. Dietary sugars alter hepatic fatty acid oxidation via transcriptional and post-translational modifications of mitochondrial proteins. Cell Metab 2019;30:735–753.e4. https://doi.org/10.1016/j.cmet.2019.09.003.

[39] Ambade A, Satishchandran A, Saha B, Gyongyosi B, Lowe P, Kodys K, et al. Hepatocellular carcinoma is accelerated by NASH involving M2 macrophage polarization mediated by hif-1αinduced IL-10. Oncoimmunology 2016;5:e1221557. https://doi.org/10.1080/2162402X.2016.1221557.

[40] Mukai K, Miyagi T, Nishio K, Yokoyama Y, Yoshioka T, Saito Y, et al. S100A8 Production in CXCR2-expressing CD11b + Gr-1 high cells aggravates hepatitis in mice fed a high-fat and high-cholesterol Diet . J Immunol 2016;196:395–406. https://doi.org/10.4049/jimmunol.1402709.

[41] Koliaki C, Szendroedi J, Kaul K, Jelenik T, Nowotny P, Jankowiak F, et al. Adaptation of hepatic mitochondrial function in humans with non-alcoholic fatty liver is lost in steatohepatitis. Cell Metab 2015;21:139–46. https://doi.org/10.1016/j.cmet.2015.04.004.

[42] Gornicka A, Morris-Stiff G, Thapaliya S, Papouchado BG, Berk M, Feldstein AE. Transcriptional profile of genes involved in oxidative stress and antioxidant defense in a dietary murine model of steatohepatitis. Antioxidants Redox Signal 2011;15:437–45. https://doi.org/10.1089/ars.2010.3815.

[43] Wang H, Liu Y, Wang D, Xu Y, Dong R, Yang Y, et al. The upstream pathway of mTOR-mediated autophagy in liver diseases. Cells 2019;8: pii: E1597. https://doi.org/10.3390/cells8121597.

[44] Lian J, Watts R, Quiroga AD, Beggs MR, Alexander RT, Lehner R. Ces1d deficiency protects against high-sucrose diet-induced hepatic triacylglycerol accumulation. J Lipid Res 2019;60:880–891. https://doi.org/10.1194/jlr.M092544.

[45] Tanaka S, Hikita H, Tatsumi T, Sakamori R, Nozaki Y, Sakane S, et al. Rubicon inhibits autophagy and accelerates hepatocyte apoptosis and lipid accumulation in nonalcoholic fatty liver disease in mice. Hepatology 2016;64:1994–2014.

https://doi.org/10.1002/hep.28820.

[46] Miyagawa K, Oe S, Honma Y, Izumi H, Baba R, Harada M. Lipid-induced endoplasmic reticulum stress impairs selective autophagy at the step of autophagosome-lysosome fusion in hepatocytes. Am J Pathol 2016;186:1861–1873. https://doi.org/10.1016/j.ajpath.2016.03.003.

[47] Koga H, Kaushik S, Cuervo AM. Altered lipid content inhibits autophagic vesicular fusion. FASEB J 2010;24:3052–65. https://doi.org/10.1096/fj.09-144519.

[48] Lee K, Haddad A, Osme A, Kim C, Borzou A, Ilchenko S, et al. Hepatic mitochondrial defects in a nonalcoholic fatty liver disease mouse model are associated with increased degradation of oxidative phosphorylation subunits. Mol Cell Proteomics 2018;17:2371–2386. https://doi:10.1074/mcp.RA118.000961.

[49] Guo Y, Darshi M, Ma Y, Perkins GA, Shen Z, Haushalter KJ, et al. Quantitative proteomic and functional analysis of liver mitochondria from high fat diet (HFD) diabetic mice. Mol Cell Proteomics 2013;12:3744–3758. https://doi:10.1074/mcp.M113.027441.

[50] Ma X, Jin M, Cai Y, Xia H, Long K, Liu J, et al. Mitochondrial electron transport chain complex III is required for antimycin A to inhibit autophagy. Chem Biol 2011;18:1474–81. https://doi:10.1016/j.chembiol.2011.08.009.

[51] Thomas HE, Zhang Y, Stefely JA, Veiga SR, Thomas G, Kozma SC, et al. Mitochondrial complex I activity is required for maximal autophagy. Cell Rep 2018 Aug;24:2404–2417.e8. https://doi: 10.1016/j.celrep.2018.07.101.

[52] López de Figueroa P, Lotz MK, Blanco FJ, Caramés B. Autophagy activation and protection from mitochondrial dysfunction in human chondrocytes. Arthritis Rheumatol 2015;67:966–976. https://doi: 10.1002/art.39025.

[53] Martín-Maestro P, Sproul A, Martinez H, Paquet D, Gerges M, Noggle S, et al. Autophagy induction by bexarotene promotes mitophagy in presenilin 1 familial Alzheimer's disease iPSC-derived neural stem cells. Mol Neurobiol 2019;56:8220–8236. https://doi: 10.1007/s12035-019-01665-y.

[54] Yang X, Wang J, Dai J, Shao J, Ma J, Chen C, et al. Autophagy protects against dasatinib-induced hepatotoxicity via p38 signaling. Oncotarget 2015;6:6203–17. https://doi.org/10.18632/oncotarget.3357.

[55] Liu J, Chang F, Li F, Fu H, Wang J, Zhang S, et al. Palmitate promotes autophagy and

apoptosis through ROS-dependent JNK and p38 MAPK. Biochem Biophys Res Commun 2015;463:262–7. https://doi.org/10.1016/j.bbrc.2015.05.042.

[56] Chen Y, Dorn GW. PINK1-phosphorylated mitofusin 2 is a parkin receptor for culling damaged mitochondria. Science 2013;340:471–5. https://doi.org/10.1126/science.1231031.

[57] Sebastián D, Hernández-Alvarez MI, Segalés J, Sorianello E, Muñoz JP, Sala D, et al. Mitofusin 2 (Mfn2) links mitochondrial and endoplasmic reticulum function with insulin signaling and is essential for normal glucose homeostasis. Proc Natl Acad Sci U S A 2012;109:5523–8. https://doi.org/10.1073/pnas.1108220109.

[58] Akundi RS, Huang Z, Eason J, Pandya JD, Zhi L, Cass WA, et al. Increased mitochondrial calcium sensitivity and abnormal expression of innate immunity genes precede dopaminergic defects in Pink1-deficient mice. PLoS One 2011;6:e16038. https://doi.org/10.1371/journal.pone.0016038.

[59] Yamada T, Dawson TM, Yanagawa T, Iijima M, Sesaki H. SQSTM1/p62 promotes mitochondrial ubiquitination independently of PINK1 and PRKN/parkin in mitophagy. Autophagy 2019;15:2012–2018. https://doi.org/10.1080/15548627.2019.1643185.

[60] Lim JS, Mietus-Snyder M, Valente A, Schwarz JM, Lustig RH. The role of fructose in the pathogenesis of NAFLD and the metabolic syndrome. Nat Rev Gastroenterol Hepatol 2010;7:251–64. https://doi.org/10.1038/nrgastro.2010.41.

[61] Simoes ICM, Janikiewicz J, Bauer J, Karkucinska-Wieckowska A, Kalinowski P. Dobrzyn A et al. Fat and Sugar-A Dangerous Duet. A Comparative Review on Metabolic Remodeling in Rodent Models of Nonalcoholic Fatty Liver Disease. Nutrients. 2019;11(12):2871. doi:10.3390/nu11122871

[62] Hu Y, Semova I, Sun X, Kang H, Chahar S, Hollenberg AN, et al. Fructose and glucose can regulate mammalian target of rapamycin complex 1 and lipogenic gene expression via distinct pathways. J Biol Chem 2018;293:2006–14. https://doi.org/10.1074/jbc.M117.782557.

[63] Montgomery MK, Fiveash CE, Braude JP, Osborne B, Brown SHJ, Mitchell TW, et al. Disparate metabolic response to fructose feeding between different mouse strains. Sci Rep 2015;5:18474. https://doi.org/10.1038/srep18474.

[64] Gaude E, Schmidt C, Gammage PA, Dugourd A, Blacker T, Chew SP, et al. NADH Shuttling Couples Cytosolic Reductive Carboxylation of Glutamine with Glycolysis in Cells with Mitochondrial Dysfunction. Mol Cell 2018;69:581-593. https://doi.org/10.1016/j.molcel.2018.01.034.

[65] Chen Q, Kirk K, Shurubor YI, Zhao D, Arreguin AJ, Shahi I, et al. Rewiring of glutamine metabolism is a bioenergetic adaptation of human cells with mitochondrial DNA mutations. Cell Metab 2018;27:1007–1025. https://doi.org/10.1016/j.cmet.2018.03.002.

[66] Tang Y, Wallace M, Sanchez-Gurmaches J, Hsiao WY, Li H, Lee PL, et al. Adipose tissue mTORC2 regulates ChREBP-driven de novo lipogenesis and hepatic glucose metabolism. Nat Commun 2016:7:11365. https://doi.org/10.1038/ncomms11365.

[67] Cao H, Gerhold K, Mayers JR, Wiest MM, Watkins SM, Hotamisligil GS. Identification of a lipokine, a lipid hormone linking adipose tissue to systemic metabolism. Cell 2008;134:933–44. https://doi.org/10.1016/j.cell.2008.07.048.

[68] Yore MM, Syed I, Moraes-Vieira PM, Zhang T, Herman MA, Homan EA, et al. Discovery of a class of endogenous mammalian lipids with anti-diabetic and anti-inflammatory effects. Cell 2014;159:318–32. https://doi.org/10.1016/j.cell.2014.09.035.

[69] Yew Tan C, Virtue S, Murfitt S, Robert LD, Phua YH, Dale M, et al. Adipose tissue fatty acid chain length and mono-unsaturation increases with obesity and insulin resistance. Sci Rep 2015;5:18366. https://doi.org/10.1038/srep18366.

[70] Thörne A, Lönnqvist F, Apelman J, Hellers G, Arner P. A pilot study of long-term effects of a novel obesity treatment: Omentectomy in connection with adjustable gastric banding. Int J Obes 2002;26:193–9. https://doi.org/10.1038/sj.ijo.0801871.

[71] Muzumdar R, Allison DB, Huffman DM, Ma X, Atzmon G, Einstein FH, et al. Visceral adipose tissue modulates mammalian longevity. Aging Cell 2008;7:438–40. https://doi.org/10.1111/j.1474-9726.2008.00391.x.

[72] Tran TT, Kahn CR. Transplantation of adipose tissue and stem cells: Role in metabolism and disease. Nat Rev Endocrinol 2010;6:195–213. https://doi.org/10.1038/nrendo.2010.20.

[73] Booth AD, Magnuson AM, Fouts J, Wei Y, Wang D, Pagliassotti MJ, et al. Subcutaneous adipose tissue accumulation protects systemic glucose tolerance and muscle

metabolism. Adipocyte 2018;7:261–272. https://doi.org/10.1080/21623945.2018.1525252.

[74] Cox-York K, Wei Y, Wang D, Pagliassotti MJ, Foster MT. Lower body adipose tissue removal decreases glucose tolerance and insulin sensitivity in mice with exposure to high fat diet. Adipocyte 2015;4:32–43. https://doi.org/10.4161/21623945.2014.957988.

[75] Zhang Y, Wang H, Zhang L, Yuan Y, Yu D. Codonopsis lanceolata polysaccharide CLPS alleviates high fat/high sucrose diet-induced insulin resistance via anti-oxidative stress. Int J Biol Macromol 2019; pii: S0141-8130(19)35823-4. https://doi.org/10.1016/j.ijbiomac.2019.09.185.

[76] Gaballah HH, El-Horany HE, Helal DS. Mitigative effects of the bioactive flavonol fisetin on high-fat/high-sucrose induced nonalcoholic fatty liver disease in rats. J Cell Biochem 2019;120:12762–774. https://doi.org/10.1002/jcb.28544.

[77] Anhê FF, Nachbar RT, Varin T V., Vilela V, Dudonné S, Pilon G, et al. A polyphenol-rich cranberry extract reverses insulin resistance and hepatic steatosis independently of body weight loss. Mol Metab 2017;6:1563–73. https://doi.org/10.1016/j.molmet.2017.10.003.

[78] Chu MJJ, Hickey AJR, Jiang Y, Petzer A, Bartlett ASJR, Phillips ARJ. Mitochondrial dysfunction in steatotic rat livers occurs because a defect in complex i makes the liver susceptible to prolonged cold ischemia. Liver Transplant 2015;21:396–407. https://doi.org/10.1002/lt.24024.

[79] Milton-Laskibar I, Aguirre L, Etxeberria U, Milagro FI, Martínez JA, Portillo MP. Involvement of autophagy in the beneficial effects of resveratrol in hepatic steatosis treatment. A comparison with energy restriction. Food Funct 2018;9:4207–15. https://doi.org/10.1039/c8fo00930a.

[80] Sun Y, Xia M, Yan H, Han Y, Zhang F, Hu Z, et al. Berberine attenuates hepatic steatosis and enhances energy expenditure in mice by inducing autophagy and fibroblast growth factor 21. Br J Pharmacol 2018;175:374–87. https://doi.org/10.1111/bph.14079.

[81] Hemmings BA, Restuccia DF. PI3K-PKB/Akt pathway. Cold Spring Harb Perspect Biol 2012;4:a011189. https://doi.org/10.1101/cshperspect.a011189.

FIGURE LEGENDS

Fig. 1. High-fat high-sucrose diet promotes steatohepatitis. Changes in body weight (A), cumulative food intake (B), energy intake (C), biochemical parameters (D), liver weight and histological variables (E and F) in mice fed with a chow diet (CD), high-fat diet (HFD) or high-fat high sucrose diet (HF-HSD). Results are shown as means and standard error of the mean. *p<0.05, **p<0.01, ***p<0.001; NAS: Non-alcoholic fatty liver activity score

Fig. 2. High-fat high-sucrose diet increases hepatic oxidative stress.
Immunohistochemical analyses (A) enzyme activity assays (B), and immunoblotting analyses (C) of oxidative stress markers and antioxidant enzymes in mice fed with a chow diet (CD), high-fat diet (HFD) or high-fat high-sucrose diet (HF-HSD). Results are shown as means and standard error of the mean; *p<0.05, **p<0.01

Fig. 3. Loss of hepatic metabolic adaptation in mice with steatohepatitis. .
Immunoblotting analyses (A) of mitochondrial complexes, and key proteins involved in the *de novo* lipogenic pathway and expression of mitochondrial and cytosolic genes (B) in mice fed with a chow diet (CD), high-fat diet (HFD) or high-fat high-sucrose diet (HF-HSD). Results are shown as means and standard error of the mean; *p < 0.05.
ACC: acetyl-CoA carboxylase; ACLY: ATP-citrate lyase; IDH 1: Isocitrate dehydrogenase 1; IDH 2: Isocitrate dehydrogenase 2; FAH: fumarylacetoacetate hydrolase; FASN, fatty acid synthase; OGDH: Oxoglutarate dehydrogenase; SDHA: succinate dehydrogenase. The other parameters analyzed in (A) are different complexes of oxidative phosphorylation.

Fig. 4. High-fat high-sucrose diet induces mitophagy defects. ((A) Immunoblotting analyses of autophagy and mitophagy components. Results are shown as means and standard error of the mean; *p<0.05
AMPK: AMP-activated protein kinase; ATG7: autophagy-related protein 7; LC3: microtubule-associated proteins 1A/1B light chain 3; MFN2: mitofusin 2; MAPK:

mitogen activated protein kinase; mTOR: mammalian target of rapamycin; P62: sequestosome 1; PARKIN: E3 ubiquitin- protein ligase parkin; PINK1: PTEN-induced putative kinase 1; TOM20: translocase outer membrane 20.

Fig. 5. The loss of adipose tissue dynamics is associated with an increase in adipocyte size. (A to C): Histological analyses of perigonadal white adipose tissue (pgWAT) and inguinal white adipose tissue (iWAT) were performed to determine the adipocyte size. (D): Immunoblotting analyses of proteins regulating lipolysis, lipogenesis, and mitochondrial status. Results are shown as means and standard error of the mean; *p<0.01, **p<0.001

ACC: acetyl-CoA carboxylase; AMPK: AMP-activated protein kinase; FAH: fumarylacetoacetate hydrolase; FASN, fatty acid synthase, HSL, hormone sensitive lipase; TOM20: translocase outer membrane 20; UCP-1, uncoupling protein 1. The other parameters analyzed in (D) are different complexes of oxidative phosphorylation

Fig. 6. Changes in the levels of lipid species in perigonadal adipose tissue linked to the high-fat high-sucrose diet. Graphical representation of the acetyl-CoA metabolism focusing on β-oxidation and the synthesis of fatty acid, bile acids, steroid, and phospholipids

CA: acid cholic; CDCA: chenodeoxycholic acid; DAG: diacilglicerol; DCA: deoxycholic acid; GCA: glycocholic acid; GCDCA: glycochenodeoxycholic acid; GLCA: glycolithocholate acid; GDCA: glycodeoxycholic acid; GUDCA: glycoursodeoxycholic acid; G3P: glycerol-3-phosphate; LPA: lysophosphatidic acid; LPS: lysophosphatidylserine; PA: phosphatidic acid; TCA: taurocholic acid; TCDCA: taurochenodeoxycholic acid; lithocholic acid; TDCA: taurodeoxycholic acid; TLCA: taurolithocholic acid; TUDCA; tauroursodeoxycholic acid.

Table 1. Results of the metabolomic study in the liver. CD: Chow diet; HFD: High-fat diet; HF-HSD: High-fat high-sucrose diet. [a] $p < 0.05$, [b] $p < 0.01$, with respect to CD. Results are shown as median plus interquartile range (25-75).

Metabolite	CD	HFD	HF-HSD
Glycolysis Pathway			
Glucose 6-P	0.4 (0.3 - 0.5)	0.6 (0.5 - 0.6)[a]	0.1 (0.1 - 0.3)[b]
Fructose 6-P	0.8 (0.5 - 1.4)	2.0 (1.8 - 2.3)[a]	0.2 (0.2 - 0.6)[a]
Fructose 1,6-BisP	0.5 (0.3 - 0.6)	0.7 (0.7 - 0.8)[a]	0.1 (0.1 - 0.3)[b]
3-Phosphoglycerate	2.7 (1.0 - 3.0)	0.3 (0.2 - 0.5)[b]	3.2 (2.5 - 4.0)
Phosphoenolpyruvate	1.2 (0.3 - 1.4)	0.1 (0.04 - 0.1)[b]	1.1 (0.7 - 1.6)
Pyruvate	6.5 (3.5 - 12.6)	3.1 (1.9 - 4.2)[a]	3.7 (2.8 - 8.5)
Lactate	33.8 (28.5 - 47.8)	31.3 (29.4 - 37.0)	30.0 (30.0 - 31.4)
Pentose Phosphate Pathway			
6-P-Glucanate	0.3 (0.3 - 0.3)	0.1 (0.1 - 0.2)[a]	0.1 (0.1 - 0.2)[b]
Ribose 5-P	0.4 (0.3 - 0.5)	1.1 (0.8 - 1.6)[a]	0.2 (0.1 - 0.3)[a]
Citric Acid Cycle Pathway			
Oxaloacetate	5.2 (3.3 - 8.4)	1.2 (0.9 - 1.2)[b]	1.5 (1.1 - 2.5)[b]
Citrate	1.0 (0.6 - 0.4)	0.6 (0.4 - 1.5)[b]	0.05 (0.04 - 0.06)[a]
α-Ketoglutarate	0.6 (0.3 - 1.8)	0.2 (0.1 - 0.2)[b]	0.2 (0.1 - 0.6)[b]
Succinate	1.4 (1.3 - 1.5)	1.1 (0.9 - 1.4)[a]	1.3 (1.3 - 1.4)
Fumarate	3.4 (3.3 - 3.5)	2.2 (1.9 - 2.7)[b]	2.2 (2.2 - 2.6)[b]
Malate	12.1 (12.1 - 12.2)	7.3 (5.2 - 9.0)[b]	7.3 (6.8 - 9.3)[a]
Glutaminolysis Pathway			
Glutamine	0.9 (0.3 - 3.0)	0.4 (0.1 - 0.7)[a]	1.2 (0.9 - 1.8)
Glutamate	9.0 (8.5 - 12.8)	7.1 (6.8 - 8.1)[a]	8.5 (7.7 - 9.8)
Amino acids metabolism			
Alanine	9.9 (9.3 - 10.3)	9.0 (7.1 - 11.1)	9.6 (7.8 - 12.4)
Aspartate	2.4 (2.0 - 2.6)	1.1 (0.9 - 1.4)[b]	1.9 (1.3 - 2.5)
Isoleucine	3.3 (3.0 - 4.2)	2.4 (2.3 - 2.7)[b]	4.0 (3.5 - 5.0)
Leucine	8.0 (7.6 - 8.9)	5.5 (4.6 - 6.2)[b]	8.1 (7.3 - 9.3)
Serine	10.0 (9.6 - 10.7)	7.5 (6.8 - 7.8)[b]	11.0 (9.8 - 11.3)
Valine	5.5 (4.8 - 5.8)	4.1 (3.4 - 4.4)[b]	5.1 (4.5 - 5.7)
Ketone bodies			
3-Hydroxybutyrate	2.9 (2.3 -5.4)	2.4 (1.6 - 4.1)	4.1 (3.3 - 6.9)

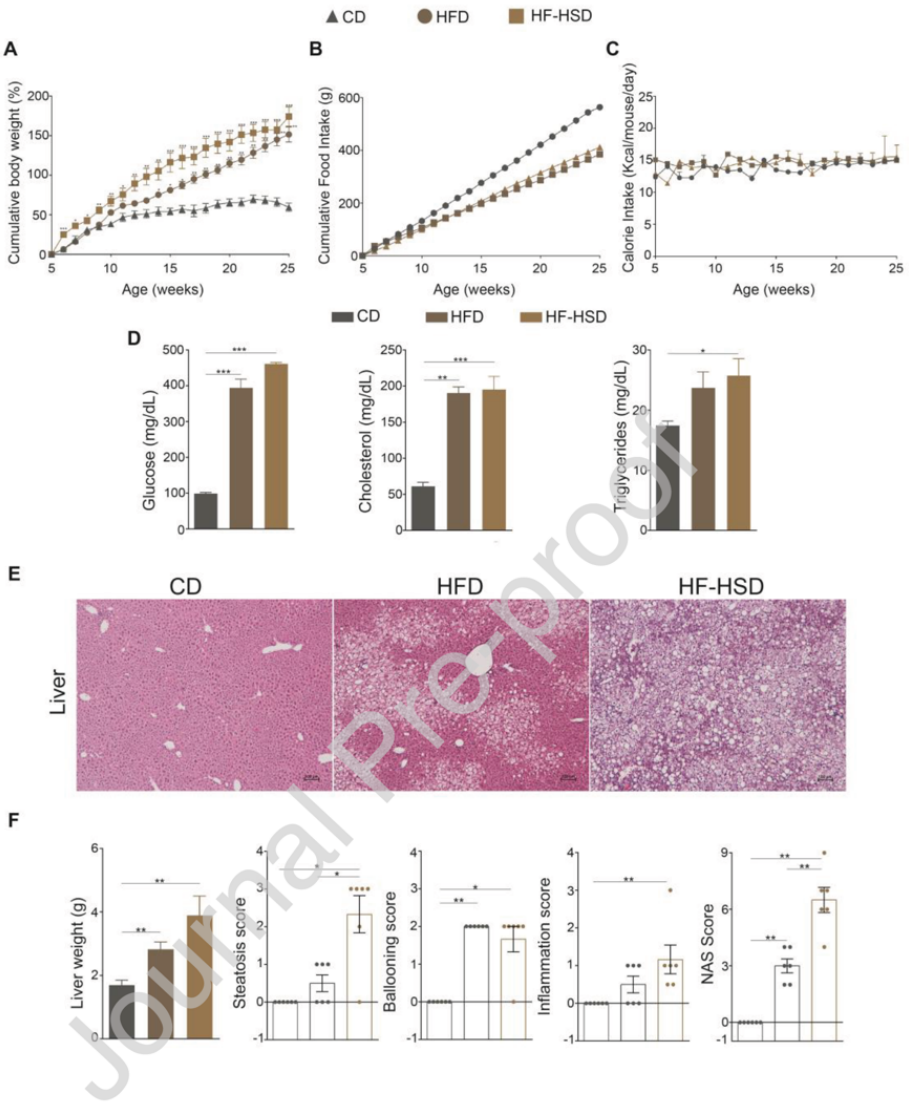

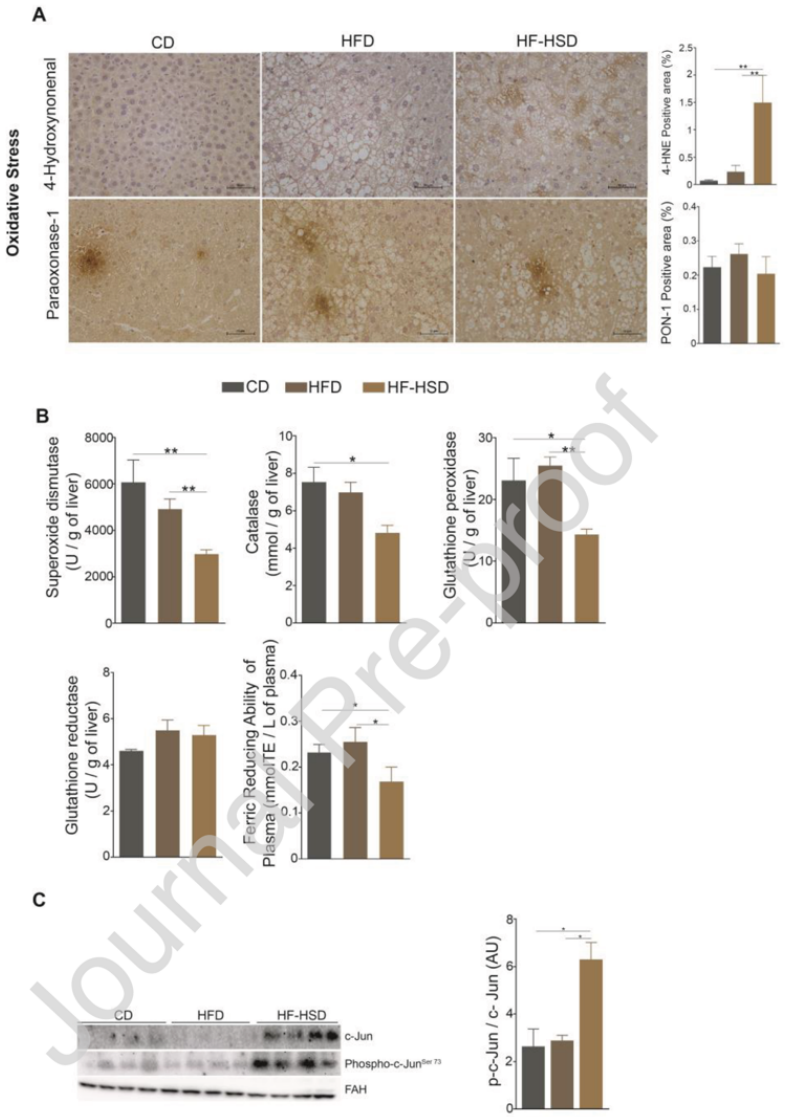

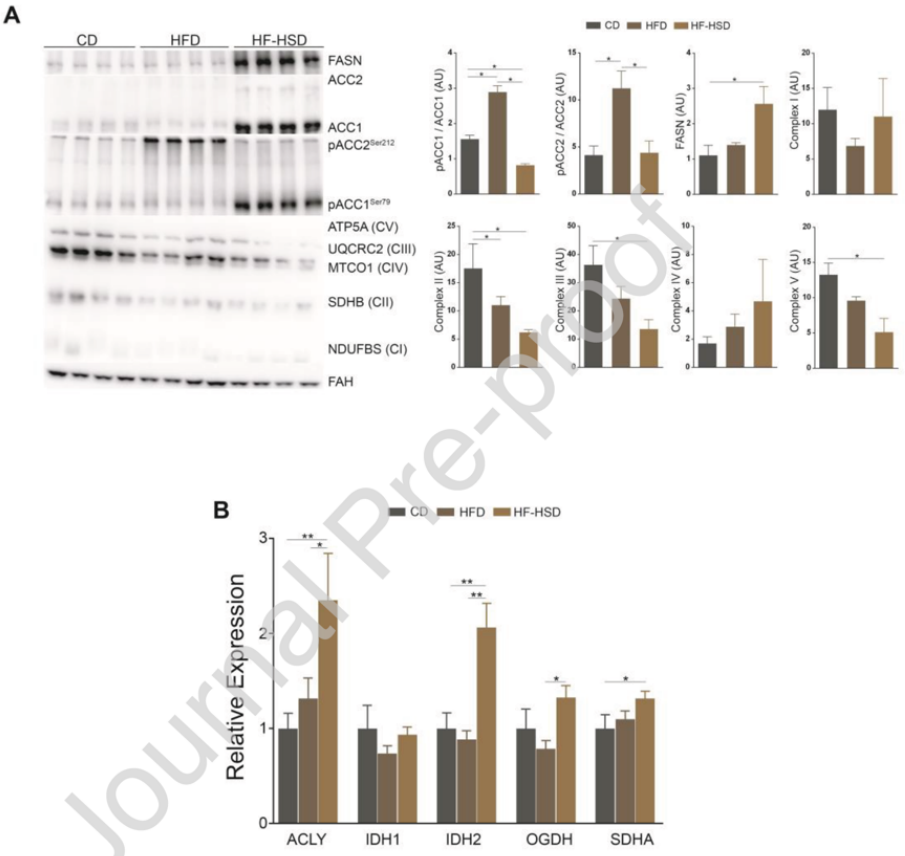

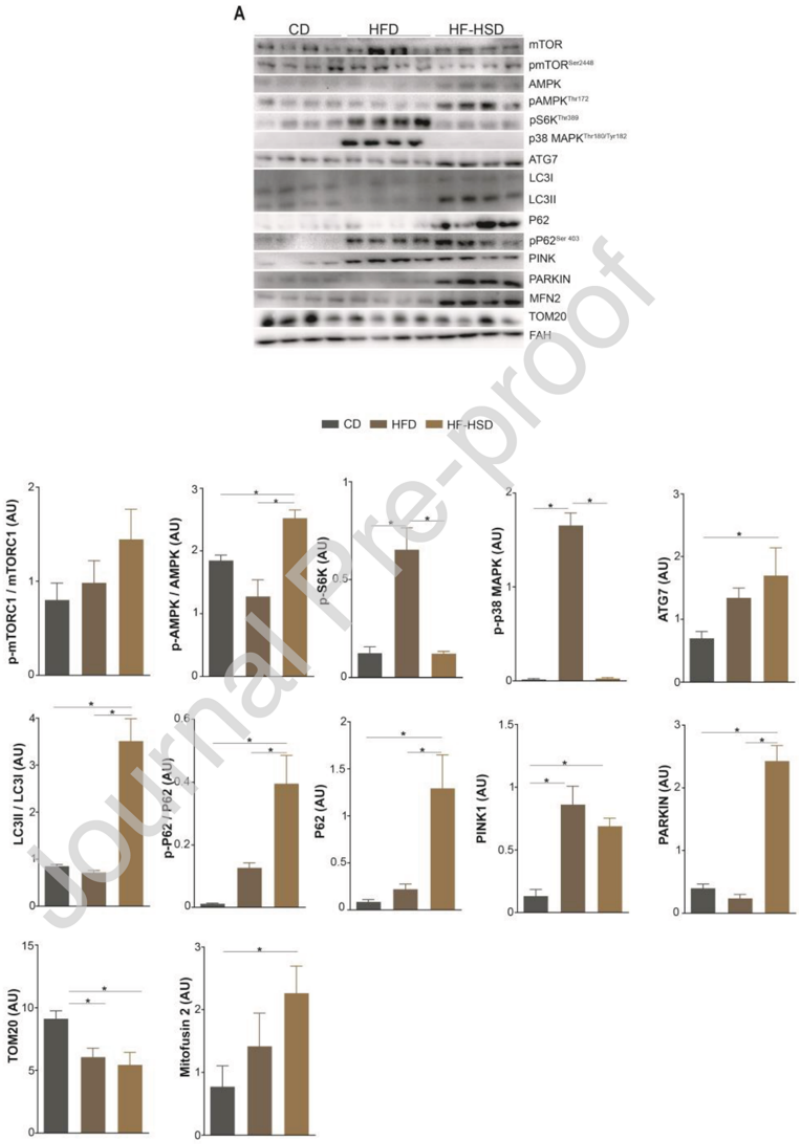

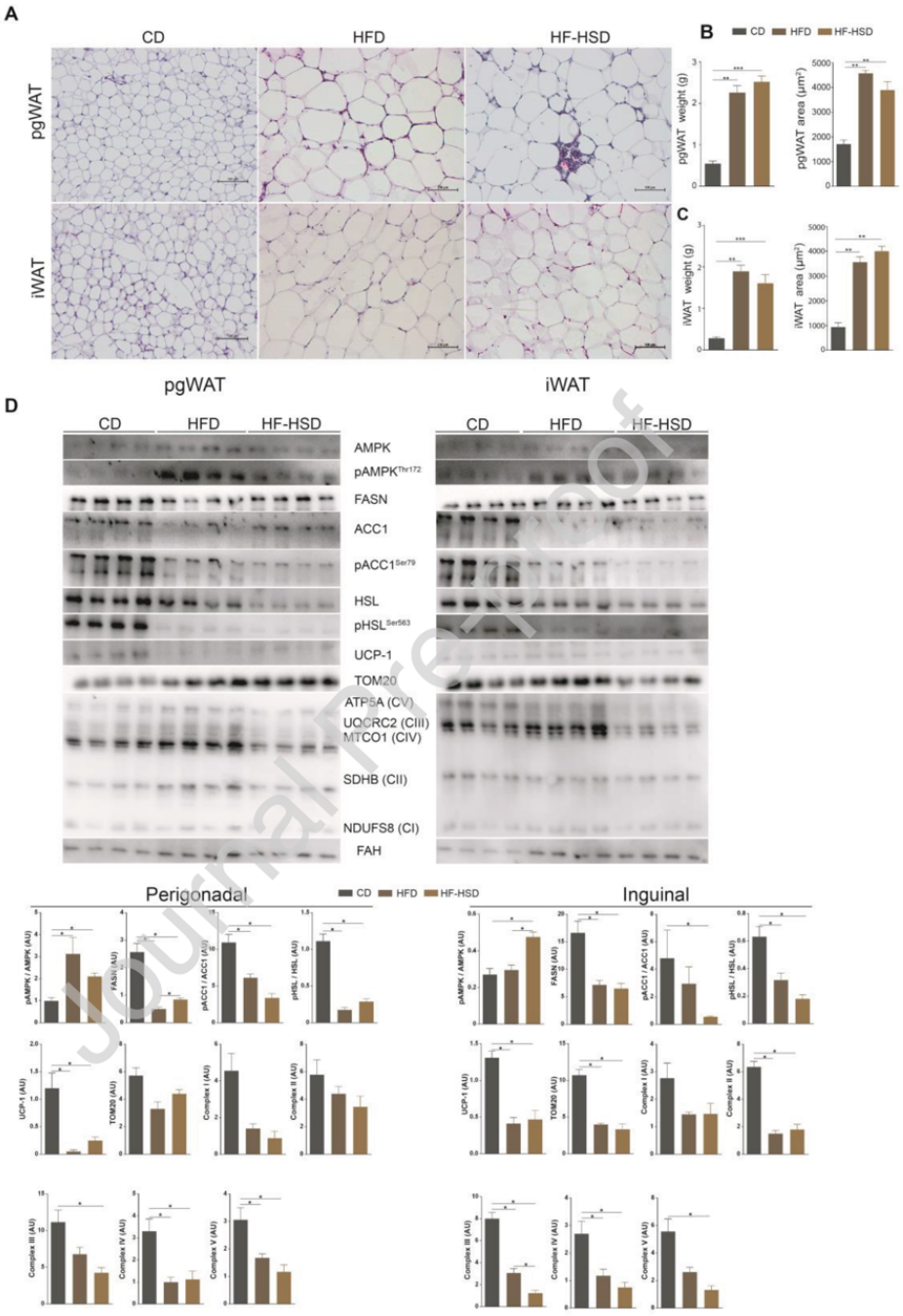

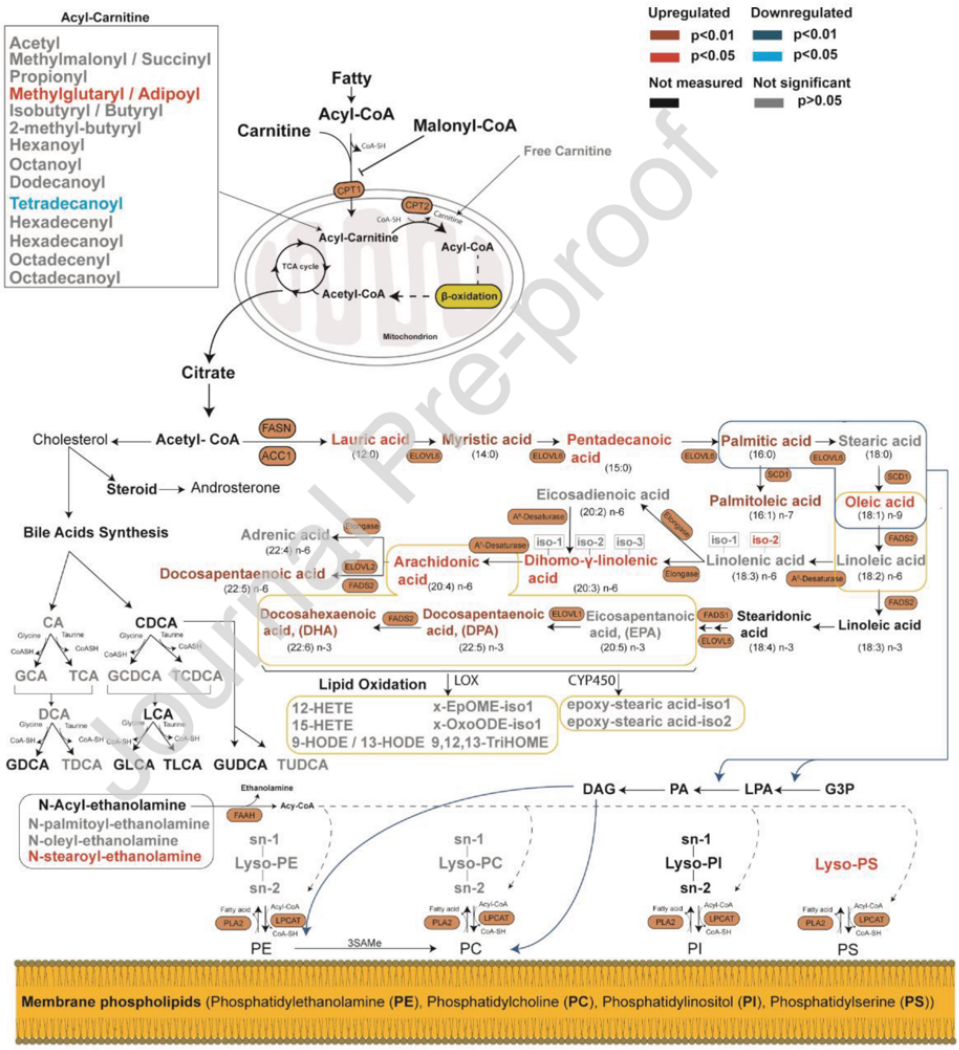

Graphical Abstract

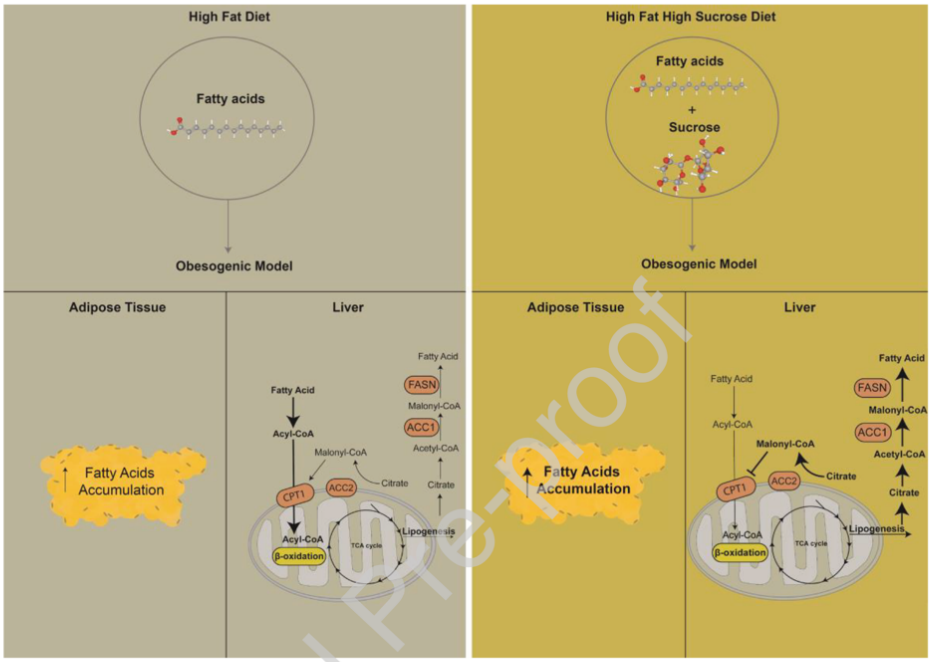

Supporting Information Table S1. Nutritional composition of chow diet (CD), high-fat diet (HFD), and high-fat high-sucrose diet (HF-HSD)
ND: Not detected.

	CD	HFD	HF-HSD
Crude Nutrients			
Crude protein, %	16.1	24.10	17.3
Crude fat, %	3.1	34.60	23.2
Crude fiber, %	3.9	7.2	5.0
Carbohydrate (available), %	71.8	24.80	47.6
Crude ash, %	4.2	8.5	ND
Nitrogen-free extracts, %	43.5	23.30	ND
Energy			
Energy density, Kcal/g (Kj/g))	3.3 (13.97)	5.7 (24)	4.7 (19.7)
Calories from protein, %	19.3	19	14.7
Calories from fat, %	8.3	60	44.6
Calories from carbohydrate, %	72.4	21	40.7
Minerals			
Calcium, %	1.38	0.98	0.62
Phosphorus, %	0.99	0.65	0.33
Sodium, %	0.47	0.20	0.13
Magnesium, %	0.34	0.17	0.06
Potassium, %	1.45	0.98	0.44
Chloride, %	0.69	-	0.19
Fatty acids			
Caprid acid (C10:0), %	ND	0.04	0.42
Lauric acid (C12:0), %	ND	0.07	0.65
Myristic acid (C14:0), %	ND	0.44	2.46
Palmitic acid (C16:0), %	0.87	7.72	5.72
Palmitoleic acid (C16:1), %	0.03	0.94	0.4
Margaric acid (C17:0), %	ND	-	ND
Stearic acid (C18:0), %	0.08	4.34	2.71
Oleic acid (C18:1), %	0.53	13.57	6.39
Linoleic acid (C18:2), %	1.34	4.75	1.67
Linolenic acid (C18:3), %	0.15	0.51	0.27
Arachidic acid (C20:0), %	ND	0.02	ND
Paullinic acid (C20:1), %	ND	0.01	ND
Arachidonic acid (C20:4), %	ND	0.53	ND
Cholesterol (mg/kg)	ND	265	576.6
Amino acids			
Lysine, %	3.9	1.98	1.37
Methionine, %	1.49	0.83	0.45
Cystine, %	1.08	0.46	0.35
Threonine, %	ND	1.07	0.74
Tryptophan, %	0.88	0.31	0.2
Arginine, %	4.75	0.88	0.64
Histidine, %	ND	0.76	0.49
Valine, %	ND	1.64	1.17
Isoleucine, %	ND	1.25	0.98
Leucine, %	ND	2.36	1.56
Phenylalanine, %	ND	1.29	0.86
Phe+Tyr, %	ND	2.57	ND
Glycine, %	0.41	0.50	0.31
Glutamic acid, %	ND	5.41	3.55
Aspartic acid, %	ND	1.79	1.17
Proline, %	ND	2.76	1.76
Alanine, %	ND	0.79	0.51
Serine, %	ND	1.43	0.98
Vitamins			
Vitamin A, IU/kg	7500	15000	14068
Vitamin D_3, IU/kg	1000	1500	1900
Vitamin E, IU/kg	120	225	143
Vitamin K (as menadione), mg/Kg	2.5	20	1.4
Vitamin C, mg/Kg	ND	30	0
Thiamin (B_1), mg/Kg	7	16	9.2
Riboflavin (B_2), mg/Kg	6.5	16	11.4
Pyridoxime (B_6), mg/Kg	2.6	18	10.9
Cyanocobalamin (B_{12}), µg/Kg	20	30	0.05
Nicotinic acid, mg/Kg	75	45	57
Pantothenic acid, mg/Kg	17	55	27.8
Folic acid, mg/Kg	0.5	19	3.8
Biotin, µg/Kg	40	310	380
Choline-Chloride, mg/Kg	1600	2300	1337
Inositol, mg/Kg	ND	80	ND
Trace elements			
Iron, mg/Kg	280	139	45.4
Manganese, mg/Kg	90	82	12.9
Zinc, mg/Kg	64	56	49.6
Copper, mg/Kg	18	12	7.6
Iodine, mg/Kg	ND	0.97	0.23
Selenium, mg/Kg	ND	0.13	0.18
Cobalt, mg/Kg	ND	0.13	ND

Supporting Information Table S2. Primary antibodies, and dilutions of primary and secondary antibodies used in immunohistochemistry and immunoblotting analyses

Protein	Protein name	Primary antibody	Primary antibody dilution	Secondary antibody dilution
Immunohistochemistry				
CD163	Cluster of Differentiation 163	Anti-CD163 antibody (ab182422, Abcam)	1/500	1/200
CCL2	Chemokine (C-C Motif) Ligand 2	Anti-MCP-1 antibody (ab25124, Abcam)	1/200	1/200
CD11b	Cluster of Differentiation 11b	Anti-CD11b antibody (ab133357, Abcam)	1/4000	1/200
CLEC4F	C-type lectin domain; family 4	Mouse CLEC4F/CLECSF13 Antibody (AF2784, R&D Systems)	1/200	1/200
F4/80	EGF-like module-containing mucin-like hormone receptor-like 1	Anti-F4/80 antibody (ab100790, Abcam)	1/100	1/200
PON1	Paraoxonase-1	In-house	1/100	1/200
TNFα	Tumor Necrosis Factor-α	Anti-TNFα antibody (ab6671, Abcam)	1/200	1/200
4-HNE	4-Hydroxy-2-nonenal	Anti-4 Hydroxynonenal antibody (ab46545, Abcam)	1/200	1/200
Immunoblotting				
ACC	Acetyl-CoA Carboxylase	Acetyl-CoA Carboxylase antibody (#3662, Cell signaling)	1/1000	1/1000
pACC	phospho-Acetyl-CoA Carboxylase	Phospho-Acetyl-CoA Carboxylase (Ser79) (D7D11) Rabbit mAb (#11818, Cell signaling)	1/1000	1/1000
pAMPK	phospho AMP-activated Protein Kinase	Anti-phospho-AMPKα (Thr172) antibody (#2531A, Cell signaling)	1/1000	1/5000
AMPK	AMP-activated Protein Kinase	Anti-AMPKα antibody (#2532, Cell signaling)	1/1000	1/5000
ATG7	Autophagy-related protein 7	Anti-ATG7 (D12B11) antibody (#8558, Cell signaling)	1/1000	1/5000
CCL2	Chemokine (C-C Motif) Ligand 2	Anti-MCP-1 antibody (ab25124, Abcam)	1/1000	1/5000
CD163	Cluster of Differentiation 163	Anti-CD163 antibody (ab182422, Abcam)	1/1000	1/5000
CD11b	Cluster of Differentiation 11b	Anti-CD11b antibody (ab133357, Abcam)	1/1000	1/5000
c-Jun	c-Jun	c-Jun (60A8) Rabbit mAb antibody (#9165, Cell signalin)	1/1000	1/1000
FAH	Fumarylacetoacetate hydrolase	FAH Polyclonal Antibody (PA5-30027, Invitrogen)	1/1000	1/5000
FASN	Fatty Acid Synthase	FASN Antibody (C20G5) Rabbit mAb (#3180, Cell signaling)	1/1000	1/1000
LC3B	Microtubule-associated proteins 1A/1B light chain 3B	Anti-LC3B antibody (#2775, Cell signaling)	1/1000	1/5000
MFN2	Mitofusin 2	Recombinant Anti-Mitofusin 2 antibody [NIAR164] (ab124773, Abcam)	1/1000	1/5000
mTOR	Mammalian target of rapamycin complex I	mTOR Antobody (#2972, Cell signaling)	1/1000	1/1000
pmTOR	phospho-Mammalian target of rapamycin complex I	Phospho-mTOR (Ser2448) antibody (#2971, Cell signaling)	1/1000	1/1000
HSL	Hormone Sensitive Lipase	HSL Antibody #4107	1/1000	1/1000
pHSL	phospho-Hormone Sensitive Lipase	Phospho-HSL (Ser563) Antibody (#4139, Cell signaling)	1/1000	1/1000
OXPHOS	Oxidative Phosphorylation	Total OXPHOS Rodent WB antibody cocktail (ab110413, Abcam)	1/250	1/1000

P62	Sequestosome-1	p62/ SQSTM1 antibody (#5114, Cell signaling)	1/1000	1/5000
p-c-Jun	Phospho-c-Jun	Phospho-c-Jun (Ser73) Antibody (#9164, Cell signaling)	1/1000	1/1000
pMAPK	Phospho-p38 MAPK	Phospho-p38 MAPK (Thr180/Tyr182) Antibody (#9211, Cell signaling)	1/1000	1/1000
pP62	phospho-Sequestosome-1	Phospho-SQSTM1/P62 (Ser403) (D8D6T) Rabbit mAb (#39786, Cell signaling)	1/1000	1/5000
PINK1	PTEN-induced putative kinase 1	Anti-PINK1 antibody (ab23707, Abcam)	1/1000	1/5000
pS6K	Phospho-p70 S6 Kinase	Phospho-p70 S6 Kinase (Thr389) Antibody (#9205, Cell signaling)	1/1000	1/1000
PARKIN	E3 ubiquitin- protein ligase parkin	Parkin Antibody (#2132, Cell signaling)	1/1000	1/5000
TOM20	Translocase outer membrane 20	Tom20 (D8T4N) Rabbit mAb (#42406, Cell signaling)	1/1000	1/1000
UCP-1	Uncoupling protein 1	Anti-UCP1 antibody (ab10983, Abcam)	1/1000	1/1000

Supporting Information Table S3. Internal standards and their final concentrations used for the lipidomics analysis

Internal Standard	Final concentration (μM)
Acetylcarnitine-d3	0.25
Arachidonic acid-d_8	7.5
Butyrylcarnitine-d3	0.5
Cholic acid-d_5	1
Free carnitine-d9	1
Isovalerylcarnitine-d9	0.5
Lysophosphatidylcholine 18:1-d_7	7.5
Myristic acid-d_{27}	7.5
Myristoylcarnitine-d9	0.5
Octanoylcarnitine-d3	0.5
Palmitoylcarnitine-d3	0.1
Propionylcarnitine-d3	0.5
Taurocholic acid-d_5	0.5

Supporting Information Table S4. Standards and their highest concentrations used in the calibration curves of lipidomics analysis**.** Ten serial dilutions containing the internal standards mixture were prepared for quantitation purposes

Standard	Highest concentration (μM)
5-Hydroxyeicosatetraenoic acid	2
Arachidonic acid	200
Carnitine	0.5
Chenodeoxycholic acid	50
Cholic acid	50
Dehydroisoandrosterone 3-sulphate	50
Deoxycholic acid	50
Hydrocortisone	50
Lysophosphatidylcholine 16:0	50
Lysophosphatidylcholine 18:1	50
Sphingosine 1-phosphate	50
Taurocholic acid	50

Supporting Information Table S5. Retention times, *m/z and* polarity used to characterize lipid species. Standards used to quantify lipids and internal standards employed to correct the quantitation

Lipid	Retention time (min)	*m/z*	Polarity	Standard	Internal standard
11,12-DiHETE	6.29	335.2228	Negative	15-HETE	Myristic-27d
11,13-Eicosadienoic acid	11.96	307.2643	Negative	Arachidonic acid	Arachidonic Acid-d8
12-HETE	8.18	319.2279	Negative	15-HETE	Myristic-27d
15-HETE	7.86	319.2279	Negative	15-HETE	Myristic -27d
17-HDHA	7.49	343.2279	Negative	15-HETE	Myristic -27d
2-Methyl-butyryl-carnitine/Isovaleryl-carnitine/Valeryl-carnitine	3.35	246.17	Positive	Free carnitine	Isovalerylcarnitine-d9
5-HETE	9.17	319.2279	Negative	15-HETE	Myristic -27d
9,12,13-TriHOME	4.70	329.2333	Negative	15-HETE	Myristic -27d
9-HODE/13-HODE	7.66	295.2279	Negative	15-HETE	Myristic -27d
Adrenic acid	11.54	331.2643	Negative	Arachidonic acid	Arachidonic Acid-d8
Androsterone sulfate	4.29	369.1741	Negative	Dehydroepiandrosterone sulfate	Taurocholic acid-d5
Arachidonic acid	10.67	303.233	Negative	Arachidonic acid	Arachidonic Acid-d8
Cholic acid	5.36	407.2803	Negative	Deoxycholic acid	Cholic acid-d5
cis-Palmitoleic acid (palmitoleic)	10.57	253.2173	Negative	Arachidonic acid	Arachidonic Acid-d8
Decanoyl-carnitine/Fumaryl-carnitine	5.09	316.2482	Positive	Free carnitine	Octanoylcarnitine-d3
Deoxycholic acid	6.72	391.2854	Negative	Deoxycholic acid	Cholic acid-d5
Deoxycholic acid-iso1	5.29	391.2854	Negative	Deoxycholic acid	Cholic acid-d5
Dihomo-y-linolenic acid	11.22	305.2486	Negative	Arachidonic acid	Arachidonic Acid-d8
Dihomo-y-linolenic acid (isomer 2)	11.22	305.2486	Negative	Arachidonic acid	Arachidonic Acid-d8
Dihomo-y-linolenic acid (isomer 3)	11.51	305.2486	Negative	Arachidonic acid	Arachidonic Acid-d8
Docosahexaenoic acid (DHA)	10.40	327.233	Negative	Arachidonic acid	Arachidonic Acid-d8
Dodecanoyl-carnitine	5.88	344.2795	Positive	Free carnitine	Octanoylcarnitine-d3
Eicosapentaenoic acid (EPA)	9.88	301.2173	Negative	Arachidonic acid	Arachidonic Acid-d8
Epoxy-stearic acid (isomer 1)	7.89	297.2435	Negative	Arachidonic acid	Arachidonic Acid-d8
Epoxy-stearic acid (isomer 2)	10.06	297.2435	Negative	Arachidonic acid	Arachidonic Acid-d8
Free carnitine	1.19	162.1125	Positive	Free carnitine	Free carnitine-d9
Glycochenodeoxycholic acid	5.44	448.3068	Negative	Deoxycholic acid	Cholic acid-d5
Glycocholic cid	4.73	464.3018	Negative	Deoxycholic acid	Cholic acid-d5
Hexadecanoyl-carnitine	8.17	400.3421	Positive	Free carnitine	Palmitoylcarnitine-d3
Hexanoyl-carnitine	3.73	260.1856	Positive	Free carnitine	Octanoylcarnitine-d3
Isobutyryl-carnitine/Butyryl-carnitine	2.98	232.1543	Positive	Free carnitine	Butyrylcarnitine-d3
Lauric acid	8.79	199.1704	Negative	Arachidonic acid	Arachidonic Acid-d8

Linoleic acid (isomer 1)	10.88	279.233	Negative	Arachidonic acid	Arachidonic Acid-d8
Linolenic acid (isomer 1)	10.04	277.2173	Negative	Arachidonic acid	Arachidonic Acid-d8
Linolenic acid (isomer 2)	10.17	277.2173	Negative	Arachidonic acid	Arachidonic Acid-d8
LPC14:0-sn1	6.65	512.2994	Negative	LPC18:1-sn1	LPC18:1-d7
LPC14:0-sn2	6.41	512.2994	Negative	LPC18:1-sn1	LPC18:1-d7
LPC15:0-sn1	7.33	526.315	Negative	LPC18:1-sn1	LPC18:1-d7
LPC16:0-sn1	8.05	540.3307	Negative	LPC18:1-sn1	LPC18:1-d7
LPC16:0-sn2	7.77	540.3307	Negative	LPC18:1-sn1	LPC18:1-d7
LPC16:1-sn1	7.01	538.315	Negative	LPC18:1-sn1	LPC18:1-d7
LPC16:1-sn2	6.77	538.315	Negative	LPC18:1-sn1	LPC18:1-d7
LPC17:0-sn1	8.82	554.3463	Negative	LPC18:1-sn1	LPC18:1-d7
LPC17:0-sn2	8.63	554.3463	Negative	LPC18:1-sn1	LPC18:1-d7
LPC17:1-sn1	7.36	552.3307	Negative	LPC18:1-sn1	LPC18:1-d7
LPC17:1-sn2	7.18	552.3307	Negative	LPC18:1-sn1	LPC18:1-d7
LPC18:0-sn1	9.60	568.362	Negative	LPC18:1-sn1	LPC18:1-d7
LPC18:0-sn2	9.30	568.362	Negative	LPC18:1-sn1	LPC18:1-d7
LPC18:1-sn1	8.38	566.3463	Negative	LPC18:1-sn1	LPC18:1-d7
LPC18:1-sn2	8.13	566.3463	Negative	LPC18:1-sn1	LPC18:1-d7
LPC18:2-sn1	7.45	564.3307	Negative	LPC18:1-sn1	LPC18:1-d7
LPC18:2-sn2	7.21	564.3307	Negative	LPC18:1-sn1	LPC18:1-d7
LPC18:3-sn1	6.73	562.315	Negative	LPC18:1-sn1	LPC18:1-d7
LPC19:0-sn1	10.37	582.3776	Negative	LPC18:1-sn1	LPC18:1-d7
LPC19:0-sn2	10.09	582.3776	Negative	LPC18:1-sn1	LPC18:1-d7
LPC20:0-sn1	11.15	596.3933	Negative	LPC18:1-sn1	LPC18:1-d7
LPC20:1-sn1	9.81	594.3776	Negative	LPC18:1-sn1	LPC18:1-d7
LPC20:1-sn2	9.52	594.3776	Negative	LPC18:1-sn1	LPC18:1-d7
LPC20:2-sn1	8.74	592.362	Negative	LPC18:1-sn1	LPC18:1-d7
LPC20:2-sn2	8.47	592.362	Negative	LPC18:1-sn1	LPC18:1-d7
LPC20:3-sn1	7.94	590.3463	Negative	LPC18:1-sn1	LPC18:1-d7
LPC20:3-sn2	7.71	590.3463	Negative	LPC18:1-sn1	LPC18:1-d7
LPC20:4-sn1	7.43	588.3307	Negative	LPC18:1-sn1	LPC18:1-d7
LPC20:4-sn2	7.24	588.3307	Negative	LPC18:1-sn1	LPC18:1-d7
LPC20:5-sn2	6.56	586.315	Negative	LPC18:1-sn1	LPC18:1-d7
LPC22:3-sn2	9.22	618.3776	Negative	LPC18:1-sn1	LPC18:1-d7
LPC22:4-sn1	8.48	616.362	Negative	LPC18:1-sn1	LPC18:1-d7
LPC22:4-sn2	8.25	616.362	Negative	LPC18:1-sn1	LPC18:1-d7
LPC22:5-sn1	7.71	614.3463	Negative	LPC18:1-sn1	LPC18:1-d7

LPC22:5-sn2	7.52	614.3463	Negative	LPC18:1-sn1	LPC18:1-d7
LPC22:6-sn1	7.36	612.3307	Negative	LPC18:1-sn1	LPC18:1-d7
LPC22:6-sn2	7.17	612.3307	Negative	LPC18:1-sn1	LPC18:1-d7
LPE14:0-sn1	6.60	424.247	Negative	LPC18:1-sn1	LPC18:1-d7
LPE15:0-sn1	7.27	438.2626	Negative	LPC18:1-sn1	LPC18:1-d7
LPE16:0-sn1	7.99	452.2783	Negative	LPC18:1-sn1	LPC18:1-d7
LPE16:0-sn2	7.71	452.2783	Negative	LPC18:1-sn1	LPC18:1-d7
LPE16:1-sn1	7.04	450.2626	Negative	LPC18:1-sn1	LPC18:1-d7
LPE16:1-sn2	6.71	450.2626	Negative	LPC18:1-sn1	LPC18:1-d7
LPE17:0-sn1	8.77	466.2939	Negative	LPC18:1-sn1	LPC18:1-d7
LPE17:1-sn1	7.63	464.2783	Negative	LPC18:1-sn1	LPC18:1-d7
LPE18:0-sn1	9.55	480.3096	Negative	LPC18:1-sn1	LPC18:1-d7
LPE18:0-sn2	9.24	480.3096	Negative	LPC18:1-sn1	LPC18:1-d7
LPE18:1-sn1	8.34	478.2939	Negative	LPC18:1-sn1	LPC18:1-d7
LPE18:1-sn2	8.08	478.2939	Negative	LPC18:1-sn1	LPC18:1-d7
LPE18:2-sn1	7.39	476.2783	Negative	LPC18:1-sn1	LPC18:1-d7
LPE18:2-sn2	7.16	476.2783	Negative	LPC18:1-sn1	LPC18:1-d7
LPE20:1-sn1	9.78	506.3252	Negative	LPC18:1-sn1	LPC18:1-d7
LPE20:1-sn2	9.50	506.3252	Negative	LPC18:1-sn1	LPC18:1-d7
LPE20:2-sn1	8.69	504.3096	Negative	LPC18:1-sn1	LPC18:1-d7
LPE20:3-sn1	7.90	502.2939	Negative	LPC18:1-sn1	LPC18:1-d7
LPE20:3-sn2	7.68	502.2939	Negative	LPC18:1-sn1	LPC18:1-d7
LPE20:4-sn1	7.39	500.2783	Negative	LPC18:1-sn1	LPC18:1-d7
LPE20:4-sn2	7.19	500.2783	Negative	LPC18:1-sn1	LPC18:1-d7
LPE20:5-sn1	6.71	498.2626	Negative	LPC18:1-sn1	LPC18:1-d7
LPE20:5-sn2	6.53	498.2626	Negative	LPC18:1-sn1	LPC18:1-d7
LPE22:4-sn1	8.44	528.3096	Negative	LPC18:1-sn1	LPC18:1-d7
LPE22:4-sn2	8.22	528.3096	Negative	LPC18:1-sn1	LPC18:1-d7
LPE22:5-sn1	7.66	526.2939	Negative	LPC18:1-sn1	LPC18:1-d7
LPE22:5-sn2	7.33	526.2939	Negative	LPC18:1-sn1	LPC18:1-d7
LPE22:6-sn1	7.31	524.2783	Negative	LPC18:1-sn1	LPC18:1-d7
LPE22:6-sn2	7.14	524.2783	Negative	LPC18:1-sn1	LPC18:1-d7
LPI16:1	6.60	569.2732	Negative	LPC18:1-sn1	LPC18:1-d7
LPS17:1	5.34	508.2681	Negative	LPC18:1-sn1	LPC18:1-d7
LPS18:2	7.98	520.2681	Negative	LPC18:1-sn1	LPC18:1-d7
LPS18:3	7.05	518.2524	Negative	LPC18:1-sn1	LPC18:1-d7
LPS22:5	6.65	570.2837	Negative	LPC18:1-sn1	LPC18:1-d7

Methylglutaryl-carnitine/Adipoyl-carnitine	2.89	290.1598	Positive	Free carnitine	Butyrylcarnitine-d3
Methyl-malonyl-carnitine/Succinyl-carnitine	1.34	262.1285	Positive	Free carnitine	Acetylcarnitine-d3
Myristic acid	10.36	227.2017	Negative	Arachidonic acid	Myristic-27d
N-linoleoyl ethanolamine	9.75	368.2806	Negative	Arachidonic acid	Myristic-27d
N-oleoyl ethanolamine	10.26	370.2963	Negative	Arachidonic acid	Myristic-27d
N-palmitoyl ethanolamine	9.95	344.2806	Negative	Arachidonic acid	Myristic-27d
N-stearoyl-ethanolamine	11.43	372.3119	Negative	Arachidonic acid	Myristic-27d
Octadecadienyl-carnitine	7.62	424.3421	Positive	Free carnitine	Palmitoylcarnitine-d3
Octadecanoyl-carnitine	9.23	428.3734	Positive	Free carnitine	Palmitoylcarnitine-d3
Octadecenyl-carnitine	8.41	426.3578	Positive	Free carnitine	Palmitoylcarnitine-d3
Octanoyl-carnitine	4.30	288.2169	Positive	Free carnitine	Octanoylcarnitine-d3
Oleic acid	11.81	281.2486	Negative	Arachidonic acid	Arachidonic Acid-d8
Palmitic acid	11.69	255.233	Negative	Arachidonic acid	Arachidonic Acid-d8
Pentadecanoic acid	11.05	241.2173	Negative	Arachidonic acid	Arachidonic Acid-d8
Propionyl-carnitine	2.05	218.1387	Positive	Free carnitine	Propionylcarnitine-d3
Stearic acid	12.78	283.2643	Negative	Arachidonic acid	Arachidonic Acid-d8
Stearidonic acid	9.31	275.2017	Negative	Arachidonic acid	Arachidonic Acid-d8
Taurochenodeoxycholic acid	4.75	498.2895	Negative	Taurocholic acid	Taurocholic acid-d5
Taurocholic acid	4.34	514.2844	Negative	Taurocholic acid	Taurocholic acid-d5
Taurodeoxycholic acid	4.89	498.2895	Negative	Taurocholic acid	Taurocholic acid-d5
Tauroursodeoxycholic acid	4.32	498.2895	Negative	Taurocholic acid	Taurocholic acid-d5
Tetradecanoyl-carnitine	7.00	372.3108	Positive	Free carnitine	Miristoylcarnitine-d9
Ursodeoxycholic/Hyodeoxicholic acid	5.50	391.2854	Negative	Deoxycholic acid	Cholic acid-d5
w3-Docosapentaenoic acid	10.83	329.2486	Negative	Arachidonic acid	Arachidonic Acid-d8
w6-Docosapentaenoic acid	11.16	329.2486	Negative	Arachidonic acid	Arachidonic Acid-d8
x-EpOME (isomer 1)	9.03	295.2279	Negative	15-HETE	Myristic-27d
x-EpOME (isomer 2)	9.49	295.2279	Negative	15-HETE	Myristic-27d

HDHA, hydroxydocosahexaenoic acid; HETE, 5-hydroxyeicosatetraenoic acid; HODE, hydroxyoctadecadienoic acid HOME, hydroxyoctadecenoic acid; LPE, lysophosphatidylethanolamine; LPC, lysophosphatidylcholine; LPI, lysophosphatidylinositol; LPS, lysophosphatidylserine

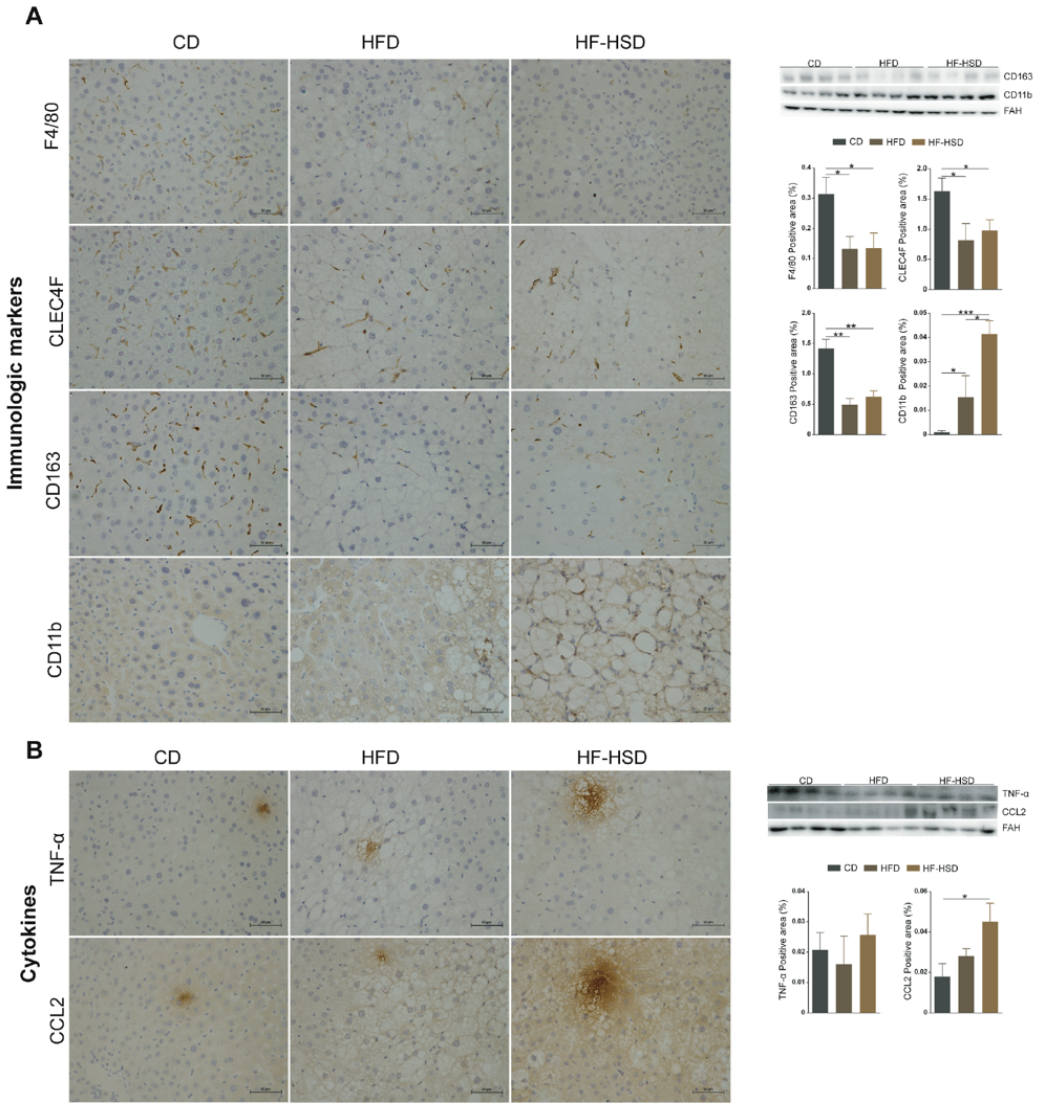

Supporting Information Figure S1. Immunohistochemical and immunoblotting analyses of immunologic markers and cytokines in mice fed with a chow diet (CD), high-fat diet (HFD) or high-fat high-sucrose diet (HF-HSD). Results are shown as means and standard error of the mean. *p < 0.05, **p < 0.01, ***p < 0.001. CCL2, chemokine (C-C motif) ligand 2; CD11b, cluster of differentiation 11b; CD163, cluster of differentiation 163; CLEC4F, c-type lectin domain family 4; F4/80, EGF-like module-containing mucin-like hormone receptor-like 1; FAH, fumarylacetoacetate hydrolase; TNFα, tumor necrosis factor-α

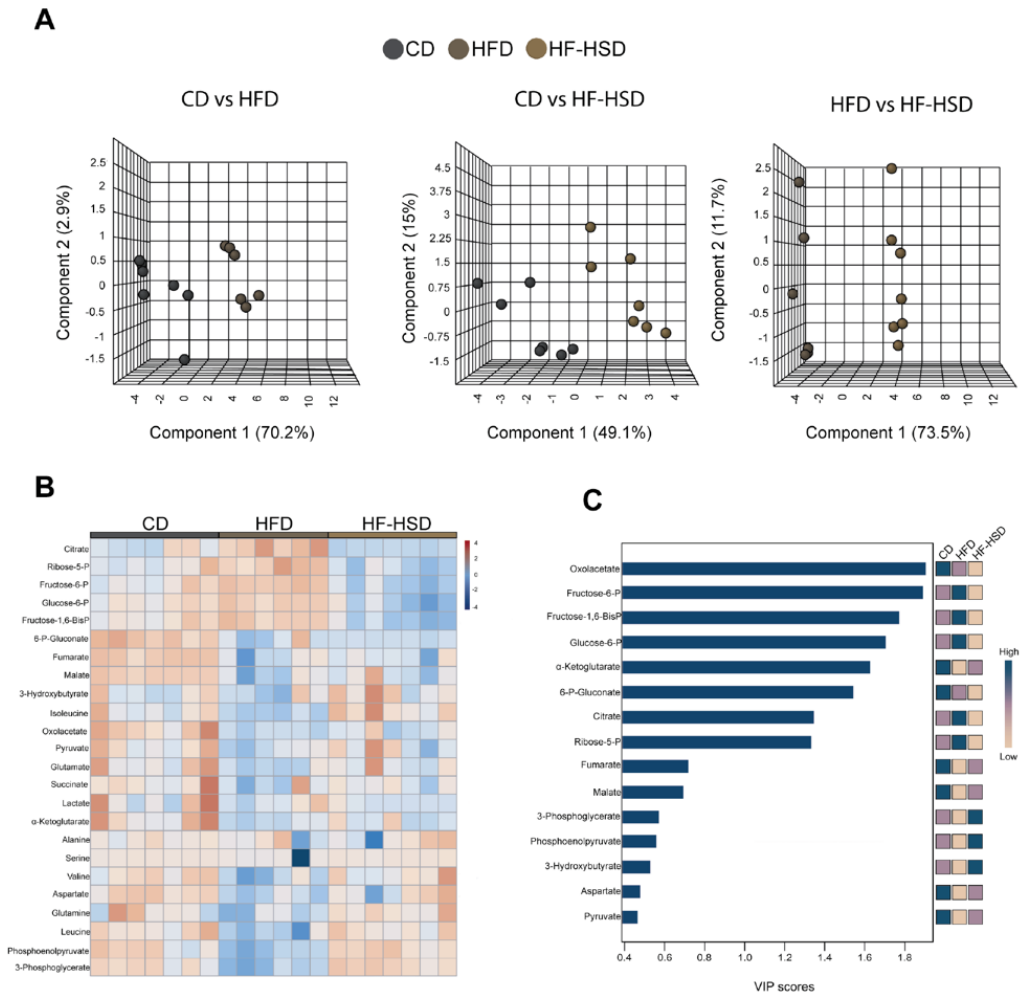

Supporting Information Figure S2. Partial least squares discriminant analysis (A), heatmap (B), variable importance in projection (VIP) score (C) of the global liver differences in energy balance-related metabolites between mice fed with a chow diet (CD), high-fat diet (HFD) or high-fat high-sucrose diet (HF-HSD)

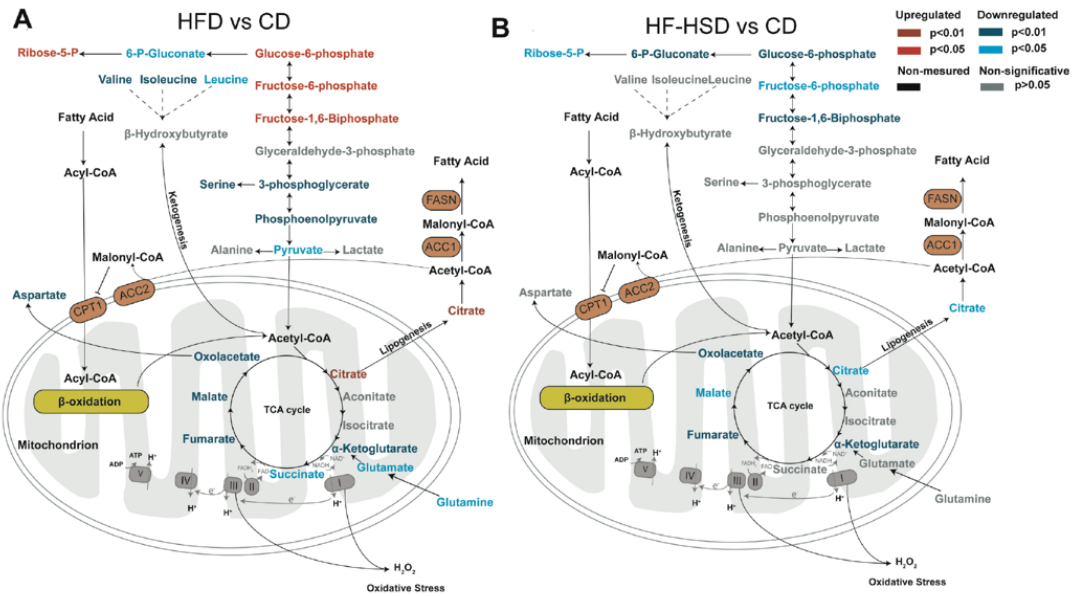

Supporting Information Figure S3. Graphical representation of the results obtained of hepatic energy metabolism depending on dietary treatment high fat diet (A) or high fat high sucrose diet (B). Metabolites are represented in red (significant increase), blue (significant decrease), grey (not significant) or black (not measured).

Supporting Information Table S6. Results of the lipidomics study in the liver. CD: Chow diet; HFD: High-fat diet; HF-HSD: High-fat high-sucrose diet. [a] $p < 0.05$, [b] $p < 0.01$, with respect to CD

Liver	CD	HFD	HF-HSD
Acyl-carnitines (µmol/g)			
Free carnitine	1.75 (0.69 - 3.59)	2.25 (1.77 - 2.56)	1.06 (0.76 - 2.21)
Methylmalonyl-carnitine / Succinyl-carnitine	5.93E-2 (4.05E-2 - 2.39E-1)	0.14 (9.99E-2 - 0.20)	9.27E-2 (6.03E-2 - 0.10)
Propionyl-carnitine	8.10E-3 (5.18E-3 - 3.34E-2)	7.37E-3 (2.84E-3 - 1.11E-2)	4.68E-3 (1.31E-3 - 6.24E-3)[a]
Methylglutaryl-carnitine / Adipoyl-carnitine	3.29E-2 (1.31E-2 - 8.15E-2)	2.19E-2 (1.56E-2 - 2.70E-2)	5.27E-3 (4.57E-3 - 6.28E-3)[b]
Isobutyryl-carnitine / Butyryl-carnitine	3.47E-3 (1.25E-3 - 1.05E-2)	1.97E-3 (1.87E-3 - 1.99E-3)	1.37E-3 (1.16E-3 - 3.04E-3)
2-methyl-butyryl-carnitine / Isovaleryl-carnitine / Valeryl-carnitine	3.09E-3 (1.51E-3 - 2.10E-2)	2.45E-3 (2.10E-3 - 2.57E-3)	2.73E-3 (2.46E-3 - 3.39E-3)
Hexanoyl-carnitine	1.42E-4(7.63E-5 - 2.30E-4)	7.25E-5 (5.70E-5 - 1.10E-4)	1.72E-4 (1.71E-4 - 1.89E-4)
Octanoyl-carnitine	1.52E-4 (6.74E-5 - 2.10E-4)	7.08E-5 (4.60E-5 - 1.03E-4)[a]	1.52E-4 (6.74E-5 - 2.10E-4)
Decanoyl-carnitine / Fumaryl-carnitine	2.93E-4 (1.42E-4 - 1.71E-3)	1.87E-4 (7.72E-5 - 3.38E-4)	1.36E-4 (7.29E-5 -5.42E-4)
Dodecanoyl-carnitine	3.14E-4 (1.58E-4 - 8.44E-4)	1.07E-4 (1.01E-4 - 1.13E-4)[b]	1.07E-4 (1.01E-4 - 2.22E-4)
Tetradecanoyl-carnitine	8.43E-4 (4.60E-4 - 3.15E-3)	4.44E-4 (2.63E-4 - 7.43E-4)	4.27E-4 (2.88E-4 - 1.12E-3)
Octadecadienyl-carnitine	2.38E-3 (1.26E-3 - 5.65E-3)	1.12E-3 (5.99E-4 - 1.74E-3)	5.71E-4 (4.90E-4 - 6.27E-4)[b]
Hexadecanoyl-carnitine	4.38E-3 (1.26E-3 - 8.16E-3)	3.53E-3 (1.77E-3 - 6.21E-3)	3.72E-3 (1.79E-3 - 4.77E-3)
Octadecenyl-carnitine	4.43E-3 (2.50E-3 - 1.13E-2)	6.35E-3 (3.39E-3 - 8.94E-3)	7.43E-3 (3.88E-3 - 9.96E-3)
Octadecanoyl-carnitine	7.95E-4 (4.14E-4 - 1.25E-3)	1.23E-3 (7.93E-4 - 1.58E-3)	4.99E-4 (2.84E-4 - 7.63E-4)
N-acylethanolamines (µmol/g)			
N-palmitoyl ethanolamine	12.00 (4.85 - 14.95)	11.40 (6.37 - 19.22)	29.71 (15.04 - 41.03)[a]
N-oleoyl ethanolamine	2.85 (2.60 - 8.54)	2.01 (0.64 - 3.34)	6.30 (5.18 - 7.15)
N-stearoyl-ethanolamine	1.02 (0.37 - 1.98)	1.38 (1.08 - 3.83)	1.66 (0.60 - 3.36)
N-linoleoyl-ethanolamine	175.84 (21.47 - 289.10)	10.22 (4.57 - 33.38)[a]	36.72 (13.31 - 73.99)
Steroids (µmol/g)			
Androsterone sulfate	8.51E-4 (8.43E-4 - 9.42E-4)	1.81E-4 (4.35E-5 - 7.91E-4)	6.84E-4 (2.35E-4 - 1.16E-2)
Bile acids (µmol/g)			
Tauroursodeoxycholic acid	1.04 (0.50 - 4.52)	2.26 (1.47 - 3.58)	0.32 (0.19 - 0.85)
Taurocholic acid	42.38 (23.78 - 117.81)	24.56 (19.64 - 36.54)	12.37 (11.89 - 12.78)[b]
Taurochenodeoxycholic acid	4.03 (8.61E-3 -16.84)	1.61 (1.10 - 2.86)	0.60 (0.27 - 1.43)
Taurodeoxycholic acid	3.97 (9.12E-3 - 16.61)	1.63 (1.09 - 2.86)	0.60 (0.27 - 1.45)
Cholic acid	0.56 (0.16 - 7.26)	5.32E-2 (3.55E-2 - 8.03E-2)[b]	6.34E-2 (5.47E-2 - 8.86E-2)[b]
Glycochenodeoxycholic acid	3.02E-3 (2.68E-3 - 3.75E-3)	4.15E-3 (3.56E-3 - 4.35E-3)[a]	3.70E-3 (2.79E-3 - 4.53E-3)
Glycocholic acid	3.10E-3 (2.55E-3 - 1.78E-2)	2.59E-3 (1.13E-3 - 4.68E-3)	4.45E-4 (3.13E-4 - 5.27E-4)[b]
Deoxycholic acid-iso1	2.36E-3 (1.65E-3 - 1.09E-2)	1.87E-3 (8.81E-4 - 3.43E-3)	1.97E-3 (5.13E-4 - 3.43E-3)[c]
Deoxycholic acid	2.15E-2 (3.21E-3 - 0.37)	6.14E-3 (2.14E-3 - 1.07E-2)	1.98E-3 (1.15E-3 - 3.58E-3)[a]
Ursodeoxycholic acid / Hyodeoxicholic acid	9.01E-3 (7.69E-3 - 0.13)	4.70E-3 (2.29E-3 - 9.76E-3)	1.43E-2 (9.48 E-3 - 1.82E-2)
Lysophosphatidylserines (µmol/g)			
LPS 17:1	2.87E-3 (1.83E-3 - 3.63E-3)	1.43E-3 (8.28E-4 - 1.62E-3)[b]	1.40E-3 (1.25E-3 - 2.34E-3)[a]
LPS 18:2	2.97E-2 (2.76E-2 - 3.91E-2)	2.99E-2 (2.61E-2 - 3.18E-2)	3.58E-2 (3.41E-2 - 3.80E-2)
LPS 18:3	1.22E-2 (1.01E-2 – 1.29E-2)	5.94E-3 (5.43E-3 - 5.97E-3)[b]	8.91E-3 (6.02E-3 - 1.18E-2)
LPS 22:5	0.10 (5.56E-2 - 0.15)	3.19E-2 (1.57E-2 - 5.37E-2)[b]	2.97E-2 (1.64E-2 - 3.89E-2)[a]

Lysophosphatidylcholines (µmol/g)			
sn1-LPC 14:0	0.50 (0.21 - 0.77)	0.26 (0.17 - 0.27)	0.49 (0.28 - 1.15)
sn2-LPC 14:0	5.41E-4 (5.23E-4 - 2.22E-3)	5.65E-3 (5.65E-3 - 6.46E-3)[b]	4.01E-4 (2.40E-4 - 1.07E-3)
sn1-LPC 15:0	0.31 (0.21 - 0.34)	0.11 (0.11 - 0.13)[b]	0.50 (0.37 - 0.78)
sn1-LPC 16:0	66.58 (26.15 - 85.34)	59.79 (47.72 - 69.74)	77.72 (48.61 - 133.10)
sn2-LPC 16:0	6.22 (4.87 - 9.29)	5.19 (5.03 - 5.77)	6.47 (4.60 - 7.59)
sn1-LPC 16:1	9.72 (5.06 - 13.59)	8.59 (7.53 - 8.95)	12.10 (6.62 - 16.66)
sn2-LPC 16:1	1.34 (0.59 - 2.50)	0.40 (0.34 - 0.45)[b]	1.61 (0.64 - 2.75)
sn1-LPC 17:0	0.27 (0.19 - 0.31)	0.49 (0.45 - 0.59)[b]	0.68 (0.68 - 1.25)[b]
sn2-LPC 17:0	0.10 (8.75E-2 - 0.17)	0.21 (0.19 - 0.23)[b]	0.75 (0.68 - 0.96)[b]
sn1-LPC 17:1	0.19 (0.15 - 0.33)	0.24 (0.19 - 0.24)	0.53 (0.34 - 0.66)
sn2-LPC 17:1	0.26 (0.16 - 0.70)	0.49 (0.40 - 0.52)	0.68 (0.44 - 0.98)
sn1-LPC 18:0	20.04 (20.04 - 21.31)	27.03 (18.55 - 35.74)	29.12 (17.33 - 47.54)
sn2-LPC 18:0	0.45 (0.28 - 0.67)	0.94 (0.80 - 1.20)[b]	0.80 (0.77 - 1.06)[a]
sn1-LPC 18:1	18.26 (9.99 - 29.07)	26.00 (23.87 - 27.16)	38.60 (33.83 - 76.12)[a]
sn2-LPC 18:1	5.39 (4.13 - 12.83)	9.15 (6.91 - 12.28)	12.40 (12.40 - 12.79)
sn1-LPC 18:2	8.55 (7.14 - 13.32)	9.19 (9.00 - 9.75)	12.15 (5.76 - 17.52)
sn2-LPC 18:2	11.29 (7.07 - 24.23)	9.48 (7.65 - 11.42)	11.35 (8.60 - 22.68)
sn1-LPC 18:3	0.44 (0.38 - 0.52)	0.21 (0.17 - 0.24)[a]	0.10 (6.20E-2 - 0.22)[a]
sn1-LPC 19:0	6.15E-3 (5.75E-3 - 6.43E-3)	6.24E-3 (3.99E-3 - 8.08E-3)	2.91E-3 (2.33E-3 - 5.84E-3)
sn2-LPC 19:0	2.18E-2 (1.86E-2 - 3.48E-2)	2.64E-2 (2.07E-2 - 3.13E-2)	0.10 (8.12E-2 - 0.18)[b]
sn1-LPC 20:0	2.04E-3 (9.11E-4 - 5.70E-3)	3.64E-3 (2.06E-3 - 4.96E-3)	1.60E-3 (1.29E-3 - 2.62E-3)
sn1-LPC 20:1	0.17 (9.62E-2 -0.25)	0.26 (0.21 - 0.28)	0.26 (0.26 - 0.34)[a]
sn2-LPC 20:1	9.72E-3 (4.75E-3 - 1.17E-2)	9.00E-3 (8.17E-3 - 1.03E-2)	1.50E-2 (1.01E-2 - 3.07E-2)
sn1-LPC 20:2	5.03E-2 (2.86E-2 - 7.15E-2)	2.50E-2 (2.23E-2 - 3.36E-2)	3.07E-2 (1.74E-2 - 4.98E-2)
sn2-LPC 20:2	0.24 (0.19 - 0.29)	0.10 (7.76E-2 - 0.13)[b]	0.14 (9.36E-2 - 0.24)
sn1-LPC 20:3	0.18 (0.15 - 0.37)	0.85 (0.69 - 0.93)[b]	1.21 (0.75 - 1.44)[b]
sn2-LPC 20:3	2.16 (1.16 - 4.40)	9.39 (8.44 - 10.84)[b]	7.84 (5.30 - 15.69)[b]
sn1-LPC 20:4	2.69 (1.72 - 3.50)	10.23 (7.86 - 10.64)[b]	6.90 (4.59 - 9.22)[b]
sn2-LPC 20:4	10.29 (7.76 - 20.02)	26.54 (18.27 - 35.61)[a]	21.99 (14.24 - 35.31)
sn2-LPC 20:5	0.21 (8.82E-2 - 0.23)	1.11E-2 (6.24E-3 - 2.01E-2)[b]	0.21 (5.87E-2 - 0.70)
sn2-LPC 22:3	2.02E-2 (7.96E-3 -3.07E-2)	5.54E-3 (3.58E-3 - 7.48E-3)[a]	7.57E-3 (3.07E-3 - 7.84E-3)
sn1-LPC 22:4	4.07E-3 (3.02E-3 - 6.66E-3)	1.23E-2 (1.05E-2 - 1.37E-2)[a]	1.06E-2 (6.04E-3 - 1.32E-2)[a]
sn2-LPC 22:4	2.08E-2 (1.08E-2 - 2.39E-2)	7.74E-2 (6.36E-2 - 9.13E-2)[b]	3.61E-2 (3.29E-2 - 4.69E-2)
sn1-LPC 22:5	1.70 (0.82 - 4.96)	1.28 (0.44 - 2.44)	2.47 (1.30 - 5.25)
sn2-LPC 22:5	0.10 (7.47E-2 - 0.28)	0.11 (5.40E-2 - 0.14)	0.22 (0.21 - 0.32)
sn1-LPC 22:6	3.74 (2.79 - 5.47)	3.70 (3.35 - 4.47)	8.10 (4.92 - 9.24)
sn2-LPC 22:6	6.41 (4.88 - 18.36)	10.56 (7.84 - 12.37)	16.59 (9.59 - 24.05)
Lysophosphatidylethanolamines (µmol/g)			
sn1-LPE 14:0	1.78E-2 (1.02E-2 - 2.67E-2)	1.39E-3 (4.46E-4 - 1.96E-3)[b]	7.97E-3 (2.89E-3 - 1.73E-2)
sn1-LPE 15:0	1.15E-2 (9.09E-3 - 1.40E-2)	1.70E-3 (1.51E-3 - 2.13E-3)[b]	1.50E-2 (1.28E-2 - 1.83E-2)
sn1-LPE 16:0	42.86 (21.53 - 54.64)	21.05 (17.63 - 24.43)[a]	37.88 (35.78 - 55.29)
sn2-LPE 16:0	2.24 (1.49 - 2.85)	0.47 (0.42 - 0.51)[b]	1.14 (1.02 - 2.31)

sn1-LPE 16:1	4.31 (3.22 - 7.65)	0.98 (0.93 - 1.28)[b]	2.24 (1.15 - 4.28)
sn2-LPE 16:1	0.26 (0.23 - 0.26)	2.00E-2(1.44E-2 - 2.10E-2)[b]	6.13E-2 (3.83E-2 - 0.13)[b]
sn1-LPE 17:0	0.21 (0.16 - 0.25)	0.10 (7.60E-2 - 0.17)	0.36 (0.27 - 0.86)
sn1-LPE 17:1	6.02E-2 (3.40E-2 - 8.39E-2)	3.37E-2 (3.32E-2 - 3.61E-2)	8.37E-2 (5.88E-2 - 0.16)
sn1-LPE 18:0	27.28 (14.55 - 28.71)	28.99 (28.93 - 29.28)[a]	40.4 (38.53 - 41.50)[b]
sn2-LPE 18:0	0.67 (0.57 - 1.28)	0.70 (0.59 - 1.07)	1.07 (0.96 - 2.58)
sn1-LPE 18:1	31.28 (20.86 - 47.27)	31.89 (30.28 - 33.42)	41.37 (40.90 - 53.69)
sn2-LPE 18:1	0.82 (0.59 - 1.74)	0.27 (0.17 - 0.32)[b]	0.58 (0.56 - 0.63)
sn1-LPE 18:2	2.30 (1.65 - 2.54)	0.58 (0.46 - 0.68)[b]	1.43 (0.75 - 1.47)[a]
sn2-LPE 18:2	1.65 (0.97 - 2.56)	0.60 (0.60 - 0.62)[b]	1.03 (0.60 - 1.30)
sn1-LPE 20:1	0.12 (7.19E-2 - 0.21)	0.13 (9.60E-2 - 0.21)[b]	0.19 (0.19 - 0.19)
sn2-LPE 20:1	1.31E-2 (1.25E-2 - 1.76E-2)	6.04E-3 (5.96E-3 - 7.12E-3)	1.04E-2 (9.70E-3 - 1.32E-2)
sn1-LPE 20:2	2.36E-2 (1.92E-2 - 3.19E-2)	6.71E-3 (6.29E-3 - 7.18E-3)[b]	6.22E-3 (4.39E-3 - 1.15E-2)[b]
sn1-LPE 20:3	5.46E-2 (4.01E-2 - 8.45E-2)	4.30E-2 (3.80E-2 - 4.95E-2)	9.50E-2 (6.48E-2 - 0.14)[a]
sn2-LPE 20:3	0.40 (0.24 - 0.68)	0.28 (0.23 - 0.29)	0.44 (0.41 - 0.50)
sn1-LPE 20:4	8.16 (5.54 - 10.21)	7.66 (7.13 - 7.90)	13.57 (10.79 - 16.65)[a]
sn2-LPE 20:4	19.89 (8.70 - 27.88)	20.38 (15.22 - 27.11)	27.39 (19.25 - 36.92)
sn1-LPE 20:5	5.24E-2 (3.41E-2 - 0.10)	ND	8.23E-2 (6.03E-2 - 0.14)
sn2-LPE 20:5	0.12 (0.54 - 0.22)	3.19E-3 (2.20E-3 - 4.89E-3)[b]	8.39E-2 (3.96E-2 - 0.25)
sn1-LPE 22:4	9.12E-3 (7.96E-3 - 2.76E-2)	1.11E-2 (8.38E-3 - 1.54E-2)	1.29E-2 (1.14E-2 - 1.78E-2)
sn2-LPE 22:4	0.24 (0.22 - 0.60)	0.40 (0.32 - 0.72)	0.37 (0.22 - 0.39)
sn1-LPE 22:5	3.95E-2 (1.87E-2 -4.79E-2)	2.74E-3 (2.29E-3 - 5.18E-3)[b]	2.84E-2 (1.80E-2 - 3.18E-2)
sn2-LPE 22:5	0.40 (0.15 - 0.59)	0.10 (6.86E-2 - 0.15)[b]	0.39 (0.31 - 0.53)
sn1-LPE 22:6	13.46 (9.29 - 17.39)	3.88 (2.39 - 5.26)[b]	12.4 (9.95 - 16.7)
sn2-LPE 22:6	17.74 (14.02 - 43.15)	16.49 (14.93 - 18.88)	29.73 (18.73 - 31.34)
L-alpha-lysophosphatidylinositol (µmol/g)			
LPI 16:1	1.13 (0.57 - 1.56)	0.34 (0.18 - 0.59)[a]	0.32 (0.18 - 0.44)[a]
Saturated fatty acids (µmol/g)			
Lauric acid	2.03E-3 (1.18E-3 - 6.20E-3)	7.66E-4 (6.09E-5 - 9.21E-4)[b]	2.19E-3 (1.89E-3 - 3.93E-3)
Myristic acid	21.09 (8.16 - 56.64)	15.37 (7.57 - 24.42)	28.34 (22.62 - 32.52)
Pentadecanoic acid	7.65E-4 (2.24E-4 - 1.78E-3)	5.91E-4 (3.53E-4 - 1.04E-3)	3.39E-3 (3.38E-3 - 3.92E-3)[a]
Palmitic acid	1.30 (0.59 - 2.75)	2.70 (1.02 - 6.13)	2.75 (1.29 - 4.36)
Stearic acid	2.05E-4 (1.54E-4 - 4.20E-4)	2.63E-4 (1.39E-4 - 3.78E-4)	3.38E-4 (2.35E-4 - 5.65E-4)
Monounsaturated fatty acids (µmol/g)			
Palmitoleic acid	9.98 (2.88 - 15.16)	5.42 (5.24 - 5.92)	4.56 (3.57 - 6.64)
Oleic acid	8.18 (2.24 - 17.44)	46.12 (23.84 - 52.28)[a]	24.83 (10.53 - 39.83)[a]
Polyunsaturated fatty acids (µmol/g)			
Stearidonic acid	0.21 (6.47E-2 - 0.43)	3.59E-2 (1.17E-2 - 5.84E-2)[a]	1.88E-2 (1.25E-2 - 2.53E-2)[b]
Eicosapentaenoic acid	138.36 (109.40 - 190.49)	31.81 (9.23 - 58.29)[b]	147.30 (87.36 - 218.17)
Docosahexaenoic acid	1800.27 (1140.31 - 2403.17)	789.79 (507.06 - 1241.48)[a]	1471.23 (1295.11 - 1870.67)
ω3-Docosapentaenoic acid	6.64 (6.48 - 10.63)	3.33 (0.81 - 5.62)	3.50 (2.26 - 5.61)[a]
ω6-Docosapentaenoic acid	3.67 (2.58 - 38.20)	23.75 (12.58 - 26.22)	4.02 (2.17 - 5.50)
Arachidonic acid	780.86 (500.60 – 1748.27)	931.99 (536.14 - 1714.20)[a]	1340.58 (1241.57 - 1639.47)

Iso-1-linolenic acid	1.33 (0.41 - 2.14)	0.27 (0.10 - 0.42)[a]	0.30 (0.21 - 0.42)
Iso-2-linolenic acid	2.27 (1.55 - 9.13)	2.71 (1.27 - 6.28)	0.52 (0.42 - 0.91)[d]
Iso-1-linoleic acid	68.22 (27.79 - 236.65)	56.74 (16.83 - 131.92)	30.15 (16.11 - 34.55)
ω6-Dihomo-dietary γ-linolenic acid	1.09 (0.70 - 3.90)	1.60 (0.91 - 4.66)	3.97 (2.17 - 4.55)
ω6-Dihomo-dietary γ-linolenic acid – iso2	3.91E-2 (2.31E-2 - 0.19)	3.42E-2 (1.90E-2 – 9.76E-2)	0.15 (0.12 - 0.24)[a]
ω6-Dihomo-dietary γ-linolenic acid – iso3	1.07 (0.41 - 4.46)	3.08 (1.03 - 5.10)	3.46 (3.25 - 7.47)
Adrenic acid	0.99 (0.25 - 1.16)	0.68 (0.22 - 1.50)	0.19 (0.13 - 0.47)[a]
ω6- Eicosadienoic acid	4.15E-3 (1.65E-3 – 1.09E-2)	2.43E-3 (8.76E-4 - 5.25E-3)	2.32E-3 (1.64E-3 - 3.32E-3)
Peroxidized fatty acids (µmol/g)			
9-HODE / 13-HODE	142.40 (142.40 - 146.19)	54.68 (48.72 - 57.50)[b]	56.84 (44.12 - 105.17)[b]
Epoxy-stearic acid-iso1	0.16 (0.14 - 0.17)	7.18E-2 (5.38E-2 - 8.48E-1)[b]	0.30 (0.13 - 0.55)
Epoxy-stearic acid-iso2	0.23 (0.14 - 0.34)	1.67 (1.20 - 2.58)[b]	0.23 (0.13 - 0.36)
5-HETE	2.99 (2.79 - 7.12)	3.68 (2.37 - 6.95)	4.15 (2.55 - 4.82)
15-HETE	12.12 (8.50 - 13.67)	10.02 (9.10 - 11.23)	12.84 (9.44 - 26.17)
12-HETE	129.38 (63.52 - 437.05)	61.47 (23.26 - 182.21)	180.13 (52.63 - 891.88)
x-EpOME-iso1	35.37 (25.64 - 51.23)	34.21 (25.73 - 45.20)	18.86 (18.66 - 20.09)[a]
x-EpOME-iso2	12.42 (10.04 - 27.81)	14.36 (9.91 - 22.29)	8.80 (5.03 - 10.90)
11,12-DiHETE	5.29 (2.75 - 9.19)	3.53 (2.84 – 3.98)	2.63 (2.00 - 3.30)
17-HDHA	6.17 (4.50 - 9.46)	5.06 (2.20 - 6.61)	3.74 (2.77 - 4.74)
9,12,13-TriHOME(10)	121.08 (97.04 - 176.10)	59.17 (25.59 - 87.23)[a]	90.80 (79.62 - 103.14)

HDHA, hydroxydocosahexaenoic acid; HETE, 5-hydroxyeicosatetraenoic acid; HODE, hydroxyoctadecadienoic acid HOME, hydroxyoctadecenoic acid; LPE, lysophosphatidylethanolamine; LPC, lysophosphatidylcholine; LPI, lysophosphatidylinositol; LPS, lysophosphatidylserine

Supporting Information Table S7. Results of the lipidomics study in perigonadal adipose tissue (pgWAT). CD: Chow diet; HFD: High-fat diet; HF-HSD: High-fat high-sucrose diet. [a] $p < 0.05$, [b] $p < 0.01$, with respect to CD

pgWAT	CD	HFD	HF-HSD
Acyl-carnitines (µmol/g)			
Free carnitine	0.20 (0.14 - 0.22)	0.22 (0.18 - 0.30)	0.31 (0.17 - 0.35)
Acetyl-carnitine	0.30 (0.30 - 0.31)	0.35 (0.21 - 0.93)	0.41 (0.26 - 0.53)
Methylmalonyl-carnitine / Succinyl-carnitine	6.90E-3 (5.11E-3 - 1.25E-2)	1.37E-2 (1.03E-2 - 1.59E-2)	1.23E-2 (3.99E-3 - 1.36E-2)
Propionyl-carnitine	7.09E-3 (5.25E-3 - 1.52E-2)	1.17E-2 (6.15E-3 - 1.65E-2)	5.47E-3 (3.65E-3 - 1.42E-2)
Methylglutaryl-carnitine / Adipoyl-carnitine	2.60E-4 (2.30E-4 - 2.94E-4)	4.34E-4 (3.42E-4 - 5.85E-4)[b]	4.82E-4 (3.63E-4 - 5.08E-4)[a]
Isobutyryl-carnitine / Butyryl-carnitine	9.20E-3 (4.52E-3 - 1.11E-2)	6.80E-3 (3.51E-3 - 1.54E-2)	2.82E-3 (1.61E-3 - 1.09E-2)
2-Methyl-butyryl-carnitine	1.56E-3 (9.65E-4 - 1.74E-3)	1.23E-3 (1.08E-3 - 1.42E-3)	1.43E-3 (7.13E-4 - 2.65E-3)
Hexanoyl-carnitine	1.07E-4 (8.05E-5 - 2.05E-4)	1.41E-4 (8.57E-5 - 2.50E-4)	9.53E-5 (9.29E-5 - 1.38E-4)
Octanoyl-carnitine	1.53E-4 (6.06E-5 - 2.10E-4)	8.52E-5 (5.44E-5 - 2.40E-4)	1.04E-4 (8.92E-5 - 1.39E-4)
Dodecanoyl-carnitine	2.11E-4 (1.39E-4 - 2.64E-4)	1.13E-4 (4.38E-5 - 6.35E-5)	9.57E-5 (6.94E-5 - 2.09E-4)
Tetradecanoyl-carnitine	1.95E-3 (1.79E-3 - 2.02E-3)	1.06E-3 (3.44E-4 - 3.56E-3)	6.68E-4 (5.07E-4 - 8.06E-4)[a]
Hexadecenyl-carnitine	2.32E-3 (8.01E-4 - 6.06E-3)	2.09E3 (3.36E-4 - 7.59E-3)	8.32E-4 (7.77E-4 - 8.66E-4)
Hexadecanoyl-carnitine	1.18E-2 (5.28E-3 - 1.88E-2)	1.48E-2 (7.79E-3 - 5.30E-2)	5.38E-3 (3.14E-3 - 2.13E-2)
Octadecenyl-carnitine	6.80E-3 (3.86E-3 - 1.30E-2)	1.30E-2 (4.62E-3 - 5.32E-2)	3.78E-3 (2.99E-3 - 5.20E-3)
Octadecanoyl-carnitine	1.76E-3 (1.65E-3 - 1.78E-3)	7.94E-3 (5.50E-3 - 1.68E-2)[b]	1.40E-3 (9.46E-4 - 4.58E-3)
N-acylethanolamines (µmol/g)			
N-palmitoyl ethanolamine	1.49 (0.63 - 2.56)	9.46 (1.73 - 26.89)	3.26 (1.57 - 6.40)
N-oleoyl ethanolamine	3.04 (2.23 - 4.85)	13.19 (8.36 - 38.38)[b]	4.64 (1.97 - 12.13)
N-stearoyl-ethanolamine	0.19 (0.14 - 0.32)	5.89 (1.49 - 13.30)[b]	0.81 (0.51 - 2.40)[a]
Steroids (µmol/g)			
Androsterone sulfate	1.20E-4 (1.63E-5 - 4.10E-3)	2.86E-4 (1.23E-4 - 5.54E-3)	6.57E-4 (1.80E-4 - 1.19E-3)
Bile acids (µmol/g)			
Tauroursodeoxycholic acid	6.35E-4 (1.94E-4 - 4.19E-2)	1.12E-2 (1.94E-3 - 3.44E-2)	3.82E-2 (3.74E-3 - 8.31E-2)
Taurocholic acid	7.05E-2 (1.07E-2 - 1.28)	0.53 (5.98E-2 - 1.42)	0.81 (9.45E-2 - 3.24)
Taurochenodeoxycholic acid	3.79E-4 (2.76E-4 - 3.73E-2)	1.20E-3 (1.01E-3 - 1.26E-3)	9.37E-3 (9.52E-4 - 0.14)
Taurodeoxycholic acid	3.68E-4 (2.76E-4 - 3.73E-2)	1.17E-3 (3.23E-4 - 5.32E-3)	9.45E-3 (9.58E-4 - 0.14)
Cholic acid	3.83E-3 (1.03E-3 - 2.94E-2)	2.04E-3 (1.54E-3 - 2.96E-3)	8.72E-3 (3.70E-3 - 0.10)
Glycochenodeoxycholic acid	3.28E-3 (2.92E-3 - 4.35E-3)	3.95E-3 (3.44E-3 - 5.16E-3)	4.57E-3 (3.37E-3 - 5.47E-3)
Deoxycholic acid	7.38E-4 (6.75E-4 - 1.06E-3)	1.33E-3 (6.86E-4 - 5.55E-2)	1.35E-3 (9.94E-4 - 3.40E-3)
Lysophosphatidylserines (µmol/g)			
LPS 17:1	7.45E-4 (5.79E-4 - 1.01E-3)	9.64E-4 (7.38E-4 - 1.13E-3)	9.80E-4 (8.26E-4 - 1.15E-3)
LPS 18:2	1.16E-2 (1.02E-2 - 1.20E-2)	9.47E-3 (7.93E-3 - 1.41E-2)	1.73E-2 (1.30E-2 - 2.35E-2)[b]
LPS 18:3	5.62E-4 (5.62E-4 - 1.16E-3)	ND	1.48E-3 (1.11E-3 - 1.59E-3)
Lysophosphatidylcholines (µmol/g)			
sn1-LPC 14:0	1.68E-4 (1.68E-4 - 1.76E-4)	3.96E-4 (2.97E-4 - 5.81E-4)[b]	1.09E-3 (1.07E-3 - 1.22E-3)[b]

sn1-LPC 16:0	6.06 (4.52 - 9.32)	5.63 (3.78 - 9.59)	6.77 (4.48 - 7.94)[a]
sn2-LPC 16:0	0.60 (0.52 - 0.67)	0.30 (0.17 - 0.31)[a]	0.19 (0.18 - 0.90)
sn1-LPC 16:1	3.73E-2 (3.40E-2 - 3.83E-2)	1.50E-2 (1.39E-2 - 1.93E-2)[b]	6.61E-2 (5.23E-2 - 9.61E-2)[a]
sn2-LPC 16:1	2.28E-2 (1.10E-2 - 6.74E-2)	8.20E-3 (4.12E-3 - 1.32E-2)[a]	3.86E-2 (3.16E-2 - 5.08E-2)
sn1-LPC 17:0	4.26E-2 (2.76E-2 - 5.87E-2)	2.93E-2 (1.37E-2 - 4.32E-2)	5.76E-2 (3.17E-2 - 7.91E-2)
sn2-LPC 17:1	8.05E-4 (6.03E-4 - 1.16E-3)	4.96E-4 (3.77E-4 - 8.39E-4)	1.26E-3 (1.02E-3 - 1.90E-3)
sn1-LPC 18:0	3.08 (2.39 - 4.41)	4.55 (2.97 - 6.66)	4.32 (2.63 - 4.71)
sn2-LPC 18:0	5.80E-2 (5.51E-2 - 6.06E-2)	8.64E-2 (6.12E-2 - 0.18)	7.61E-2 (2.67E-2 - 0.10)
sn1-LPC 18:1	0.63 (0.42 - 1.06)	0.78 (0.21 - 1.09)	0.77 (0.54 - 0.95)
sn2-LPC 18:1	0.23 (0.15 - 0.71)	0.44 (0.20 - 0.85)	0.60 (0.46 - 0.70)
sn1-LPC 18:2	0.43 (0.32 - 0.67)	0.33 (0.22 - 0.89)	0.43 (0.22 - 0.84)
sn2-LPC 18:2	2.24 (1.42 - 2.45)	1.82 (1.24 - 2.36)	1.71 (0.69 - 2.28)
sn1-LPC 19:0	8.60E-3 (7.02E-3 - 1.01E-2)	1.52E-3 (8.65E-4 - 1.78E-3)[b]	2.86E-3 (9.36E-4 - 1.25E-2)
sn2-LPC 19:0	5.30E-3 (3.33E-3 - 6.99E-3)	1.34E-3 (1.25E-3 - 1.61E-3)[b]	4.74E-3 (3.81E-3 - 1.04E-2)
sn1-LPC 20:0	3.23E-3 (3.06E-3 - 3.82E-3)	1.52E-3 (7.05E-4 - 2.53E-3)	5.37E-4 (5.20E-4 - 7.00E-4)[a]
sn1-LPC 20:1	1.19E-2 (5.64E-3 - 1.89E-2)	5.53E-3 (3.36E-3 - 8.60E-3)[a]	7.46E-3 (2.45E-3 - 2.66E-2)[a]
sn1-LPC 20:2	1.97E-3 (1.09E-3 - 2.23E-3)	1.89E-3 (1.36E-3 - 4.31E-3)	4.33E-3 (4.33E-3 - 4.33E-3)[b]
sn2-LPC 20:2	9.32E-4 (6.27E-4 - 1.70E-3)	9.92E-4 (7.82E-4 - 1.35E-3)	1.37E-3 (1.12E-3 - 2.21E-3)
sn1-LPC 20:3	6.41E-3 (4.66E-3 - 1.67E-2)	5.54E-3 (2.38E-3 - 1.28E-2)	1.21E-2 (4.59E-3 - 1.49E-2)
sn2-LPC 20:3	1.71E-2 (1.19E-2 - 3.46E-2)	1.03E-2 (5.31E-3 - 1.60E-2)	2.07E-2 (1.71E-2 - 2.60E-2)
sn1-LPC 20:4	4.76E-2 (2.64E-2 - 0.13)	9.41E-2 (3.38E-2 - 0.18)	0.10 (6.67E-2 - 0.13)
sn2-LPC 20:4	0.12 (9.65E-2 - 0.42)	0.19 (0.16 - 0.28)	0.21 (0.20 - 0.32)
sn2-LPC 22:4	6.88E-4 (4.43E-4 - 1.55E-3)	1.08E-3 (4.09E-4 - 3.61E-3)	6.49E-4 (5.95E-4 - 8.38E-4)
sn1-LPC 22:6	1.60E-2 (1.05E-2 - 3.35E-2)	1.62E-2 (3.92E-3 - 2.81E-2)	2.26E-2 (1.76E-2 - 3.97E-2)
sn2-LPC 22:6	1.84E-2 (1.44E-2 - 3.58E-2)	1.71E-2 (9.20E-3 - 2.25E-2)	2.58E-2 (2.33E-2 - 5.04E-2)
Lysophosphatidylethanolamines (µmol/g)			
sn1-LPE 16:0	0.82 (0.81 - 0.83)	0.63 (0.41 - 0.89)	1.27 (1.03 - 2.52)[a]
sn2-LPE 16:0	3.38E-2 (2.01E-2 - 4.83E-2)	1.17E-2 (9.80E-3 - 1.46E-2)[b]	5.02E-2 (2.94E-2 - 7.57E-2)
sn1-LPE 16:1	3.50E-2 (2.31E-2 - 7.38E-2)	9.83E-3 (5.97E-3 - 1.36E-2)[b]	8.15E-2 (5.12E-2 - 9.78E-2)
sn2-LPE 16:1	1.10E-2 (9.99E-3 - 1.10E-2)	1.45E-3 (9.27E-4 - 2.56E-3)[b]	1.51E-2 (5.40E-3 - 2.72E-2)
sn1-LPE 17:0	7.62E-3 (4.32E-3 - 3.50E-2)	6.80E-3 (4.75E-3 - 1.06E-2)	2.16E-2 (9.88E-3 - 3.69E-2)
sn1-LPE 17:1	1.37E-3 (1.37E-3 - 1.37E-3)	2.58E-4 (2.47E-4 - 3.28E-4)[b]	1.03E-3 (6.87E-4 - 2.57E-3)
sn1-LPE 18:0	0.88 (0.38 - 2.04)	2.17 (1.43 - 3.10)	1.72 (1.01 - 3.70)
sn2-LPE 18:0	8.44E-3 (7.24E-3 - 6.13E-2)	1.88E-2 (9.93E-3 - 5.02E-2)	2.44E-2 (1.23E-2 - 7.34E-2)
sn1-LPE 18:1	0.47 (0.43 - 1.59)	0.65 (0.37 - 1.02)	0.69 (0.54 - 0.83)
sn2-LPE 18:1	0.40 (0.23 - 0.59)	0.27 (0.22 - 0.39)	0.44 (0.29 - 0.67)
sn1-LPE 18:2	0.10 (6.20E-2 - 0.36)	6.19E-2 (5.23E-2 - 7.75E-2)	0.15 (7.66E-2 - 0.37)
sn2-LPE 18:2	0.70 (0.59 - 0.73)	0.29 (0.19 - 0.43)[b]	0.67 (0.52 - 0.68)
sn1-LPE 20:1	1.52E-3 (1.29E-3 - 2.48E-3)	7.93E-4 (4.41E-4 - 1.24E-3)[a]	2.89E-3 (7.72E-4 - 4.32E-3)
sn2-LPE 20:1	5.80E-3 (5.37E-3 - 6.37E-3)	1.20E-3 (8.54E-4 - 1.74E-3)[b]	1.14E-2 (3.47E-3 - 1.14E-2)
sn1-LPE 20:4	0.11 (0.10 - 0.14)	0.13 (0.10 - 0.31)	0.40 (0.18 - 1.91)
sn2-LPE 20:4	1.13 (1.04 - 1.32)	2.16 (2.04 - 2.78)[b]	2.84 (1.43 - 4.43)[b]
sn1-LPE 22:4	2.88E-3 (1.57E-3 - 6.81E-3)	3.74E-3 (1.74E-3 - 7.08E-3)	2.79E-3 (1.21E-3 - 2.87E-3)

sn2-LPE 22:4	5.44E-2 (4.00E-2 - 7.19E-2)	6.19E-2 (4.90E-2 - 8.53E-2)	3.98E-2 (2.67E-2 - 4.70E-2)
sn2-LPE 22:5	3.24E-2 (2.53E-2 - 4.95E-2)	2.32E-2 (1.54E-2 - 3.89E-2)	2.59E-2 (2.20E-2 - 3.81E-2)
sn1-LPE 22:6	0.15 (0.11 - 0.16)	2.90E-2 (2.89E-2 - 3.15E-2)[b]	2.26E-2 (1.76E-2 - 3.97E-2)
sn2-LPE 22:6	0.88 (0.61 - 1.38)	0.28 (0.16 - 0.68)[a]	1.30 (0.55 - 1.48)
Saturated fatty acids (µmol/g)			
Lauric acid	9.93E-4 (5.08E-4 - 3.47E-3)	8.26E-4 (4.94E-4 - 1.10E-3)	1.48E-2 (1.41E-2 - 1.48E-2)[a]
Myristic acid	8.67 (8.39 - 8.95)	10.63 (5.83 - 24.00)	154.10 (153.11 - 155.09)[b]
Pentadecanoic acid	7.35E-4 (6.10E-4 - 2.17E-3)	3.17E-4 (1.44E-4 - 8.85E-4)	4.80E-3 (4.62E-3 - 4.98E-3)[a]
Palmitic acid	1.44 (0.85 - 0.14)	1.34 (0.46 - 5.40)	3.60 (3.32 - 3.67)[b]
Stearic acid	4.09E-4 (3.19E-4 - 5.07E-4)	6.06E-4 (4.03E-4 - 7.88E-4)	6.28E-4 (3.40E-4 - 7.11E-4)
Monounsaturated fatty acids (µmol/g)			
Palmitoleic acid	3.89 (3.51 - 4.29)	1.07 (0.70 - 2.97)	7.96 (7.77 - 8.20)[b]
Oleic acid	21.14 (15.27 - 25.71)	47.17 (21.98 - 74.37)	42.52 (37.59 - 48.91)[a]
Polyunsaturated fatty acids (µmol/g)			
Stearidonic acid	3.10E-3 (2.74E-3 - 3.71E-3)	ND	1.59E-3 (8.11E-4 - 1.96E-3)[b]
Eicosapentaenoic acid	2.20 (1.51 - 8.17)	0.61 (0.49 - 1.05)[b]	3.96 (1.58 - 7.68)
Docosahexaenoic acid	36.15 (34.51 - 36.55)	37.09 (21.63 - 78.37)	47.43 (46.52 - 47.58)[b]
ω3-Docosapentaenoic acid	0.99 (0.82 - 1.10)	035 (0.28 - 0.65)[b]	2.13 (1.78 - 2.36)[b]
ω6-Docosapentaenoic acid	0.56 (0.42 - 0.60)	2.50 (2.11 - 3.48)[b]	1.11 (0.98 - 1.28)[b]
Arachidonic acid	43.37 (20.91 - 65.60)	73.76 (61.03 - 139.52)[a]	72.47 (51.25 - 94.05)[a]
Iso-1-linolenic acid	0.67 (0.60 - 0.75)	0.14 (9.01E-2 - 0.42)	0.61 (0.56 - 0.68)
Iso-2-linolenic acid	4.95E-2 (4.16E-2 - 9.25E-2)	0.10 (6.98E-2 - 0.13)	0.10 (9.15E-2 - 0.13)[a]
Iso-1-linoleic acid	42.06 (22.13 - 51.51)	21.61 (11.56 - 43.61)	19.91 (17.75 - 58.46)
ω6-Dihomo-dietary γ-linolenic acid	0.13 (0.11 - 0.24)	0.23 (0.12 - 0.67)	0.34 (0.24 - 0.43)[a]
ω6-Dihomo-dietary γ-linolenic acid – iso2	5.16E-3 (4.28E-3 - 1.09E-2)	3.16E-2 (3.11E-2 - 3.43E-2)[b]	2.26E-2 (9.56E-3 - 5.30E-2)
ω6-Dihomo-dietary γ-linolenic acid – iso3	0.31 (0.21 - 1.97)	1.20 (1.16 - 1.33)	0.53 (0.44 - 3.40)
Adrenic acid	7.36E-2 (3.23E-2 - 0.14)	0.30 (0.18 - 1.08)[b]	0.13 (0.13 - 0.16)
ω6- Eicosadienoic acid	9.99E-4 (4.06E-4 - 2.01E-3)	2.73E-3 (1.49E-3 - 9.12E-3)[b]	7.33E-4 (4.83E-4 - 2.18E-3)
Peroxidized fatty acids (µmol/g)			
9-HODE / 13-HODE	73.07 (49.41 - 83.33)	57.74 (49.52 - 67.44)	71.06 (32.15 - 143.36)
Epoxy-stearic acid-iso1	0.10 (6.49E-2 - 0.18)	2.64E-2 (2.51E-2 - 2.87E-2)[b]	0.19 (9.95E-2 - 0.21)
Epoxy-stearic acid-iso2	4.75E-3 (3.24E-3 - 2.19E-2)	2.72E-2 (1.64E-2 - 4.31E-2)	1.08E-2 (3.79E-3 - 4.22E-2)
15-HETE	1.62 (1.08 - 5.25)	4.30 (3.70 - 8.41)	3.14 (2.23 - 5.33)
12-HETE	4.17 (2.84 - 34.52)	11.20 (8.68 - 25.79)	20.51 (10.70 - 27.42)
x-OxoODE-iso1	576.18 (251.52 - 710.18)	754.94 (404.74 - 855.18)	631.14 (554.05 - 891.45)
x-EpOME-iso1	8.15 (2.32 - 13.69)	8.95 (7.45 - 12.40)	12.38 (10.49 - 15.67)
9,12,13-TriHOME(10)	34.69 (18.38 - 41.63)	36.11 (33.36 - 37.90)	34.97 (15.91 – 59.77)

HDHA, hydroxydocosahexaenoic acid; HETE, 5-hydroxyeicosatetraenoic acid; HODE, hydroxyoctadecadienoic acid; HOME, hydroxyoctadecenoic acid; LPE, lysophosphatidylethanolamine; LPC, lysophosphatidylcholine; LPS, lysophosphatidylserine

Supporting Information Table S8. Results of the lipidomics study in inguinal adipose tissue (iWAT). CD: Chow diet; HFD: High-fat diet; HF-HSD: High-fat high-sucrose diet. [a] $p < 0.05$, [b] $p < 0.01$, with respect to CD

iWAT	CD	HFD	HF-HSD
Acyl-carnitine (µmol/g)			
Free carnitine	0.18 (0.18 - 0.26)	0.19 (0.17 - 0.24)	0.18 (0.17 - 0.22)
Acetyl-carnitine	0.34 (0.27 - 0.40)	0.27 (0.18 - 0.36)	0.23 (0.18 - 0.29)[a]
Methylmalonyl- carnitine / Succinyl-carnitine	8.08E-3 (7.43E-3 - 8.24E-3)	6.53E-3 (4.17E-3 - 1.32E-2)	9.43 (6.26 - 1.06)
Propionyl-carnitine	6.15E-3 (3.34E-3 - 9.94E-3)	1.22E-2 (1.10E-2 - 1.31E-2)[b]	3.04E-3 (2.12E-3 - 5.81E-3)
Methylglutaryl-carnitine / Adipoyl-carnitine	2.64E-4 (2.15E-4 - 3.86E-4)	3.38E-4 (3.27E-4 - 3.72E-4)	4.02E-4 (3.95E-4 - 5.08E-4)[a]
Isobutyryl-carnitine / Butyryl-carnitine	6.50E-3 (6.50E-3 - 6.55E-3)	5.67E-3 (3.98E-3 - 8.60E-3)	2.14E-3 (1.39E-3 - 2.53E-3)[b]
2-methyl-butyryl-carnitine / Isovaleryl-carnitine / Valeryl-carnetine	1.89E-3 (1.64E-3 - 2.11E-3)	2.27E-3 (1.10E-3 - 2.86E-3)	9.76E-4 (7.62E-4 - 1.15E-3)[b]
Hexanoyl-carnitine	4.27E-4 (3.82E-4 - 4.85E-4)	1.07E-4 (6.75E-5 - 1.79E-4)[b]	9.00E-5 (7.04E-5 - 1.04E-4)[b]
Octanoyl-carnitine	2.50E-4 (1.62E-4 - 3.53E-4)	8.46E-5 (5.99E-5 - 1.03E-4)[b]	9.68E-5 (7.72E-5 - 1.94E-4)[b]
Dodecanoyl-carnitine	1.16E-3 (2.27E-4 - 2.94E-3)	2.12E-4 (4.12E-5 - 4.36E-4)	1.17E-4 (7.46E-5 - 1.38E-4)[a]
Tetradecanoyl-carnitine	5.63E-3 (5.46E-3 - 6.30E-3)	1.27E-3 (5.26E-4 - 2.09E-3)[b]	5.55E-4 (4.82E-4 - 8.50E-4)[b]
Hexadecenyl-carnitine	1.24E-2 (2.42E-3 - 3.70E-2)	2.33E-3 (1.87E-3 - 2.78E-3)	7.56E-4 (6.00E-4 - 1.05E-3)[b]
Hexadecanoyl-carnitine	3.74E-2 (1.32E-2 - 5.414E-2)	1.07E-2 (7.59E-3 - 1.48E-2)	3.07E-3 (2.47E-3 - 3.90E-3)[b]
Octadecenyl-carnitine	2.64E-2 (8.34E-2 - 7.96E-2)	1.32E-2 (1.30E-2 - 1.38E-2)	3.72E-3 (1.90E-3 - 4.38E-3)[b]
Octadecanoyl-carnitine	8.24E-3 (5.34E-3 - 3.91E-2)	8.48E-3 (5.95E-3 - 1.05E-2)	8.73E-4 (6.27E-4 - 1.62E-3)[b]
N-acylethanolamines (µmol/g)			
N-palmitoyl ethanolamine	3.78 (2.03 - 4.95)	7.12 (3.50 - 11.01)	2.45 (1.81 - 2.97)
N-oleoyl ethanolamine	5.50 (2.62 - 7.73)	15.71 (7.27 - 23.89)[a]	3.51 (1.65 - 4.88)
N-stearoyl-ethanolamine	0.63 (0.26 - 0.88)	2.83 (1.88 - 6.10)[b]	0.73 (0.29 - 0.84)
Steroids (µmol/g)			
Androsterone sulfate	2.09E-5 (1.31E-5 - 1.00E-4)	3.25E-4 (1.82E-4 - 5.85E-4)[b]	1.48E-4 (1.29E-4 - 1.71E-4)[b]
Bile acids (µmol/g)			
Tauroursodeoxycholic acid	9.40E-3 (2.95E-4 - 2.65E-2)	3.36E-3 (3.95E-4 - 3.23E-2)	2.01E-4 (1.36E-4 - 7.65E-4)
Taurocholic acid	0.68 (9.73E-2 - 0.71)	0.13 (6.2E-3 - 0.82)	1.04E-2 (7.46E-3 - 5.45E-2)[b]
Taurochenodeoxycholic acid	3.06E-2 (2.66E-2 - 5.09E-2)	1.13E-3 (3.71E-5 - 7.01E-3)[b]	1.72E-4 (3.15E-5 - 2.54E-4)[b]
Taurodeoxycholic acid	3.05E-2 (2.68E-2 - 5.09E-2)	9.08E-4 (3.35E-5 - 6.79E-3)[b]	1.62E-4 (2.43E-5 - 2.37E-4)[b]
Cholic acid	1.76E-2 (3.53E-3 - 4.01E-2)	2.10E-3 (1.81E-3 - 2.32E-3)	2.08E-3 (1.74E-3 - 2.56E-3)[a]
Glycochenodeoxycholic acid	4.86E-3 (4.01E-3 - 5.61E-3)	3.67E-3 (3.22E-3 - 5.11E-3)	3.64E-3 (3.45E-3 - 4.38E-3)
Deoxycholic acid	2.07E-3 (8.50E-4 - 3.10E-3)	2.88 (8.06E-2 - 7.68)[a]	7.74E-3 (7.44E-3 - 1.35E-2)[b]
Lysophosphatidylserines (µmol/g)			
LPS 17:1	9.44E-4 (8.74E-4 - 9.59E-4)	8.34E-4 (5.91E-4 - 9.90E-4)	7.89E-4 (7.41E-4 - 8.24E-4)[a]
LPS 18:2	1.04E-2 (7.18E-3 - 1.72E-2)	1.49E-2 (6.97E-3 - 1.77E-2)	2.26E-2 (1.57E-2 - 3.24E-2)[a]
LPS 18:3	1.31E-3 (1.22E-3 - 1.71E-3)	3.74E-4 (2.01E-4 - 5.60E-4)[b]	8.40E-4 (6.31E-4 - 1.71E-3)
Lysophosphatidylcholines (µmol/g)			
sn1-LPC 14:0	6.92E-4 (3.42E-4 - 1.00E-3)	2.29E-4 (1.41E-4 - 4.55E-4)	9.71E-4 (5.55E-4 - 1.33E-3)
sn1-LPC 16:0	8.63 (7.72 - 10.52)	5.13 (3.81 - 6.22)[a]	0.14 (0.12 - 0.20)[b]

sn2-LPC 16:0	0.80 (0.60 - 1.06)	0.21 (0.17 - 0.34)[b]	3.61 (3.16 - 4.95)[a]
sn1-LPC 16:1	6.91E-2 (5.13E-2 - 0.16)	3.70E-2 (3.55E-2 - 3.80E-2)[a]	7.07E-2 (5.04E-2 - 0.10)
sn2-LPC 16:1	2.91 (1.64E-2 - 5.98E-2)	1.28E-2 (1.09E-2 - 1.46E-2)[a]	4.91E-2 (2.80E-2 - 8.07E-2)
sn1-LPC 17:0	5.91E-2 (3.66E-2 - 6.45E-2)	3.13E-2 (1.40E-2 - 4.28E-2)	3.19E-2 (2.47E-2 - 5.04E-2)
sn2-LPC 17:1	9.72E-4 (9.72E-4 - 1.14E-3)	6.23E-4 (3.79E-4 - 7.65E-4)[b]	1.19E-3 (8.10E-4 - 2.20E-3)
sn1-LPC 18:0	4.31 (3.10 - 5.36)	5.48 (3.07 - 7.17)	2.71 (2.24 - 4.18)
sn2-LPC 18:0	9.49E-2 (8.97E-2 - 0.10)	0.12 (7.44E-2 - 0.21)	3.99E-2 (3.12E-2 - 6.87E-2)[a]
sn1-LPC 18:1	1.01 (0.72 - 1.80)	0.66 (0.21 - 0.89)	0.59 (0.42 - 0.84)
sn2-LPC 18:1	0.27 (0.26 - 0.32)	0.64 (0.34 - 0.82)	0.63 (0.54 - 0.73)[b]
sn1-LPC 18:2	0.76 (0.71 - 0.83)	0.37 (0.18 - 0.70)[b]	0.29 (0.26 - 0.34)[b]
sn2-LPC 18:2	1.30 (1.16 - 1.37)	2.00 (0.99 - 2.65)	1.23 (0.93 - 1.35)
sn1-LPC 19:0	1.39E-2 (9.84E-2 - 1.98E-2)	1.65E-3 (9.96E-4 - 2.80E-3)[b]	8.85E-4 (7.36E-4 - 1.54E-3)[b]
sn2-LPC 19:0	7.13E-3 (4.48E-3 - 1.01E-2)	1.27E-3 (8.78E-4 - 1.82E-3)[b]	4.66E-3 (3.28E-3 - 9.85E-3)
sn1-LPC 20:0	3.87E-3 (3.72E-3 - 4.39E-3)	1.18E-3 (5.73E-4 - 2.41E-3)[a]	2.91E-4 (2.50E-4 - 3.63E-4)[b]
sn1-LPC 20:1	1.69E-2 (1.54E-2 - 3.64E-2)	7.03E-3 (2.66E-3 - 9.32E-3)[b]	4.21E-3 (3.53E-3 - 9.33E-3)[b]
sn1-LPC 20:2	3.37E-3 (2.86E-3 - 5.06E-3)	2.59E-3 (2.54E-3 - 2.62E-3)[b]	1.20E-3 (1.20E-3 - 1.20E-3)
sn2-LPC 20:2	2.09E-3 (1.94E-3 - 2.23E-3)	1.62E-3 (6.62E-4 - 2.16E-3)	1.10E-3 (1.10E-3 - 1.10E-3)[b]
sn1-LPC 20:3	8.69E-3 (6.12E-3 - 1.37E-2)	5.68E-3 (1.98E-3 - 7.07E-3)	9.49E-3 (9.34E-3 - 9.96E-3)
sn2-LPC 20:3	1.22E-2 (8.55E-3 - 1.35E-2)	1.96E-2 (8.83E-3 - 3.02E-2)	4.08E-2 (3.56E-2 - 4.54E-2)[b]
sn1-LPC 20:4	5.59E-2 (3.52E-2 - 7.57E-2)	8.31E-2 (4.03E-2 - 0.11)	7.39E-2 (5.26E-2 - 8.37E-2)
sn2-LPC 20:4	0.14 (0.13 - 0.17)	0.20 (0.14 - 0.27)	0.20 (0.16 - 0.25)[b]
sn2-LPC 22:4	5.33E-4 (2.15E-4 - 8.95E-4)	9.95E-4 (4.96E-4 - 1.88E-2)	6.40E-4 (4.82E-4 - 6.91E-4)
sn1-LPC 22:6	3.25E-2 (2.28E-2 - 6.19E-2)	1.11E-2 (6.87E-3 - 1.54E-2)[a]	1.89E-2 (1.72E-2 - 2.28E-2)
sn2-LPC 22:6	3.13E-2 (1.42E-2 - 4.89E-2)	2.02E-2 (1.26E-2 - 2.76E-2)	3.67E-2 (3.53E-2 - 3.82E-2)
Lysophosphatidylethanolamines (µmol/g)			
sn1-LPE 16:0	0.81 (0.57 - 1.49)	0.85 (0.40 - 1.18)	1.53 (1.16 - 1.99)
sn2-LPE 16:0	6.42E-2 (4.34E-2 - 0.11)	2.06E-2 (1.80E-2 - 3.26E-2)[b]	3.34E-2 (2.30E-2 - 5.07E-2)[a]
sn1-LPE 16:1	7.93E-2 (6.62E-2 - 0.14)	1.52E-2 (9.49E-3 - 2.38E-3)[b]	4.34E-2 (3.07E-2 - 0.12)
sn2-LPE 16:1	2.05E-2 (1.83E-2 - 3.17E-2)	2.31E-3 (1.82E-3 - 4.25E-3)[b]	1.04E-2 (4.77E-3 - 1.68E-2)[b]
sn1-LPE 17:0	5.70E-3 (4.23E-3 - 6.86E-3)	1.56E-2 (1.53E-2 -1.63E-2)[a]	3.07E-2 (1.52E-2 - 3.80E-2)[b]
sn1-LPE 17:1	9.50E-4 (9.50E-4 - 9.5E-4)	8.85E-4 (7.61E-4 - 1.01E-3)	1.07E-3 (1.01E-3 - 1.09E-3)[a]
sn1-LPE 18:0	0.90 (0.89 - 1.60)	5.48 (3.07 - 7.17)	2.49 (1.96 - 3.37)[a]
sn2-LPE 18:0	1.82E-2 (7.82E-3 - 2.43E-2)	5.45E-2 (1.61E-2 - 9.19E-2)	4.94E-2 (2.73E-2 - 5.73E-2)[a]
sn1-LPE 18:1	0.93 (0.36 - 2.32)	1.38 (1.28 - 1.44)	0.90 (0.87 - 0.95)
sn2-LPE 18:1	1.08 (0.44 - 2.82)	0.64 (0.24 - 0.88)	0.31 (0.21 - 0.47)[b]
sn1-LPE 18:2	8.28E-2 (7.64E-2 - 0.13)	0.15 (9.91E-2 - 0.41)	0.47 (0.12 - 0.67)[a]
sn2-LPE 18:2	0.71 (0.43 - 1.20)	0.56 (0.21 - 1.32)	0.63 (0.22 - 0.83)
sn1-LPE 20:1	6.51E-3 (1.90E-3 - 9.33E-3)	1.53E-3 (1.53E-3 - 1.62E-3)[b]	1.52E-3 (1.34E-3 - 1.75E-3)[b]
sn2-LPE 20:1	1.30E-2 (8.44E-3 - 1.94E-2)	1.29E-3 (1.06E-3 - 2.09E-3)[b]	1.14E-3 (9.85E-4 - 2.61E-3)
sn1-LPE 20:4	0.35 (0.22 - 0.70)	0.30 (0.17 - 0.48)	0.65 (0.32 - 0.99)
sn2-LPE 20:4	2.19 (2.06 - 2.39)	2.06 (1.68 - 3.49)	2.44 (1.61 - 2.72)
sn2-LPE 22:1	ND	ND	ND
sn1-LPE 22:4	3.75E-3 (2.26E-3 - 6.96E-3)	4.54E-2 (4.13E-2 - 5.06E-2)	1.72E-3 (1.36E-3 - 2.04E-3)

sn2-LPE 22:4	5.27E-2 (3.11E-2 - 9.27E-2)	7.92E-2 (7.89E-2 - 8.03E-2)	3.26E-2 (2.31E-2 - 5.84E-2)
sn2-LPE 22:5	3.03E-2 (2.47E-2 - 5.42E-2)	2.04E-2 (1.48E-2 - 3.45E-2)	2.97E-2 (2.64E-2 - 3.88E-2)
sn1-LPE 22:6	0.48 (0.22 - 1.22)	7.26E-2 (6.83E-2 - 7.93E-2)[b]	0.32 (0.24 - 1.10)
sn2-LPE 22:6	1.70 (1.25 - 1.80)	0.51 (0.45 - 0.57)[b]	0.87 (0.72 - 1.72)
Saturated fatty acids (µmol/g)			
Lauric acid	6.31E-4 (5.23E-4 - 8.38E-4)	5.07E-4 (4.67E-4 - 6.18E-4)	5.58E-3 (3.43E-3 - 9.33E-3)[b]
Myristic acid	16.17 (11.32 - 26.59)	5.00 (3.00 - 6.15)[a]	56.74 (38.93 - 73.41)[a]
Pentadecanoic acid	4.96E-4 (2.14E-4 - 7.18E-4)	1.03E-4(7.12E-5 - 1.82E-4)[b]	1.81E-3 (1.79E-3 - 2.11E-3)[b]
Palmitic acid	1.44 (0.81 - 1.83)	0.15 (5.53E-2 - 0.22)[b]	0.36 (0.15 - 0.50)[b]
Stearic acid	3.57E-4 (3.22E-4 - 6.68E-4)	4.26E-4 (4.21E-4 - 4.43E-4)	4.13E-4 (3.49E-4 - 4.87E-4)
Monounsaturated fatty acid (µmol/g)			
Palmitoleic acid	5.94 (4.34 - 6.68)	0.37 (0.34 - 0.55)[b]	1.95 (1.31 - 3.29)[b]
Oleic acid	19.66 (1.62E-3 - 2.94E-3)	4.34 (3.19 - 7.18)[b]	7.89 (1.88 - 11.47)[b]
Polyunsaturated fatty acid (µmol/g)			
Stearidonic acid	6.76E-3 (5.37E-3 - 7.34E-3)	ND	2.01E-4 (1.31E-4 - 7.58E-4)[b]
Eicosapentaenoic acid	2.22 (1.75 - 2.80)	8.41E-2 (3.75E-2 - 0.19)[b]	1.51 (1.06 - 1.95)
Docosahexaenoic acid	54.26 (38.89 - 71.99)	22.29 (11.87 - 24.43)[a]	32.61 (32.61 - 33.32)[a]
ω3-Docosapentaenoic acid	1.05 (0.84 - 1.24)	0.13 (5.17E-2 - 0.24)[b]	0.64 (0.42 - 0.81)[a]
ω6-Docosapentaenoic acid	0.53 (0.50 - 0.62)	0.69 (0.14 - 1.28)	0.29 (0.25 - 0.38)[b]
Arachidonic acid	39.91 (36.94 - 45.93)	72.69 (58.42 - 75.36)[b]	74.61 (52.92 - 93.07)[b]
Iso-1-linolenic acid	0.91 (0.91 - 0.91)	5.33E-2 (5.26E-2 - 8.89E-2)[b]	0.22 (0.14 - 0.27)[b]
Iso-2-linolenic acid	7.89E-2 (7.03E-2 - 8.38E-2)	4.21E-2 (2.91E-2 - 4.95E-2)[b]	3.13E-2 (2.45E-2 - 4.78E-2)[b]
Iso-1-linoleic acid	59.03 (54.71 - 68.83)	5.31 (4.67 - 6.67)[b]	6.10 (3.27 - 7.35)[d]
ω6-Dihomo-dietary γ-linolenic acid	0.13 (0.12 - 0.15)	6.15E-2 (3.06E-2 - 0.14)	0.13 (0.10 - 0.23)
ω6-Dihomo-dietary γ-linolenic acid – iso2	6.13E-3 (5.63E-3 - 8.09E-3)	7.17E-3 (3.68E-3 - 1.47E-3)	8.46E-3 (7.07E-3 - 9.39E-3)
ω6-Dihomo-dietary γ-linolenic acid – iso3	0.17 (0.15 - 0.18)	6.90E-2 (4.96E-2 - 0.26)	0.22 (0.10 - 0.34)
Adrenic acid	7.21E-2 (5.02E-2 - 8.18E-2)	6.46E-2 (3.07E-2 - 0.11)	4.72E-2 (4.30E-2 - 5.29E-2)[a]
ω6- Eicosadienoic acid	1.89E-3 (1.62E-3 - 2.94E-2)	6.43E-4 (3.39E-4 - 1.13E-3)[b]	2.18E-4 (1.61E-4 - 2.36E-4)[b]
Peroxidized fatty acids (µmol/g)			
9-HODE / 13-HODE	75.78 (58.19 - 130.90)	33.37 (30.08 - 41.48)[b]	13.99 (12.36 - 22.04)[b]
Epoxy-stearic acid-iso1	0.13 (8.68E-2 - 0.23)	1.78E-2 (5.75E-3 - 3.23E-2)[a]	9.32E-2 (4.75E-2 - 0.27)[d]
Epoxy-stearic acid-iso2	7.46E-3 (6.37E-3 - 8.12E-3)	2.74E-2 (9.47E-3 - 4.86E-2)[b]	1.09E-2 (9.77E-3 - 1.7E-2)[b]
15-HETE	1.45 (1.14 - 1.55)	2.58 (2.23 - 3.48)[b]	2.05 (1.47 - 2.99)
12-HETE	4.62 (2.92 - 8.91)	25.55 (19.18 - 30.32)[b]	13.31 (10.40 - 26.77)[a]
x-OxoODE-iso1	529.28 (477.10 - 693.25)	648.309 (491.09 - 735.53)	606.16 (455.46 - 673.46)
x-EpOME-iso1	8.21 (4.41 - 12.03)	10.19 (7.81 - 13.23)	6.90 (6.89 - 7.31)
9,12,13-TriHOME(10)	39.52 (20.93 - 53.17)	31.19 (21.22 - 35.00)	23.33 (22.84 - 24.17)

HDHA, hydroxydocosahexaenoic acid; HETE, 5-hydroxyeicosatetraenoic acid; HODE, hydroxyoctadecadienoic acid; HOME, hydroxyoctadecenoic acid; LPE, lysophosphatidylethanolamine; LPC, lysophosphatidylcholine; LPS, lysophosphatidylserine

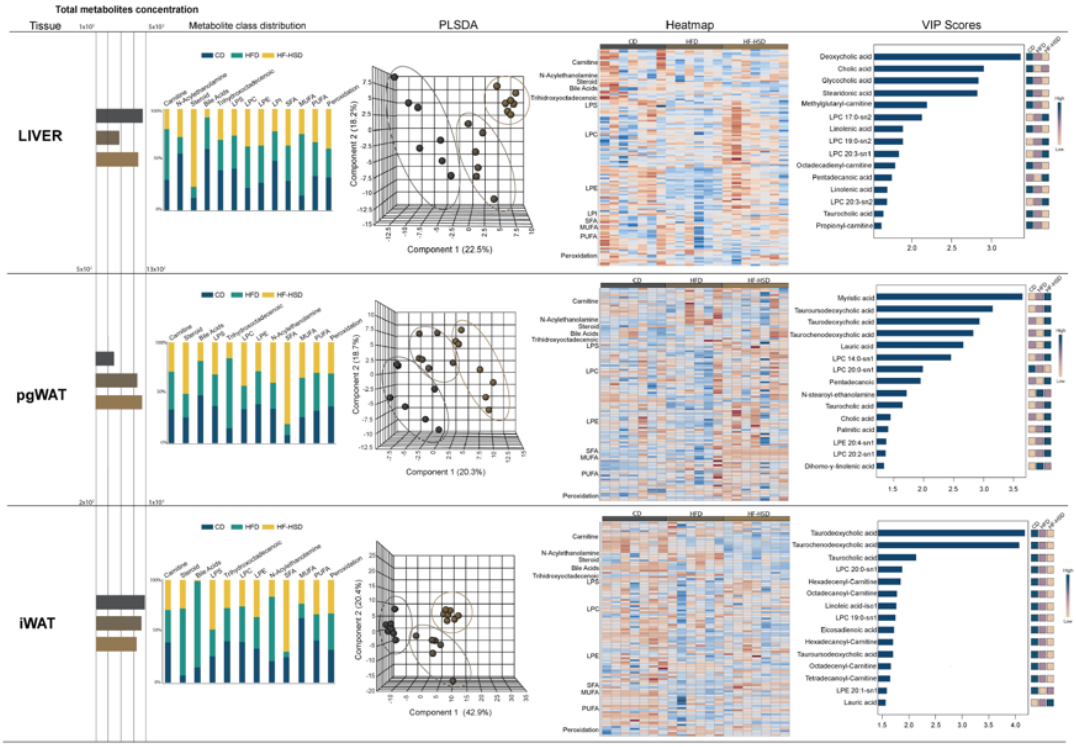

Supporting Information Figure S4. Lipidomic analysis in the liver, perigonadal white adipose tissue (pgWAT) and inguinal white adipose tissue (iWAT) of mice fed with a chow diet (CD), high-fat diet (HFD) or high-fat high-sucrose diet (HF-HSD). From left to right: total metabolite concentrations, class distribution, partial least squares discriminant analysis (PLSDA), heatmap and variable importance in projection (VIP) scores

Uncropped blots from figure 2 (Liver)

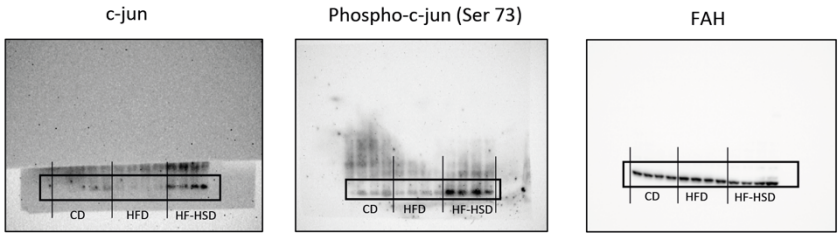

Uncropped blots from figure 3 (Liver)

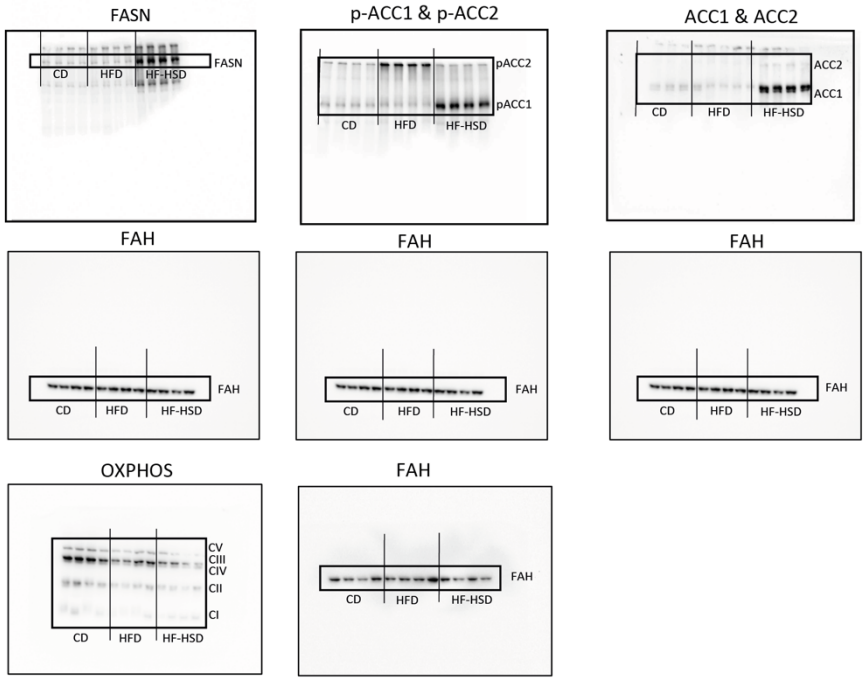

Uncropped blots from figure 4 (Liver)

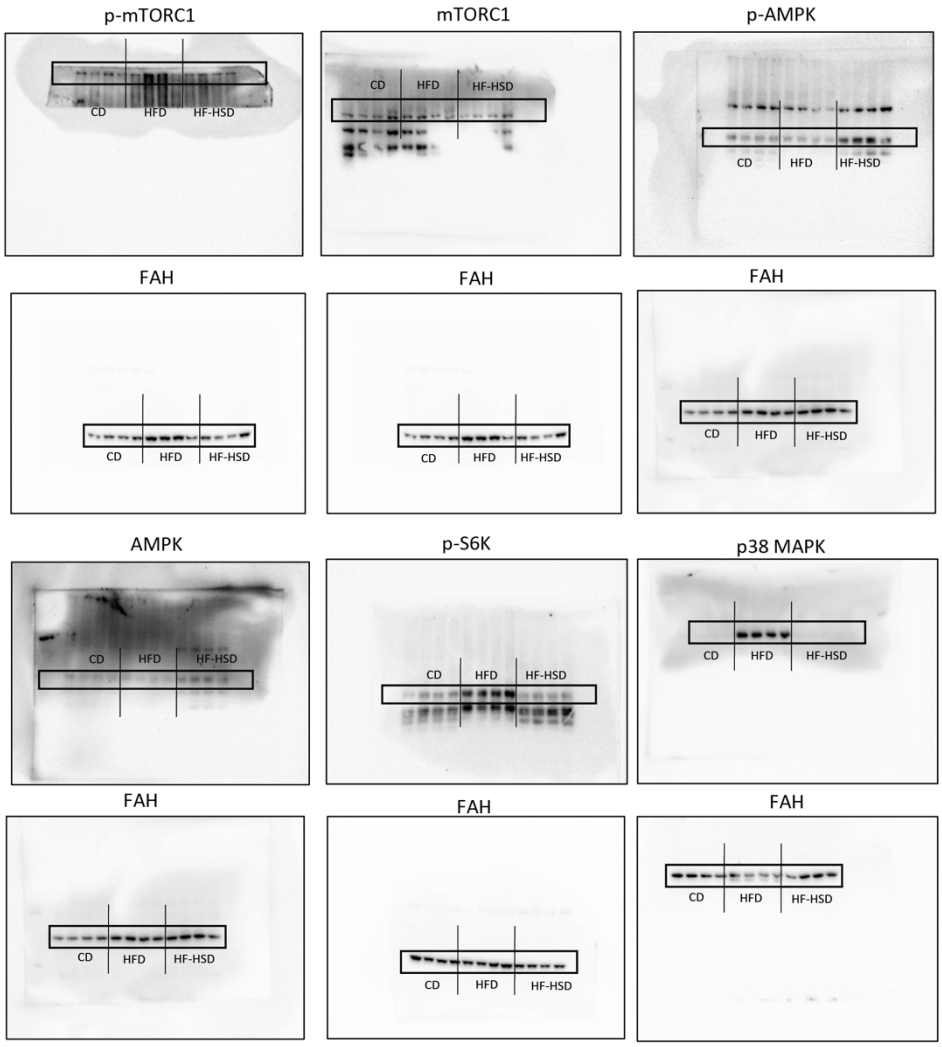
p-mTORC1
CD HFD HF-HSD
mTORC1
CD HFD HF-HSD
p-AMPK
CD HFD HF-HSD
FAH
CD HFD HF-HSD
FAH
CD HFD HF-HSD
FAH
CD HFD HF-HSD
AMPK
CD HFD HF-HSD
p-S6K
CD HFD HF-HSD
p38 MAPK
CD HFD HF-HSD
FAH
CD HFD HF-HSD
FAH
CD HFD HF-HSD
FAH
CD HFD HF-HSD

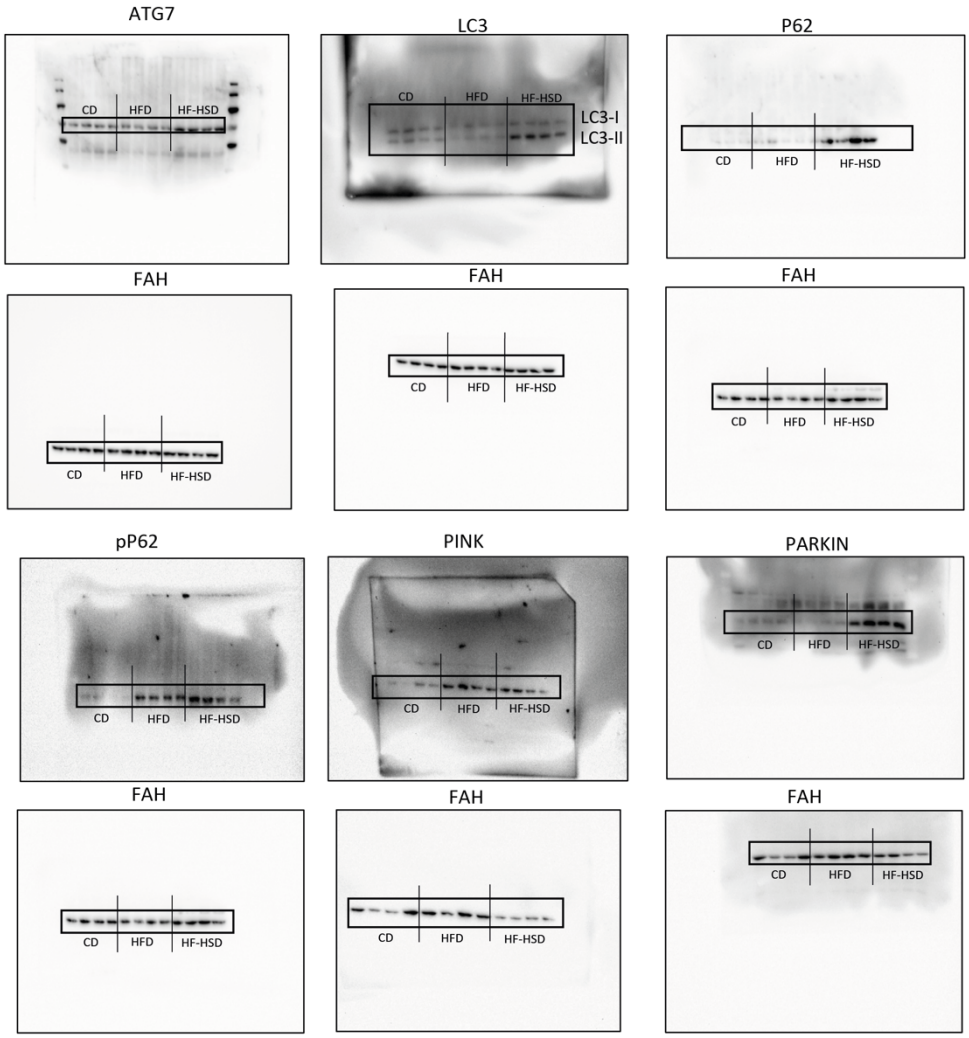
ATG7
CD
HFD
HF-HSD
LC3
CD
HFD
HF-HSD
LC3-I
LC3-II
P62
CD
HFD
HF-HSD
FAH
CD
HFD
HF-HSD
FAH
CD
HFD
HF-HSD
FAH
CD
HFD
HF-HSD
pP62
CD
HFD
HF-HSD
PINK
CD
HFD
HF-HSD
PARKIN
CD
HFD
HF-HSD
FAH
CD
HFD
HF-HSD
FAH
CD
HFD
HF-HSD
FAH
CD
HFD
HF-HSD

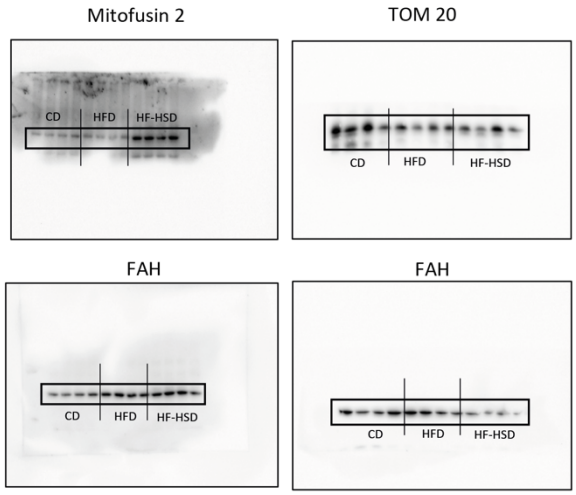

Uncropped blots from figure 5 (pgWAT)

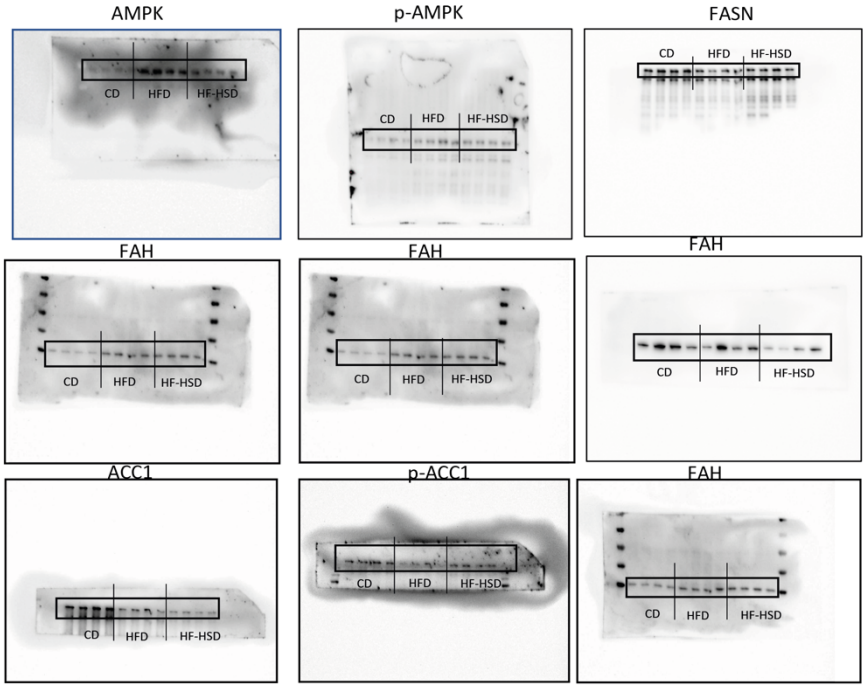

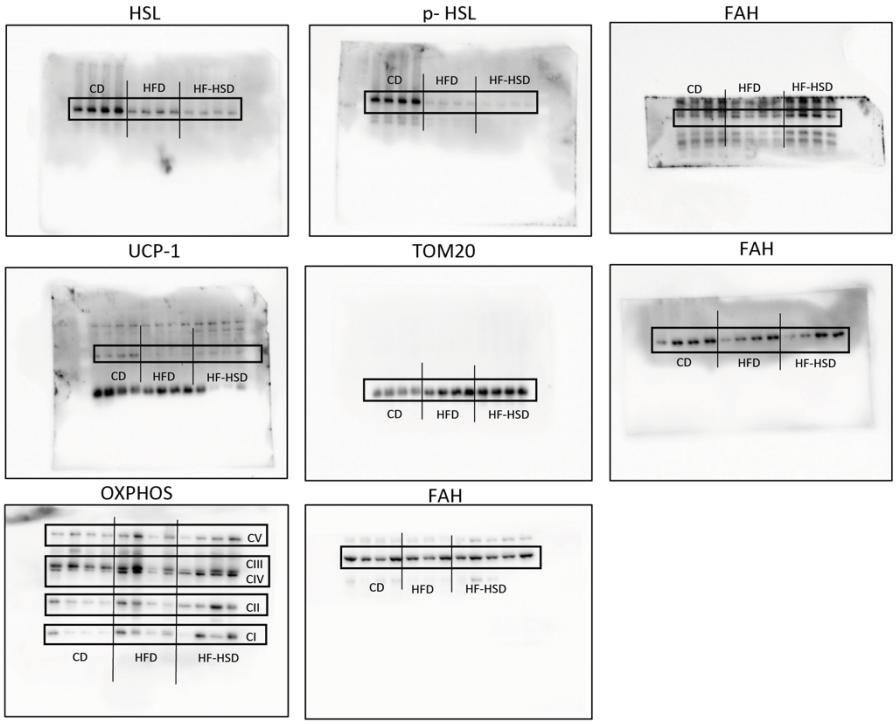

Uncropped blots from figure 5 (iWAT)

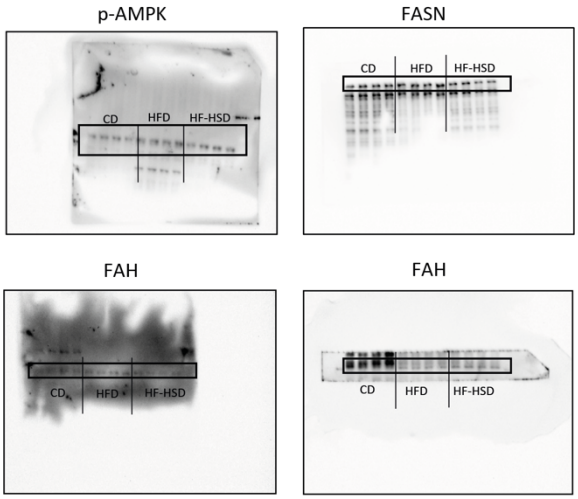

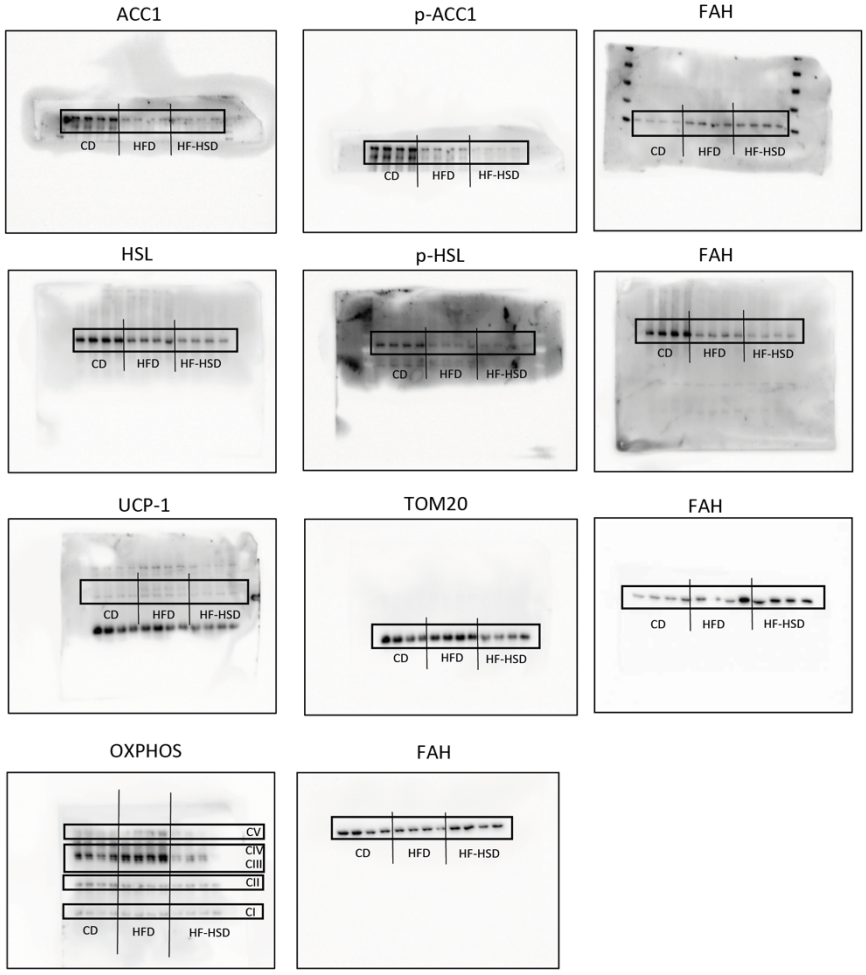
ACC1
CD
HFD
HF-HSD
p-ACC1
CD
HFD
HF-HSD
FAH
CD
HFD
HF-HSD
HSL
CD
HFD
HF-HSD
p-HSL
CD
HFD
HF-HSD
FAH
CD
HFD
HF-HSD
UCP-1
CD
HFD
HF-HSD
TOM20
CD
HFD
HF-HSD
FAH
CD
HFD
HF-HSD
OXPHOS
CV
CIV
CIII
CII
CI
CD
HFD
HF-HSD
FAH
CD
HFD
HF-HSD

Uncropped blots from Supplementary figure 1 (liver)

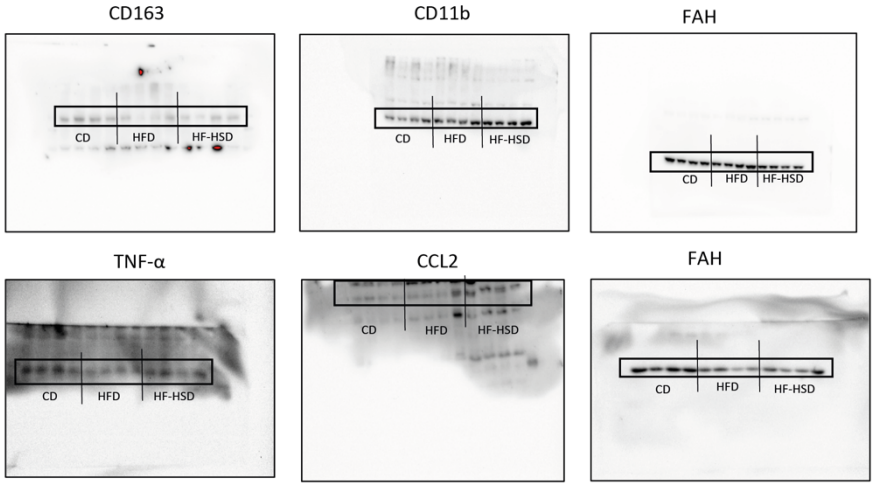

Study II: Combining caloric restriction with metformin treatment enhances NAFLD remission in mice fed a high-fat high-sucrose diet

UNIVERSITAT ROVIRA I VIRGILI
EXPLORING LIVER AND ADIPOSE TISSUE ALTERATIONS IN THE NATURAL COURSE OF NON-ALCOHOLIC FATTY LIVER DISEASE: A LIPIDOMIC
Gerard Baiges Gaya

JHEP Reports

Combining caloric restriction with metformin treatment enhances NAFLD remission in mice fed a high-fat high-sucrose diet

--Manuscript Draft--

Manuscript Number:	
Article Type:	Original Article
Section/Category:	NAFLD and alcohol-related liver disease
Keywords:	Mice, Obesity, Adipocytes, Liver, NAFLD, Lipidomic
Corresponding Author:	Jordi Camps Hospital Universitari Sant Joan de Reus Reus, Catalunya SPAIN
First Author:	Gerard Baiges-Gaya
Order of Authors:	Gerard Baiges-Gaya
	Elisabet Rodríguez-Tomàs
	Helena Castañé
	Andrea Jiménez-Franco
	Núria Amigó
	Jordi Camps
	Jorge Joven
Abstract:	Background & Aims: Non-alcoholic fatty liver disease (NAFLD) and non-alcoholic steatohepatitis (NASH) are serious health concerns in which lifestyle interventions are the only effective first-line treatments. Caloric restriction is effective in body weight reduction, but not much in the way of improvement in insulin sensitivity and hepatic lipid mobilization. Conversely, metformin increases insulin sensitivity and promotes the inhibition of de novo hepatic lipogenesis. In this study we evaluate the metformin effectiveness in NASH prevention and treatment, when combined with caloric restriction in male mice fed a high-fat high-sucrose diet (HFHSD). Methods: Eighty 5-week old C57BL/6J male mice were fed a chow or HFHSD diets and sacrificed at 20 or 40 weeks. Serum as well as hepatic and adipose tissues were obtained for lipoprotein, lipidomics, biochemical, and histological analyses. Results: HFHSD-fed mice developed NASH after 20 weeks. Lipoprotein and lipidomic analyses showed that the changes associated with diet were not prevented by metformin administration. Conversely, the age of mice worsened the lipoprotein profile. Lipidomic analysis of visceral and subcutaneous adipocytes showed that the age of mice was the main factor in the lipid remodeling process; specifically increasing lipid storage and decreasing glycerophospholipid levels. HFHSD-fed mice subject to caloric restriction (CR) combined with metformin showed a 19.6% body weight reduction compared to 9.8% in those mice subjected to CR alone. Lower hepatic steatosis scores were induced. Our lipidomic data showed that both types of intervention reversed hepatic and adipocytes lipidome, as well as the biochemical and lipoprotein profiles. Conclusions: We conclude that metformin should not be considered as a preventive option in NAFLD, but it is effective in the treatment of this disorder when combined with CR.

Combining caloric restriction with metformin treatment enhances NAFLD remission in mice fed a high-fat high-sucrose diet

Gerard Baiges-Gaya[1,2], Elisabet Rodríguez-Tomàs[1,2], Helena Castañé[1,2], Andrea Jiménez-Franco[1], Núria Amigó[1,3,4], Jordi Camps[1,2,⋈], Jorge Joven[1,2,5⋈]

[1] *Universitat Rovira i Virgili, Department of Medicine and Surgery, 43201 Reus, Spain*

[2] *Unitat de Recerca Biomèdica (URB-CRB), Hospital Universitari de Sant Joan,Institut d'Investigacio Sanitaria Pere Virgili, Universitat Rovira i Virgili, 43201 Reus, Spain*

[3] *CIBER de Diabetes y Enfermedades Metabólicas Asociadas (CIBERDEM)- Instituto de Salud Carlos III, 28029, Madrid, Spain*

[4] *Biosfer Teslab SL Plaça Prim, 10 2on 5a, 43201, Reus, Spain*

[5] *Campus of International Excellence Southern Catalonia, Tarragona, Spain*

⋈ **Corresponding authors: jorge.camps@salutsantjoan.cat (J. Camps) or jorge.joven@salutsantjoan.cat (J. Joven)**

Unitat de Recerca Biomèdica (URB-CRB), Hospital Universitari de Sant Joan,Institut d'Investigacio Sanitaria Pere Virgili, Universitat Rovira i Virgili, Reus, Spain. Carrer Sant Joan s/n, 43201, Reus, Spain

Email addresses:

GBG: gerard.baiges@iispv.cat; ERT: elisabet.rodriguez@urv.cat;

HC: helena.castane@iispv.cat; A.J.F: andrea.jimenez@urv.cat;

N.A: nuriaamigo@gmail.com; JC: jorge.camps@salutsantjoan.cat;

JJ: jorge.joven@salutsantjoan.cat.

Electronic word count:

Number of figures: 4

Conflicts of interest

The authors declare no competing interests.

Financial support

This study was supported by grants PI18/00921 and PI21/00510 from the *Instituto de Salud Carlos III* (Madrid, Spain) and the *Agència de Gestió d'Ajuts Universitaris I de Recerca by Generalitat de Catalunya* (AGAUR, SGR00436). G.B.G is recipient of PFIS fellowship (FI19/00097) co-financed by the European Social Fund (ESF) "investing in your future".E.R.T is recipient of a fellowship from AGAUR (2020FI_d1 00215). H.C is recipient of a fellowship of the Department of Health of Catalonia (Generalitat de Catalunya). "Pla Estratègic de Recerca I Innovació en Salut" (PERIS-SLT017/3501/2020)

Authors' contributions

Gerard Baiges-Gaya, Jordi Camps, Jorge Joven: Conceptualization; Gerard Baiges-Gaya, Jordi Camps: Data curation; Gerard Baiges-Gaya, Jordi Camps, Jorge Joven: Formal analysis; Jorge Joven: Funding acquisition; Gerard Baiges-Gaya, Elisabet Rodríguez-Tomàs, Helena Castañé, Andrea Jiménez-Franco: Investigation; Gerard Baiges-Gaya, Elisabet Rodríguez-Tomàs, Helena Castañé, Andrea Jiménez-Franco: Methodology; Jordi Camps, Jorge Joven: Project administration; Núria Amigó, Jorge Joven: Resources; Gerard Baiges-Gaya: Software; Jordi Camps, Jorge Joven: Supervision; Gerard Baiges-Gaya, Jordi Camps, Jorge Joven: Validation; Jordi Camps: Visualization; Gerard Baiges-Gaya: Writing – original draft; Jordi Camps: Writing – review & editing.

Acknowledgments

The authors thank Dr. Peter R. Turner for critical review and language editing of the manuscript. The EURECAT-Technology Centre of Catalonia (Reus, Spain) contributed its expertise and advice in lipidomics measurements.

ABSTRACT

Background & Aims: Non-alcoholic fatty liver disease (NAFLD) and non-alcoholic steatohepatitis (NASH) are serious health concerns in which lifestyle interventions are the only effective first-line treatments. Caloric restriction is effective in body weight reduction, but not much in the way of improvement in insulin sensitivity and hepatic lipid mobilization. Conversely, metformin increases insulin sensitivity and promotes the inhibition of *de novo* hepatic lipogenesis. In this study we evaluate the metformin effectiveness in NASH prevention and treatment, when combined with caloric restriction in male mice fed a high-fat high-sucrose diet (HFHSD).

Methods: Eighty 5-week old C57BL/6J male mice were fed a chow or HFHSD diets and sacrificed at 20 or 40 weeks. Serum as well as hepatic and adipose tissues were obtained for lipoprotein, lipidomics, biochemical, and histological analyses.

Results: HFHSD-fed mice developed NASH after 20 weeks. Lipoprotein and lipidomic analyses showed that the changes associated with diet were not prevented by metformin administration. Conversely, the age of mice worsened the lipoprotein profile. Lipidomic analysis of visceral and subcutaneous adipocytes showed that the age of mice was the main factor in the lipid remodeling process; specifically increasing lipid storage and decreasing glycerophospholipid levels. HFHSD-fed mice subject to caloric restriction (CR) combined with metformin showed a 19.6% body weight reduction compared to 9.8% in those mice subjected to CR alone. Lower hepatic steatosis scores were induced. Our lipidomic data showed that both types of intervention reversed hepatic and adipocytes lipidome, as well as the biochemical and lipoprotein profiles.

Conclusions: We conclude that metformin should not be considered as a preventive option in NAFLD, but it is effective in the treatment of this disorder when combined with CR.

Abstract words: 275

Keywords: Mice, Obesity, Adipocytes, Liver, NAFLD, Lipidomic

Lay summary:

Caloric restriction is an accepted manner of reducing weight in morbid obesity, but does not greatly improve insulin sensitivity or liver lipid accumulation. Our data show that, in mice fed a diet high in fat and sucrose, the combination of metformin administration and caloric restriction

is more effective than restriction alone in decreasing body weight and normalizing the hepatic derangements in NAFLD.

Lay summary words: 65

1. Introduction

Obesity is a metabolic disease that increases the risk pf developing non-alcoholic fatty liver disease (NAFLD). The onset of NAFLD consists of an increase in the lipid content of the liver and, over time, alterations leading to non-alcoholic steatohepatitis (NASH), which is characterized by hepatocyte death, inflammation, and fibrosis. Lipid metabolism requires complex regulations to maintain plasma membrane fluidity, and lipoprotein synthesis needed for cellular viability [1–3]. Under normal conditions, excessive intracellular lipid levels are metabolized, or transported in secreted lipoproteins or stored as lipid droplets. However, in NAFLD, the lipoprotein secretion and glycerophospholipid synthesis by endoplasmic reticulum may be impaired; and lead to alterations in very-low-density lipoprotein (VLDL) size and glycerophospholipid profile [4–7]. In this metabolic context, lipid mobilization deteriorates, causing accumulation of cholesterol esters in the hepatocyte, leading to NASH development [8–10]. The lack of effective pharmacological strategies makes the management of NAFLD difficult, and becomes an important health challenge worldwide. Metformin is the first-line drug in type 2 diabetes mellitus management; a function of increasing insulin sensitivity. However, there is insufficient evidence on the role of metformin within the spectrum of metabolic derangements of NAFLD. Earlier animal studies suggested that metformin is effective in reducing hepatic steatosis by inhibiting *de novo* hepatic lipogenesis and, as such, preventing the onset and progression of NAFLD. However, most of these studies had been conducted in animals fed a high-fat diet (HFD) [11–13] and results from our group [14] and others [15] have reported that, compared to HFD-fed mice,, high-fat high-sucrose diets (HFHSD) promote a phenotype characterized by higher hepatic steatosis scores, oxidative stress and inflammatory environment, together with alterations in autophagy. The results suggest that such a diet could be a better mouse model for the study of NASH. Caloric restriction is effective in body weight reduction, while amelioration of the hepatic fat content [16] is less effective in increasing insulin sensitivity and adipose tissue lipid mobilization [17] Thus, the present study addressed the effects of caloric restriction and metformin treatment in the context of severe obesity and NASH; the outcome would have clinical relevance in the treatment of morbid obesity. Using a lipidomic approach, the objectives of the study were to evaluate: 1) if metformin treatment protects against NASH

development in HFHSD-fed mice; 2) the possible synergistic effects of caloric restriction and metformin administration in NAFLD resolution.

2. Material and methods

2.1. Mice study protocol

Four-week-old C57BL/6J mice were obtained from ENVIGO (Barcelona, Spain), and were housed 4 per cage in a temperature-controlled room (22 ± 2ºC) with a 12hr light/dark cycle, with “lights on” corresponding to 8 am. All mice were male, acclimatized to the animal house for 1 week. They were fed a diet (TD.2018, Teklad) composed of 58% carbohydrates, 24% protein and 18% fat.

During the study, mice were fed with a chow diet (TD.2014, Teklad), composed of 67% carbohydrates, 20% protein, and 13% fat, or a HF-HSD (TD.08811, Teklad) containing 40.7% carbohydrates (29% sucrose), 14.7% protein and 44.6% fat.

Mice were monitored daily for well-being and signs of discomfort and distress. Body weight, food and water intakes were monitored weekly, and metformin was administrated in drinking water daily (300 mg/kg body weight/day). Animal experiments were approved by the Animal Ethics Committee of *Rovira i Virgili University* and authorized by the Directorate General of Environmental Policies and the Natural Environment of the Government of Catalonia (reference number: 10281).

2.2. Mice study design

The study was carried out on 80 male mice. Five-week-old animals were randomly divided into 6 experimental groups. Sixteen mice were fed CD and were sacrificed by cervical dislocation under general anesthesia in groups of 8 at 25 and 45 weeks of age. The same design was repeated for animals fed CD+metformin, HFHSD alone and HFHSD + metformin. The remaining 16 animals received HFHSD or HFHSD + metformin. Halfway through the study the regimen was swapped (see scheme in Fig. S1). The animals were sacrificed at 45 weeks of age.

2.3. Glucose tolerance test

Two weeks before scheduled sacrifice, the mice were fasted for 14h (from 6 pm to 8 am) and were injected a glucose solution (2g glucose per kg body weight, i.p.). Blood samples for glucose measurement were taken at 15, 30, 60 and 120 min post-injection, and glucose measured using a handheld glucometer (Accu-Check glucose reader, Roche).

2.4. Histological analysis

Liver and adipose tissue samples at the conclusion of each dietary period were removed and fixed in formalin and embedded in paraffin for hematoxylin/eosin staining. The degree of hepatic impairment was estimated using the NAFLD activity score (NAS score). This scoring system is based on histological features classified into three categories: steatosis (graded from 0 to 3), lobular inflammation (graded from 0 to 2) and hepatocellular ballooning (graded from 0 to 2) [18]. Samples were assessed by an experienced pathologist of the team (J.J.) who was blinded with respect to the provenance of the samples. NASH was considered when the NAS score was ≥5. The average adipocyte size from visceral and subcutaneous adipose tissue was estimated using the Image J 1.51 software (National Institutes of Health, Bethesda, MD, USA) with the macro MRI's adipocyte tool.
Sections were assessed using optical microscopy (Eclipse E600, Nikon) and images recorded using NIS-Elements F 4.00.00 software.

2.5. Lipoprotein analyses by nuclear magnetic resonance (^{1}H-NMR) spectroscopy

The lipoprotein profiles of serum samples were analyzed by ^{1}H-NMR, as previously described [5] .

2.6. Isolation of mature adipocytes

Visceral (epididymal and retroperitoneal) and subcutaneous (inguinal and anterior) adipose tissues were removed post-sacrifice, and resuspended in digestion solution containing 10 mL of DMEM/F12 and 10 mg of collagenase type II (C6885, Sigma) for 50 minutes at 37ºC with agitation at 100 rpm. Digested samples were then passed through 250 µm cell strainer (S1020, Sigma) into fresh sample tubes and centrifuged at room temperature at 300g for 5 min to separate adipocytes from the stromal

vascular fraction. Adipocytes were separated by pipetting, washed in phosphate-buffered saline solution, and used directly for lipid analysis.

2.7. Semi-targeted lipidomics

Apolar lipids were extracted from liver and adipocytes with methanol, and polar lipids with methanol and chloroform, as described in detail [14,19]. Lipid samples were analyzed by liquid chromatography coupled to time-of-flight mass spectrometry. We detected 292 and 190 lipid species from liver and adipocytes respectively, The following categories were identified: Fatty acyls (FAs) [fatty acids (FA), acyl-carnitines (CAR), hydroxy fatty acids (HFA), N-acyl-ethanolamine (NAE)]; glycerolipids (GLs) [triglycerides (TG), diglycerides (DG)]; glycerophospholipids (GPs) [ester-linked phosphatidylcholines (PC), ester linked lysophosphatidylcholines (LPC), ester linked lysophosphatidylethanolamines (LPE)]; sphingophospholipids (SPs) [sphingomyelins (SM)]; and sterol lipids (ST) [bile acids (BAs), cholesterol ester (CE), steroid hormones]. Data are expressed as internal standard response ratios.

2.8. Statistical analysis

All data from box plots are represented as means, with bars showing the minimum and maximum values. Error bars of bar plots represent standard deviation values. Some data are represented in lollipop and volcano plots. Statistical significance of quantitative variables of lipid species was assessed using Wilcoxon rank-sum test. A $p<0.05$ was considered statistically significant. Dimensionality reduction techniques (scikit-learn package) [20], lollipop (matplotlib package) [21] and volcano plots (bioinfokit package) were constructed using the Jupyter Notebook via the Anaconda environment [22] and written in Python code. Finally, GraphPad Prism (version 9.0.1) was used to generate box and bar plots.

2.8.1 Dimensionality reduction analysis

Linear discriminant analysis (LDA) was used as supervised technique method. LDA projects the data onto a low-dimensional space and is useful in exploring differences between groups.

3. Results

3.1. Metformin does not prevent HFHSD-associated NAFLD development and metabolic derangements

The average daily caloric intake in HFHSD-fed mice was almost double than in CD-fed animals (Fig. 1A). Body weight increased significantly and independently of metformin administration (Fig. 1B). We observed that diet and age contributed to the increase in tissue weight (Fig. 1C and 1D). Mice fed on a HFHSD developed a phenotype characterized by a higher concentration of glucose, cholesterol, and lower triglyceride concentrations together with higher alanine aminotransferase activities than mice fed on CD (Fig. 1E). In CD-fed mice, metformin administration slightly increased the cholesterol concentration in 45-week old mice, whereas in HFHSD-fed mice with metformin, cholesterol and triglyceride concentrations were decreased (Fig. S2). In addition, metformin improved glucose tolerance in 25-week old mice, but not in 45-week old mice (Fig. S3A and S3B). We found that cholesterol levels and alanine aminotransferase activities increased with age in HFHSD-fed mice (Fig. 1E).

In mice receiving HFHSD, the total number of lipoprotein particles was higher than in those given CD, with an increase in the number of low-density lipoprotein particles (LDL-p) and decreases in very low-density and high-density lipoprotein particles (VLDL-p) and (HDL-p), respectively (Fig. S4A). Medium-sized VLDL-p and large HDL-p increased in HFHSD-fed mice; a phenomenon that is accentuated with age (Fig. S4B). Total lipoprotein cholesterol was higher in mice fed HFHSD, whereas the total lipoprotein triglycerides were higher in mice fed CD. We found that the LDL-p population in HFHSF-fed mice was enriched with cholesterol and triglycerides, and these alterations were exacerbated with age (Fig. S4C and S4D). In addition, we observed that metformin slightly decreased the VLDL-p as well as the TG and cholesterol content linked to VLDL in 25-week-old mice fed CD. In 45-week-old mice, fed HFHSD, slightly decreased VLDL-p and increased TG content linked to IDL was observed (Fig. S5). Further,, we observed that 25-week-old mice fed CD+metformin had smaller VLDL-p than mice not receiving metformin (Fig. S6A). In summary: age worsened the HFHSD-associated lipoprotein profile, while metformin administration did not ameliorate it.

Hepatic histological analysis showed that dietary treatment was the main cause of NAFLD development, increase in hepatic steatosis, lobular inflammation, and ballooning scores. As a result, HFHSD-fed mice exhibited a phenotype associated with the diagnosis of probable NASH (NAS = 3-4) and definite NASH (NAS≥5), independently of metformin administration (Fig. 1F and S7). Also, the hepatic steatosis scores tended to increase with age.

3.2. NAFLD was associated with alterations in cholesterol-related lipids and glycerophospholipids

LDA showed that overall hepatic lipidome was altered mainly by the dietary treatment, while age and metformin played secondary roles (Fig. 2A-C, S8A-C). As such, hepatic glycerolipids (GLs) were the most abundant lipid category, followed by glycerophospholipids (GPs), fatty acyls (FAs), sphingophospholipids (SPs) and sterol lipids (ST) in CD-fed mice. HFHSD-fed animals had higher levels of ST than SPs. Despite the importance of diet in modifying the lipid category relative abundance, we also found alterations in the lipid composition of FAs, GPs and ST i.e. the FAs pool in mice with NAFLD was characterized by decrease in hydroxy fatty acids, an oxylipin type, and increase in carnitines (CAR) and fatty acids (FA) (Fig. 2D). In the GPs pool, the levels of phosphatidylcholines (PC) decreased, whereas the levels of lysophosphatidylcholines (LPC) increased, suggesting that phospholipid hydrolysis is increased (Fig. 2F). Finally, in the ST pool we found that free cholesterol was mainly depleted in forming cholesterol esters (CE) and, therefore, decreased the concentrations of bile acids (BA), and steroid hormones (St) (Fig. 2H).

In parallel with these findings, we observed that diglycerides (DG), CE, triglycerides (TG), LPC, and lysophosphatidylethanolamines (LPE) increased the monounsaturated fatty acid (MUFA) content in NAFLD mice, whereas the polyunsaturated fatty acids (PUFA) content linked to PC increased (Fig. 2F, 2E and 2H).

With respect to age contribution to hepatic lipid remodeling, we found that N-acyl-ethanolamines (NAE) and LPE decreased with age, while the LPC species increased, independently of diet and metformin administration (Fig. 2A and 2F). We did not find any alterations associated with metformin.

3.3. Age determined the lipid remodeling in adipocytes

To ascertain whether metformin affected the lipid signature of adipocytes, we analyzed the histological adipocyte size and lipid alterations from visceral (epididymal and retroperitoneal) and subcutaneous (inguinal and anterior) adipocytes in 25-week and 45-week-old mice. Our data showed that epididymal adipocyte size increased with age, HFHSD and metformin, whereas the retroperitoneal adipocyte size decreased with age and HFHSD. Inguinal subcutaneous depots increased with age and HFHSD, while being decreased in metformin-treated mice. Finally, anterior subcutaneous adipocyte size decreased in HFHSD-fed mice (Fig. 3 A-D, S9 and S10 A-C).

White adipose tissue acts as the main lipid storage facility by incorporating TG and DG into the adipocytes. Thus, adipocyte lipidome in CD-fed mice revealed that GLs were the main lipid category in visceral as well as subcutaneous depots in 25-week-old mice. The FAs, GPs, SPs and ST were the most important lipid categories in epididymal and inguinal regions, whereas in retroperitoneal and anterior adipocytes the categories were SPs, FAs, GPs and ST; suggesting that the adipocyte lipid signature is specific to the anatomical region (Fig. S11, S12, S13 and S14).

When 25-week-old CD-fed mice received metformin, we observed a remodeling of the lipid signature in epididymal, retroperitoneal and anterior adipocytes depots in epididymal regions. We observed an increase in TG and a decrease in HFA, LPE and LPC species, while in retroperitoneal adipocytes HFA was increased. Finally, in anterior adipocytes we observed a decrease in TG and an increase in SM compared to mice without metformin (Fig. S11, S12, S13, S14). However, the metformin effects on HFSHD-fed 25-week-old mice were less relevant; increases only in the SM in epididymal adipocytes being observed (Fig. S8E).

These alterations in CD-fed mice contributed to the lipid class weight redistribution within each lipid category. Thus, we observed an increase of fatty acids in the FAs pool of epididymal adipocytes, and an increase of DG in the GLs pool of anterior adipocytes (Fig. S9E-G).

With respect to the effects of HFHSD, we observed that the increase in NAE levels in visceral depots, and the increase in PC species in retroperitoneal adipocytes, were

independent of metformin administration. Moreover, in mice treated with metformin, we found specific alterations characterized by the increase in LPE species in epididymal, and decrease in retroperitoneal regions. Finally, we observed that mice without metformin had decreased levels of steroid hormones in retroperitoneal adipocytes (Fig. S10E and S10F).

In subcutaneous depots, we found that inguinal adipocytes increased the bile acid concentrations while the steroid hormones decreased in mice with and those without metformin; the decrease in SM species were specific to metformin treatment. Finally, in anterior adipocytes, we observed a decrease in SM in metformin-treated mice and a decrease in FA in mice without metformin (Fig. S10G and S10H). Our lipidomic data also revealed the contribution of diet to qualitatively modifying the lipid aspects i.e. we found that both visceral and subcutaneous depots increased the MUFA content in TG, DG, FA, and LPC species, independently of metformin administration (Fig. S10E-H).

Of note, we found that age acts as the main factor in remodeling the lipid signature of adipocytes (Fig. 3E-H, S11-14). We observed that all the 45-week-old groups of mice exhibited the same signature in both visceral and subcutaneous adipocytes, independently of diet and metformin administration i.e. the adipocytes developed a phenotype associated with reduced lipid mobilization and, favoring lipid storage as triglycerides and diglycerides. Moreover, we found that GPs levels, which are related to plasma membrane lipids, decreased (Fig. S15). These alterations induced changes in the lipid class distribution, increasing the importance of steroid hormones within the ST pool as well as the FA in the pool of FAs due to the decrease of NAE levels. The GPs pools were characterized by decrease LPC species and increase LPE species; subcutaneous depots also increased the PC species (Fig. 3E-H).

Finally, we observed that age contributes to an increase in the saturated fatty acid content in CAR, and PUFA content in LPE and NAE (Fig. 3D-H).

In summary, metformin administration can modify the adipocyte lipid signature in young mice fed on CD, whereas these changes are reduced when HFHSD is administrated, or completely lost as age advances.

3.4. Combining caloric restriction with metformin treatment promotes hepatic steatosis remission

Body weight was significantly reduced under caloric restriction, with the largest reduction occurring when the diet switch was combined with metformin treatment (Fig. 4 A-B). Glucose, total lipoprotein particles, and lipoprotein profile improved compared to mice fed HFHSD without caloric restriction, independently of metformin treatment, and without any improvement in the glucose tolerance test (Fig. 4 D-H, S3C). Further, the hepatic lipidome returned to normal when mice were treated with caloric restriction. Thus, cholesterol metabolism was ameliorated, resulting in the decrease in CE and the increase in BAs and steroid hormones levels. Additionally, we found that the CAR and FA levels decreased, while the HFA increased.

Liver histology revealed less hepatic steatosis in mice treated with caloric restriction + metformin than in animals treated with caloric restriction alone. Alanine aminotransferase activity, lobular inflammation and ballooning improved compared to HFSHD, independently of metformin treatment (Fig. 4I). The lipid signature of adipocytes from visceral and subcutaneous adipose tissue also improved (Fig. S16A-G). In all adipocytes, we observed an increase in PUFA-containing TG and DG, as well as an increase in PUFA-containing LPC in both visceral depots (Fig. S16B-H). We did not observe relevant alterations relating to metformin treatment.

Discussion

We did not find any protective effect of metformin alone in the liver histology after 20 and 40 weeks of dietary treatment (25 and 45 weeks of age) i.e. the observations of changes in biochemical parameters, lipoprotein particles, weight gain, and hepatic lipidome in mice fed HFHSD and metformin, were similar to those of mice fed with HFHSD alone. Unlike other reports, these data do not support the use of metformin as a therapeutic strategy to prevent NAFLD in obese mice. Previous studies in *ob/ob* mice treated with metformin for 4 weeks showed weight reduction and hepatic steatosis prevention [23,24], but these experiments had been performed in animals fed on a CD diet. As such, the effect of metformin administered in this model with a hypercaloric diet, had not been explored. Despite the controversial effect of metformin in *in vivo* studies, some human studies suggested that metformin maintains the intrahepatic TG content [25–27].The hepatic levels of cholesterol

esters (CE) were increased in our model, whereas triglycerides and diglycerides were enriched with MUFA. These data indicated that hepatic lipid signature from mice with a NASH phenotype may be characterized by CE accumulation in the lipid droplets. When the lipid flux entering hepatocytes increases, free fatty acids are esterified into triglycerides by diacylglycerol-*O*-acyltransferases (DGATs) as well as into cholesterol esters by acyl-CoA cholesterol acyltransferases (ACATs) and incorporated into hepatic lipid droplets. Taking into consideration that the increase of hepatic free cholesterol is associated with NASH development, the increase of hepatic CE in HFHSD-fed mice would confirm the NASH phenotype of our model [28] . Indeed, ACAT2$^{-/-}$ (also abbreviated as SOAT2) mice had improved insulin sensitivity, decreased lipid storage, and increased lipid oxidation pathways [29].

While we did not observe any preventive effect in the liver with respect to metformin treatment, we found that the adipocyte size in eWAT (visceral) and aWAT (subcutaneous) had higher and lower sizes, respectively, than in HFHSD-fed mice alone. CD, and metformin-treatment of 25-week-old mice, exhibited lower levels of SM in anterior adipocytes than those mice without metformin. Further, 25-week-old mice receiving HFHSD and metformin had lower levels of SM in subcutaneous depots than metformin-treated mice in CD group, suggesting than metformin could mediate the sphingophospholipid metabolism. Indeed, a human study in women with polycystic ovary syndrome observed that metformin treatment decreases serum SM levels as well as oxidized lipids, although the mechanisms were not fully explained [30].

Also, our data showed that adipocytes from visceral and subcutaneous adipose tissue displayed lipid remodeling in HFHSD-fed mice; with decrease in PUFA content in DG, TG, FA and LPC. Indeed, an earlier study demonstrated that adipose tissue macrophages in obesity display higher PC turnover resulting in an increase in the amount of saturated fatty acids in plasma membrane phospholipids [31]. We found, as well, that these changes were followed by a decrease in steroid hormones and increase in bile acid levels. Another finding of note was the decrease in glycerophospholipids and the increase in glycolipids with age, independently of the diet and metformin treatment. As has been described, the levels of phospholipids in blood, liver, and brain decrease with age, and have higher degree of saturated fatty

acids [32,33]. *In vitro* studies in PEMT$^{-/-}$ (enzyme involved in the synthesis of PC through the PE trimethylation) adipocytes, demonstrate that the low levels in PC causes a smaller-sized adipocyte, and higher basal hydrolysis of triglycerides [34]. Despite PC being an important factor in adipocyte metabolism, we did not observe higher serum triglyceride concentrations, and decreased adipocyte size with age. The increase in age-related lipid accumulation in adipocytes may be due to DGAT activity, i.e. esterification of DG with FA in TG synthesis. Indeed, DGAT1 gene deletion in mice has been shown to promote longevity and body leanness; indicating that losses in lipid mobilization could be an indication of an organism's aging [35].

Taken together, these data indicate that metformin, at least in a long-term study, cannot prevent the development of age- and HFHSD-associated metabolic derangements.

In contrast to our earlier hypotheses, our data strongly suggest that metformin, combined with caloric restriction, promotes greater beneficial NASH remission than caloric restriction alone. Metformin-treated mice showed a greater body weight reduction (19.6% vs 9.8% weight loss) and rapid reversal of hepatic steatosis i.e. experimental animal studies have indicated that the combination of caloric restriction with metformin can be more beneficial than either of these interventions alone [11,36]. The improvement in biochemical parameters, such as lipoprotein concentrations and profiles were not metformin specific, whereas the glucose tolerance test did not improve in either intervention. Our findings demonstrate that caloric restriction modifies the lipid signature in liver and adipocytes, independently of metformin administration. Our lipidomic results indicate that hepatic CE decreases, while the bile acids and steroid hormones increase (mimicking CD-fed mice), while adipocytes from visceral and subcutaneous depots increased PUFA-containing DG, TG and LPC. I.e. the effects of caloric restriction in liver are quantitative, but more qualitative in adipocytes. Caloric restriction *per se* does not modify the lipid composition, but the type of diet may determine the qualitative lipid aspects such that dietary sources enriched with PUFA modify the phospholipid plasma membrane composition, promoting better metabolic outcomes, than SFA-enriched diets [37–39].

In summary, we have shown that metformin cannot prevent hepatic steatosis and age-related lipid alterations. As such its administration for the preventive treatment of NAFLD should be taken with caution [27]. Most NAFLD models described in the literature are based on HFD, and the period of treatment is shorter than in our study. However, our data indicate a synergy between caloric restriction and metformin resulting in better weight reduction, and a better amelioration of hepatic steatosis than caloric restriction alone. Of further note is the age contribution to lipid remodeling of adipocytes. For example, all 45-week-old mice groups exhibited similar lipid signatures independently of diet and metformin group assignment in the study. These remodeling processes were characterized by increase in lipid storage (mainly triglycerides and diglycerides), and decrease in glycerophospholipids; which are important regulators of adipocyte size, plasma membrane fluidity, and lipoprotein metabolism. Our results suggest that, during the aging process, the metabolic program changes from lipid mobilization to lipid storage resulting in alterations in adipocyte plasma membrane. This scenario invites the consideration of whether current therapies are appropriate, or whether a new treatment approach is necessary in older subjects with NAFLD.

6. Conclusions

Our data show that age affects changes in the adipocyte lipidome, and that HFHSD diets promote alterations in hepatic lipidome leading to NASH phenotype. This is independently of metformin administration. As such, we would suggest that metformin ought not to be considered a preventive strategy in attenuating NAFLD development. However, using CR in combination with metformin could be an efficient treatment, and a good strategy in inducing greater CR effects.

7. Abbreviations

ALT, alanine aminotransferase; ACAT, acyl-CoA cholesterol acyltransferase; aWAT, anterior white adipose tissue; BA, bile acids; CAR, carnitine; CD, chow diet; CE, cholesterol ester; CR, caloric restriction; DG, diglyceride; DGAT, diacylglycerol-*O*-acyltransferase; eWAT, epididymal white adipose tissue; FA, fatty acid; FAs, fatty acyls; GLs, glycerolipids; GPs, glycerophospholipids, HDL, high density lipoprotein; HFA, hydroxy fatty acid; HFD, high fat diet; HFHSD, high fat high sucrose diet; IDL, intermediate density lipoprotein; iWAT, inguinal white adipose tissue; LDA, linear

discriminant analysis; LDL, low density lipoprotein; LPC, lysophosphatidylcholine; LPE, lysophosphatidylethanolamine; MUFA, monounsaturated fatty acid; NAE, N-acyl-ethanolamine; NAFLD, non-alcoholic fatty liver disease; NAS, NAFLD activity score; NASH, non-alcoholic steatohepatitis, PC, phosphatidylcholine; PEMT, phosphatidylethanolamine methyltransferase; PUFA, polyunsaturated fatty acid; rWAT, retroperitoneal white adipose tissue; SFA, saturated fatty acid, SM, sphingomyelin; SPs, sphingophospholipid; St, steroid hormone; ST, sterol lipids; TG, triglyceride; VLDL, very low density lipoprotein

.

8. References

[1] Fajardo VA, McMeekin L, LeBlanc PJ. Influence of phospholipid species on membrane fluidity: a meta-analysis for a novel phospholipid fluidity index. The Journal of Membrane Biology 2011;244:97–103. https://doi.org/10.1007/s00232-011-9401-7.

[2] van der Veen JN, Kennelly JP, Wan S, Vance JE, Vance DE, Jacobs RL. The critical role of phosphatidylcholine and phosphatidylethanolamine metabolism in health and disease. Biochimica et Biophysica Acta (BBA) - Biomembranes 2017;1859:1558–72. https://doi.org/10.1016/j.bbamem.2017.04.006.

[3] Li Z, Agellon LB, Allen TM, Umeda M, Jewell L, Mason A, et al. The ratio of phosphatidylcholine to phosphatidylethanolamine influences membrane integrity and steatohepatitis. Cell Metabolism 2006;3. https://doi.org/10.1016/j.cmet.2006.03.007.

[4] Cali AMG, Zern TL, Taksali SE, de Oliveira AM, Dufour S, Otvos JD, et al. Intrahepatic fat accumulation and alterations in lipoprotein composition in obese adolescents. Diabetes Care 2007;30:3093–8. https://doi.org/10.2337/dc07-1088.

[5] Cabré N, Gil M, Amigó N, Luciano-Mateo F, Baiges-Gaya G, Fernández-Arroyo S, et al. Laparoscopic sleeve gastrectomy alters 1H-NMR-measured lipoprotein and glycoprotein profile in patients with severe obesity and nonalcoholic fatty liver disease. Scientific Reports 2021;11:1343. https://doi.org/10.1038/s41598-020-79485-7.

[6] Lebeaupin C, Vallée D, Hazari Y, Hetz C, Chevet E, Bailly-Maitre B. Endoplasmic reticulum stress signalling and the pathogenesis of non-alcoholic fatty liver disease. Journal of Hepatology 2018;69:927–47. https://doi.org/10.1016/j.jhep.2018.06.008.

[7] Heeren J, Scheja L. Metabolic-associated fatty liver disease and lipoprotein metabolism. Molecular Metabolism 2021;50:101238. https://doi.org/10.1016/j.molmet.2021.101238.

[8] Subramanian S, Goodspeed L, Wang S, Kim J, Zeng L, Ioannou GN, et al. Dietary cholesterol exacerbates hepatic steatosis and inflammation in obese LDL receptor-deficient mice. Journal of Lipid Research 2011;52:1626–35. https://doi.org/10.1194/jlr.M016246.

[9] van Rooyen DM, Larter CZ, Haigh WG, Yeh MM, Ioannou G, Kuver R, et al. Hepatic free cholesterol accumulates in obese, diabetic mice and causes nonalcoholic steatohepatitis. Gastroenterology 2011;141:1393-1403.e5. https://doi.org/10.1053/j.gastro.2011.06.040.

[10] Park H, Shima T, Yamaguchi K, Mitsuyoshi H, Minami M, Yasui K, et al. Efficacy of long-term ezetimibe therapy in patients with nonalcoholic fatty liver disease. Journal of Gastroenterology 2011;46:101–7. https://doi.org/10.1007/s00535-010-0291-8.

[11] Riera-Borrull M, García-Heredia A, Fernández-Arroyo S, Hernández-Aguilera A, Cabré N, Cuyàs E, et al. Metformin potentiates the benefits of dietary restraint: a metabolomic study. International Journal of Molecular Sciences 2017;18:2263. https://doi.org/10.3390/ijms18112263.

[12] Li M, Sharma A, Yin C, Tan X, Xiao Y. Metformin ameliorates hepatic steatosis and improves the induction of autophagy in HFD-induced obese mice. Molecular Medicine Reports 2017;16:680–6. https://doi.org/10.3892/mmr.2017.6637.

[13] Woo S-L, Xu H, Li H, Zhao Y, Hu X, Zhao J, et al. Metformin ameliorates hepatic steatosis and inflammation without altering adipose phenotype in diet-induced obesity. PLoS ONE 2014;9:e91111. https://doi.org/10.1371/journal.pone.0091111.

[14] Baiges-Gaya G, Fernández-Arroyo S, Luciano-Mateo F, Cabré N, Rodríguez-Tomàs E, Hernández-Aguilera A, et al. Hepatic metabolic adaptation and adipose tissue expansion are altered in mice with steatohepatitis induced by high-fat high sucrose diet. The Journal of Nutritional Biochemistry 2021;89. https://doi.org/10.1016/j.jnutbio.2020.108559.

[15] Kishida Y, Okubo H, Ohno H, Oki K, Yoneda M. Effect of miglitol on the suppression of nonalcoholic steatohepatitis development and improvement of the gut environment in a rodent model. Journal of Gastroenterology 2017;52:1180–91. https://doi.org/10.1007/s00535-017-1331-4.

[16] Semmler G, Datz C, Reiberger T, Trauner M. Diet and exercise in NAFLD/NASH: beyond the obvious. Liver International 2021;41:2249–68. https://doi.org/10.1111/liv.15024.

[17] Magkos F, Hjorth MF, Astrup A. Diet and exercise in the prevention and treatment of type 2 diabetes mellitus. Nature Reviews Endocrinology 2020;16:545–55. https://doi.org/10.1038/s41574-020-0381-5.

[18] Kleiner DE, Brunt EM, van Natta M, Behling C, Contos MJ, Cummings OW, et al. Design and validation of a histological scoring system for nonalcoholic fatty liver disease. Hepatology 2005. https://doi.org/10.1002/hep.20701.

[19] Fernández-Arroyo S, Hernández-Aguilera A, de Vries MA, Burggraaf B, van der Zwan E, Pouw N, et al. Effect of vitamin D3 on the postprandial lipid profile in obese patients: A Non-Targeted Lipidomics Study. Nutrients 2019;11. https://doi.org/10.3390/nu11051194.

[20] Pedregosa F, Varoquaux G, Gramfort A, Michel V, Thirion B, Grisel O, et al. Scikit-learn: machine learning in Python 2012.

[21] Hunter J.D. "Matplotlib: a 2D graphics environment", computing in science & engineering 2007;9:90–5. https://doi.org/https://doi.org/10.5281/zenodo.6513224.

[22] Anaconda Software Distribution [Internet]. Anaconda documentation. Anaconda Inc.; 2020. Available from: https://docs.anaconda.com/ n.d.

[23] Liu F, Wang C, Zhang L, Xu Y, Jang L, Gu Y, et al. Metformin prevents hepatic steatosis by regulating the expression of adipose differentiation-related protein. International Journal of Molecular Medicine 2014;33:51–8. https://doi.org/10.3892/ijmm.2013.1560.

[24] Song YM, Lee Y, Kim J-W, Ham D-S, Kang E-S, Cha BS, et al. Metformin alleviates hepatosteatosis by restoring SIRT1-mediated autophagy induction via an AMP-activated protein kinase-independent pathway. Autophagy 2015;11:46–59. https://doi.org/10.4161/15548627.2014.984271.

[25] Green CJ, Marjot T, Walsby-Tickle J, Charlton C, Cornfield T, Westcott F, et al. Metformin maintains intrahepatic triglyceride content through increased hepatic de novo lipogenesis. European Journal of Endocrinology 2022;186:367–77. https://doi.org/10.1530/EJE-21-0850.

[26] Loomba R, Lutchman G, Kleiner DE, Ricks M, Feld JJ, Borg BB, et al. Clinical trial: pilot study of metformin for the treatment of non-alcoholic steatohepatitis. Alimentary Pharmacology & Therapeutics 2009;29:172–82. https://doi.org/10.1111/j.1365-2036.2008.03869.x.

[27] Green CJ, Marjot T, Tomlinson JW, Hodson L. Of mice and men: Is there a future for metformin in the treatment of hepatic steatosis? diabetes, obesity and metabolism 2019;21:749–60. https://doi.org/10.1111/dom.13592.

[28] Paul B, Lewinska M, Andersen JB. Lipid alterations in chronic liver disease and liver cancer. JHEP Reports 2022;4:100479. https://doi.org/10.1016/j.jhepr.2022.100479.

[29] Pramfalk C, Ahmed O, Pedrelli M, Minniti ME, Luquet S, Denis RG, et al. *Soat2* ties cholesterol metabolism to β- oxidation and glucose tolerance in male mice. Journal of Internal Medicine 2022. https://doi.org/10.1111/joim.13450.

[30] Pradas I, Rovira-Llopis S, Naudí A, Bañuls C, Rocha M, Hernandez-Mijares A, et al. Metformin induces lipid changes on sphingolipid species and oxidized lipids in polycystic ovary syndrome women. Scientific Reports 2019;9:16033. https://doi.org/10.1038/s41598-019-52263-w.

[31] Petkevicius K, Virtue S, Bidault G, Jenkins B, Çubuk C, Morgantini C, et al. Accelerated phosphatidylcholine turnover in macrophages promotes adipose tissue inflammation in obesity. Elife 2019;8. https://doi.org/10.7554/eLife.47990.

[32] Johnson AA, Stolzing A. The role of lipid metabolism in aging, lifespan regulation, and age- related disease. Aging Cell 2019;18. https://doi.org/10.1111/acel.13048.

[33] Modi HR, Katyare SS, Patel MA. Ageing-induced alterations in lipid/phospholipid profiles of rat brain and liver mitochondria: implications for mitochondrial energy-linked functions. Journal of Membrane Biology 2008;221:51–60. https://doi.org/10.1007/s00232-007-9086-0.

[34] Hörl G, Wagner A, Cole LK, Malli R, Reicher H, Kotzbeck P, et al. Sequential synthesis and methylation of phosphatidylethanolamine promote lipid droplet biosynthesis and stability in tissue culture and in vivo. Journal of Biological Chemistry 2011;286. https://doi.org/10.1074/jbc.M111.234534.

[35] Streeper RS, Grueter CA, Salomonis N, Cases S, Levin MC, Koliwad SK, et al. Deficiency of the lipid synthesis enzyme, DGAT1, extends longevity in mice. Aging 2012;4:13–27. https://doi.org/10.18632/aging.100424.

[36] Linden MA, Lopez KT, Fletcher JA, Morris EM, Meers GM, Siddique S, et al. Combining metformin therapy with caloric restriction for the management of type 2 diabetes and nonalcoholic fatty liver disease in obese rats. Applied Physiology, Nutrition, and Metabolism 2015;40:1038–47. https://doi.org/10.1139/apnm-2015-0236.

[37] Field CJ, Toyomizu M, Clandinin MT. Relationship between dietary fat, adiopcyte membrane composition and insulin binding in the rat. The Journal of Nutrition 1989;119:1483–9. https://doi.org/10.1093/jn/119.10.1483.

[38] Field CJ, Ryan EA, Thomson AB, Clandinin MT. Diet fat composition alters membrane phospholipid composition, insulin binding, and glucose metabolism in adipocytes from control and diabetic animals. J Biol Chem 1990;265:11143–50.

[39] Lindqvist HM, Bärebring L, Gjertsson I, Jylhä A, Laaksonen R, Winkvist A, et al. A randomized controlled dietary intervention improved the serum lipid signature towards a less atherogenic profile in patients with rheumatoid arthritis. Metabolites 2021;11:632. https://doi.org/10.3390/metabo11090632.

Figure 1. Metformin does not reduce body weight gain and hepatic lipid accumulation in obesity-induced mice

(A) Caloric intake and (B) body weight gain curves of CD- and HFHSD-fed mice (n=8/group); (C-D) Tissue weights in relation to dietary treatment and age; (E) Glucose, cholesterol, triglycerides, and alanine aminotransferase activity (ALT) in animals sacrificed at 25 and 45 weeks of age (n=8/group); (F) Representative histological images of liver sections of mice (n=8/group) according to the type of diet, age, and metformin administration (on the left), and scores of hepatic steatosis, lobular inflammation, ballooning and NAFLD activity score (on the right). Scatter and bar plots are presented as a means and SD, while box plots are shown as means, maximum and minimum. P values < 0.05 are considered significant. (Wilcoxon-rank sum test). aWAT: anterior white adipose tissue; CD: chow diet; eWAT: epididymal white adipose tissue; HFHSD: high-fat high sucrose diet; iWAT: inguinal white adipose tissue; Met: metformin; rWAT: retroperitoneal white adipose tissue; w: weeks

Figure 2. Hepatic lipid remodeling in mice, segregated by diet, age, and metformin; (A-C) Linear discriminant analysis (LDA) showing the lipid signature of liver tissue according to dietary type, age, and metformin administration; (D-H) Lollipop plots showing the age of mice in sky-blue dots (25w) and blue dots (45w). Horizontal axis displays the mean relative abundance of lipids, while the vertical axis reflects the group of mice (n=4/group) P values < 0.05 are considered significant. (Wilcoxon-rank sum test). CD: chow diet; HFHSD: high-fat high-sucrose diet; Met: metformin; MUFA: monounsaturated fatty acids; PUFA: polyunsaturated fatty acids; SFA: saturated fatty acids; w: weeks.

Figure 3. Adipocyte lipid signature segregated according to age

The density plots show the relative frequency of histological adipocyte size; (A) epididymal; (B) retroperitoneal; (C) inguinal; (D) anterior white adipose tissues. The age of mice depicted by colored dots; sky-orange (25-week-old) and sky-blue (45-week-old). Representation of significant lipid classes, showing mean log2 [fold change (45-week-old mice / 25-week-old mice) and the changes in the degree of unsaturation of lipid; (E) epididymal (top left); (F) retroperitoneal (top right); (G) inguinal (bottom left); (H) anterior (bottom right) adipocytes. Each group of mice (n=4/group) represented by colored dots: sky-orange (CD-fed mice); orange (CD-fed mice + metformin); sky-blue (HFHSD-fed mice); blue (HFHSD-fed mice + metformin). P values < 0.05 are considered significant. (Wilcoxon-rank sum test). BA: bile acids; CAR: carnitines; CD: chow diet; HFHSD: high-fat high-sucrose diet; DG: diglycerides; FA: fatty acids; HFA: hydroxy fatty acids; LPC: lysophosphatidylcholines; LPE: lysophosphatidylethanolamines; Met: metformin; MUFA: monounsaturated fatty acids; NAE: N-acyl-ethanolamine's; PC: phosphatidylcholine; PUFA: polyunsaturated fatty acids; SFA: saturated fatty acids; SM: sphingomyelins; St: steroid hormones; w: weeks.

Figure 4. Synergistic effects of caloric restriction and metformin in the NAFLD remission; (A) final body weight; (B) body weight curve (n=8/group),; The concentration of: (C) glucose (n=8/group); (D) total lipoprotein parameters (n=4/group); (E-G) VLDL-p, LDL-p and HDL-p molar abundance (expressed as a percentage of total measured lipoprotein particles) (n=4/group); (I) lipid signature

analysis and significant alterations in liver comparing the effects of calorie restriction with or without metformin versus obese mice lipidome (n=4/group); (H) significant hepatic lipid alterations in NAFLD remission (n=4/group); (I) representative histology images of liver sections with the NAFLD activity score, and alanine aminotransferase activity (n=8/group). Scatter and bar plots are presented as means and SD, while box plots are shown as means, maximum and minimum. P values < 0.05 are considered significant. (Wilcoxon-rank sum test). ALT: alanine aminotransferase; BA: bile acids; CAR: carnitines; CD: chow diet; CE: cholesterol esters; CR: caloric restriction; FA: fatty acids; HDL: high-density lipoproteins; HFA: hydroxy fatty acids; HFHSD: high-fat high-sucrose diet; LDL: low-density lipoproteins; LPC: lysophosphatidylcholines; NAS: NAFLD activity score; p: particles; SM: sphingomyelins; St: steroid hormones; VLDL: very low-density lipoproteins

Figures

Click here to access/download;Figure;FIGURES-JHEPR.pdf

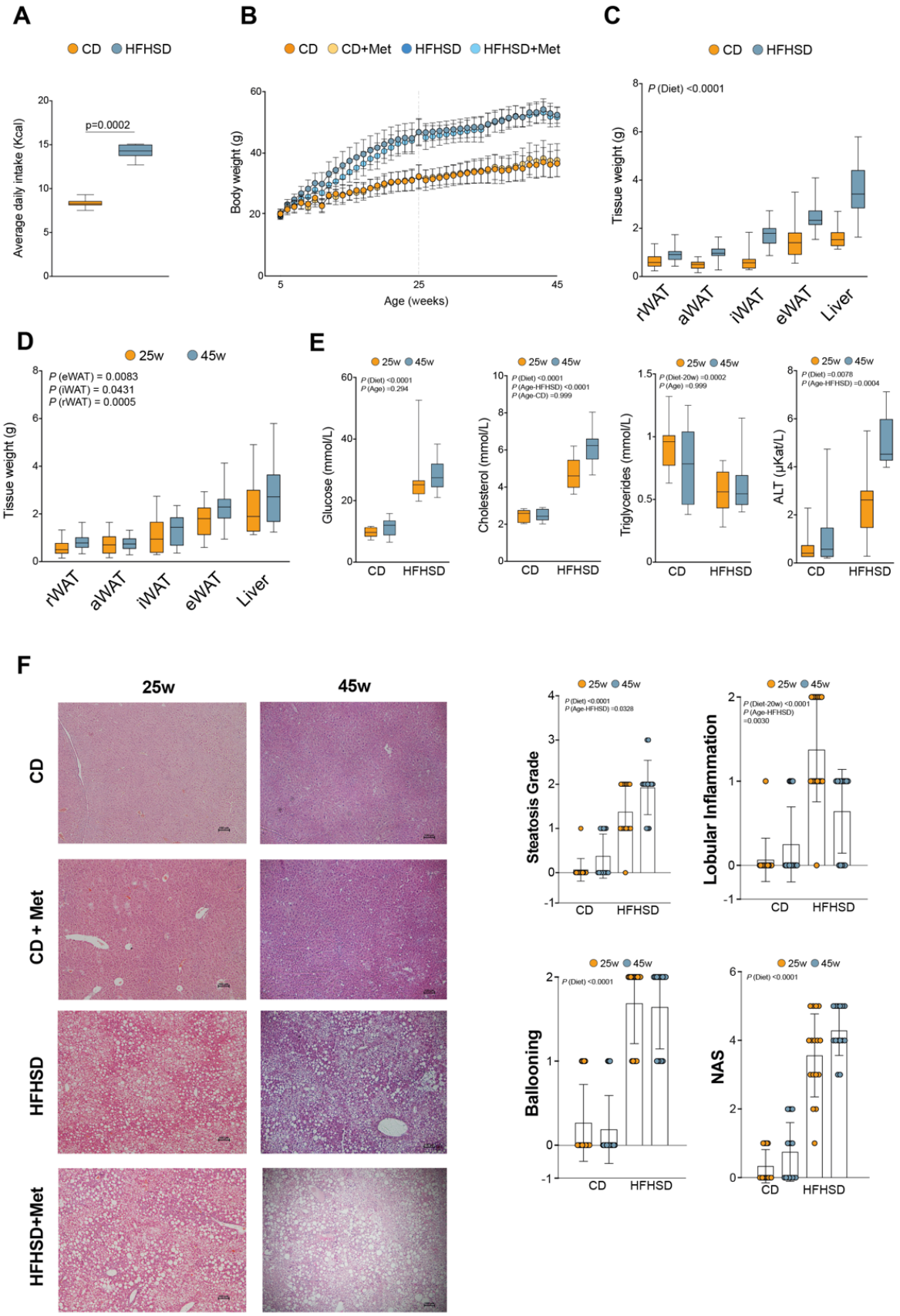

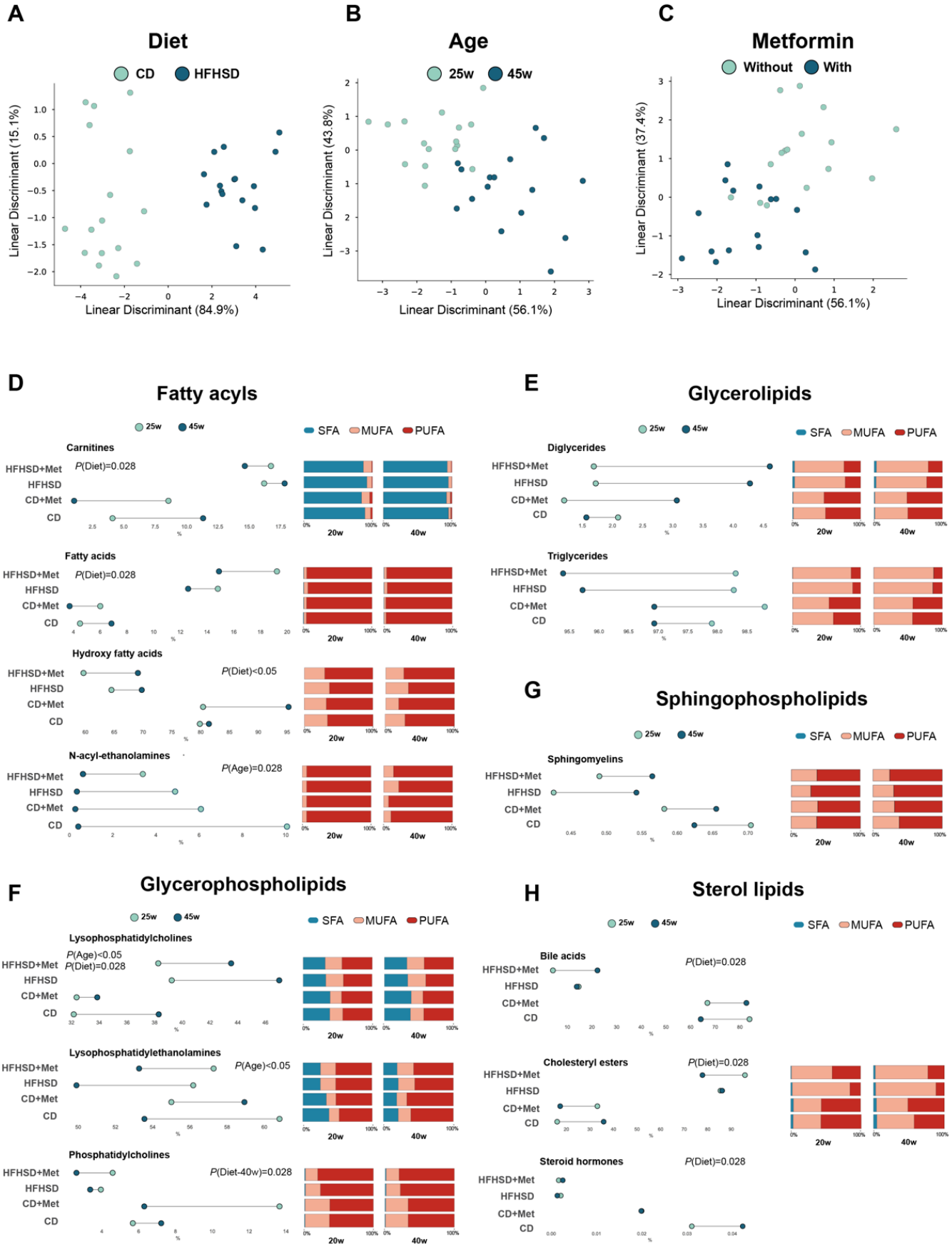
A
Diet
CD
HFHSD
Linear Discriminant (15.1%)
Linear Discriminant (84.9%)
B
Age
25w
45w
Linear Discriminant (43.8%)
Linear Discriminant (56.1%)
C
Metformin
Without
With
Linear Discriminant (37.4%)
Linear Discriminant (56.1%)
D
Fatty acyls
Carnitines
P(Diet)=0.028
Fatty acids
P(Diet)=0.028
Hydroxy fatty acids
P(Diet)<0.05
N-acyl-ethanolamines
P(Age)=0.028
E
Glycerolipids
Diglycerides
Triglycerides
G
Sphingophospholipids
Sphingomyelins
F
Glycerophospholipids
Lysophosphatidylcholines
P(Age)<0.05
P(Diet)=0.028
Lysophosphatidylethanolamines
P(Age)<0.05
Phosphatidylcholines
P(Diet-40w)=0.028
H
Sterol lipids
Bile acids
P(Diet)=0.028
Cholesteryl esters
P(Diet)=0.028
Steroid hormones
P(Diet)=0.028
HFHSD+Met
HFHSD
CD+Met
CD
SFA
MUFA
PUFA
20w
40w

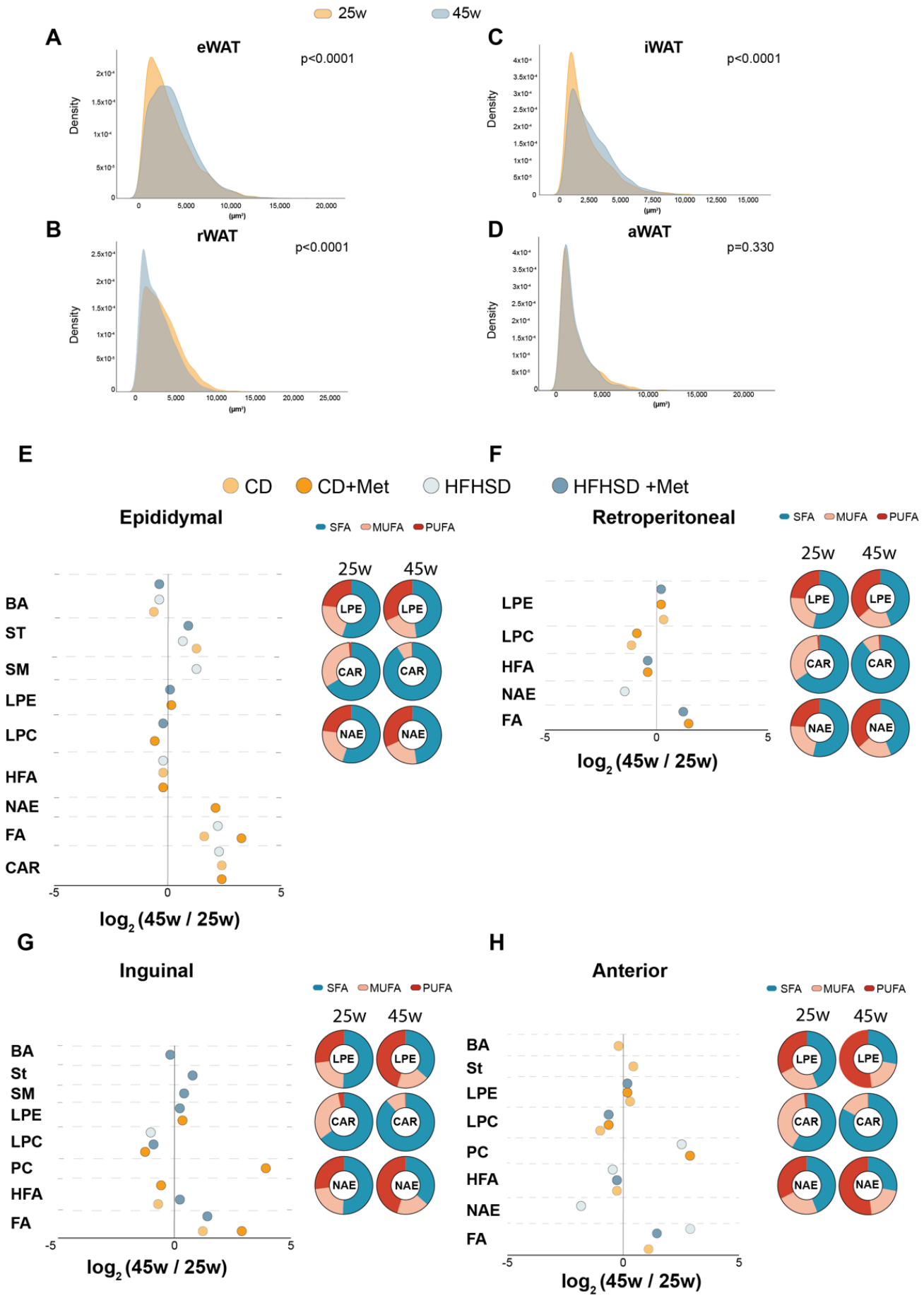
25w
45w
A
eWAT
p<0.0001
B
rWAT
p<0.0001
C
iWAT
p<0.0001
D
aWAT
p=0.330
Density
E
F
CD
CD+Met
HFHSD
HFHSD +Met
Epididymal
Retroperitoneal
SFA
MUFA
PUFA
LPE
CAR
NAE
BA
ST
SM
LPC
HFA
FA
log2 (45w / 25w)
G
H
Inguinal
Anterior
St
PC

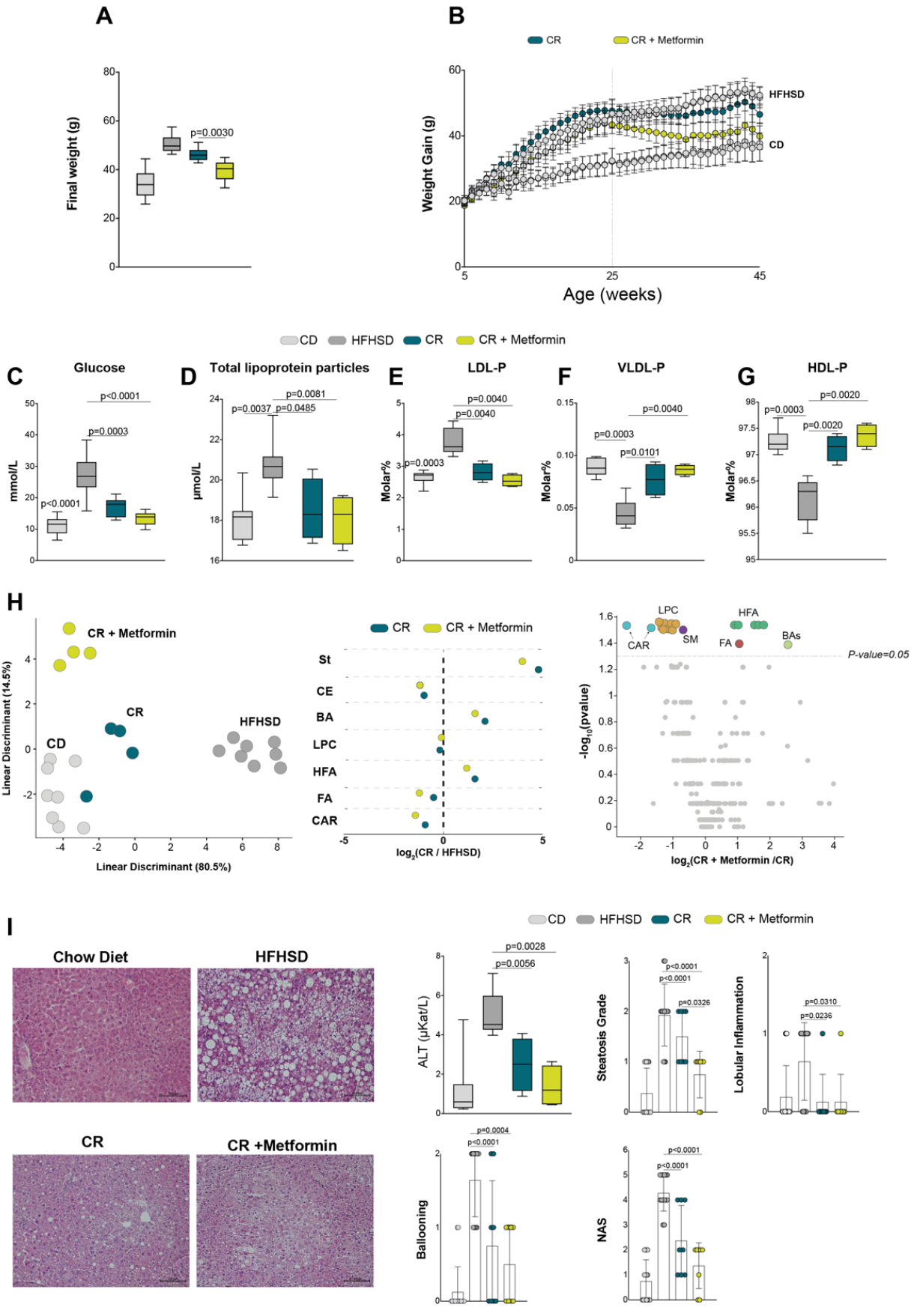
A
Final weight (g)
p=0.0030
B
CR
CR + Metformin
Weight Gain (g)
HFHSD
CD
Age (weeks)
CD
HFHSD
CR
CR + Metformin
C
Glucose
mmol/L
p<0.0001
p=0.0003
p<0.0001
D
Total lipoprotein particles
µmol/L
p=0.0081
p=0.0037
p=0.0485
E
LDL-P
Molar%
p=0.0040
p=0.0040
p=0.0003
F
VLDL-P
Molar%
p=0.0040
p=0.0003
p=0.0101
G
HDL-P
Molar%
p=0.0020
p=0.0003
p=0.0020
H
CR + Metformin
CR
CD
HFHSD
Linear Discriminant (14.5%)
Linear Discriminant (80.5%)
CR
CR + Metformin
St
CE
BA
LPC
HFA
FA
CAR
log2(CR / HFHSD)
LPC
HFA
CAR
SM
FA
BAs
P-value=0.05
-log10(pvalue)
log2(CR + Metformin /CR)
I
CD
HFHSD
CR
CR + Metformin
Chow Diet
HFHSD
CR
CR +Metformin
ALT (µKat/L)
p=0.0028
p=0.0056
Steatosis Grade
p<0.0001
p<0.0001
p=0.0326
Lobular Inflammation
p=0.0310
p=0.0236
Ballooning
p=0.0004
p<0.0001
NAS
p<0.0001
p<0.0001

Combining caloric restriction with metformin treatment enhances NAFLD remission in mice fed a high-fat high-sucrose diet.

Gerard Baiges-Gaya, Elisabet Rodríguez-Tomàs, Helena Castañé, Andrea Jiménez-Franco, Núria Amigó, Jordi Camps, Jorge Joven

Table of contents

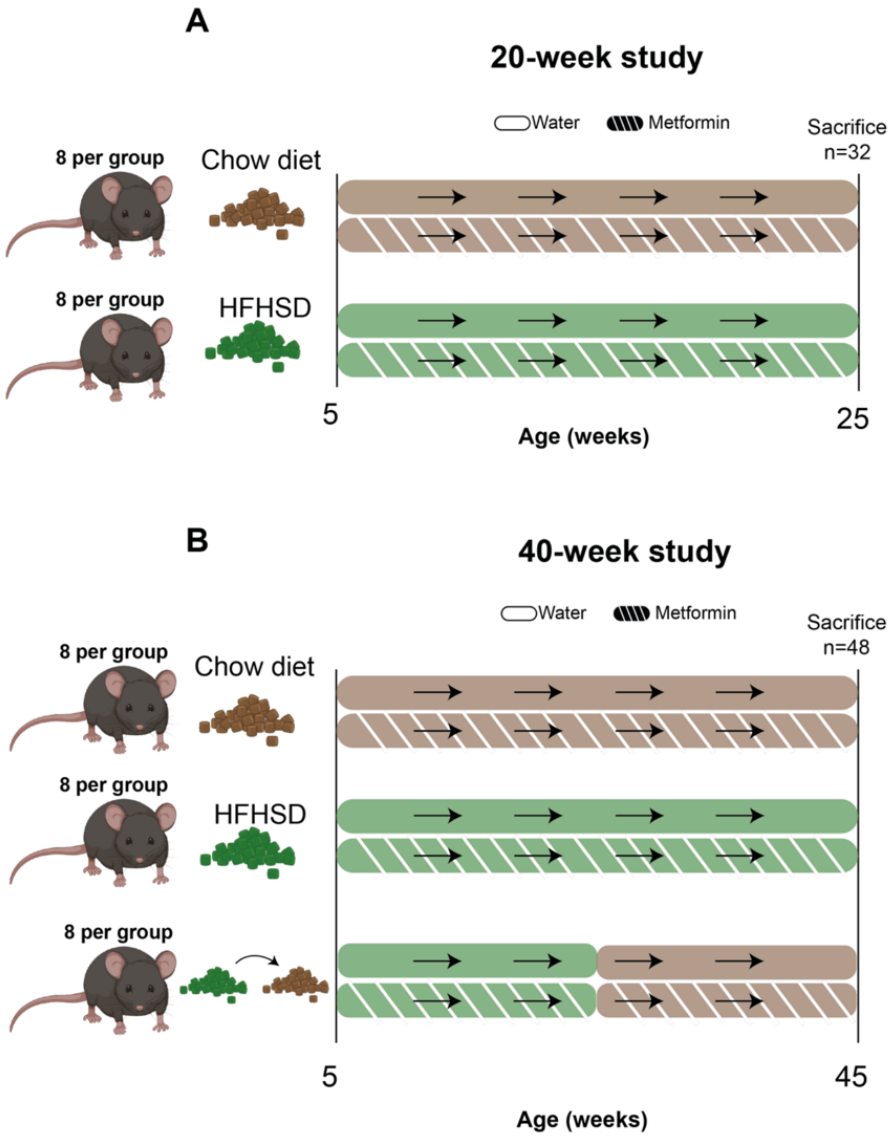

Fig. S1. Study design scheme
(**A**) Scheme of 20-week and (**B**) 40-week study design. HFHSD, high-fat high-sucrose diet.

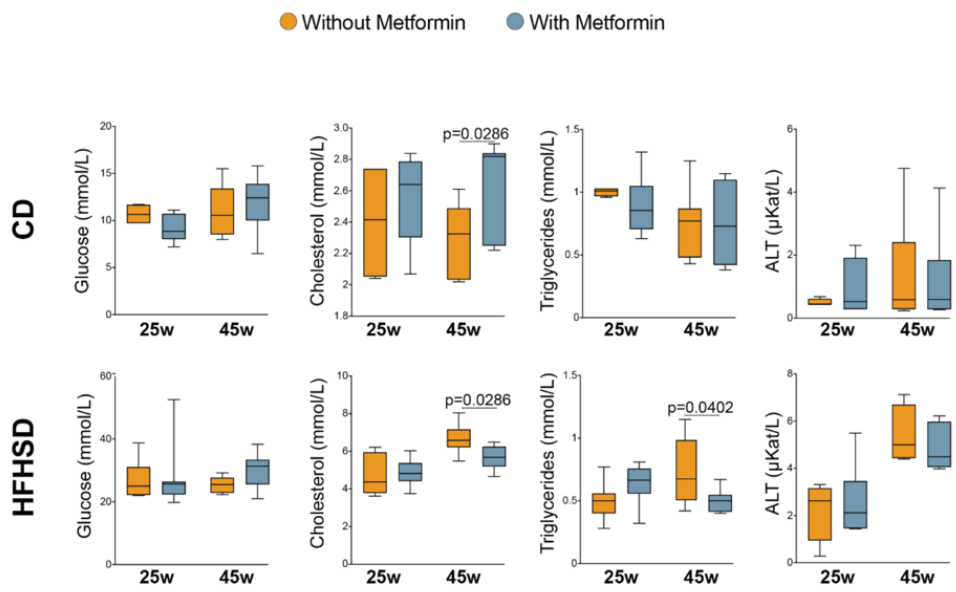

Fig. S2. Effects of metformin on biochemical variables
Glucose, cholesterol, and triglyceride concentrations, and alanine aminotransferase (ALT) activities in mice fed with chow or high-fat high-sucrose diets (CD and HFHSD, respectively) (n=8/group). Data are presented as means, maximum and minimum. P values < 0.05 are considered significant. (Wilcoxon-rank sum test).

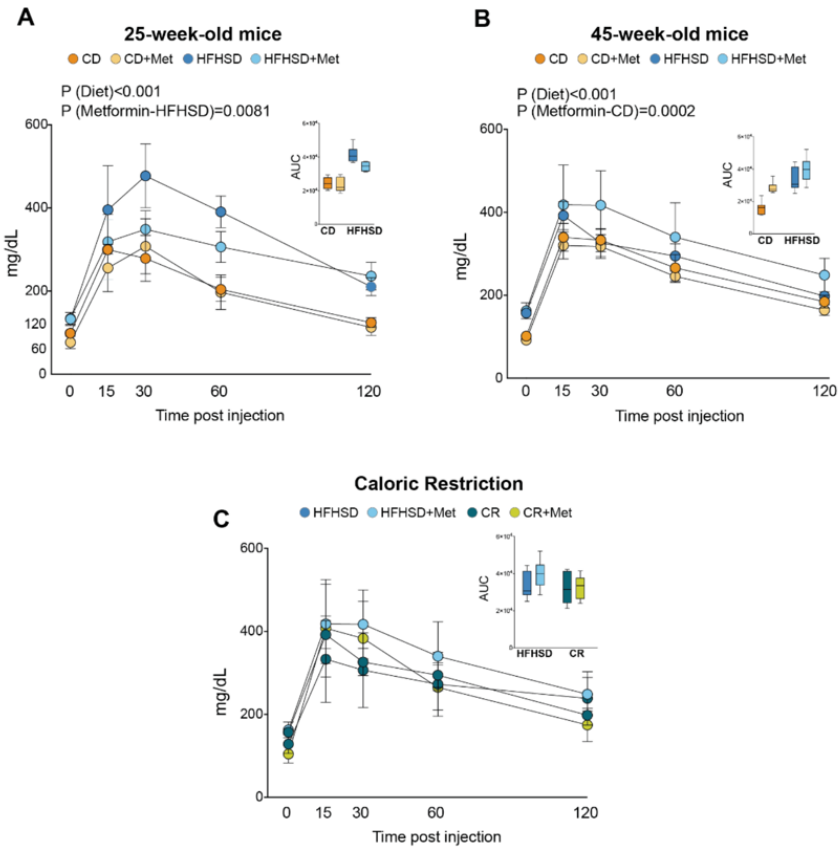

Fig. S3. Metformin does not improve glucose tolerance test in obese mice
(**A**) Glucose tolerance test curves and areas under the curve (AUC) of 25-week-old mice, and (**B**) 45-week-old mice. (**C**) Effect of caloric restriction, with or without metformin treatment, on glucose tolerance test (n=8/group). Data are shown as means and SD. P values < 0.05 are considered significant. (Wilcoxon-rank sum test). CD: chow diet; CR, caloric restriction; HFHSD: high-fat high-sucrose diet; Met: metformin.

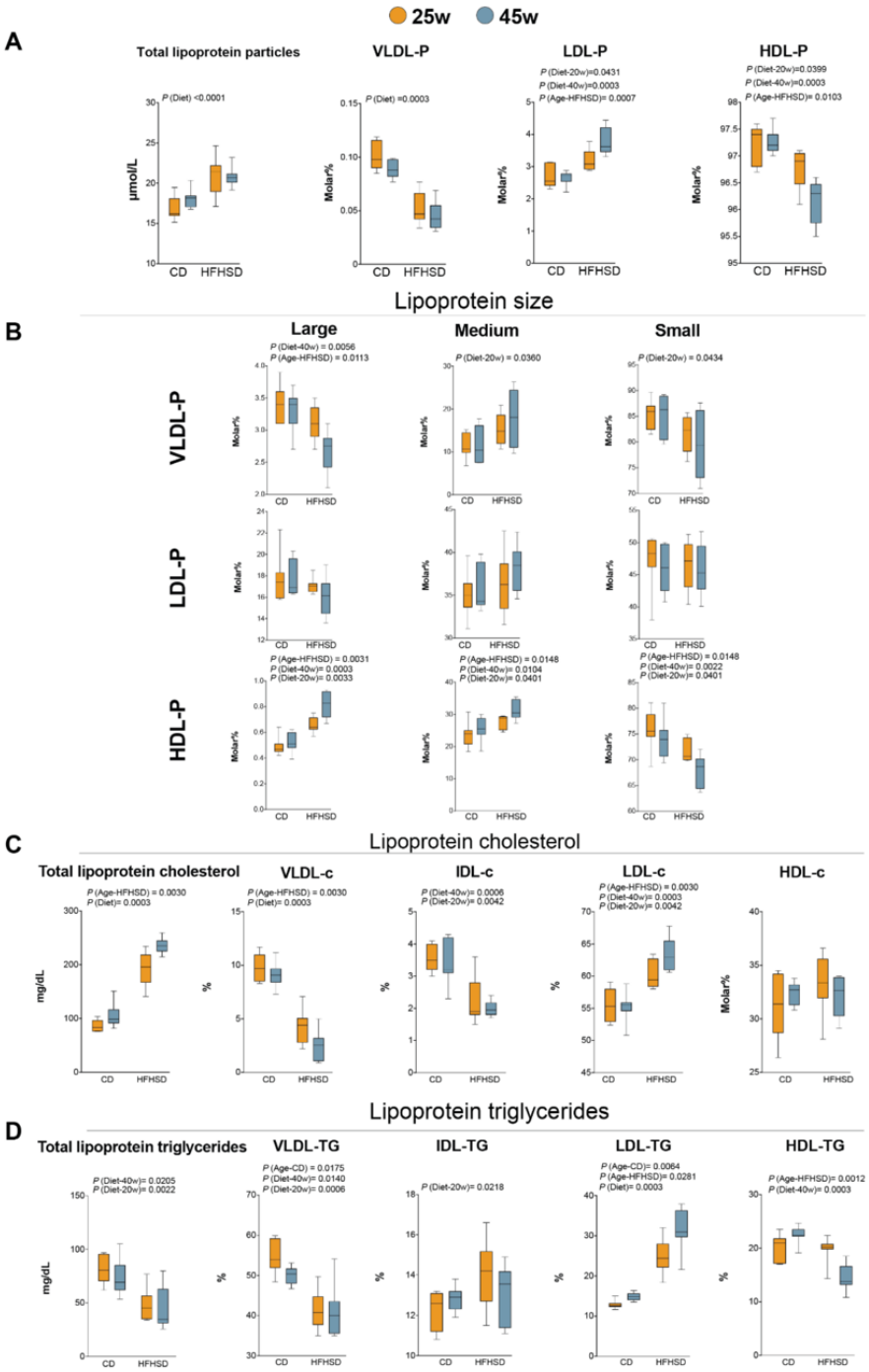

Fig. S4. High-fat high-sucrose diet and age adversely affect the lipoprotein profile
(**A**)Total concentration of lipoprotein particles and VLDL-p, LDL-p, and HDL-p molar abundance (expressed as a percentage of total measured lipoprotein particles) (n=4/group). (**B**) The molar abundance of lipoprotein size (expressed as a percentage of total measured VLDL-p, LDL-p or HDL-p) (n=4/group). (**C**) Total lipoprotein cholesterol concentration and abundance of VLDL-c, IDL-c,

LDL-c and HDL-c (expressed as a percentage of total measured lipoprotein cholesterol) (n=4/group). (**D**)Total lipoprotein triglyceride concentrations and abundance of VLDL-TG, IDL-TG, LDL-TG and HDL-TG (expressed as a percentage of total measured lipoprotein triglycerides) (n=4/group). Data are shown as means, maximum and minimum. P values < 0.05 are considered significant. (Wilcoxon-rank sum test). CD: chow diet; HDL: High-density lipoproteins; HFHSD: high-fat high-sucrose diet; IDL: intermediate-density lipoproteins; LDL: low-density lipoproteins; p: particles; TG: triglycerides; VLDL: very low-density lipoproteins; w: weeks.

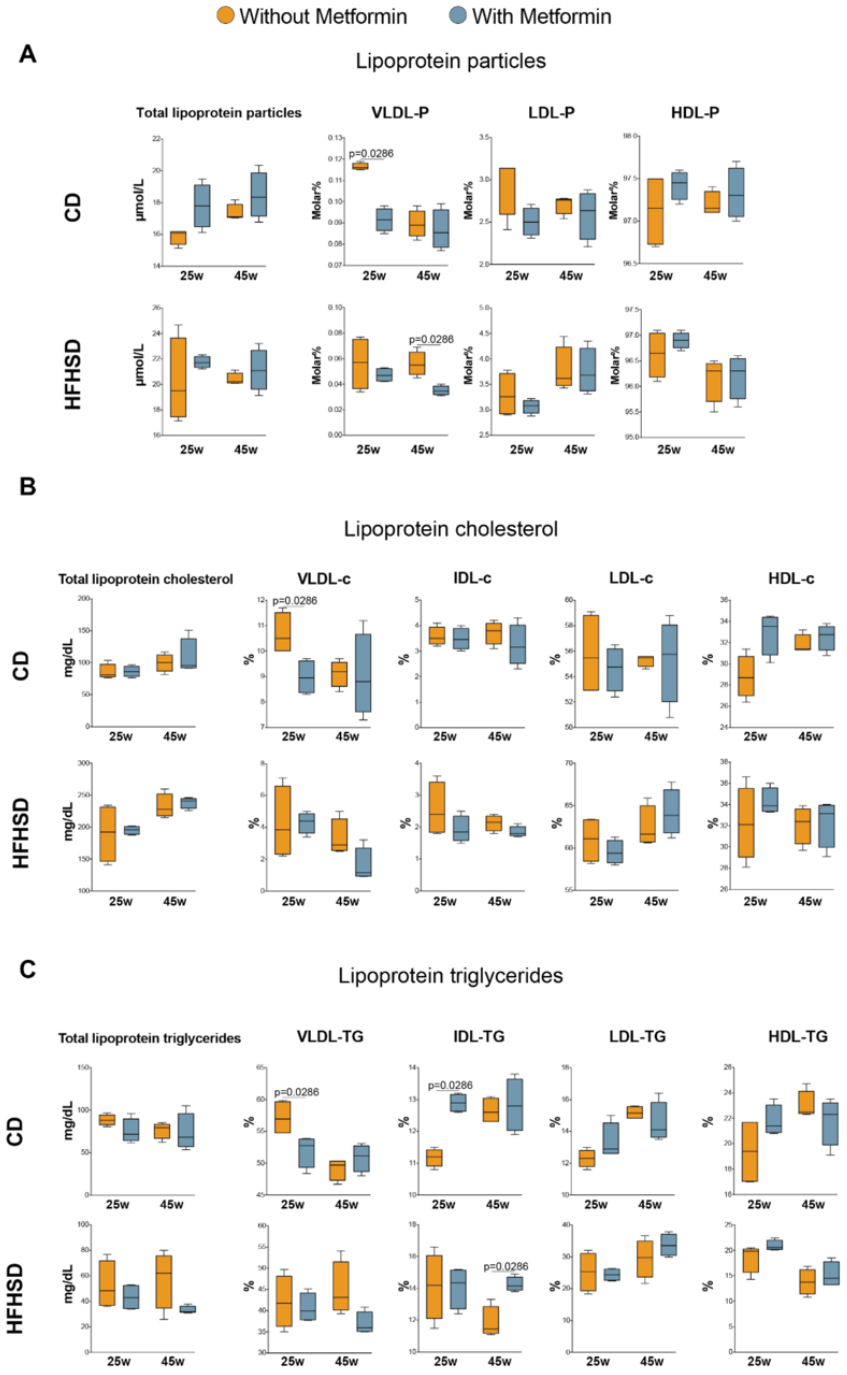

Fig. S5. Effects of metformin on lipoproteins profiles
(**A**) Concentration of total lipoprotein particles and VLDL-p, LDL-p and HDL-p molar abundance (expressed as a percentage of total measured lipoprotein particles) in CD or HFHSD-fed mice (n=4/group). (**B**) Total lipoprotein cholesterol concentration and abundance of VLDL-c, IDL-c, LDL-c and HDL-c (expressed as a percentage of total measured lipoprotein cholesterol) in CD or HFHSD-fed mice (n=4/group). (**C**)Total lipoprotein triglyceride concentrations and abundance of VLDL-TG,

IDL-TG, LDL-TG and HDL-TG (expressed as a percentage of total measured lipoprotein triglycerides) in CD or HFHSD-fed mice (n=4/group). Data are shown as means, maximum and minimum. P values < 0.05 are considered significant. (Wilcoxon-rank sum test). CD: chow diet; HDL: high-density lipoproteins; HFHSD: high-fat high-sucrose diet; IDL: intermediate-density lipoproteins; LDL: low-density lipoproteins; p: particles; TG: triglycerides; VLDL: very low-density lipoproteins; w: weeks.

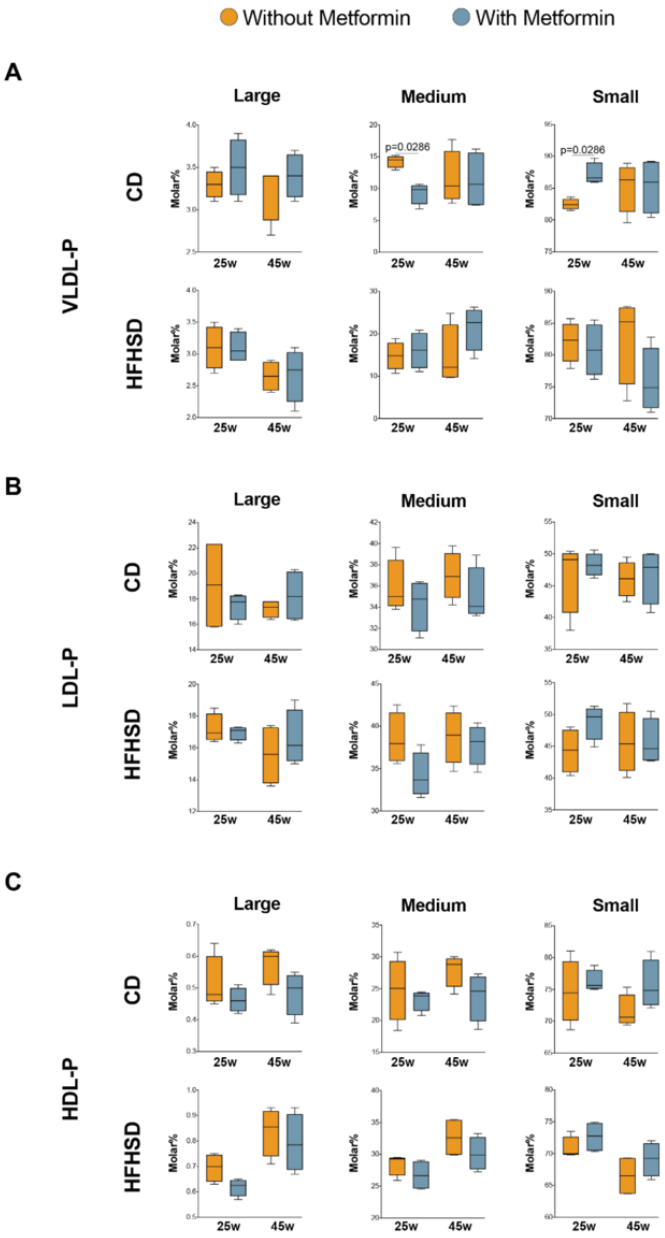

Fig. S6. Effects of metformin on lipoprotein particle size
(**A-C**) The molar abundance of lipoprotein size (expressed as a percentage of total measured VLDL-p, LDL-p or HDL-p) in CD or HFHSD-fed mice (n=4/group). Data are shown as means, maximum and minimum. P values < 0.05 are considered significant. (Wilcoxon-rank sum test). CD: chow diet; HDL: high-density lipoproteins; HFHSD: high-fat high-sucrose diet; IDL: intermediate-density lipoproteins; LDL: low-density lipoproteins; p: particles; TG: triglycerides; VLDL: very low-density lipoproteins; w: weeks.

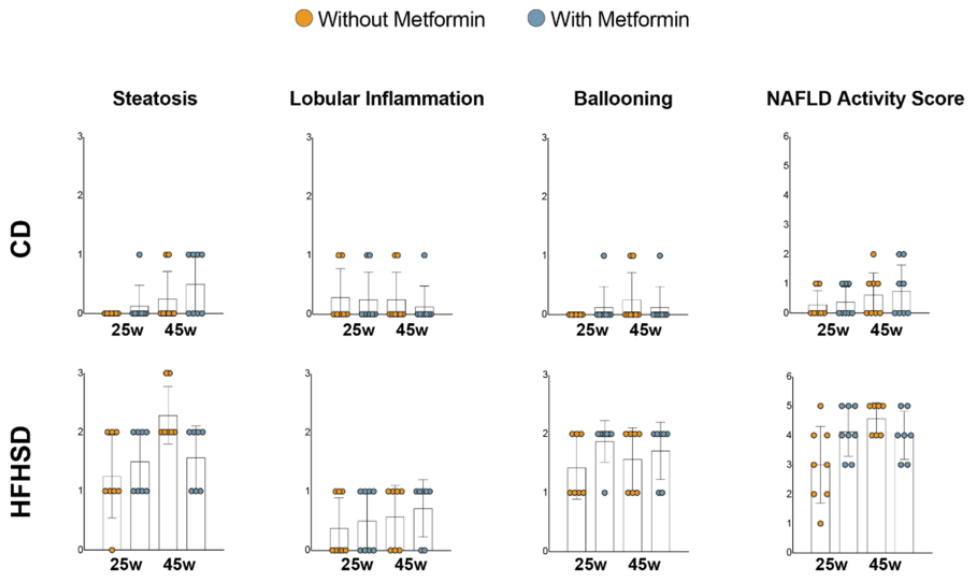

Fig. S7. Effects of metformin on hepatic histology
Hepatic steatosis, lobular inflammation, ballooning, and NAFLD activity scores in CD or HFHSD-fed mice with or without metformin treatment (n=8/group). Data shown as means and SD. P values < 0.05 are considered significant. (Wilcoxon-rank sum test). CD: chow diet; HFHSD: high-fat high sucrose diet; w: weeks.

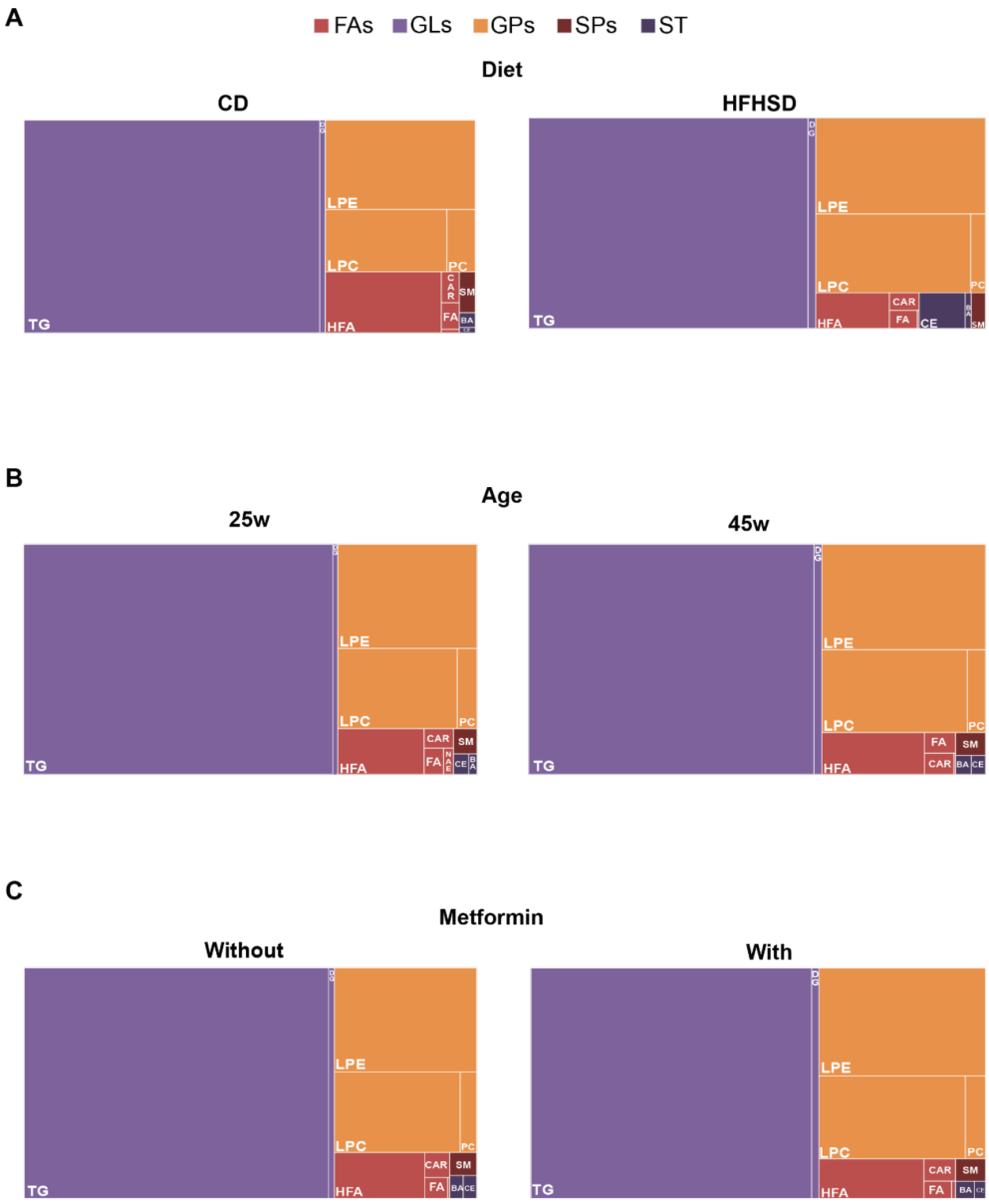

Fig. S8. Hepatic lipid signature according to diet, age, and metformin treatment
Treemaps show the relative distribution of main lipid categories and classes (n=4/group). These relative distributions serve as a comparative metric of hepatic lipidome between (**A**) dietary treatments, (**B**) age, (**C**) metformin treatment. FAs, fatty acyls; GLs, glycerolipids; GPs, glycerophospholipids; BA: bile acids; CAR: carnitines; CE: cholesterol esters; DG, diglycerides; FA: fatty acids; HFA: hydroxy fatty acids; LPC: lysophosphatidylcholine; LPE: lysophosphatidylethanolamine; PC: phosphatidylcholines; SM: sphingomyelins; SPs: sphingophospholipids, ST: sterol lipids; w: weeks.

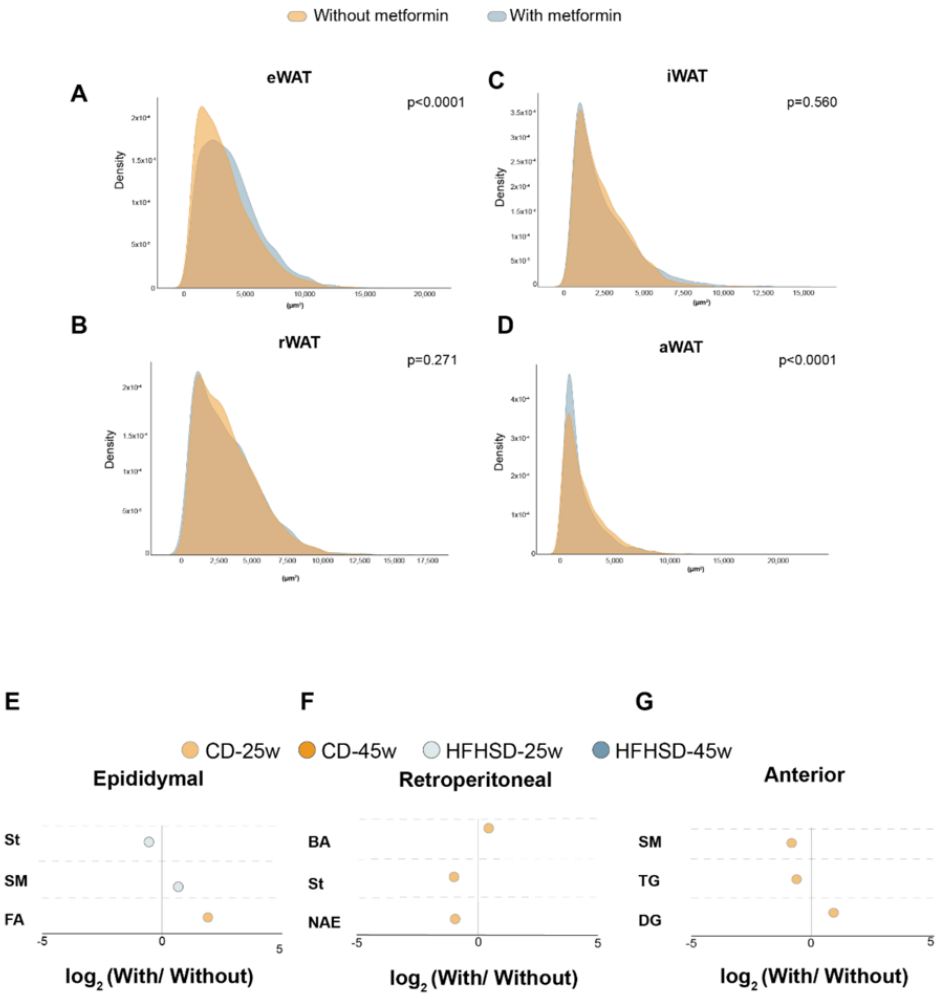

Fig. S9. Adipocyte lipid signature according to metformin treatment
Density plots show the relative frequency of histological adipocyte size from (**A**) epididymal (eWAT), (**B**) retroperitoneal (rWAT), (**C**) inguinal (iWAT) and (**D**) anterior (aWAT) white adipose tissues. The metformin treatment highlighted in sky-orange (mice without metformin) and sky-blue (mice with metformin) (n=8/group). Representation of significant lipid classes, showing the mean log_2 (with metformin / without metformin) in (E) epididymal, (**F**) retroperitoneal, and (**G**) anterior adipocytes (n=4/group). Groups of mice represented in sky-orange (25-week-old mice with CD) or orange (45-week-old mice with CD) (n=4/group) and sky-blue (25-week-old mice with HFHSD) or blue (45-week-old mice with HFHSD) dots (n=4/group). P values < 0.05 are considered significant. (Wilcoxon-rank sum test). BA: bile acids; CD: chow diet; DG: diglycerides; FA: fatty acids; HFHSD: high-fat high-sucrose diet; NAE: N-acyl-ethanolamine's; SM: sphingomyelins; St: steroid hormones; TG: triglycerides; w: weeks.

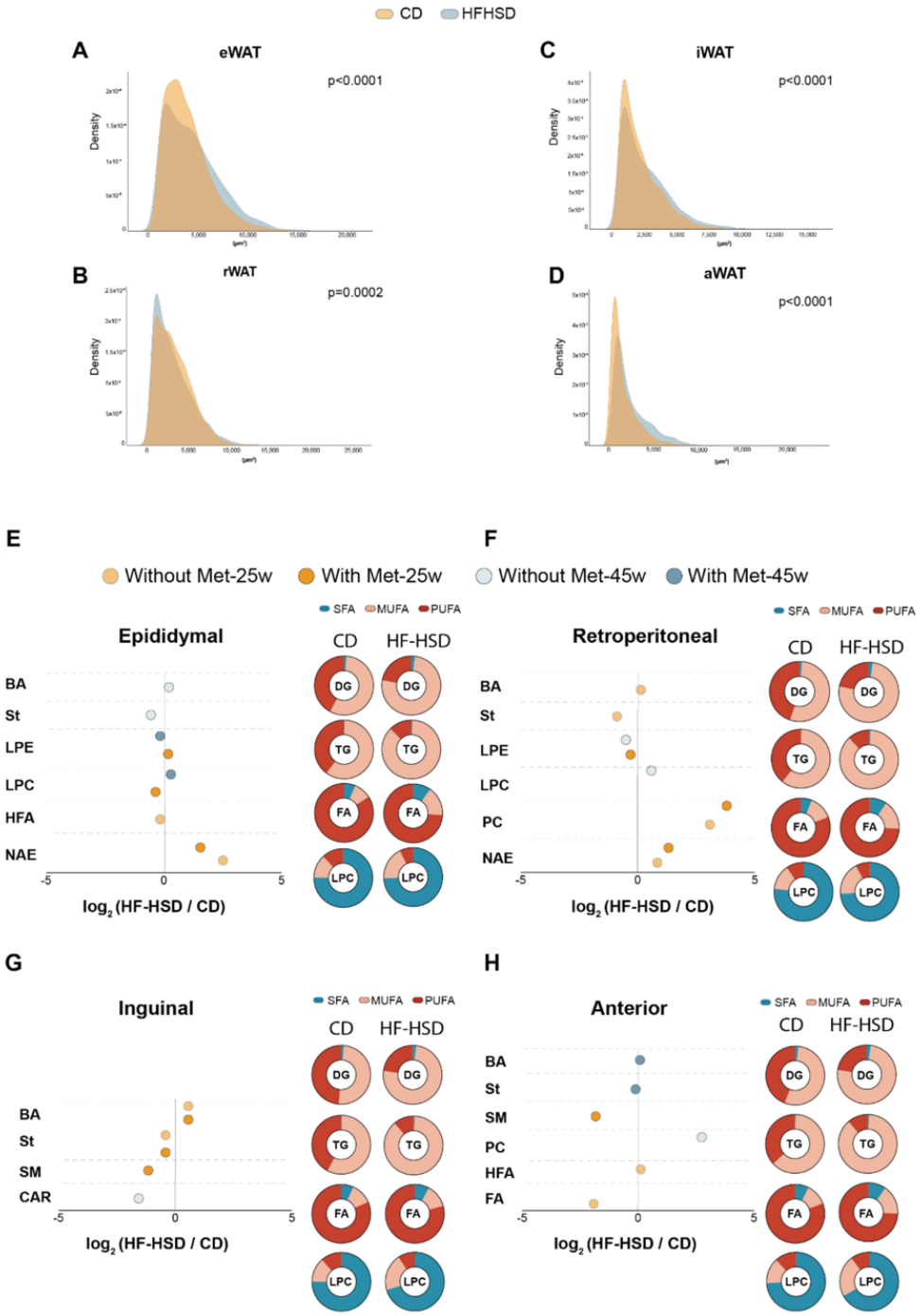
CD
HFHSD
A
eWAT
p<0.0001
C
iWAT
p<0.0001
B
rWAT
p=0.0002
D
aWAT
p<0.0001
Density
E
Without Met-25w
With Met-25w
Epididymal
F
Without Met-45w
With Met-45w
Retroperitoneal
G
Inguinal
H
Anterior
SFA
MUFA
PUFA
CD
HF-HSD
DG
TG
FA
LPC
BA
St
LPE
LPC
HFA
NAE
PC
SM
CAR
log2 (HF-HSD / CD)

Fig. S10. Adipocyte lipid signature according to dietary treatment
Density plots show the relative frequency of histological adipocyte size from (**A**) epididymal (eWAT), (**B**) retroperitoneal (rWAT), (**C**) inguinal (iWAT) and (**D**) anterior (aWAT) white adipose tissues. Diets of mice colored in sky-orange (CD-fed mice) and sky-blue (HFHSD-fed mice) (n=8/group). Representation of significant lipid classes showing the mean log_2 (HFHSD-fed mice / CD-fed mice) and the unsaturation changes in (**E**) epididymal (top left), (**F**) retroperitoneal (top right), (**G**) inguinal (bottom left) and (**H**) anterior (bottom right) adipocytes. Groups of mice represented in sky-orange (without metformin) or orange (with metformin) dots in 25-week-old mice (n=4/group) and sky-blue (without metformin) or blue (with metformin) dots in 45-week-old mice (n=4/group). P values < 0.05 are considered significant. (Wilcoxon-rank sum test). BA: bile acids; CAR: carnitines; CD: chow diet; DG: diglyceride; FA: fatty acid; HFA: hydroxy fatty acids; HFHSD: high-fat high-sucrose diet; LPC: lysophosphatidylcholines; LPE: lysophosphatidylethanolamines; Met: metformin; MUFA: monounsaturated fatty acids; NAE: N-acyl-ethanolamine's; PC: phosphatidylcholines; PUFA: polyunsaturated fatty acids; SM: sphingomyelins; SFA: saturated fatty acids; ST: steroid hormones; TG: triglycerides; w: weeks.

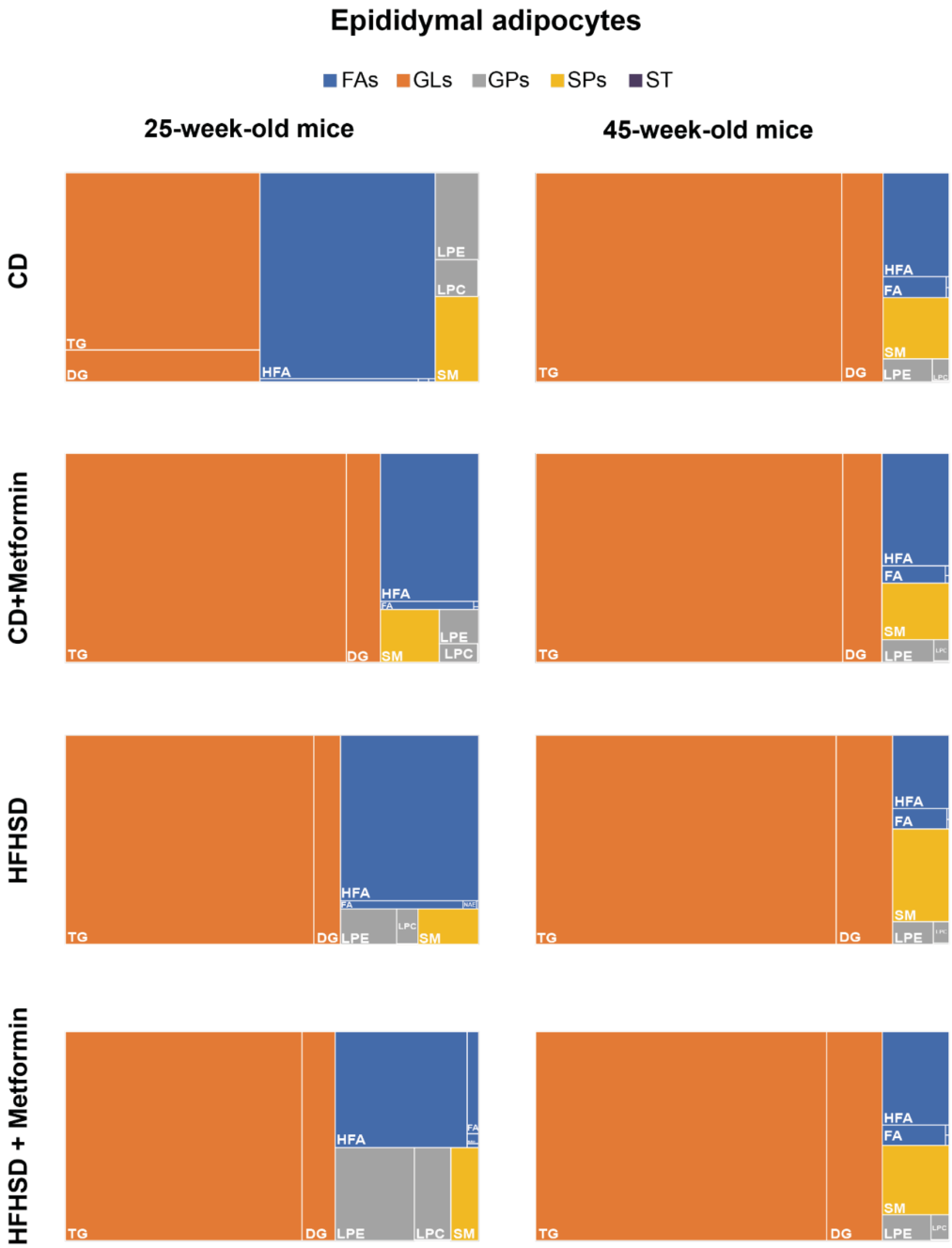

Fig. S11. Lipid class distribution in epididymal adipocytes
Treemaps show the relative distribution of main lipid categories and classes in epididymal adipocytes (n=4/group). These relative distributions serve as a comparative metric of epididymal lipidome between dietary treatments, age, and metformin treatment. BA: bile acids; CAR: carnitine; CD: chow diet; DG: diglycerides; FA: fatty acids; FAs: fatty acyls; GLs: glycerolipids; GPs: glycerophospholipids, HFA: hydroxy fatty acids; HFHSD: high-fat high sucrose diet; LPC: lysophosphatidylcholines; LPE: lysophosphatidylethanolamines; NAE: N-acyl-ethanolamine's; PC: phosphatidylcholines; SM: sphingomyelins; SPs: sphingophospholipids; St: steroid hormones; ST: sterol lipids, TG: triglycerides.

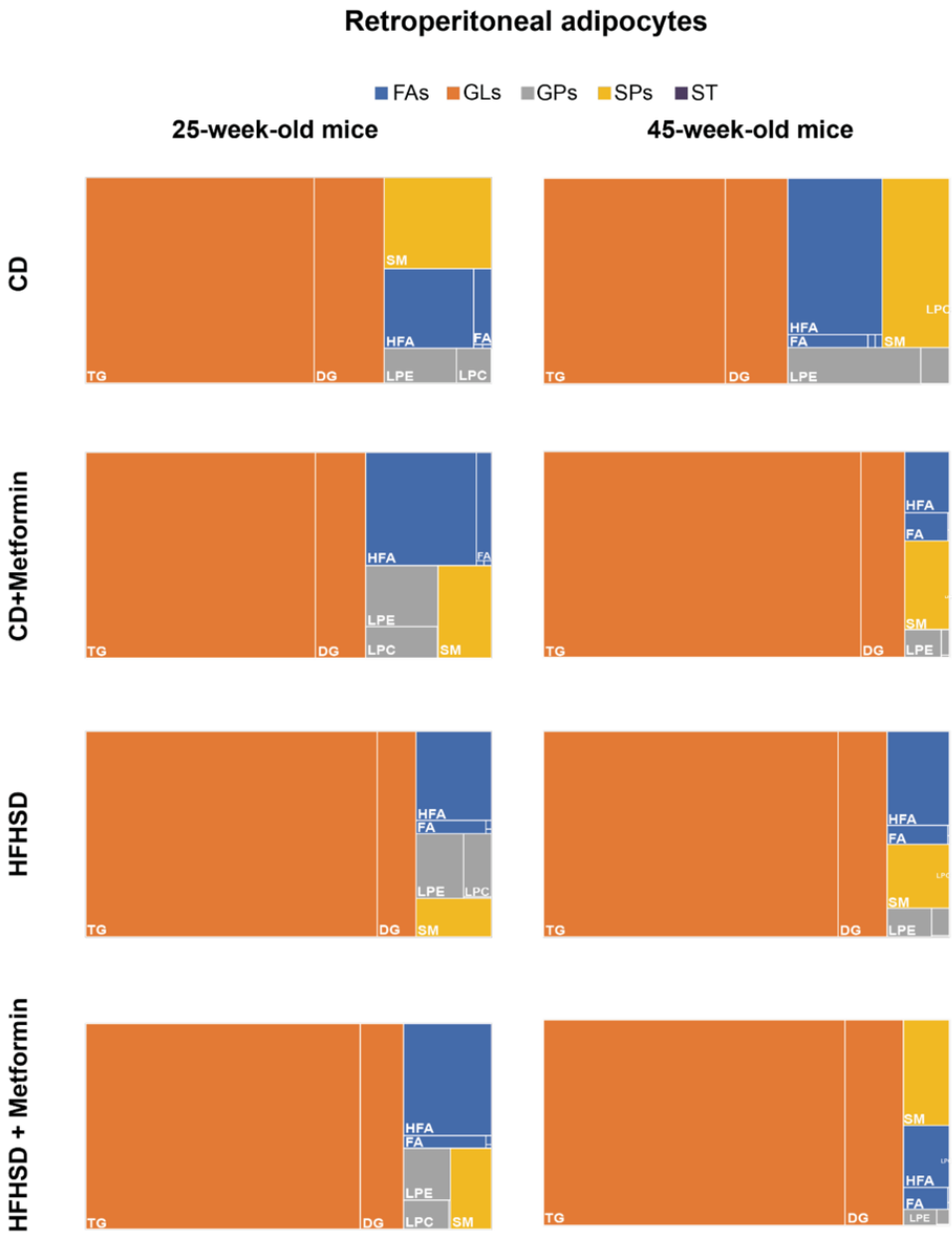

Fig. S12. Lipid class distribution in retroperitoneal adipocytes
Treemaps show the relative distribution of main lipid categories and classes in retroperitoneal adipocytes (n=4/group). These relative distributions serve as a comparative metric of retroperitoneal lipidome between dietary treatments, age, and metformin treatment. BA: bile acids; CAR: carnitine; CD: chow diet; DG: diglycerides; FA: fatty acids; FAs: fatty acyls; GLs: glycerolipids; GPs: glycerophospholipids, HFA: hydroxy fatty acids; HFHSD: high-fat high sucrose diet; LPC: lysophosphatidylcholines; LPE: lysophosphatidylethanolamines; NAE: N-acyl-ethanolamine's; PC: phosphatidylcholines; SM: sphingomyelins; SPs: sphingophospholipids; St: steroid hormones; ST: sterol lipids, TG: triglycerides.

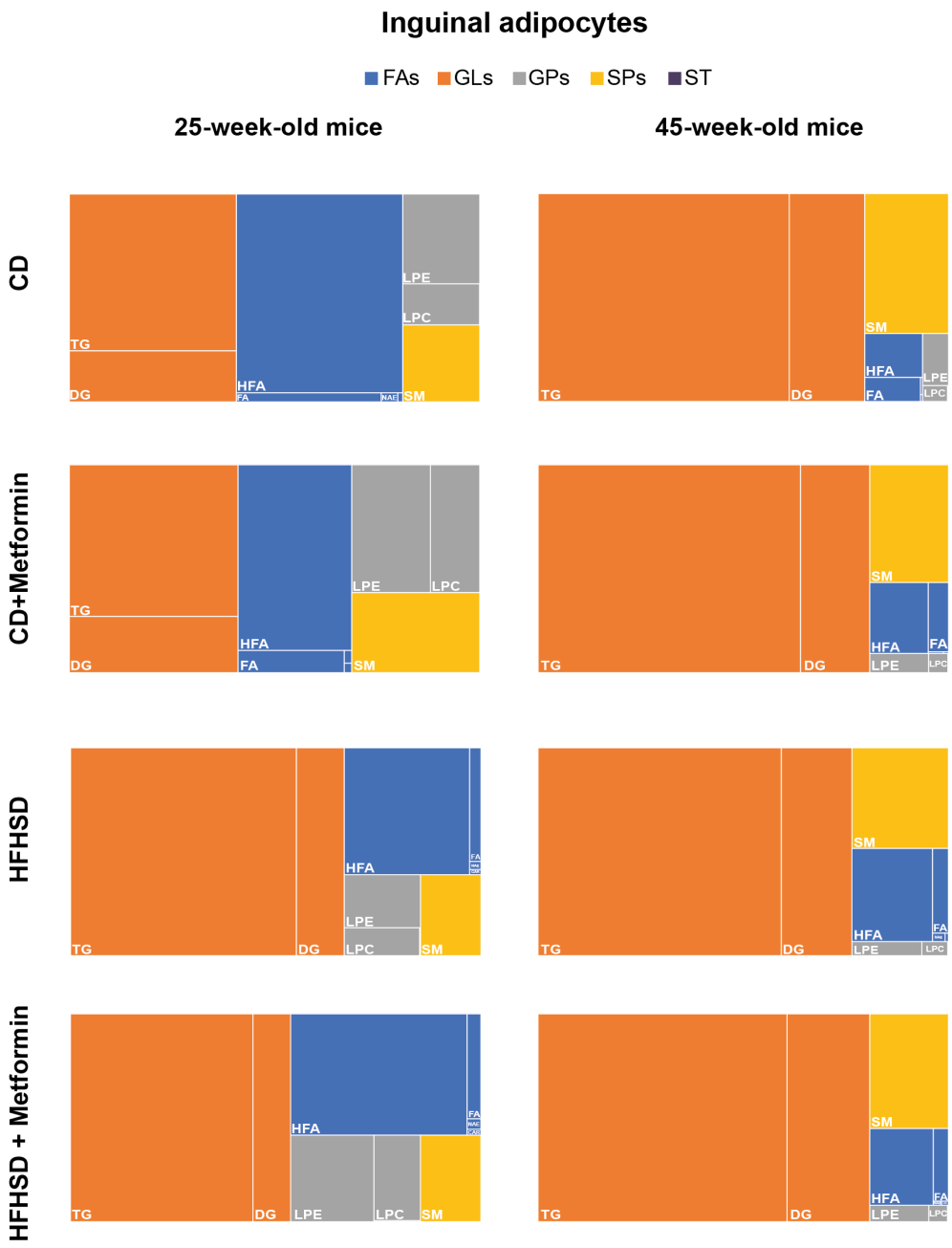

Fig. S13. Lipid class distribution in inguinal adipocytes
Treemaps show the relative distribution of main lipid categories and classes in inguinal adipocytes (n=4/group). These relative distributions serve as a comparative metric of inguinal lipidome between dietary treatments, age, and metformin treatment. BA: bile acids; CAR: carnitine; CD: chow diet; DG: diglycerides; FA: fatty acids; FAs: fatty acyls; GLs: glycerolipids; GPs: glycerophospholipids, HFA: hydroxy fatty acids; HFHSD: high-fat high sucrose diet; LPC: lysophosphatidylcholines; LPE: lysophosphatidylethanolamines; NAE: N-acyl-ethanolamine's; PC: phosphatidylcholines; SM: sphingomyelins; SPs: sphingophospholipids; St: steroid hormones; ST: sterol lipids, TG: triglycerides.

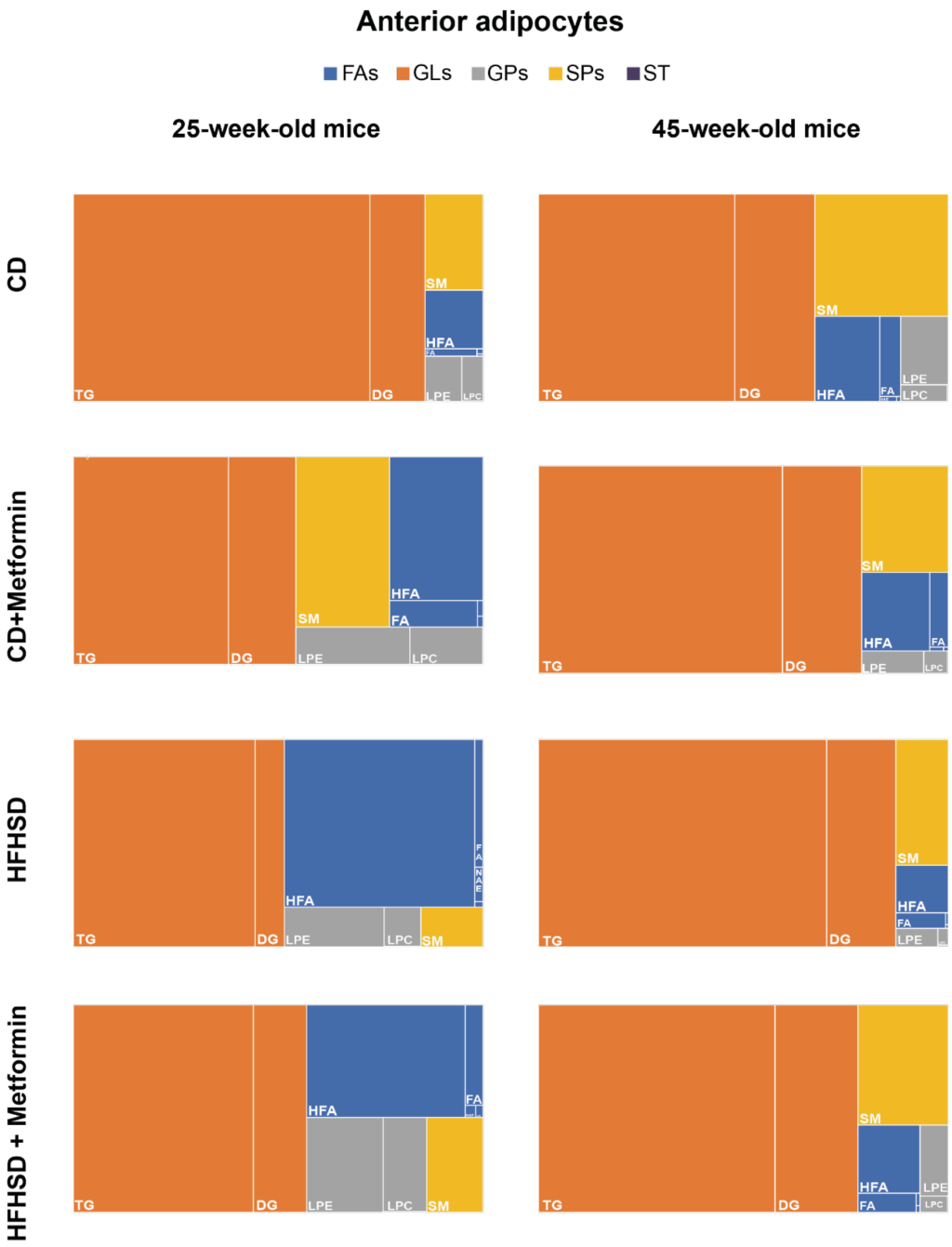

Fig. S14. Lipid class distribution in anterior adipocytes
Treemaps show the relative distribution of main lipid categories and classes in anterior adipocytes (n=4/group). These relative distributions serve as a comparative metric of anterior lipidome between dietary treatments, age, and metformin treatment. BA: bile acids; CAR: carnitine; CD: chow diet; DG: diglycerides; FA: fatty acids; FAs: fatty acyls; GLs: glycerolipids; GPs: glycerophospholipids, HFA: hydroxy fatty acids; HFHSD: high-fat high sucrose diet; LPC: lysophosphatidylcholines; LPE: lysophosphatidylethanolamines; NAE: N-acyl-ethanolamine's; PC: phosphatidylcholines; SM: sphingomyelins; SPs: sphingophospholipids; St: steroid hormones; ST: sterol lipids, TG: triglycerides.

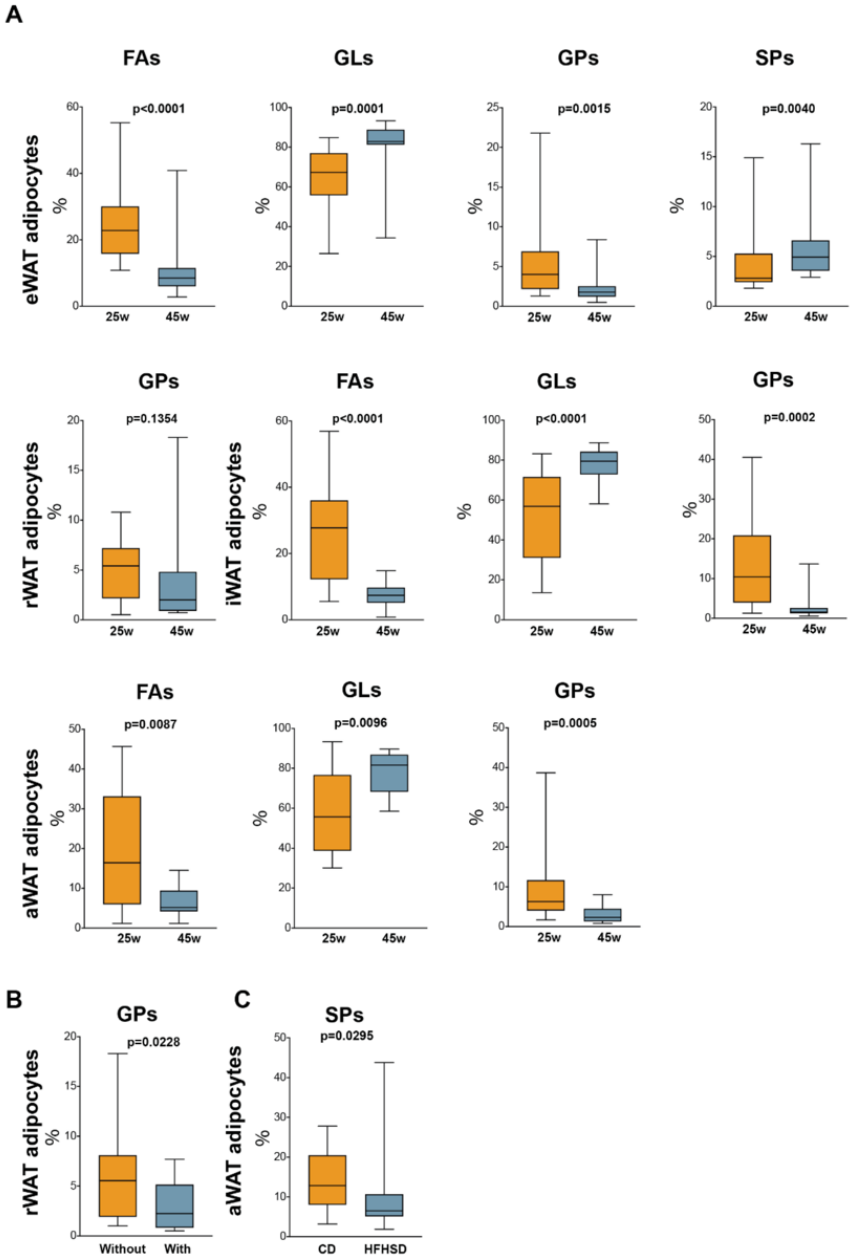

Fig. S15. Age, diet and metformin effects in adipocyte lipid categories
(**A**) Box plots show the lipid category alterations in visceral and subcutaneous adipocytes according to age, (**B**) metformin and (**C**) diet (n=4/group). Data are presented as means, maximum and minimum. P values < 0.05 are considered significant. (Wilcoxon-rank sum test). aWAT: anterior white adipose tissue; CD: show diet; eWAT: epididymal white adipose tissue; FAs: fatty acyls; GLs: glycerolipids; GPs: glycerophospholipids; HFHSD: high-fat high sucrose diet; iWAT: inguinal white adipose tissue; rWAT: retroperitoneal white adipose tissue; SPs: sphingophospholipids, ST: sterol lipids.

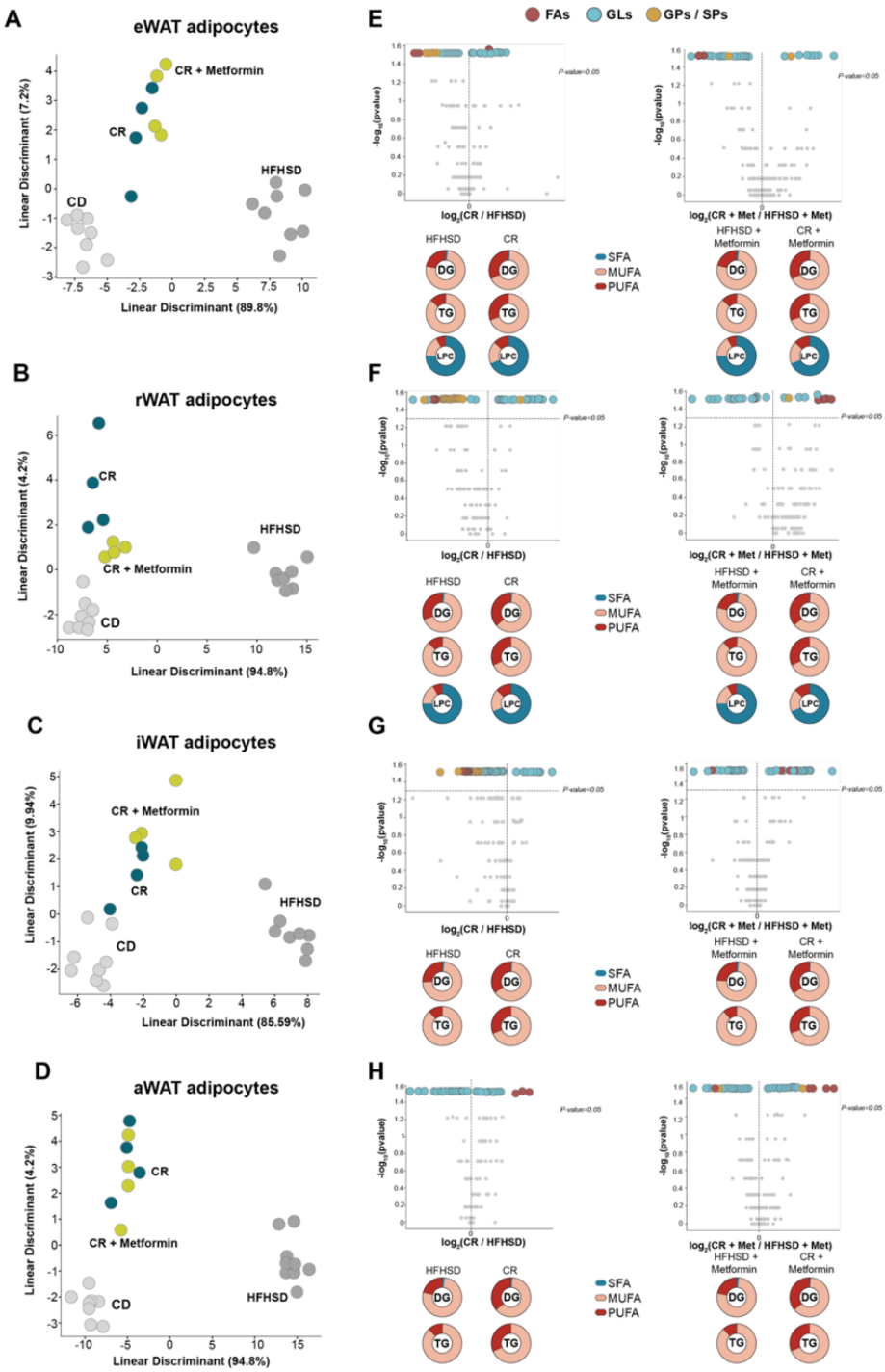

Fig. S16. Caloric restriction increased the lipid unsaturation in adipocytes
Lipid signature analysis between caloric restriction with or without metformin in obese mice in (**A**) epididymal (eWAT), (**C**) retroperitoneal (rWAT), (**E**) inguinal (iWAT),(**G**) anterior (aWAT) adipocytes (n=4/group). (**B**) Volcano plots of the effect of caloric restriction with or without metformin

administration in (**B**-**D**) visceral and (F-**H**) subcutaneous adipocytes (n=4/group). Significant lipid species are colored according to the lipid category. Levels of significance below 0.05 were considered significant (Wilcoxon-rank sum test).CD: chow diet; CR: caloric restriction; DG: diglycerides; FAs: fatty acyls; GLs: glycerolipids; GPs: glycerophospholipids; HFHSD: high-fat high-sucrose diet LPC: lysophosphatidylcholines; Met: metformin; MUFA: monounsaturated fatty acids; PUFA: polyunsaturated fatty acids, SFA: saturated fatty acids; SPs: sphingophospholipids; TG: triglycerides.

SUMMARY OF RESULTS

UNIVERSITAT ROVIRA I VIRGILI
EXPLORING LIVER AND ADIPOSE TISSUE ALTERATIONS IN THE NATURAL COURSE OF NON-ALCOHOLIC FATTY LIVER DISEASE: A LIPIDOMIC
Gerard Baiges Gaya

6.1 STUDY I

In Study I, we set up a NASH mouse model in the context of obesity to recapitulate the disorder observed in the human population. Mice receiving a high-fat diet (HFD) and high-fat high-sucrose diet (HFHSD) were obese after 20 weeks of dietary treatment. Both showed alterations in biochemical parameters such as glucose, cholesterol, and triglycerides. After liver histological analyses HFHSD-fed mice exhibited higher hepatic steatosis and lobular inflammation grades than HFD-fed mice, leading to the diagnosis of NASH (NAS≥5). To confirm these findings, we studied the inflammation and oxidative stress in liver samples and compared with those mice fed on a CD and HFD. Immunohistochemistry results revealed that mice receiving an HFHSD showed higher levels of hepatic markers associated with pro-inflammatory macrophages such as CD11b and CCL2, as well as 4-HNE related to oxidative stress. These findings were also confirmed by western blot analyses. Additionally, our metabolic data from liver samples showed that energy metabolism was altered differently according to the dietary treatment. In this sense, we observed that mice receiving an HFHSD had higher gene expression of genes implicated with the reductive glutamine pathway to form citrate through the reduction of alpha-ketoglutarate. In parallel, we found that the enzymes involved in the hepatic *de novo* lipogenesis, such as acetyl-CoA carboxylase and fatty acid synthase, were higher than in HFD and CD-fed mice. In adipose tissue, we found that after 20 weeks, both HFD and HFHSD-fed mice showed an increase in histological adipocyte size in visceral and subcutaneous white adipose tissue compared to mice fed a CD. In both diets, we found lower levels of hormone sensible lipase, suggesting that lipid mobilization was impaired in both obese mice groups. Our lipidomic analyses revealed that mice fed on an HFHSD showed higher concentrations of saturated and polyunsaturated fatty acids in visceral adipose tissue than CD-fed mice, whereas in subcutaneous adipose tissue, we found an increase in polyunsaturated fatty acids.

In summary, we conclude that mice receiving HFHSD develop a NASH phenotype characterized by the presence of inflammation and oxidative stress after 20 weeks of dietary treatment, while mice fed an HFD recapitulate the simple steatosis.

6.2 STUDY II

Given the unmet need to find new therapeutical drugs against NASH and the point that hepatic *de novo* lipogenesis is one of the strongest pathways activated in our NASH mouse model, we considered testing the efficacy of metformin as a *de novo* lipogenesis inhibitor for the prevention of NASH. After 20 weeks of experimental study, we found that mice fed on an HFHSD developed obesity independently of metformin administration. The biochemical and lipoprotein profiles were also altered, increasing the concentrations of glucose and cholesterol as well as the low-density lipoprotein particles in both groups. After liver histological analyses we found that mice receiving HFHSD with or without metformin developed a liver characterised by the diagnosis of probable NASH (NAS 3-4) or NASH (NAS>5). This phenotype was associated in both groups with alterations in glycerophospholipid and cholesterol metabolism. Thus, we found a decrease in the levels of hepatic phosphatidylcholines and an increase in lysophospatidylcholines. We also found an increase in cholesterol esters and a decrease in bile acids and steroid hormones, suggesting that free cholesterol is esterified to be incorporated in the hepatic lipid droplets. In visceral and subcutaneous adipocytes, the content of polyunsaturated fatty acids decreased in triglycerides, diglycerides, and lysophosphatidylcholines in both groups of animals. Additionally, we observed that in mice receiving HFHSD with metformin, the sphingomyelins species decreased in subcutaneous adipocytes. At 40 weeks of study, we observed the same trend as aforementioned; That is, mice receiving HFHSD had higher concentrations of glucose and cholesterol as well as alanine aminotransferase activities compared to CD-fed mice. Lipoprotein profiles were characterised by the increase of low-density lipoprotein particles and the decrease of high-density lipoproteins and very low-density lipoproteins compared to CD-fed mice. Liver histological analyses revealed a phenotype associated with the diagnosis of NASH. When we focused on the effects of age by comparing between 25- and 45-week-old mice, we found that alterations in biochemical and lipoprotein profiles were accentuated in mice fed an HFHSD. In this sense, 45-week-old mice with HFHSD had higher cholesterol levels and showed an increase in the alanine aminotransferase activity compared to 25-week-old mice. Lipoprotein profiles were characterised by the increase in very low-density particles and the decrease in high-density lipoprotein particles compared to 25-week-old mice. In parallel, we observed

that particle sizes decreased in very low-density lipoprotein particles and increased in high-density lipoprotein particles. In the lipidome of the liver, we found that the N-acyl-ethanolamine species decreased with age, which is associated with the contribution to inflammation and hepatic lipogenesis as well as the relative deficiency in insulin secretion. In adipocytes from visceral and subcutaneous white adipose tissue, age contributed to remodel the lipidome independently of diet and metformin administration. Thus, we found an increase in lipid species related to lipid storage, such as triglycerides and diglycerides, whereas the lipids related to plasma membranes, such as phosphatidylcholines and lysophospholipids, decreased.

Finally, we focused on the effects of caloric restriction (CR) in combination with metformin. We found that the body weight reduction was higher when the CR was combined with metformin (19.6% vs 9.8%) than with CR alone. Despite we did not observe differences in the biochemical and lipoprotein profiles, we found that mice given CR with metformin had lower hepatic steatosis grades than those given CR alone. In both groups of animals, the hepatic accumulation of cholesterol esters decreased, and the levels of bile acids and steroid hormones were restored as well as the qualitative lipid aspects such as the content increase in polyunsaturated fatty acids linked to triglycerides, diglycerides in the liver and adipocytes.

In summary, we conclude that metformin does not prevent non-alcoholic fatty liver disease progression but potentiates the caloric restriction effects during NASH remission.

DISCUSSION

UNIVERSITAT ROVIRA I VIRGILI
EXPLORING LIVER AND ADIPOSE TISSUE ALTERATIONS IN THE NATURAL COURSE OF NON-ALCOHOLIC FATTY LIVER DISEASE: A LIPIDOMIC
Gerard Baiges Gaya

Although a high-fat diet has been reported to induce obesity and non-alcoholic fatty liver disease in mice after 12 weeks of dietary treatment (79), there is little evidence about which type of diet is suitable for developing NASH. To recapitulates human NASH, we used C57BL/6J male mice under a high-fat diet (HFD) and high-fat high sucrose diet (HFHSD) for 20 weeks. This resulted in changes in the basal metabolism that increased the body weight and the concentrations of glucose, cholesterol, triglycerides, and alanine-aminotransferase activities in animals given either diet. Importantly, these changes proved to be strictly dependent on dietary fat content considering that caloric intake was similar between both diets and chow diet-fed mice (80). HFHSD-fed mice exhibited higher hepatic steatosis scores than HFD-fed mice and, as a result, developed a phenotype associated with the diagnosis of NASH (NAS≥5). These effects appear to be mediated by dietary composition rather than diet caloric density (81). This selectivity has been reported before, for example, with diets enriched with saturated fatty acids that induce a greater degree of insulin resistance than diets enriched with monounsaturated or polyunsaturated fatty acids (82). The content of sucrose or fructose in diets also contributes to the risk of metabolic syndrome, increasing the hepatic triglycerides content and insulin resistance (83,84), suggesting the diet qualitative aspect is an important factor in the contribution of metabolic disorders. The fructose effects on hepatic de novo lipogenesis are mediated by the upregulation of transcription factors that regulate the expression of lipogenic enzymes such as acetyl-CoA carboxylase and fatty acid synthase (85). Indeed, the hepatic gene expression signature we observed in HFHSD-fed mice resulted in a higher expression of ATP-citrate lyase and higher protein levels of ACC and FASN than in HFD-fed mice, both related to hepatic *de novo* lipogenesis. This suggests that the higher hepatic scores observed in HFHSD-fed mice were associated with the content of sucrose, which results in NASH induction (86).

Of note, we observed that HFHSD-fed mice had an alteration of autophagy-associated proteins, such as an increase in both p62/SQSTM1 (sequestosome 1) and microtubule-associated protein 1A/1B-light chain 3 (LC3). This agrees with other reports in established NAFLD models. In the early stage of NAFLD, the LC3-II protein increases as a response to hepatic lipid accumulation and avoids lipotoxicity by the increase of autophagy. However, as the liver disease advances from simple steatosis to

steatohepatitis, the protein p62 increase, which in turn is associated with autophagic flux inhibition resulting in the accumulation of autophagosomes (87). Additionally, the hepatic levels of phosphatase and tensin homolog (PTEN)-induced an increase in putative kinase protein 1 (PINK1) in mice fed an HFHSD, which is associated with damaged mitochondria (88). In agreement with other reports, PINK1 is a key component in mitochondrial quality control (89). The accumulation of PINK1 occurs on the outer mitochondrial membrane in situations of mitochondrial depolarization (mitochondria dysfunction)(89). In parallel, PINK1 phosphorylates E3 ubiquitin-protein ligase parkin (PARKIN), which results in mitochondrial ubiquitination being degraded through the autophagosome-lysosome pathway (mitophagy) (89). This suggests that HFHSD-fed mice result in autophagy inhibition leading to the accumulation of damaged mitochondria. Of note, the mitophagy reduction in human patients correlates with the severity of NAFLD (90–93).

In addition to the importance of autophagy in maintaining cellular quality control, it also contributes to the degradation of lipid droplets (lipophagy). In normal conditions, triglycerides and cholesterol esters are incorporated into lipid droplets and then can be degraded via lipolysis or lipophagy. Thus, mice receiving an HFHSD showed an accumulation of hepatic cholesterol esters mediated by Acyl-CoA: cholesterol acyltransferases (ACATs), which are activated when the levels of free cholesterol and fatty acids are elevated. Therefore, the free cholesterol is transformed into cholesterol ester through the incorporation of saturated or monounsaturated very long chain fatty acids, reducing the hepatic lipotoxicity of cholesterol and saturated fatty acids (94). Indeed, ACAT2 $^{-/-}$ mice exhibit protection against hepatic neutral lipids (triglycerides and cholesterol ester) accumulation but have increased plasma triglycerides (95).

The increase of hepatic CE in HFHSD-fed mice was concomitant with a reduction in the hepatic levels of PC as well as the increase in lysophosphatidylcholines (LPC). Indeed, the lipid droplet surface is composed by a monolayer of phospholipids, and changes in the composition of phospholipids can affect the lipid droplet dynamics. Of note, the inhibition of PC biosynthesis results in lipid droplet size increase. On the other side, the enrichment of lipid droplet surface in PE also promotes the size increase through lipid

droplet fusion (96). Other studies found that the deletion of phosphate cytidylyltransferase 1 A (PCYT1A) gene in mice, which is involved in the regulation of PC biosynthesis by the Kennedy pathway, showed lower levels of hepatic PC (resulting in 7-fold higher levels of hepatic triglycerides) was associated with the diagnosis of NASH compared to those in control mice (97,98). This suggests that the major presence of hepatic macro steatosis (large lipid vacuole) in HFHSD-fed mice could be mediated, at least in part, by the loss of content in PC.

On the other side, glycerophospholipid metabolism is also a key regulator in lipoprotein metabolism, and the inhibition of PC synthesis leads to the reduction of circulatory VLDL-p (99). The lipoprotein signature we observed in HFHSD-fed mice resulted in high total lipoprotein concentration characterized by enrichment in LDL-p and a decrease in VLDL-p and HDL-p compared to CD-fed mice. This observation was also found in patients with NASH, which displayed a decrease in HDL-p, whereas the small LDL-p increased compared to non-NASH patients (100). Our data did not reveal any change in the size of LDL-p, but we found an increase in medium and large HDL-p subfractions. Of note, large and medium HDL particles confer protection against vascular complications and a better lipoprotein profile in humans (101,102). Other reports revealed that a small HDL subpopulation acts as a potent protector of LDL oxidation as well as displays anti-inflammatory and atheroprotective properties rather than larger subpopulations (103). In this sense, it has been observed that small HDL-p display a major capacity to uptake free cholesterol from peripheral tissue and exchange triglycerides with triglyceride-rich lipoproteins (104). This suggests that HFHSD-fed mice show a lipoprotein profile with less capacity to remove the excess cholesterol leading to a lipotoxicity environment and a high likelihood to have a cardiovascular event.

In normal conditions, triglycerides are packaged into chylomicrons and VLDL-p to be transported into adipocytes for their safe storage. In this sense, we measured the relative levels of key proteins involved in the lipogenesis and lipolysis metabolism of adipose tissue. The protein levels of hormone sensible lipase (HSL), which is involved in the hydrolysis of diglycerides, decreased in HFHSD-fed mice compared to CD-fed mice. This suggests that adipose tissue fat mobilization could be reduced in HFHSD-fed mice.

Of note, human patients with low levels in HSL and $HSL^{-/-}$ mice show greater grades of insulin resistance and diglycerides accumulation in organs such as muscle, testis, and adipose tissue (105). The low relative lipolysis rates in HFHSD-fed mice resulted in the preference for fat accumulation, increasing the histological adipocyte size. Of the four adipose depots we analysed, epididymal, retroperitoneal, and inguinal adipocytes increased the levels of triglycerides but not the anterior depots.

In agreement with other reports, the more abundant lipid in adipocytes were the glycerolipids (comprising triglycerides and diglycerides), followed by fatty acyls, glycerophospholipids, sphingophoshpolipids, and a minor amount of sterol lipids (106). The most abundant lipid species in the fatty acyls were the hydroxy fatty acids (oxylipin type) that may increase in the context of metabolic syndrome. It has been reported that alterations in n-3/n-6 polyunsaturated fatty acids (PUFAs) derived from oxylipins can promote inflammatory responses (107). In this sense, we observed that the content of PUFAs in triglycerides, diglycerides, and fatty acids decreased in mice under an HFHSD, which in turn could modify the oxylipins profile and promotes an inflammatory environment in the adipose depots.

Metformin has been shown to reduce hepatic *de novo* lipogenesis (108), phospholipids, lysophospholipids (produced by hydrolysis of phospholipids), and sphingomyelins (109,110). Data from other authors suggest that metformin inhibits hepatic lipogenesis upon AMP-activated protein kinase (AMPK) activation, which in turn regulates the acetyl-CoA carboxylase (ACC) activity through the phosphorylation at the Ser212 site and inhibits the conversion of acetyl-CoA to malonyl-CoA, a precursor of fatty acid synthesis (111). However, our data did not support such effects since the lipid accumulation in the liver was similar to that of mice without metformin. This suggests that metformin treatment does not affect hepatic lipid metabolism. Moreover, it has been observed in humans that metformin administration does not reduce the intrahepatic content of triglycerides (112,113) and even they found an increase in the hepatic *de novo* lipogenesis rates has been found (113). Although little evidence exists about the metformin's effects on lipid metabolism, a report revealed that women population with polycystic ovary syndrome after metformin treatment exhibited a plasma profile

characterized by lower concentration in sphingomyelins and glycerophospholipids as well as a reduction in oxidized lipid species (110). Our lipidomic data revealed a decrease in SM in subcutaneous anterior adipocytes in mice fed on a CD, but these effects disappeared in mice of 45-week-old mice. Of note, ageing process is related to endoplasmic reticulum (ER) stress, which can affect the synthesis of glycerophospholipids. Indeed, the levels of PC are necessry for triglycerides storage in adipocytes. For example, during the differentiation of 3T3-L1 fibroblasts into mature adipocytes, the expression of phosphatidylethanolamine N- methyltransferase (PEMT) is high (114). In this sense, adipocytes from $PEMT^{-/-}$ mice exhibited higher basal hydrolysis of triglycerides rates resulting in smaller adipocyte size (70). This suggests that glycerophospholipid levels are essential in adipocyte metabolism, regulating the capacity of lipid storage. In this context, we found that 45-week-old mice had lower concentrations of glycerophospholipids compared to 25-week-old mice. However, their lipid signature was characterized by increased glycerolipids (comprising triglycerides and diglycerides) and not by a decrease, suggesting that other drivers are implicated in the regulation of the capacity of adipocytes to store triglycerides. The decreased content of glycerophospholipids has been reported in the ageing process. For example, in 94-week-old mice, the levels of PC, PE, and SM in kidney samples decreased in comparison to 14-week-old mice (115). Moreover, 108-week-old mice showed glycerophospholipid alterations in the heart and serum (116). However, this decrease in the content of glycerophospholipids appears to be tissue-specific, considering that the brain hippocampus in ageing mice accumulates PC. It is not surprising that older people have a major risk of developing NAFLD than younger people (117,118), taking into consideration that the severity of NAFLD is associated with a decrease in the hepatic PC/PE molar ratio, and age contributes to a reduction the content of glycerophospholipids. In the context of the hepatic lipid signature, we observed that 45-week-old mice showed lower levels of N-acyl ethanolamines. Indeed, the N-acyl ethanolamines are phospholipid-derived lipids of the endocannabinoids family, which can be synthetised by any organ and act mainly as paracrine mediators. Thus, high plasma levels of this type of lipids are correlated with cardiovascular events, insulin resistance, and hepatic steatosis. However, we do not know if the low hepatic levels correlate with higher plasma levels (119,120).

Caloric restriction (CR) has been reported to counteract several age-associated alterations and improve weight loss and cardiometabolic risk factors in patients with obesity (121). Moreover, CR upregulates the autophagy flux through the activation of AMPK. In this context, catabolic pathways are upregulated, as exemplified by β-oxidation of fatty acids as well as the lipophagy of hepatic lipid droplets. Thus, our NASH model after CR had decreased the content of cholesterol esters, fatty acids and carnitines, suggesting that the mechanisms of lipid oxidation were restored. However, the hepatic PC content remained low, which could indicate an impairment of glycerophospholipid synthesis related to age. CR promoted body weight reduction (9.8%), but this reduction increased when CR was combined with metformin (19.1%). The lipoprotein profile improved, resulting in the increase of very low-density and high-density lipoprotein particles and a decrease in low-density lipoprotein particles. Our results agree with other reports performed on patients with obesity after CR. (122,123). However, these studies did not observe an improvement in high-density lipoprotein concentration. On the other side, when lean people receive CR, only decreases in very-low-density particles are observed (124), suggesting the CR effects on lipoprotein profile vary according to the metabolic background of the patient.

The gene expression profile in white adipose tissue of aged mice displays a down-regulation of genes involved in lipid metabolism. However, these changes are prevented in mice under CR (125). For example, the genes involved in the peroxisome proliferator-activated receptor gamma (PPARγ) are downregulated with age but preserved under CR (125). This suggests that old mice under CR maintain the capacity to enlarge adipose tissue and therefore store lipids safely (126). Despite these transcriptional effects, our lipidomic data revealed that visceral and subcutaneous adipocytes had decreased content of monounsaturated fatty acids, whereas the content of polyunsaturated fatty acids increased, improving the qualitative lipid aspect of triglycerides and diglycerides. Proteomic data (127) of male Wistar rats showed that old rats under CR had higher levels of long-chain fatty acid CoA ligase 1 (ACSL1), which is involved in the activation of polyunsaturated fatty acids. This suggests that the increase of ACSL1 proteins could explain the increase of polyunsaturated fatty acids content in triglycerides and diglycerides.

UNIVERSITAT ROVIRA I VIRGILI
EXPLORING LIVER AND ADIPOSE TISSUE ALTERATIONS IN THE NATURAL COURSE OF NON-ALCOHOLIC FATTY LIVER DISEASE: A LIPIDOMIC
Gerard Baiges Gaya

PERSPECTIVES

UNIVERSITAT ROVIRA I VIRGILI
EXPLORING LIVER AND ADIPOSE TISSUE ALTERATIONS IN THE NATURAL COURSE OF NON-ALCOHOLIC FATTY LIVER DISEASE: A LIPIDOMIC
Gerard Baiges Gaya

We demonstrated that mice receiving an HFHSD develop a phenotype associated with the diagnosis of NASH. This phenotype results in higher hepatic inflammatory and oxidative stress markers, an increase in atherogenic lipoproteins such as LDL-p, hepatic accumulation of cholesterol ester, and a decrease in PC content. Additionally, the adipose tissue increases in size, resulting in a reduction of the degree of polyunsaturated fatty acid-containing lipids.

Taken together, our findings suggest that during NASH development, many players are involved. However, the enormous biomolecular complexity of this metabolic disorder requires experimental designs to 1) identify and understand the metabolic regulation of hepatic cell subtypes in health and disease as well as 2) understand the underlying molecular mechanisms of inter-organ crosstalk between the liver and other metabolic key organs such as adipose tissue and muscle.

The liver cell population comprises distinct cell subtypes. These include hepatocytes (~70% of total cells) and non-parenchymal cells (~30% of total cells), such as cholangiocytes, endothelial cells, Kupffer cells, hepatic stellate cells and, hepatic stem cells. The use of RNA-seq methods enables the study of hepatic cell subtypes to identify candidate genes altered in mice receiving HFHSD. In order to study the role of candidate genes in different primary cell lines, we shall perform a gene expression gain and loss of function study to evaluate the impact on the secretion of cytokines, collagen, and exosomes. Moreover, we shall evaluate the synthesis rate of fatty acids and the capacity of hepatocytes to release VLDL-p. Therefore, these results would provide an understanding of the molecular mechanisms involved in NASH development and the effects on such cell subtypes. Additionally, taking into consideration the importance of hepatocytes in regulating the lipoprotein metabolism and the biogenesis of lipid droplets, the subcellular organelles would be isolated to perform proteomics and lipidomic analysis, which can provide valuable information about changes in the composition of these compartments during NASH development.

.

Second, to study the crosstalk between organs, we shall use exosomes as a mode of cellular communication. Exosomes are complex 20-100 nm vesicles containing protein, lipids, metabolites, DNA, and RNA that promote metabolic effects in the target cells. Therefore, the exosome profile from hepatocytes in mice fed on a CD and HFHSD should be analysed. In order to identify the specific function of isolated exosomes, primary-cell lines should be used to evaluate their effects on adipocytes, myocytes as well immune cells. After that, labelled exosomes with radioactive isotopes from hepatocytes of CD-fed mice should intravenously be injected into HFHSD-fed mice to track and identify the target cell line as well as to explore the metabolic effects. The same design should be conducted in CD-fed mice with an intravenous injection of exosomes derived from HFHSD-fed mice. Therefore, this approach will provide evidence about the effects of exosome vesicles on health and disease, as well as the target-cell-specificity according to the exosome signature.

Third, the results in mouse models will be validated in human samples to initiate a drug discovery program. This approach will use a protein database to identify the best protein candidates that can inhibit exosomes and/or pathways altered in NASH.

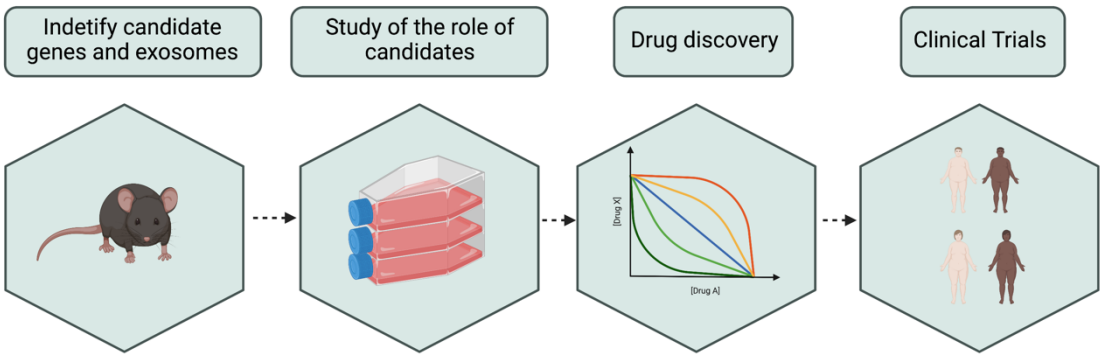

Fig.10. Drug discovery design

UNIVERSITAT ROVIRA I VIRGILI
EXPLORING LIVER AND ADIPOSE TISSUE ALTERATIONS IN THE NATURAL COURSE OF NON-ALCOHOLIC FATTY LIVER DISEASE: A LIPIDOMIC
Gerard Baiges Gaya

CONCLUSIONS

UNIVERSITAT ROVIRA I VIRGILI
EXPLORING LIVER AND ADIPOSE TISSUE ALTERATIONS IN THE NATURAL COURSE OF NON-ALCOHOLIC FATTY LIVER DISEASE: A LIPIDOMIC
Gerard Baiges Gaya

- After 20 weeks of dietary treatment, HFHSD-fed mice developed a phenotype associated with the diagnosis of NASH. (Objective 1, Study I)

- The NASH mouse model showed features of metabolic syndrome, such as an increase in glucose, cholesterol, and total lipoprotein particle concentrations. Additionally, the liver showed strong activation of hepatic de novo lipogenesis, autophagy-associated protein alteration, as well as accumulation of hepatic neutral lipids such as cholesterol esters and markers associated with mitochondrial damage (Objective 2, Study I and Study II).

- 45-week-old mice showed hepatic decreases in N-acyl-ethanolamine species, which are involved in the promotion of an inflammatory response. On the other side, the adipocytes of 45-week-old mice showed a loss of phospholipids content and an increase in storage-related lipids such as triglycerides and diglycerides. (Objective 3, Study II)

- Caloric restriction promoted a decrease in glucose, cholesterol, and total lipoprotein concentration and alanine aminotransferase activity, as well as reductions in body weight. Additionally, it restored the hepatic lipid alteration observed in our NASH mouse model, resulting in lower hepatic steatosis scores (Objective 4, Study II).

- Metformin is not effective in the prevention of NAFLD. However, the use of metformin in combination with caloric restriction potentiates the effects of body weight and hepatic steatosis reduction (Objective 5, Study II).

OVERALL CONCLUSION

Herein, we demonstrate that mice receiving a high-fat high-sucrose diet recapitulates the metabolic disorders observed in patients with NASH and could be used as a mouse model to study NASH in the context of obesity. Moreover, we recommend that metformin should not be used as a preventive strategy to avoid NAFLD development but may be useful to potentiate the effect of dietary interventions.

UNIVERSITAT ROVIRA I VIRGILI
EXPLORING LIVER AND ADIPOSE TISSUE ALTERATIONS IN THE NATURAL COURSE OF NON-ALCOHOLIC FATTY LIVER DISEASE: A LIPIDOMIC
Gerard Baiges Gaya

REFERENCES

UNIVERSITAT ROVIRA I VIRGILI
EXPLORING LIVER AND ADIPOSE TISSUE ALTERATIONS IN THE NATURAL COURSE OF NON-ALCOHOLIC FATTY LIVER DISEASE: A LIPIDOMIC
Gerard Baiges Gaya

1. Roust LR, Jensen MD. Postprandial free fatty acid kinetics are abnormal in upper body obesity. Diabetes. 1993 Nov;42(11):1567–73.
2. Lytle KA, Bush NC, Triay JM, Kellogg TA, Kendrick ML, Swain JM, et al. Hepatic fatty acid balance and hepatic fat content in humans with severe obesity. The Journal of Clinical Endocrinology & Metabolism. 2019 Dec 1;104(12):6171–81.
3. Sen P, Govaere O, Sinioja T, McGlinchey A, Geng D, Ratziu V, et al. Quantitative modelling of human liver reveals dysregulation of glycosphingolipid pathways in nonalcoholic fatty liver disease. iScience. 2022 Aug;104949.
4. Musso G, Cassader M, Paschetta E, Gambino R. Bioactive lipid species and metabolic pathways in progression and resolution of nonalcoholic steatohepatitis. Gastroenterology. 2018 Aug;155(2):282-302.e8.
5. Obesity. Nature Reviews Disease Primers. 2017 Dec 15;3(1):17035.
6. Okorodudu DO, Jumean MF, Montori VM, Romero-Corral A, Somers VK, Erwin PJ, et al. Diagnostic performance of body mass index to identify obesity as defined by body adiposity: a systematic review and meta-analysis. International Journal of Obesity. 2010 May 2;34(5):791–9.
7. World Bank Country and Lending Groups [Internet]. 2021 [cited 2022 Aug 5]. Available from: https://datahelpdesk.worldbank.org/knowledgebase/articles/906519-world-bank-country-and-lending-groups
8. Prevalence of obesity among adults, BMI >30, age-standarized estimates by World Bank income groups [Internet]. 2017 [cited 2022 Aug 5]. Available from: https://apps.who.int/gho/data/view.main.WB2480A?lang=en
9. White UA, Tchoukalova YD. Sex dimorphism and depot differences in adipose tissue function. Biochimica et Biophysica Acta (BBA) - Molecular Basis of Disease. 2014 Mar;1842(3):377–92.
10. Tchkonia T, Thomou T, Zhu Y, Karagiannides I, Pothoulakis C, Jensen MD, et al. Mechanisms and metabolic implications of regional differences among fat depots. Cell Metabolism. 2013 May;17(5):644–56.
11. Karastergiou K, Fried SK, Xie H, Lee MJ, Divoux A, Rosencrantz MA, et al. Distinct developmental signatures of human abdominal and gluteal subcutaneous adipose tissue depots. The Journal of Clinical Endocrinology & Metabolism. 2013 Jan;98(1):362–71.

12. Pinnick KE, Nicholson G, Manolopoulos KN, McQuaid SE, Valet P, Frayn KN, et al. Distinct developmental profile of lower-body adipose tissue defines resistance against obesity-associated metabolic complications. Diabetes. 2014 Nov 1;63(11):3785–97.
13. McQuaid SE, Humphreys SM, Hodson L, Fielding BA, Karpe F, Frayn KN. Femoral adipose tissue may accumulate the fat that has been recycled as VLDL and nonesterified fatty acids. Diabetes. 2010 Oct 1;59(10):2465–73.
14. Hoffstedt J, Arner E, Wahrenberg H, Andersson DP, Qvisth V, Löfgren P, et al. Regional impact of adipose tissue morphology on the metabolic profile in morbid obesity. Diabetologia. 2010 Dec 10;53(12):2496–503.
15. Petta S, Amato MC, di Marco V, Cammà C, Pizzolanti G, Barcellona MR, et al. Visceral adiposity index is associated with significant fibrosis in patients with non-alcoholic fatty liver disease. Alimentary Pharmacology & Therapeutics. 2012 Jan;35(2):238–47.
16. Karpe F, Pinnick KE. Biology of upper-body and lower-body adipose tissue—link to whole-body phenotypes. Nature Reviews Endocrinology. 2015 Feb 4;11(2):90–100.
17. Hotamisligil GS, Shargill NS, Spiegelman BM. Adipose expression of tumor necrosis factor-α: direct role in obesity-linked insulin resistance. Science (1979). 1993 Jan;259(5091):87–91.
18. Weisberg SP, McCann D, Desai M, Rosenbaum M, Leibel RL, Ferrante AW. Obesity is associated with macrophage accumulation in adipose tissue. Journal of Clinical Investigation. 2003 Dec 15;112(12):1796–808.
19. Bastard JP, Jardel C, Bruckert E, Blondy P, Capeau J, Laville M, et al. Elevated levels of interleukin 6 are reduced in serum and subcutaneous adipose tissue of obese women after weight loss. The Journal of Clinical Endocrinology & Metabolism. 2000 Sep 1;85(9):3338–42.
20. Tourniaire F, Romier-Crouzet B, Lee JH, Marcotorchino J, Gouranton E, Salles J, et al. Chemokine expression in inflamed adipose tissue is mainly mediated by NF-κB. PLoS ONE. 2013 Jun 18;8(6):e66515.
21. Kawakami M, Murase T, Ogama H, Ishibashi S, Mori N, Takau F, et al. Human recombinant TNF suppresses lipoprotein lipase activity and stimulates lipolysis in 3T3-L1 cells1. The Journal of Biochemistry. 1987 Feb;101(2):331–8.

22. Piché ME, Parry SA, Karpe F, Hodson L. Chylomicron-derived fatty acid spillover in adipose tissue: a signature of metabolic health? The Journal of Clinical Endocrinology & Metabolism. 2018 Jan 1;103(1):25–34.
23. Combs TP, Marliss EB. Adiponectin signaling in the liver. Reviews in Endocrine and Metabolic Disorders. 2014 Jun 3;15(2):137–47.
24. Ludwig J, Viggiano TR, McGill DB, Oh BJ. Nonalcoholic steatohepatitis: Mayo Clinic experiences with a hitherto unnamed disease. Mayo Clin Proc. 1980 Jul;55(7):434–8.
25. Ayonrinde OT. Historical narrative from fatty liver in the nineteenth century to contemporary NAFLD – Reconciling the present with the past. JHEP Reports. 2021 Jun;3(3):100261.
26. Ferguson D, Finck BN. Emerging therapeutic approaches for the treatment of NAFLD and type 2 diabetes mellitus. Nature Reviews Endocrinology. 2021 Aug 15;17(8):484–95.
27. Younossi ZM, Koenig AB, Abdelatif D, Fazel Y, Henry L, Wymer M. Global epidemiology of nonalcoholic fatty liver disease-Meta-analytic assessment of prevalence, incidence, and outcomes. Hepatology. 2016 Jul;64(1):73–84.
28. Gorden DL, Ivanova PT, Myers DS, McIntyre JO, VanSaun MN, Wright JK, et al. Increased diacylglycerols characterize hepatic lipid changes in progression of Human Nonalcoholic Fatty Liver Disease; Comparison to a Murine Model. PLoS ONE. 2011 Aug 9;6(8):e22775.
29. Luukkonen PK, Sädevirta S, Zhou Y, Kayser B, Ali A, Ahonen L, et al. Saturated fat is more metabolically harmful for the human liver than unsaturated fat or simple sugars. Diabetes Care. 2018 Aug 1;41(8):1732–9.
30. Luukkonen PK, Zhou Y, Sädevirta S, Leivonen M, Arola J, Orešič M, et al. Hepatic ceramides dissociate steatosis and insulin resistance in patients with non-alcoholic fatty liver disease. Journal of Hepatology. 2016 May;64(5):1167–75.
31. Ioannou GN. The role of cholesterol in the pathogenesis of NASH. Trends in Endocrinology & Metabolism. 2016 Feb;27(2):84–95.
32. Dentin R. Polyunsaturated fatty acids suppress glycolytic and lipogenic genes through the inhibition of ChREBP nuclear protein translocation. Journal of Clinical Investigation. 2005 Oct 1;115(10):2843–54.

33. Chiappini F, Coilly A, Kadar H, Gual P, Tran A, Desterke C, et al. Metabolism dysregulation induces a specific lipid signature of nonalcoholic steatohepatitis in patients. Scientific Reports. 2017 May 11;7(1):46658.
34. Pardo V, González-Rodríguez Á, Muntané J, Kozma SC, Valverde ÁM. Role of hepatocyte S6K1 in palmitic acid-induced endoplasmic reticulum stress, lipotoxicity, insulin resistance and in oleic acid-induced protection. Food and Chemical Toxicology. 2015 Jun;80:298–309.
35. Rada P, González-Rodríguez Á, García-Monzón C, Valverde ÁM. Understanding lipotoxicity in NAFLD pathogenesis: is CD36 a key driver? Cell Death & Disease. 2020 Sep 25;11(9):802.
36. Flowers MT, Keller MP, Choi Y, Lan H, Kendziorski C, Ntambi JM, et al. Liver gene expression analysis reveals endoplasmic reticulum stress and metabolic dysfunction in SCD1-deficient mice fed a very low-fat diet. Physiological Genomics. 2008 May;33(3):361–72.
37. Rolo AP, Teodoro JS, Palmeira CM. Role of oxidative stress in the pathogenesis of nonalcoholic steatohepatitis. Free Radical Biology and Medicine. 2012 Jan;52(1):59–69.
38. Ore A, Akinloye O. Oxidative stress and antioxidant biomarkers in clinical and experimental models of non-alcoholic fatty liver disease. Medicina (B Aires). 2019 Jan 24;55(2):26.
39. Koliaki C, Szendroedi J, Kaul K, Jelenik T, Nowotny P, Jankowiak F, et al. Adaptation of hepatic mitochondrial function in humans with non-alcoholic fatty liver is lost in steatohepatitis. Cell Metabolism. 2015; May 5; 21(5):739-46.
40. Rada P, González-Rodríguez Á, García-Monzón C, Valverde ÁM. Understanding lipotoxicity in NAFLD pathogenesis: is CD36 a key driver? Cell Death & Disease. 2020 Sep 25;11(9):802.
41. Mei S, Ni HM, Manley S, Bockus A, Kassel KM, Luyendyk JP, et al. Differential roles of unsaturated and saturated fatty acids on autophagy and apoptosis in hepatocytes. Journal of Pharmacology and Experimental Therapeutics. 2011 Nov;339(2):487–98.
42. Li S, Dou X, Ning H, Song Q, Wei W, Zhang X, et al. Sirtuin 3 acts as a negative regulator of autophagy dictating hepatocyte susceptibility to lipotoxicity. Hepatology. 2017 Sep;66(3):936–52.

43. Niture S, Lin M, Rios-Colon L, Qi Q, Moore JT, Kumar D. Emerging roles of impaired autophagy in fatty liver disease and hepatocellular carcinoma. Int J Hepatol. 2021;2021:6675762.
44. González-Rodríguez Á, Mayoral R, Agra N, Valdecantos MP, Pardo V, Miquilena-Colina ME, et al. Impaired autophagic flux is associated with increased endoplasmic reticulum stress during the development of NAFLD. Cell Death & Disease. 2014 Apr 17;5(4):e1179–e1179.
45. Chapman MJ, Ginsberg HN, Amarenco P, Andreotti F, Borén J, Catapano AL, et al. Triglyceride-rich lipoproteins and high-density lipoprotein cholesterol in patients at high risk of cardiovascular disease: evidence and guidance for management. European Heart Journal. 2011 Jun 1;32(11):1345–61.
46. Holmes M v., Ala-Korpela M. What is 'LDL cholesterol'? Nature Reviews Cardiology. 2019 Apr 30;16(4):197–8.
47. Kindel T, Lee DM, Tso P. The mechanism of the formation and secretion of chylomicrons. Atheroscler Suppl. 2010 Jun;11(1):11–6.
48. Dallinga-Thie GM, Franssen R, Mooij HL, Visser ME, Hassing HC, Peelman F, et al. The metabolism of triglyceride-rich lipoproteins revisited: new players, new insight. Atherosclerosis. 2010 Jul;211(1):1–8.
49. Goldstein JL, Brown MS. A century of cholesterol and coronaries: from plaques to genes to statins. Cell. 2015 Mar;161(1):161–72.
50. Brown MS, Radhakrishnan A, Goldstein JL. Retrospective on cholesterol homeostasis: the central role of scap. Annual Review of Biochemistry. 2018 Jun 20;87(1):783–807.
51. Rosenson RS, Brewer HB, Davidson WS, Fayad ZA, Fuster V, Goldstein J, et al. Cholesterol efflux and atheroprotection. Circulation. 2012 Apr 17;125(15):1905–19.
52. Rye KA, Barter PJ. Cardioprotective functions of HDLs. Journal of Lipid Research. 2014 Feb;55(2):168–79.
53. Hodson L, Gunn PJ. The regulation of hepatic fatty acid synthesis and partitioning: the effect of nutritional state. Nature Reviews Endocrinology. 2019 Dec 25;15(12):689–700.
54. Igal RA. Stearoyl-CoA desaturase-1: a novel key player in the mechanisms of cell proliferation, programmed cell death and transformation to cancer. Carcinogenesis. 2010 Sep 1;31(9):1509–15.

55. Reynolds LM, Dutta R, Seeds MC, Lake KN, Hallmark B, Mathias RA, et al. FADS genetic and metabolomic analyses identify the Δ5 desaturase (FADS1) step as a critical control point in the formation of biologically important lipids. Scientific Reports. 2020 Dec 28;10(1):15873.
56. Wang B, Wu L, Chen J, Dong L, Chen C, Wen Z, et al. Metabolism pathways of arachidonic acids: mechanisms and potential therapeutic targets. Signal Transduction and Targeted Therapy. 2021 Dec 26;6(1):94.
57. Alves-Bezerra M, Cohen DE. Triglyceride metabolism in the liver. in: comprehensive physiology. Wiley; 2017. p. 1–22.
58. Yew Tan C, Virtue S, Murfitt S, Robert LD, Phua YH, Dale M, et al. Adipose tissue fatty acid chain length and mono-unsaturation increases with obesity and insulin resistance. Scientific Reports. 2015 Dec 17;5:18366.
59. Olzmann JA, Carvalho P. Dynamics and functions of lipid droplets. Nature Reviews Molecular Cell Biology. 2019 Mar 6;20(3):137–55.
60. Stevenson J, Huang EY, Olzmann JA. Endoplasmic reticulum–associated degradation and lipid Homeostasis. Annual Review of Nutrition. 2016 Jul 17;36(1):511–42.
61. Bacle A, Gautier R, Jackson CL, Fuchs PFJ, Vanni S. Interdigitation between triglycerides and lipids modulates surface properties of lipid droplets. Biophysical Journal. 2017 Apr;112(7):1417–30.
62. Prévost C, Sharp ME, Kory N, Lin Q, Voth GA, Farese R v., et al. Mechanism and determinants of amphipathic helix-containing protein targeting to lipid droplets. Developmental Cell. 2018 Jan;44(1):73-86.e4.
63. Valm AM, Cohen S, Legant WR, Melunis J, Hershberg U, Wait E, et al. Applying systems-level spectral imaging and analysis to reveal the organelle interactome. Nature. 2017 Jun 24;546(7656):162–7.
64. Vance JE. Phospholipid synthesis and transport in mammalian cells. Traffic. 2015 Jan;16(1):1–18.
65. Kennedy EP, Weiss SB. The function of cytidine coenzymes in the biosynthesis of phospholipides. J Biol Chem. 1956 Sep;222(1):193–214.
66. Pelech SL, Vance DE. Regulation of phosphatidylcholine biosynthesis. Biochimica et Biophysica Acta (BBA) - Reviews on Biomembranes. 1984 Jun;779(2):217–51.

67. Li Z, Vance DE. Thematic Review Series: Glycerolipids. Phosphatidylcholine and choline homeostasis. Journal of Lipid Research. 2008 Jun;49(6):1187–94.
68. Vance DE. Physiological roles of phosphatidylethanolamine N-methyltransferase. Biochimica et Biophysica Acta (BBA) - Molecular and cell biology of lipids. 2013 Mar;1831(3):626–32.
69. Vance DE, Walkey CJ, Cui Z. Phosphatidylethanolamine N-methyltransferase from liver. Biochimica et Biophysica Acta (BBA) - Lipids and Lipid Metabolism. 1997 Sep;1348(1–2):142–50.
70. van der Veen JN, Kennelly JP, Wan S, Vance JE, Vance DE, Jacobs RL. The critical role of phosphatidylcholine and phosphatidylethanolamine metabolism in health and disease. Biochimica et Biophysica Acta (BBA) - Biomembranes. 2017 Sep;1859(9):1558–72.
71. Shindou H, Hishikawa D, Harayama T, Eto M, Shimizu T. Generation of membrane diversity by lysophospholipid acyltransferases. J Biochem. 2013 Jul;154(1):21–8.
72. Cole LK, Vance JE, Vance DE. Phosphatidylcholine biosynthesis and lipoprotein metabolism. Biochimica et Biophysica Acta (BBA) - Molecular and Cell Biology of Lipids. 2012 May;1821(5):754–61.
73. Vance DE. Role of phosphatidylcholine biosynthesis in the regulation of lipoprotein homeostasis. Current Opinion in Lipidology. 2008 Jun;19(3):229–34.
74. Wang B, Tontonoz P. Phospholipid Remodeling in Physiology and Disease. Annual Review of Physiology. 2019 Feb 10;81(1):165–88.
75. Guo Y, Walther TC, Rao M, Stuurman N, Goshima G, Terayama K, et al. Functional genomic screen reveals genes involved in lipid-droplet formation and utilization. Nature. 2008 May 13;453(7195):657–61.
76. Krahmer N, Guo Y, Wilfling F, Hilger M, Lingrell S, Heger K, et al. Phosphatidylcholine synthesis for lipid droplet expansion is mediated by localized activation of CTP:phosphocholine cytidylyltransferase. Cell Metabolism. 2011 Oct;14(4):504–15.
77. Hafez IM, Cullis PR. Roles of lipid polymorphism in intracellular delivery. Advanced Drug Delivery Reviews. 2001 Apr;47(2–3):139–48.
78. Moessinger C, Klizaite K, Steinhagen A, Philippou-Massier J, Shevchenko A, Hoch M, et al. Two different pathways of phosphatidylcholine synthesis, the

Kennedy Pathway and the Lands Cycle, differentially regulate cellular triacylglycerol storage. BMC Cell Biology. 2014 Dec 10;15(1):43.

79. Recena Aydos L, Aparecida do Amaral L, Serafim de Souza R, Jacobowski AC, Freitas dos Santos E, Rodrigues Macedo ML. Nonalcoholic fatty liver disease induced by high-fat diet in C57bl/6 models. Nutrients. 2019 Dec 16;11(12):3067.
80. van der Heijden RA, Sheedfar F, Morrison MC, Hommelberg PP, Kor D, Kloosterhuis NJ, et al. High-fat diet induced obesity primes inflammation in adipose tissue prior to liver in C57BL/6j mice. Aging. 2015 Apr 23;7(4):256–68.
81. Berná G, Romero-Gomez M. The role of nutrition in non-alcoholic fatty liver disease: Pathophysiology and management. Liver International. 2020 Feb 20;40(S1):102–8.
82. Lee JS, Pinnamaneni SK, Eo SJ, Cho IH, Pyo JH, Kim CK, et al. Saturated, but not n-6 polyunsaturated, fatty acids induce insulin resistance: role of intramuscular accumulation of lipid metabolites. Journal of Applied Physiology. 2006 May;100(5):1467–74.
83. Small L, Brandon AE, Turner N, Cooney GJ. Modeling insulin resistance in rodents by alterations in diet: what have high-fat and high-calorie diets revealed? American Journal of Physiology-Endocrinology and Metabolism. 2018 Mar 1;314(3):E251–65.
84. Montgomery MK, Fiveash CE, Braude JP, Osborne B, Brown SHJ, Mitchell TW, et al. Disparate metabolic response to fructose feeding between different mouse strains. Scientific Reports. 2016 Nov 22;5(1):18474.
85. Geidl-Flueck B, Hochuli M, Németh Á, Eberl A, Derron N, Köfeler HC, et al. Fructose- and sucrose- but not glucose-sweetened beverages promote hepatic de novo lipogenesis: A randomized controlled trial. Journal of Hepatology. 2021 Jul;75(1):46–54.
86. Ishimoto T, Lanaspa MA, Rivard CJ, Roncal-Jimenez CA, Orlicky DJ, Cicerchi C, et al. High-fat and high-sucrose (western) diet induces steatohepatitis that is dependent on fructokinase. Hepatology. 2013 Nov;58(5):1632–43.
87. Ding H, Ge G, Tseng Y, Ma Y, Zhang J, Liu J. Hepatic autophagy fluctuates during the development of non-alcoholic fatty liver disease. Annals of Hepatology. 2020 Sep;19(5):516–22.
88. Gao F, Zhang Y, Hou X, Tao Z, Ren H, Wang G. Dependence of PINK1 accumulation on mitochondrial redox system. Aging Cell. 2020 Sep 11;19(9).

89. McLelland GL, Soubannier V, Chen CX, McBride HM, Fon EA. Parkin and PINK1 function in a vesicular trafficking pathway regulating mitochondrial quality control. The EMBO Journal. 2014 Jan;n/a-n/a.
90. González-Rodríguez Á, Mayoral R, Agra N, Valdecantos MP, Pardo V, Miquilena-Colina ME, et al. Impaired autophagic flux is associated with increased endoplasmic reticulum stress during the development of NAFLD. Cell Death & Disease. 2014 Apr 17;5(4):e1179–e1179.
91. Kashima J, Shintani-Ishida K, Nakajima M, Maeda H, Unuma K, Uchiyama Y, et al. Immunohistochemical study of the autophagy marker microtubule-associated protein 1 light chain 3 in normal and steatotic human livers. Hepatology Research. 2014 Jul;44(7):779–87.
92. Fukuo Y, Yamashina S, Sonoue H, Arakawa A, Nakadera E, Aoyama T, et al. Abnormality of autophagic function and cathepsin expression in the liver from patients with non-alcoholic fatty liver disease. Hepatology Research. 2014 Sep;44(9):1026–36.
93. Madrigal-Matute J, Cuervo AM. Regulation of Liver Metabolism by Autophagy. Gastroenterology. 2016 Feb;150(2):328–39.
94. Wang YJ, Bian Y, Luo J, Lu M, Xiong Y, Guo SY, et al. Cholesterol and fatty acids regulate cysteine ubiquitylation of ACAT2 through competitive oxidation. Nature Cell Biology. 2017 Jul 1;19(7):808–19.
95. Alger HM, Brown JM, Sawyer JK, Kelley KL, Shah R, Wilson MD, et al. Inhibition of Acyl-Coenzyme A:Cholesterol Acyltransferase 2 (ACAT2) prevents dietary cholesterol-associated steatosis by enhancing hepatic triglyceride Mobilization. Journal of Biological Chemistry. 2010 May;285(19):14267–74.
96. Cohen BC, Raz C, Shamay A, Argov-Argaman N. Lipid droplet fusion in mammary epithelial cells is regulated by phosphatidylethanolamine metabolism. Journal of Mammary Gland Biology and Neoplasia. 2017 Dec 29;22(4):235–49.
97. Ling J, Chaba T, Zhu LF, Jacobs RL, Vance DE. Hepatic ratio of phosphatidylcholine to phosphatidylethanolamine predicts survival after partial hepatectomy in mice. Hepatology. 2012 Apr;55(4):1094–102.
98. Niebergall LJ, Jacobs RL, Chaba T, Vance DE. Phosphatidylcholine protects against steatosis in mice but not non-alcoholic steatohepatitis. Biochimica et Biophysica Acta (BBA) - Molecular and Cell Biology of Lipids. 2011 Dec;1811(12):1177–85.

99. Cole LK, Vance JE, Vance DE. Phosphatidylcholine biosynthesis and lipoprotein metabolism. Biochimica et Biophysica Acta (BBA) - Molecular and Cell Biology of Lipids. 2012 May;1821(5):754–61.
100. Corey KE, Misdraji J, Gelrud L, Zheng H, Chung RT, Krauss RM. Nonalcoholic steatohepatitis is associated with an atherogenic lipoprotein subfraction profile. Lipids in Health and Disease. 2014 Dec 21;13(1):100.
101. Vaisar T, Kanter JE, Wimberger J, Irwin AD, Gauthier J, Wolfson E, et al. High concentration of medium-sized HDL particles and enrichment in HDL Paraoxonase 1 associate with protection from vascular complications in people with long-standing type 1 diabetes. Diabetes Care. 2020 Jan 1;43(1):178–86.
102. Pascot A, Lemieux I, Prud'homme D, Tremblay A, Nadeau A, Couillard C, et al. Reduced HDL particle size as an additional feature of the atherogenic dyslipidemia of abdominal obesity. J Lipid Res. 2001 Dec;42(12):2007–14.
103. Camont L, Chapman MJ, Kontush A. Biological activities of HDL subpopulations and their relevance to cardiovascular disease. Vol. 17, Trends in Molecular Medicine. 2011. p. 594–603.
104. Kontush A. HDL and reverse remnant-cholesterol transport (RRT): televance to cardiovascular disease. Trends in Molecular Medicine. 2020 Dec;26(12):1086–100.
105. Grabner GF, Xie H, Schweiger M, Zechner R. Lipolysis: cellular mechanisms for lipid mobilization from fat stores. Nature Metabolism. 2021 Nov 19;3(11):1445–65.
106. Jové M, Moreno-Navarrete JM, Pamplona R, Ricart W, Portero-Otín M, Fernández-Real JM. Human omental and subcutaneous adipose tissue exhibit specific lipidomic signatures. The FASEB Journal. 2014 Mar 21;28(3):1071–81.
107. Mendonça AM, Cayer LGJ, Pauls SD, Winter T, Leng S, Taylor CG, et al. Distinct effects of dietary ALA, EPA and DHA on rat adipose oxylipins vary by depot location and sex. Prostaglandins, Leukotrienes and Essential Fatty Acids. 2018 Feb;129:13–24.
108. Fullerton MD, Galic S, Marcinko K, Sikkema S, Pulinilkunnil T, Chen ZP, et al. Single phosphorylation sites in Acc1 and Acc2 regulate lipid homeostasis and the insulin-sensitizing effects of metformin. Nature Medicine. 2013 Dec 3;19(12):1649–54.

109. Wanninger J, Neumeier M, Weigert J, Liebisch G, Weiss TS, Schäffler A, et al. Metformin reduces cellular lysophosphatidylcholine and thereby may lower apolipoprotein B secretion in primary human hepatocytes. Biochimica et Biophysica Acta (BBA) - Molecular and Cell Biology of Lipids. 2008 Jun;1781(6–7):321–5.
110. Pradas I, Rovira-Llopis S, Naudí A, Bañuls C, Rocha M, Hernandez-Mijares A, et al. Metformin induces lipid changes on sphingolipid species and oxidized lipids in polycystic ovary syndrome women. Scientific Reports. 2019 Dec 5;9(1):16033.
111. Rena G, Hardie DG, Pearson ER. The mechanisms of action of metformin. Diabetologia. 2017 Sep 3;60(9):1577–85.
112. Gormsen LC, Søndergaard E, Christensen NL, Jakobsen S, Nielsen EHT, Munk OL, et al. Metformin does not affect postabsorptive hepatic free fatty acid uptake, oxidation or resecretion in humans: A 3-month placebo-controlled clinical trial in patients with type 2 diabetes and healthy controls. Diabetes, Obesity and Metabolism. 2018 Jun;20(6):1435–44.
113. Green CJ, Marjot T, Walsby-Tickle J, Charlton C, Cornfield T, Westcott F, et al. Metformin maintains intrahepatic triglyceride content through increased hepatic de novo lipogenesis. European Journal of Endocrinology. 2022 Mar 1;186(3):367–77.
114. Cole LK, Vance DE. A Role for Sp1 in Transcriptional Regulation of Phosphatidylethanolamine N-methyltransferase in liver and 3T3-L1 adipocytes. Journal of Biological Chemistry. 2010 Apr;285(16):11880–91.
115. Braun F, Rinschen MM, Bartels V, Frommolt P, Habermann B, Hoeijmakers JHJ, et al. Altered lipid metabolism in the aging kidney identified by three layered omic analysis. Aging. 2016 Feb 16;8(3):441–54.
116. Eum JY, Lee JC, Yi SS, Kim IY, Seong JK, Moon MH. Aging-related lipidomic changes in mouse serum, kidney, and heart by nanoflow ultrahigh-performance liquid chromatography-tandem mass spectrometry. Journal of Chromatography A. 2020 May;1618:460849.
117. Golabi P, Paik J, Reddy R, Bugianesi E, Trimble G, Younossi ZM. Prevalence and long-term outcomes of non-alcoholic fatty liver disease among elderly individuals from the United States. BMC Gastroenterology. 2019 Dec 16;19(1):56.

118. Arshad T, Golabi P, Henry L, Younossi ZM. Epidemiology of non-alcoholic fatty Liver disease in north america. Current Pharmaceutical Design. 2020 Apr 24;26(10):993–7.
119. van Eyk HJ, van Schinkel LD, Kantae V, Dronkers CEA, Westenberg JJM, de Roos A, et al. Caloric restriction lowers endocannabinoid tonus and improves cardiac function in type 2 diabetes. Nutrition & Diabetes. 2018 Dec 17;8(1):6.
120. Gruden G, Barutta F, Kunos G, Pacher P. Role of the endocannabinoid system in diabetes and diabetic complications. British Journal of Pharmacology. 2016 Apr;173(7):1116–27.
121. Ard JD, Gower B, Hunter G, Ritchie CS, Roth DL, Goss A, et al. Effects of calorie restriction in obese older adults: The CROSSROADS randomized controlled trial. The Journals of Gerontology Series A: Biological Sciences and Medical Sciences. 2016 Dec 21;glw237.
122. Ariel D, Kim SH, Abbasi F, Lamendola CA, Liu A, Reaven GM. Effect of liraglutide administration and a calorie-restricted diet on lipoprotein profile in overweight/obese persons with prediabetes. Nutrition, Metabolism and Cardiovascular Diseases. 2014 Dec;24(12):1317–22.
123. Hołowko J, Michalczyk MM, Zając A, Czerwińska-Rogowska M, Ryterska K, Banaszczak M, et al. Six weeks of calorie restriction improves body composition and lipid profile in obese and overweight former athletes. Nutrients. 2019 Jun 27;11(7):1461.
124. Chooi Y, Ding C, Chan Z, Lo J, Choo J, Ding B, et al. Lipoprotein subclass profile after progressive energy deficits induced by calorie restriction or exercise. Nutrients. 2018 Nov 21;10(11):1814.
125. Ou MY, Zhang H, Tan PC, Zhou SB, Li QF. Adipose tissue aging: mechanisms and therapeutic implications. Cell Death & Disease. 2022 Apr 4;13(4):300.
126. Linford NJ, Beyer RP, Gollahon K, Krajcik RA, Malloy VL, Demas V, et al. Transcriptional response to aging and caloric restriction in heart and adipose tissue. Aging Cell. 2007 Oct;6(5):673–88.
127. Valle A, Sastre-Serra J, Roca P, Oliver J. Modulation of white adipose tissue proteome by aging and calorie restriction. Aging Cell. 2010 Oct;9(5):882–94.

ANNEX

Antonio Vidal-Puig MD PhD FRCP FMedSci EMBA
Professor of Molecular Nutrition and Metabolism
Wellcome-MRC Institute of Metabolic Science-Metabolic Research Laboratories
and Medical Research Council Metabolic Diseases Unit
University of Cambridge
IMS Level 4,
Box 289, Addenbrooke's Hospital
Cambridge CB2 0QQ, UK
Tel: (44) 1223 762790
Email: ajv22@medschl.cam.ac.uk
Website: http://www.tvplab-cambridge.com

4th January 2022

Mr. Gerard Baiges Gaya
Universitat Rovira i
Virgili Reus, Catalonia,
43201

To Whom it May Concern:

This is to confirm that Gerard Baiges Gaya, a visiting PhD student from Rovira i Virgili University has been doing his placement research work in the laboratory of Toni Vidal Puig (TVP lab) located at the University of Cambridge, UK between 13th September and 18th December 2021.

During his stay, he has been working in our lab and has learnt both lab techniques and lipidomic data analysis. The work lab experience has improved his skills in tissue culture as well as related techniques to evaluate the experiments such as protein, lipid, RNA extraction and ROS assay through flow cytometry in secondary hepatocyte cell lines.

In addition, he has contributed to one of our studies in order to gain experience in how to address the lipid analysis properly. During this period, he has been an active member of our team, presented his ongoing PhD work from his University and taken part in various discussions, seminars and lab meetings.

I'd happy to provide any further information as needed.

Yours faithfully,